# OPEN-PIT MINE PRODUCTION SCHEDULING UNDER GRADE UNCERTAINTY

by

Ady A. D. Van-Dúnem

A thesis submitted to the Faculty and the Board of Trustees of the Colorado School Mines in partial fulfillment of the requirements for the degree of Doctor of Philosophy (Mining and Earth Systems Engineering).

Golden, Colorado

Date _____

Signed: _____
Ady A. D. Van-Dúnem

Signed: _____
Dr. Kadri Dagdelen
Thesis Advisor

Signed: _____
Dr. Thys Johnson
Thesis Co-Advisor

Golden, Colorado

Date _____

Signed: _____
Dr. Priscilla Nelson
Professor and Head
Department of Mining Engineering

# ABSTRACT

Common challenges associated with grade uncertainty involve failing to meet decisive operational targets, which include (among others) the following: ore tonnage sent to the mill, total metal processed at the mill, blending requirements on ore feed, total waste tonnage mined, maximum allowable proportion of potentially deleterious materials (e.g., toxic elements such as arsenic). These challenges reflect, to an important extent, the uncertainty involved in defining precisely the mineral grades in an ore deposit.

This has motivated a vast body of research directed at improving understanding stochastic mine planning techniques, with an aim of incorporating its tools to mine production scheduling. One popular paradigm for stochastic mine planning consists of formulating fully stochastic linear programming (SLP) models which adopt sets of realizations of the orebody to represent uncertainty regarding grades (Dimitrakopoulos *et al.*, 2014). Since constraints must be met with total certainty, solutions from these formulations provide a decision maker with an absolute aversion to risk, i.e., one who (invariably) favors the most certain of two possible outcomes, regardless of their corresponding payoffs. Such production schedules may be too conservative in satisfying the production targets, while simultaneously producing sub-optimal results in those circumstances in which some flexibility in meeting targets exists. In a second paradigm, mine planners overcome the shortcomings of traditional production scheduling by incorporating geologic and grade uncertainty through geostatistical conditional simulations. However, this means that it is conceivable that one could also potentially benefit from any favorable development regarding previously "uncertain" domains of the ore deposit.

The work undertaken in this dissertation focuses on generating production schedules that take into account grade uncertainty, as described by geostatistically simulated realizations of the ore deposit, and provide optimized production schedules that also consider the desired degree of risk in meeting the production planning outcomes. To do this, the production scheduling problem is formulated as a large-scale linear program (LP) that considers grade uncertainty as characterized by a resource block model. The large-scale LP problem is solved using an iterative decomposition algorithm whose subproblems are multi-time-period sequencing problems. At each iteration, one

solves a master problem that generates a series of Lagrange multipliers (dual variables) that modify the objective function of the subproblems. In turn, the subproblem solutions modify the feasible region in the master problem and the approach is proven to converge to the optimal solution (Bienstock & Zuckerberg, 2009). The resulting LP solution is a multi-time-period mine production schedule that meets mining company's required level of risk tolerance in mine production plans.

The production scheduling formulation based on new risk-quantified linear programming models (LP) and their subsequent solutions do not only provide the risk profile of a given mine production schedule, but also allow the decision maker to define the level of acceptable risk in the mine plans generated and adopted.

.

# TABLE OF CONTENTS

# LIST OF FIGURES

# LIST OF TABLES

# ACKNOWLEDGMENTS

I would like to express my deepest gratitude to the many people, inside and outside the CSM campus who have helped make this dissertation possible. First my advisor, Dr. Kadri Dagdelen. I've always marveled at his unique ability to creatively think outside the box and, within few minutes, untie apparently "impossible Gordian knots." But most of all I'm indebted to him for the infinite personal support and encouragement throughout this (at times improbable) Journey. This I will surely carry with me for the rest of my life. I wish to thank the members of my jury who generously accepted to serve on my thesis committee. I thank Dr. Priscilla Nelson, for her great leadership in the Mining Department (and also for her maternal instincts...!). I would obviously like to thank Dr. Alexandra Newman for her immense generosity, her selflessness and for - throughout the years we have shared at Mines - always believing, even when I myself had doubts. I wish to thank, Dr. Thys Johnson, the smartest man alive, for the incredible help he has given me, and most of all, for his friendship and the brotherhood we have formed in this research group. Dr. Ozbay has been the best Rock Mechanics professor I've ever had. I thank him for that, and mostly, for having always kept the door of his office open to me. Literally, but also figuratively. Dr. Rennie Kaunda arrived heaven-sent at a complicated time when the jury had to be recomposed. I wish to thank him for being so supportive and helping make this day possible. I also thank Dr. Amanda Hering (who left Mines) for her help and for having accepted my invitation.

I wish to thank the enormous generosity of Sociedade Mineira de Catoca (SMC) in funding the greater part of my stay at Mines (including the time I have spent pursuing my MSc. Degree). I am deeply indebted to my colleagues at SMC and, in particular, to its former General Manager Dr. José M. A. Ganga Jr., for his amazing stewardship of SMC and the personal investment placed in me.

Dr. Marcelo Godoy, this thesis would not be possible without your contribution. I wish to acknowledge the funding from Newmont Company which was instrumental in prosecuting the work described herein, but at least as important, were the wonderful suggestions and technical advice you gave along this journey. Thanks a lot Marcelo. I certainly owe a great debt of gratitude

to professors Marcos Goycoolea, Daniel Espinoza and Eduardo Moreno for the many exchanges and advice throughout the latter year of the research.

I have been fortunate to be surrounded by very smart people at Mines. At the risk of unfairly leaving many colleagues out, I wish to mention by name Jung Mi Lee and Ruyxiang Gu, from an earlier stage, and Ismail Traore, Matias Palma and Saquib Saki from a later stage. I wish to thank my friend and colleague Canberk Aras, I brilliant young researcher, and a brother from many anxious sleepless nights at mines who I've been fortunate to have met.

Finally, I thank my brothers (and their spouses): N'vula and Edgar, José and Carlota, Telmo and Lay, for being so incredibly supportive and for having always sacrificed so much for me. I owe them so much; my debt can never be paid. My gratitude extends to my nephews: Maura, Yana, Muary, Muana, Jacinto, Nico and Kiary for the light-heartedness and inspiration. Your love represents the one immaterial dimension of life which gives everything its meaning. I thank my wife Euridice, for being a constant champion from day one; for the endless source of steadfast support, and for the plans and dreams I have asked she forfeit so that my own could come to fruition. Mostly, I thank her for her love.

To my parents, Zeca and Nina, for their unconditional love and forgiveness;

And to my daughter Lueji, for being.

# CHAPTER 1.
# INTRODUCTION

This thesis examines the problem of determining an optimal open pit mine production schedule which allows the quantification of grade uncertainty, i.e., a precise determination of the production volumes and respective sequencing in time, that is optimal with respect to the objective of maximizing the net present value NPV of the potential cash flows to be generated over the life-of-mine of the project for a given risk tolerance. This is an important and difficult problem, with a multidisciplinary nature that might call for the simultaneous consideration of aspects from the economic, statistical and optimization sciences. The economic dimension of production scheduling directly reflects consideration of the time-value of money effects, i.e., the relative preference on the part of management to realize income, sooner rather than later, so as to capitalize on potential investment opportunities presently available.

However, there exist limits to how soon profits can be realized, that is, since most mining operations have limited resources available, the large majority of economically viable mineral deposits cannot realistically be mined "instantaneously." Instead, mining likely spans over a set of time periods, and this characteristic makes considering the time-value of money an important deliberation. By defining when cash flows (from the sales of the metal commodity) can be realized, the specific production schedule adopted is crucial in determining a mining project's $NPV$. Furthermore, any profit-maximizing production schedule must necessarily be feasible, and the meaning of feasibility is not dissociable from the manner in which the problem is modeled. However, independently of the particular modeling choice, it is widely accepted that the open pit mine production scheduling problem ($OPMPSP$) is, in its essence, a large-scale linear mathematical constrained optimization problem (Johnson, 1968).

Aiming at taking advantage of the tools from optimization theory, the problem is most commonly tackled by initially discretizing the ore deposit into individual three-dimensional blocks whose technical and economic characteristics are assumed known. These might include quantitative variables such as the block's total ore content, the block's ore recovery at the processing plant, or qualitative variables including (among others) a block's lithological group or

rock type. Subdividing the mineral deposit into discrete blocks is important, because it allows the ($OPMPSP$) to be expressed formally in terms of either binary or continuous decision variables which determine (in the case of discrete variables) when, if ever, the block should be mined and, if mined, the destination to which the block should be sent. Alternatively, in the case of continuous decision variables, it is possible to mine fractions of a given block, that is, a given block might not be extracted fully. Since the total number of blocks in the deposit may be large (possibly reaching tens of millions for realistic orebodies), the total number of variables - which increases geometrically with the number of time periods - can potentially be very large as well.

One additional complicating aspect of ($OPMPSP$) is the fact that all mining problems are subject, in different forms and degrees, to operational requirements that limit the set of feasible decision paths to be considered. Within the formalism of Operations Research, the problem requirements are expressed in terms of linear combinations of the problem's decision variables, and modeled in the form of inequalities in the set of problem constraints. The combination of a large number of decision variables and the possible existence of a large variety of problem requirements - although typically in smaller number - confers a combinatorial nature to optimization problems which makes them tendentiously hard to solve, even in deterministic terms.

Furthermore, there exists growing recognition of the fact that a true optimal solution to ($OPMPSP$) cannot be found under a deterministic framework. In effect, it has become increasingly noted that, in various dimensions, including: confidence in estimated grades, confidence in the defined geologic boundaries of the orebody, confidence in the evolution of ore prices or confidence in the performance and availability of mine equipment, among others, uncertainty pervades mining, and realistic modeling of ($OPMPSP$) must take into account the possible economic impact of the risks associated with it. Because of uncertainty it is possible one might solve a decision problem incorporating input parameters which are, in effect, quite different from the true (unknown) problem parameters, that is, one might generate an "optimal" solution to the *wrong* problem.

This dissertation addresses only grade uncertainty and, although we refer to and geological uncertainty interchangeably, it is intended that both terms allude to the degree of confidence in some estimated grade. The field of geostatistics offers the best quantitative resource modeling tools for incorporating grade uncertainty into mine production schedules (Isaaks & Srivastava, 1989;

Godoy, 2004), as well as the formal theoretical framework supporting the vast majority of grade estimation techniques (Matheron, 1968; Journel, 1990; Delfiner & Chilés, 1997). One such method - that of geostatistical conditional simulations (GCS) - has emerged as one of the most powerful tools for adequate integration of grade risk into mine production plans. GCS allow for the generation of sets of equally likely representations (realizations) of the deposit, which honor the hard data at those locations of the ore deposit which have been sampled, and are conditioned on both the sampled and newly simulated grade values. GCS are desirable because they reproduce fairly the local grade variability, its spatial continuity, and by replacing a single grade estimate with a set of possible grades, they present a viable framework for probabilistic analysis in mine planning.

It is quite common to model geological (grade) uncertainty by assigning mineral resources to three distinct resource classification categories: Inferred, Indicated, and Measured (in increasing order of confidence), which reflect objective (as well as subjective) considerations as to the degree of risk involved in achieving estimated grades. Indeed, given a particular level of risk-tolerance, a decision maker will strive to define an appropriate "mix" of the proportions of material falling into each of the resource categories, making up the composition of the mill feed for any given time period. An example composition might be one in which upper bounds on the proportion of Inferred material require it to be below 30%, and lower bounds on the proportions of Indicated and Measured material, to be at least 20% and 50% of the total mill feed ore, respectively. The natural approach to solving such problems is by directly formulating them as stochastic linear programming ($SLP$) models, in which decision variables are indexed to each of the individual, alternative scenarios. However, this is not truly a viable approach in the context of mine production scheduling, because inherently difficult-to-solve problems are made intractable by the addition of scenario-dependent variables.

In this dissertation, a solution methodology is presented whereby different categories of ore resource requirements (i.e., proportions of inferred, indicated and measured material) are enforced in the form of "ore risk constraints. A risk-quantified open pit mine production scheduling problem ($OPMPSP$) is formulated which includes ore-risk constraints, together with other common capacity or blending and sequencing constraints. Next, an iterative large-scale decomposition

algorithm, tailored to solve to proven optimality the ($OPMPSP$), is used to solve an LP relaxation of said problem.

The solution generated is confronted with a set of available geostatistical simulations of the orebody in order to verify that, to a decision maker's level of risk tolerance, it can be deemed acceptable. If the present solution meets the risk requirements, it is considered optimal; however, in the event that it does not, and assuming our concern focuses only on satisfying risk requirements, then three distinct courses of action are possible: (a) adjust the current required proportions of each of the resource categories (Inferred, Indicated or Measured) to new equally acceptable levels and resolve the problem; (b) keep the current risk requirement levels (required material proportions) and adopt the current "risky" schedule; or (c) determine whether additional drilling is justified given the tradeoff between the expected benefit from reduced uncertainty versus the costs of additional data gathering.

According to this framework, a mine production schedule is considered optimal not simply because it corresponds to the solution of an optimization problem, but only after is has been shaped by a decision maker's risk tolerance level. In this sense, our problem formulation reflects an alternative view regarding the best approach to integrating grade uncertainty into production schedules, as well as a restatement of the problem where mineral resource classification categories are incorporated. This clearly is a very simple view of the problem. However, it is also very flexible, transparent, and importantly, very practical.

## 1.1 Dissertation Contents

This thesis dissertation assumes the reader is familiar with the basic principles of open pit mine planning and design, such as outlined in Hustrulid and Kuchta (2013). The following is a chapter-by-chapter description of the contents in the dissertation:

Chapter 1: Briefly introduces the Open Pit Mine Production Scheduling Problem ($OPMPSP$) together with a description of how, traditionally, the problem has been understood and modelled within a deterministic framework. We hint at some of the characteristics which make this a challenging problem, and emphasize the need for considering uncertainty in its multiple dimensions including the one most relevant to our research: grade uncertainty. We give indication

on how mineral resource classification categories, which have been widely used in industry, can be used as a useful proxy for confidence in grade estimation. Finally, we outline a solution methodology striving to include said classification categories, together with a mine planner's tolerance to risk, in a viable and practical framework.

Chapter 2: Deals with some of the basic foundational concepts in mine planning and open pit production scheduling. It briefly reviews a subset of the mine planning literature relevant to the research, focusing on distinct solution methodologies and classifying these into the following traditional categories: (i) exact deterministic methods and (ii) suboptimal block aggregation methods.

Chapter 3: Provides the strict minimum background in geostatistics that is required for the reader to comfortably follow some of the discussions in the subsequent sections. Emphasis is placed on those concepts which have a specific earth sciences nexus and may depart slightly from more general statistical methods. It is the author's conviction that the following topics merit said distinction: data declustering, usage of scatterplots as well as their relation to measures of spatial continuity such as the correlogram, covariogram or the variogram. We discuss estimation criteria to illuminate the specific sense in which geostatistical estimation methods are considered "best" or "unbiased." We introduce kriging, highlight its basic mechanics by way of a small numerical example and point to some of its shortcomings. This chapter assumes no prior knowledge of geostatistics and reads as a tutorial on the subject. A reader more versed in the topic of geostatistics might skip this chapter.

Chapter 4: Provides a simple introduction to the topic of geostatistical sequential (conditional) simulations and, similar to kriging, a small numerical example of the method highlighting the basic steps involved is included. Conditional simulations constitute the "workhorse" for stochastic mine planning, and are often used as a valid framework for mineral resource classification. This leads the way to stochastic production scheduling in Chapter 5.

Chapter 5: Presents the current stochastic mine production scheduling ($SMPS$) framework, in particular, its use of multiple geostatistical conditional simulations as input, which contrasts with the deterministic case, in which a single estimated model constitutes the sole support for mine planning. Two distinct models are included as paradigmatic examples of ($SMPS$). Finally, we give

indication to some of the challenges with said models and - to an important extent as a consequence of the challenges mentioned - we introduce the concept of mineral resource classification categories.

Chapter 6: Provides a description of the proposed problem formulation and solution methodology. The chapter is organized as an argument motivating the solution framework adopted, covering the defining characteristics of the problem to be solved, the nature of uncertainty in mine planning, the distinction between an exact and a heuristic starting point as a basis for mine planning, and it concludes with a flowchart of the solution methodology. It describes how the research presented integrates two powerful exact solution algorithms into a framework that takes into account uncertainties as conveyed by mineral resource classification categories and risk measured through conditional simulations.

Chapter 7: Contains a description of the general mathematical models adopted for the methodology upon which this research is focused. It states the problem, its underlying assumptions, and presents general and detailed mathematical model formulations of open pit mine production scheduling problems that consider grade uncertainties associated with the resource model.

Chapter 8: Examines the two exact solution algorithms adopted for the proposed solution methodology, namely: the Bienstock-Zuckerberg ($BZ$) and the PseudoFlow ($HPF$) algorithms. Although fairly technical, the discussions are not intended as a comprehensive treatment of either algorithm, and we refer the reader to the original work by Bienstock & Zuckerberg (2009), as well as to Hochbaum (2001, 2008, and 2012) for the detailed proofs on complexity, convergence and optimality. The related work in Munoz *et al*. (2016) extends that of Bienstock & Zuckerberg (2009), shows the applicability of BZ to the broader class of Resource Constrained Project Scheduling problems (RCPSP), and is insightful in presenting the problem in the context of delayed column generation algorithms. Nonetheless, the discussions therein are sophisticated and written for an operations research audience. In our presentation, a considerable effort is directed to helping the technical practitioner understand the links between these theoretical concepts and mining practice. The chapter includes small conceptual examples of both the BZ and HPF algorithms. Knowledge of operations research techniques would be helpful, but not absolutely necessary.

Chapter 9: Presents the results from the application of the proposed methodology to a two-dimensional and a three-dimensional synthetic case study. Throughout, the presentation is framed in the context of comparing our results to those obtained in a scenario in which risk constraints are not present, and discussing some of the implications of the results obtained.

Chapter 10: Concludes the dissertation by summarizing its key findings and listing suggestions for future work.

## 1.2 Original Contributions

The research work in this dissertation provides the technical practitioner with a tool, in the form of an integrated solution methodology, which allows the user to impart a specific degree of risk tolerance into mine production planning. Differently from other approaches reported in the literature, in the methodology developed in this dissertation, incorporation of management's tolerance to grade uncertainty is transparent, and this is achieved in two specific ways: (i) by explicitly soliciting from the decision maker a threshold reflecting preferences regarding risk, and (ii) by explicitly incorporating well-established industry metrics for uncertainty in classification of mineral resources into the optimization models. Said industry metrics are commonly referred to as the Inferred, Indicated and Measured resource classification categories, and compared to a direct block-by-block consideration of scenario-based grades, resource classification categories offer the following advantages:

(i) They can be included into the optimization models similarly to traditional blending constraints, thereby circumventing the "dimensionality curse" prevalent in most stochastic optimization models for the ($OPMPSP$).

(ii) They constitute, *a priori*, the most common tool by which geologists and geostatisticians, responsible for ore resource modeling, communicate a degree of confidence in estimated mineral resource grades. This enhances transparency, increases the chances for adoption of the proposed methods in practice, and helps to bridge the gap between production schedules ignorant of uncertainty and "uncertainty-conscious" commodity markets.

The solution methodology developed relies importantly on our implementation of the Bienstock-Zuckerberg (BZ) algorithm and the integration, within it, of the PseudoFlow

algorithm (HPF), both of which constitute state-of-the-art exact solution algorithms. Indeed, a considerable effort has been dedicated to investigating the principles underlying both algorithms, in an effort to make these more transparent to a technical mining audience. Our methods demonstrate, both in two dimensional and three dimensional case studies, how said algorithms can be used to obtain mine production schedules satisfying traditional, lower and upper bounding, mining and/or milling capacity constraints, grade blending constraints, as well as less traditional (unpublished at the time of this writing) mineral resource risk constraints. In addition, by allowing for the specification of user-defined levels of risk, the tool developed empowers the user to operate what amounts to a "dial" whereby its tolerance to risk is able to shape the production schedules. It should be noted that this is not the same as simplistic sensitivity analysis on an individual operational or economic parameter. In effect, in the framework developed in this research, new requirements on either the proportions of material belonging to a given resource category, or changes in the risk tolerance threshold, imply that a *completely new* production schedule need be generated and confronted against the decision maker's preferences.

Potentially, one of the future directions for the research reported on in this dissertation consists of the generation of optimal pushback designs under uncertainty. This idea follows naturally from the work developed in this dissertation, and this exact concept is demonstrated in one of the examples presented in Section 9.2.

Our methodology also provides an incremental contribution to the problem of determining the optimal amount of infill drilling (OID) for a mining operator. This is accomplished in two ways: (i) by exposing those regions of the ore deposit whose (grade) uncertainty most directly impacts mining in any given period, and (ii) by indicating an upper bound on how much management might be willing to invest on further drilling in return for greater conversion of mineral resources from inferred to a higher confidence class.

# CHAPTER 2.
# TRADITIONAL MINE PLANNING

Broad agreement exists within mine planning practitioners as to what solving the long-term open pit mine production scheduling problem ($OPMPS$) entails. To this effect, Dagdelen (1985) outlines the following necessary steps:

1. Development of a block model (geological and economical).
2. Determination of the final economic pit limits.
3. Generating mineable pushbacks within the final pit limits.
4. Generating a production schedule spanning the life of the mine project.

At the completion of the initial exploration stage, the biggest challenge is to successfully generate a reliable, geologic block model of the ore deposit. Drawing from a limited set of collected data samples, practitioners attempt to estimate the distribution of grades throughout the deposit by using one or more of an assortment of geostatistical interpolation techniques. Typical practice consists of discretizing the ore deposit into three-dimensional blocks, compositing the drillhole sample data and, finally, using some preferred interpolation technique assigning average grades to unsampled blocks (David, 1977). At completion, every individual block in the block model is assigned a corresponding grade value. However, due to the limited number of drillhole samples within a given deposit, a certain degree of uncertainty exists in the estimated block grades. Frequently, ore resource modelers choose to classify mineral resources into distinct risk categories as a "risk mitigation strategy" against grade uncertainty. Specifically, standard practice defines three distinct mineral resource classification categories, namely, the Inferred, Indicated and Measured categories, which are defined as follows (CIM, 2006):

**(i)** An Inferred mineral resource is that part of a mineral resource for which quantity and grade or quality are estimated on the basis of limited geological evidence and sampling. Geological evidence is sufficient to imply, but not verify, geological and grade or quality continuity.

**(ii)** An Indicated mineral resource is that part of a mineral resource for which quantity, grade or quality, densities, shape and physical characteristics are estimated with sufficient confidence to allow the application of modifying factors in sufficient detail to support mine planning and evaluation of the economic viability of the deposit.

**(iii)** A Measured mineral resource is that part of a mineral resource for which quantity, grade or quality, densities, shape, and physical characteristics are estimated with confidence sufficient to allow the application of Modifying Factors to support detailed mine planning and final evaluation of the economic viability of the deposit.

Once the construction of a geological block model is completed, the subsequent task is to translate geological information, such as grades, into economic block values. This requires examining an important set of economic and operational parameters. The economic value of individual blocks reflects the net result of calculating the revenue generated from extracting the block's "metal" element and subtracting the cost of mining, hauling and processing or stockpiling it (Johnson, 1968; Lane, 1988). Block values are thus determined using a single estimate of grades from the geologic model despite the existence of a significant degree of uncertainty surrounding the estimates of the block grades. It is then possible to build a sophisticated economic model for mine valuation including consideration of minimum internal rates of return (Armstrong *et al*., 2007). It is also possible to assign other attributes to each block, including a material type, equipment hours required to mine it and plant hours required to process it, among others.

## 2.1 The Ultimate Pit Limit Problem

In traditional mine planning, the economic block model is the basis for the determination of ultimate pit limits, which contain all the blocks deemed economical to mine. This optimization problem is widely known as the Ultimate Pit Limit (UPL) problem, and includes constraints regarding the sequencing of blocks ensuring all blocks are mined only after all of its predecessor (overlying) blocks have been mined. In addition, since the (UPL) problem assumes unlimited resources are available, then no system constraints prevent a feasible solution from mining a given block as early as necessary, thereby excluding the need for consideration of multiple time periods, and allowing the (UPL) to be expressed as a single-time-period problem. In effect, it is common

to present the (UPL) problem as an integer program (IP), which is formulated as follows (Lambert *et al.*, 2014):

Indices and Sets:

$b \in B$: $set\ of\ all\ blocks\ b$,

$b' \in B_b$: $set\ of\ all\ predecessor\ blocks\ b'\ that\ must\ be\ extracted\ directly\ before\ b$,

Data:

$v_b$: $net\ value\ (revenue\ minus\ cost)\ resulting\ from\ mining\ block\ b$

Decision Variable:

$x_b$: $1\ if\ block\ b\ is\ to\ be\ extracted; 0\ otherwise.$

Objective function:

$$(UPL) \quad max \sum_{b \in B} c_b x_b \tag{2.1}$$

Constraints:

$$x_b \leq x_{b'} \quad \forall b \in B, \quad b' \in B_b \tag{2.2}$$

$$x_b\ binary \tag{2.3}$$

The objective function (2.1)(8.139) seeks to maximize to total profit realized from mining. Constraints (2.2) ensure the sequencing of mined blocks obeys precedence requirements between a given block $b$, and its set of predecessor blocks $b'$.

Within the ultimate pit limits, price parameterization is used to generate nested pits ranging from the smallest pit, with the highest value per tonne of ore, to the largest pit, with the lowest value of ore per tonne of ore.

Lerchs and Grossman (1965) are credited with having first proposed a solution algorithm (LG) that would demonstrably solve the ultimate pit limit problem (UPLP) to optimality. Similarly, having observed the special structure of the UPLP namely, the total unimodularity of its constraint matrix, Johnson (1968) formally proposed a network-flow algorithm that also solves the UPL problem to proven optimality. Both algorithms have now been implemented to solve real-life problems very efficiently (Zhao & Kim, 1992).

Hochbaum (2008) introduces a new algorithm for the maximum flow problem which the author refers to as the PseudoFlow algorithm (HPF). The algorithm uses so-called pseudoflows – a vector of flows that "floods" the network - to solve a problem that is equivalent to the maximum flow problem and which the author names the maximum blocking cut problem. Once said problem is solved, a solution to the original maximum flow problem can be determined efficiently. Development of the PseudoFlow algorithm is strongly influenced by the previous work presented in Lerchs and Grossman (1965). Accordingly, the PseudoFlow algorithm adopts some of the concepts present in LG (e.g., strong and weak tree branches) and, importantly, it adopts a data structure (a normalized tree) that allows it to quickly reach an optimal solution, provided the corresponding pseudoflows are of good quality. The author proves the finite convergence of the algorithm, as well as its optimality. The author presents a parametric PseudoFlow algorithm in addition to a simplex variant of the PseudoFlow algorithm, and show that the complexity of said algorithm is linear in the number of arcs and nodes of the network. HPF is widely considered the fastest algorithm solving the maximum problem and, given its important role in the research developed in this dissertation, it is discussed in greater detail in Section (8.2).

## 2.2 The Open Pit Mine Production Scheduling Problem (OPMPSP)

After obtaining the ultimate pit limits, the next step consists of designing pushbacks, i.e., to include haul road access contouring the limits of each nested pit, and act as a guide during the short-term scheduling of yearly production. It often occurs that (i) more than one possible destination exists to which the extracted material can be sent, and (ii) the destinations to which the individual production blocks can be sent are predetermined in advance of the actual production schedules being generated. This is achieved by determining a break-even grade that results from equating the profit generated from sending a given production block to one destination versus sending it to an alternative destination. Once all of the alternative destinations are compared, a list of breakeven cutoff grades is generated which serves to determine the best possible destination for any individual production block. Additionally, it is common to determine cutoff grades which, to some extent at least, recognize and attempt to take into account some of the mining system's potential operational constraints, which can include a milling capacity bottleneck or a mine transportation capacity bottleneck (Lane, 1988). The combination of these break-even cutoff

grades forms what is known as a cutoff grade policy, constitute the basis for differentiating ore from waste material, and further, to determine exactly how individual blocks should be processed. These steps are repeated in an iterative fashion as incremental improvements are made with respect to the adequacy of the production capacities and the estimated operational costs (Dagdelen, 2007).

The next immediate step consists of generating production schedules that should result in the highest net present value for the project while still meeting a number of operational constraints. Commonly such constraints include: limits on the total number of blocks to be mined in a period, otherwise known as production capacity constraints, limits on the average grade of the material sent to (or obtained from) the processing plants, also known as blending constraints, and an ordering of the extraction time of individual mining units in such fashion as to ensure that spatial precedence constraints are enforced. This last group of constraints is also known as the set of block sequencing (precedence) constraints.

In general, a mine production schedule answers the following questions:

a) Whether a given block in the model should be mined or not
b) If it is to be mined, when should it be mined, and
c) Once it is mined, where it should be sent.

The mathematical formulation of the Open Pit Mine Production Scheduling Problem can be stated using notation consistent with prior references (Lambert *et al*., 2014) as follows:

Indices and Sets:

$b \in B$: $set\ of\ all\ blocks\ b$

$b' \in B_b$: $set\ of\ blocks\ b'\ that\ must\ be\ extrated\ before\ block\ b\ (i.e., the\ direct\ predecessors\ of\ block\ b)$

$d \in D$: $set\ of\ all\ destinations\ d$

$t \in T$: $set\ of\ all\ time\ periods\ t$

$r \in R$: $set\ of\ all\ operational\ resources\ r$

Data:

$v_{bdt}$: $net\ present\ value\ (NPV)\ generated\ by\ extracting\ block\ b\ in\ period\ t\ and\ sending\ it\ to\ destination\ d$ ($)

$a_{rb}$: $nonnegative\ amount\ of\ operational\ resource\ r\ associated\ with\ block\ b$

$\underline{e}_{rdt}$: $nonnegative\ , per-period\ minimum\ required\ usage\ for\ operational\ resource\ r\ at\ destination\ d$

$\bar{e}^{rdt}$: $nonnegative\ , per-period\ maximum\ required\ usage\ for\ operational\ resource\ r\ at\ destination\ d$

Decision Variables:

$x_{bdt} = the\ fraction\ of\ block\ b\ that\ is\ extracted\ at\ time\ period\ t\ and\ sent\ to\ destination\ d$

Objective Function:

$$(OPMPSP) \quad \max \sum_{b\in B}\sum_{d\in D}\sum_{t\in T} v_{bdt}x_{bdt} \tag{2.4}$$

Constraints:

$$\sum_{t'<t} x_{bdt'} \leq \sum_{t'<t} x_{b'dt'} \qquad \forall b \in B, b' \in B_b, t \in T \tag{2.5}$$

$$\underline{e}_{rd} \leq \sum_{b\in B} a_{rb}x_{bdt} \leq \bar{e}^{rd} \qquad \forall r \in R, t \in T, d \in D \tag{2.6}$$

$$0 \leq \sum_{d\in D}\sum_{t\in T} x_{bdt} \leq 1 \qquad \forall b \in B \tag{2.7}$$

$$x_{bdt} \in [0,1] \qquad \forall b \in B, t \in T, d \in D \tag{2.8}$$

The objective function (2.4) seeks to maximize the discounted value of all extracted blocks. Constraints (2.5) ensure that the cumulative proportion of block $b$ (mined in period $t$ or earlier), is not greater than the cumulative proportion of any of its predecessor blocks $b'$ that is mined in time period $t$ or earlier. Constraints (2.6) enforce minimum resource requirements and maximum resource requirements per time period. Constraints (2.7) restrict (for all blocks) the sum of the fraction of a block mined - across all destinations and time periods - to be less than or equal to one. Constraints (2.8) restrict all decision variables to assume continuous values between zero and one.

Constraints (2.6) might include, among others, lower bounds on the minimum ore tonnage to be sent to the mill plant per period or even minimum average grade at the mill feed, such that financial metrics such as return on investments or payback periods can be satisfied. On the other hand, upper bounding constraints might impose limits on, among others, the total mining and/or processing capacity, the maximum allowable average grade at the mill.

The traditional approach to mine planning has been deterministic in nature. This characterization is the result of the following assumptions being satisfied (Froyland *et al*., 2004):

- A deterministic block model is given as input data,
- Mining and processing costs, the selling price of the product and future discount rates are perfectly known into the future,
- Grade control is assumed to be perfect; i.e., once a block has been blasted its content is precisely known and,
- The infrastructure is fixed throughout the life of the mine (e.g., mining and processing capacities).

Ideally, a comprehensive approach to the mine production scheduling problem ($OPMPSP$) would allow one to simply formulate and solve the problem, independently of the determination of ultimate pit limits and phases or pushbacks. However, using exact optimization methods such as mixed integer linear programming ($MILP$) leads to formulations which are intractable (very hard to solve) due to the combinatorial nature of such problems. To our knowledge, there are no known optimum open-pit mine production scheduling techniques presently able to tackle very large-scale realistic problems, i.e., problems which might include over a million variables and constraints. In discussing the steps for effective mine planning previously outlined, Dagdelen (1992) stresses the circular nature of the problem and, thus, the resulting iterative characteristics of any optimal solution algorithm.

As interest in the solution of the $OPMPSP$ widened, a larger swath of researchers studied the problem, and the breadth of solution algorithms constructed also increased. This is reflected in the diversity and depth of the technical literature on the subject. Nonetheless, the published academic literature contains work which reviews and systematizes some of the most important contributions in the field. Out of these, two particular references stand out: Osanloo *et al*., 2008 and Newman *et al.*, 2010 which provide a thorough discussion of the application of Operations Research techniques to a wide spectrum and classes of mine planning problems. It is common to catalog solution algorithms for production scheduling problems (both open-pit and underground) into one of the following categories; (a) exact methods which may or may not resort to block

aggregation, (b) heuristic (Ramazan 2001, Cullenbine *et al*. 2011, Somrit 2011) and metaheuristic methods (Lamghari *et al.*, 2012; Silva *et al.*, 2014).

Exact methods are mathematically proven to solve the OPMPSP to true optimality. Johnson (Johnson, 1968) is credited with pioneering the application of exact mathematical optimization methods to solve the production scheduling problem. The author uses Dantzig-Wolfe decomposition principles to solve the OPMPSP by separating the multi-time period subproblem into single-time period problems which are solved as ultimate pit limit problems. The master problem enforces operational constraints (i.e., production and processing requirements) while the subproblems enforce sequencing constraints. However, the optimal solutions obtained are not necessarily integer and therefore may not be feasible in practice.

Dagdelen (1985) uses an LP formulation to model the production scheduling problem including mining capacity, blending and processing capacity. The multi-time period OPMPSP is notoriously difficult to solve (i.e., it belongs to the class of NP-hard problems). Dagdelen then applies a large-scale decomposition technique - the Lagrangian relaxation method - to solve the problem by decomposing the larger and more complex multi-time period problem into smaller single time period problems which can be solved using optimal ultimate pit limit algorithms such as maximum flow. The subgradient method is applied to find the Lagrangian parameters in his formulation. He states that despite generating integer solutions, the proposed approach cannot avoid the so-called "gap problem" and hence the solutions obtained may not always be feasible.

Akaike (1999) extends the work on Lagrangian relaxation methods by Dagdelen (1985). A new scheme for updating the Lagrangian multipliers is proposed, and instead of directly solving the OPMPSP as an LP, the author converts the problem into a network relaxation formulation so that the problem can be solved expeditiously by Lerchs-Grossman (LG) or Max-Flow algorithms. The network flow problem is solved as multi-time-period sequencing maximum flow problem. All constraints other than sequencing are relaxed (i.e., moved to the objective function and multiplied by a penalty). By decreasing the overall solution time the author states this increases the applicability of the Lagrangian approach to large-scale production scheduling problems. However, the author concedes that due to the "gap problem," the algorithm is not able to consistently find feasible solutions.

Cacceta and Hill (2003), building on an idea first presented by Johnson (1968), modify the conventional integer programming (IP) formulation in which the decision variables specify that blocks are to be mined "at" a specific time period $t$, to a formulation where blocks are mined "by" a specified time period $t$. Their model accounts for inventory variables and, since the model determines whether a block is to be sent to the mill to be processed as ore, or to be sent to the waste dump (or an alternative destination), it also is an attempt at cutoff grade optimization. It should be noted that if the $OPMPSP$ could be solved to true integer optimality, the resulting cutoff grades would also be optimal (Johnson, 1968; Dagdelen, 1985).

Gaupp (2008) employs three complementary strategies for expediting the solution of a Mixed Integer Programming (MILP) formulation of the OPMPSP: (1) A variable reduction technique (implementing earliest starts and latest starts) to reduce the number of decision variables considered in the model; (2) Strengthening the solution procedure through the application of cuts; and (3) Using Lagrangian relaxation techniques. The author states that the approach allows for optimal (or near optimal) solutions to be found more quickly than by solving the original problem. The size of the problems solved by the proposed technique - in the order of tens of thousands of variables – can be considered relatively small when compared to some of the test instances reported in the literature (Espinoza *et al.*, 2012).

Bienstock & Zuckerberg (2009) present an exact Lagrangian-based algorithm to solve the LP relaxation of the Precedence Constrained Production Scheduling Problem (RCPSP); henceforth referred to as BZ algorithm. The authors frame the problem in terms of sets of jobs to be scheduled observing a set of precedence rules, and processed according to a predefined set of processing options which have limited resources. This is a problem most commonly referred to as the Mine Production Scheduling Problem (MPSP) within the technical mining literature, and a parallel exists between jobs and mine blocks, as well as between processing options and mine destinations. The BZ is a decomposition algorithm which solves an LP relaxation of the RCPSP by dividing the problem into a master problem and a subproblem which are interdependent and communicate with one another. A subset of the constraints in the original problem - considered "complicating constraints" because they cause the problem to become harder to solve – are dualized and penalized (i.e., removed from the constraint set and moved to the objective function objective with an associated penalty) thus defining a new problem in which only less complicating constraints

remain. Said problem is defined in the space of the original decision variables and constitutes the pricing subproblem of the BZ algorithm. Conversely, BZ's master problem is defined on a new space of aggregated variables generated from the solutions of the subproblem - similar to a column generation algorithm, (see Munoz *et al*., 2016) - which the authors define as partitions. Iterations of the BZ algorithm can start from either an initial set of partitions or an initial set of dual vector values. Assuming an initial set of partitions is readily available, a master problem is solved, which is expressed in terms of the individual partitions. Next, a vector of duals associated with said set of hard constraints is used to update the objective function of BZ's pricing subproblem. This is followed by a new iteration of the subproblem which generates a new partition. Importantly, BZ defines the sets of partitions at any iteration to be composed of orthogonal partitions and this requires that a newly obtained solution to the subproblem be made orthogonal with the set of preexisting partitions. The procedure of generating orthogonal partitions out of an initial set of partitions is referred to as partitioning and constitutes a crucial step to be taken before any individual partition is used in the master problem. The authors prove finite convergence and optimality of the BZ algorithm while also reporting solving efficiently very large instances of RCPSP (including millions of variables and tens of millions of constraints) in only a few seconds.

Bley, Boland, Fricke and Froyland (2010) propose a solution methodology for the production scheduling model using cutting planes. An original integer programming (IP) formulation is strengthened by adding inequalities (cuts) derived by combining precedence and capacity constraints to eliminate a substantial number of decision variables from the model as a preprocessing step preceding optimization. Testing suggests that significant reductions in the computation time required to achieve optimal integer solutions can be realized. Unfortunately, the instances tested were relatively small as they contained only a few hundred blocks and 5 to 10 time periods.

Somrit (2011) develops a fast solution methodology to solve the ultimate pit limit problem, maximizing the total dollar value for a given block model of an open pit project. The author presents a method for open pit phase design that follows in the tradition of Lagrangian relaxation methods using subgradient parameterization for long-term open pit mine production scheduling (Dagdelen, 1985; Kawahata, 2006). Similar to Dagdelen and Kawhata earlier, this methodology also encounters the so-called "gap problem." However, the author proposes a method to obtain an

exact solution to the problem when a gap exists. In addition, the author presents a revised maximum flow formulation which is developed to solve each sub-problem with a new open pit mine phase design solution methodology, based on the maximum flow problem proposed by Johnson (1968). Subproblems are solved iteratively to determine individual phases in a "backward" ordering relative to time, i.e., if P represents the set of all phases to be considered, then the first phase to be determined is phase P (the last phase to be mined), followed by phase P-1 (the penultimate phase to be mined), successively until finally the first phase is determined. For all instances studied, results indicate that the revised formulation of the maximum flow problem is much faster than widely used commercial software packages that employ the Lerchs-Grossman (LG) algorithm (Lerchs & Grossman, 1965). The author also proves that optimal solutions to the ultimate pit limit problem are always obtained using the revised maximum flow problem formulation, while some commercial software packages may not.

Cullenbine *et al*. (2011) propose a Sliding Time Window Heuristic (STWH), for problems which include lower bounds on resource constraints. The authors emphasize the significance of including such constraints and demonstrate that their presence can dramatically affect solution times. In each iteration *k* of the STWH algorithm, a sub-problem is formed by partitioning the set of time periods in the horizon (T) into three subsets (windows): $T \equiv \{T_{FIX}^k \cup T_{INT}^k \cup T_{Rlx}^k\}$, within which variables are fixed to integer values ($T_{FIX}^k$), or their integrality is either relaxed ($T_{Rlx}^k$) or enforced ($T_{INT}^k$ ). The algorithm fixes all variables in the first window to feasible integer variables, defines the current second window in which full integrality is enforced and defines the resulting (current) third window in which only a relaxed version of the model is enforced. In each successive iteration, new sub-problems are produced in which a new partition of T is constructed by sliding all three windows to an adjacent set of time periods, and the procedure is repeated. Finally, linking the partial, integer feasible solutions from each sub-problem creates a complete solution. Clearly, the window represented by $T_{INT}^k$ can be enlarged enough so as to encompass the entire set "T" and, in this "trivial" case, the problem resolves to a pure integer programming problem. However, for non-trivial instances, STWH's myopic strategy may not guarantee that an optimal integer solution is always found.

Lambert & Newman (2013) expand the previous work by Cullenbine to solve larger instances of the open pit block sequencing problem than previously possible with the STWH. Their

method employs three methodologies to reduce solution times: (i) eliminate variables which must assume a value of 0 in the optimal solution; (ii) use heuristics to generate an initial integer feasible solution for use by the branch-and-bound algorithm; and (iii) employ Lagrangian relaxation, using information obtained while generating the initial solution to select a dualization scheme for the resource constraints. The combination of these techniques allows for the determination of near-optimal solutions more quickly than solving the original problem. In addition, the method is guaranteed to always find a feasible integer solution. The authors end by demonstrating their techniques on instances containing 25,000 blocks and 10 time periods, and 10,000 blocks and 15 time periods, which are solved to near-optimality.

Munoz *et al*. (2016) study the Lagrangian decomposition algorithm recently developed by Daniel Bienstock and Mark Zuckerberg (2009) for solving the LP relaxation of a class of open pit mine production scheduling problem ($OPMPSP$). The authors show that the algorithm is, in fact, applicable to a broader class of scheduling problems, the Resource Constrained Project Scheduling Problem ($RCPSP$), of which the ($OPMPSP$) is a special case, including multi-model variants of the ($RCPSP$) that consider batch processing jobs. The authors present the BZ in the context of a Delayed Column Generation Algorithm and draw parallels with the Dantzig-Wolfe algorithm (DW). In addition, algorithmic speedups are proposed that can result in increased overall efficiency for the BZ algorithm. The authors run computational experiments and compare the performance of both BZ and DW confirming that, for the problems tested, the BZ outperforms the DW algorithm. Finally, it is shown that algorithmic tuning can improve the performance of the BZ algorithm. Given the relevance of the discussions in Munoz *et al.*, 2016 to the present research, this reference will be revisited in greater detail in Section 8.1.

## 2.3 Production Scheduling Model Based On Block Aggregation Methods

Typically, mathematical formulations of realistic instances of the Open Pit Mine Production Scheduling Problem ($OPMPSP$) require that the variables include a substantial number of integer (binary) variables, which allow for the modeling of features such as (i) blocks being mined fully or not at all, and/or (ii) scheduling "activities" which can only be started once a predecessor activity has been completely fulfilled (e.g., fully finish mining a bench before starting one underneath it). If models include integer-valued variables alone, then they belong to the realm

of integer programing (IP) or, for circumstances in which both linear and integer variables are included, they are considered mixed integer linear programs ($MILP$). Due to the typically large size of mining ore deposits, IP or MILP formulations for ($OPMPSP$) tend to be very large, leading some researchers to explore the possibility of developing block aggregation techniques that have the potential of expediting solutions. While still preserving feasibility, the majority of block aggregation techniques are not guaranteed to achieve proven optimality. Indeed, most block aggregation techniques tend to be both "static" in the sense that, once blocks are initially combined into aggregated units, they remain as part of the same unit throughout the life of the mine, and naïve in the sense that the criteria used to determine how individual blocks are to be aggregated are ignorant (or rather indifferent) to the implications of aggregation to the optimality of the solutions subsequently obtained.

In the context of aggregation techniques, Ramazan (2001) proposes the Fundamental Tree algorithm and models problems with fixed cutoff grades, blending constraints, and production and processing constraints. The model includes lower-bounding constraints on processing although not on production. Ramazan's aggregated "fundamental trees" are built according to three properties: 1) the value of the aggregated blocks is positive, 2) extraction of a Fundamental Tree does not violate allowable pit slopes, and 3) a tree cannot be subdivided into smaller trees that possess properties 1) and 2). The multi-time-period production schedules are generated by a mixed integer linear programming (MILP) formulation using the fundamental trees. The algorithm can generate multiple solutions and, in certain instances, may not produce the true optimal solution. In addition, the case study presented is also relatively small – considering twelve thousand (12,000) blocks which are then reduced to 1,600 trees.

Kawahata (2006) builds on the work pioneered by Dagdelen (1985) and extends it to include dynamic cutoff grade optimization. Additionally, his algorithm addresses multiple destinations, multiple pits, stockpiles and upper and lower bounds on capacity constraints. The author defines two subproblems, such that one represents "aggressive" mine sequencing while the other corresponds to "conservative" mine sequencing. The aggressive sequencing problem consists of mining only the strict minimum volume of waste required to reach the ore in any given bench, while the conservative schedule attempts to mine the totality of the waste present in a given bench. Variable reduction is achieved by applying two Lagrangian relaxation sub-problems, one

for the most aggressive mine sequencing case and the other for the most conservative block sequencing. Although the Lagrangian Relaxation method used constitutes an exact technique, the methodology presented in Kawahata is classified as an aggregation methodology because the algorithm groups blocks on a bench-by-bench basis, seeking to adhere to predefined phases. The algorithm is then implemented in such fashion that optimality of the final schedules generated may not always be guaranteed.

Boland, Dumitrescu, Froyland and Gleixner (2009) develop a model which, the authors state, incorporates cutoff grade optimization, but with no blending constraints and no lower bounds on resource consumption. Their methodology aggregates blocks according to precedence rules to form bins. Bins (sets of blocks) are used to schedule mine production while individual blocks determine processing decisions at the mill. Their aggregation and disaggregation techniques solve large problems (up to 96,821 blocks) in reasonable time (in as little as 420 seconds) since the aggregation of sets of blocks into bins results in a much smaller number of variables. The authors report solving instances of 96,000 and up to 25 time periods in a few hundred seconds. In general, however, the inclusion of lower bounds on resource constraints in the problem formulation can dramatically increase the required solution time for the OPMPSP, so it would be interesting to confirm if the algorithms would still fare as well as it did, had the lower bounding constraints been incorporated.

## 2.4 Production Scheduling Problem Based on Heuristic Methods

Heuristic methods are attractive for their ability to potentially solve large, realistic problems. Unfortunately, these methods are not guaranteed to solve every problem instance to optimality. To be clear, the description of heuristic solution methodologies provided includes many for which key components rely on exact solution methods. In this sense, the only approaches grouped together are those tailored techniques in which the presence of some specific algorithmic feature results in a departure from a strict exact solution method. Some methodologies based on some paradigmatic examples in the literature are presented below:

Gershon (1987) develops a mine scheduling heuristic based on a block's positional weight, "the sum of the ore qualities within the cone generated downward from a block within the ultimate

pit," to determine when a block should be mined. The positional weight of a block defines the desirability of removing that block at a particular point in time such that higher positional weights are more desirable. An accessible block with the highest rank is extracted and then the entire procedure, starting from determining the positional weight of the remaining blocks in the ultimate pit, is conducted again until all the blocks in the ultimate pit have been removed.

Elevli, Dagdelen and Salamon (1989) build an algorithm based on Lagrangian relaxation to improve the NPV of an open pit mine. The algorithm converts production scheduling for a single tonnage constraint into a series of ultimate pit limit problems which can be solved by the LG algorithm. The algorithm improved the cash flows generated compared to previous manual schedules. However, decomposing the original multi-period problem into a series of single-time period problems (solved one at a time) may not generate the optimal production schedule consistently.

Chicoisne *et al*. (2012) propose an algorithm to solve a linear relaxation of the OPMPSP and an LP-based heuristic to obtain integer feasible solutions. The authors use their algorithm to improve on the optimal LP solution obtained in a first stage and generate an integer feasible solution, and discuss the capabilities of alternative heuristic methods which are able to identify a topological ordering (sorting) of the blocks in the mine. These methods are shown to be computationally inexpensive, and, therefore, can be employed effectively to determine an initial feasible integer solution (IFIS). Additionally, the authors discuss a local search heuristic which is able to improve the quality of the incumbent IFIS so that it is very close to optimality, albeit requiring slightly more computational time. Their method is able to solve instances of up to 5 million blocks and 15 time periods. The authors discuss an extension of the algorithm which accommodates two side constraints, although not considering lower bounding constraints.

Lamghari, Dimitrakopoulos and Ferland (2014) propose a two-phase hybrid solution method to the mine production scheduling problem (OPMPSP). The first phase relies on solving a series of linear programming problems to generate an initial solution. In the second phase, a variable neighborhood descent procedure is applied to improve the solution. Upper bounds provided by CPLEX (IBM, 2012) are used to evaluate the efficiency and optimality of the proposed method. Computational experiments show that the method finds excellent solutions (less than 3.2% optimality gap) within a few seconds or up to a few minutes.

# CHAPTER 3.
# GEOSTATISTICAL QUANTIFICATION OF GRADES IN MINERAL RESOURCE MODELS

One of the most challenging tasks facing geologists and engineers alike consists of determining how to address the uncertainty associated with the estimated grades in resource models and the consequent impact such uncertainty has on mine production schedules. In general, this challenge is met by the execution of a sequence of steps beginning with the collection of drillhole samples aimed at providing the largest possible amount of information regarding the orebody's "concentration" of some mineralogical element of interest (e.g., gold, copper or silver). However, due to the typically large dimensions of viable mineral deposits, and the monetary and time expenditures associated with exploration work, actual sampling of the orebody can never be exhaustive. This, in turn, means that given the relatively small number of data samples available at the exploration stage, geologists are forced to contend with imperfect information in building geological models of the mineral deposit. Hence, building such models necessarily entails estimating grades at locations previously not sampled, resulting in a significant degree of uncertainty.

## 3.1 Background Concepts - Statistical Data Analysis in the Earth Sciences

Given the multidisciplinary nature of the research contained in this thesis, it is convenient to revisit and briefly describe a small set of elementary statistical concepts which are relevant to the discussions in the ensuing chapters. Although most of the traditional statistical tools remain applicable, their use within the realm of ore resource estimation requires significant "customization," as well as an adequate theoretical framework capable of providing sound formal support. One important example of the need for customization in ore resource estimation is the prevalence of "clustering," i.e., a tendency for the collected grade samples to be concentrated in specific areas of the orebody rather than uniformly distributed across its extension. This often justifies the fact that traditional central tendency measures such as the arithmetic average produce

very misleading results whenever a prior account of "clustering" is not taken. Likewise, the need to remain within the confines of a sound theoretical foundation is reflected, in practice, in the use of concepts such as "geostatistical domains" which help ensure that important conditions for the validity of geostatistical models are verified. One such condition is the presumption of "stationarity" which is a crucial tenet of the theory of regionalized random variables which undergirds most of geostatistics.

Clustering and consideration for "geostatistical domains" are two significant features of statistical data analysis specific to the earth sciences fields (although others have adopted some of the same concepts). However, the aspect that is likely the most distinctive component of geostatistics and which marks its sharpest boundary with traditional statistics is the nullification of the premise on independence in the data samples. In effect, it is precisely the assumption of *dependence* between (nearby) samples that geostatistical methods seek to exploit and leverage in drawing conclusions about the distribution of grades at locations yet unsampled. This is contrary to the traditional statistical analysis framework in which the premise of "independent, identically distributed" ($iid$) random variables is a central assumption. An additional challenge in ore resource modeling includes the treatment to give to distribution outliers, which typically play a disproportionate role in the economic valuation of the ore deposit.

Finally, introducing these concepts offers two important advantages, namely: contextualizing those discussions in which it is assumed enough geostatistical background exists and improving the clarity and readability of the document.

## 3.2 Data Declustering

Whenever a drilling campaign occurs, it is desirable that standards of accuracy, representativeness, efficiency (non-redundancy of the samples collected) and statistical significance be observed. In the practice of ore resource modeling, these goals are prosecuted concurrently with the need to delimit, as closely and with as much detail as possible, those portions of the deposit in which the highest grades are found. This is an inherent feature of resource estimation, as well as a sensible approach since it is legitimate to concentrate limited exploration resources on those areas of the orebody offering the biggest potential for high economic payoffs,

rather than dispersing them on delineating "barren" sections. However, the emphasis on data collection centered on high-grade domains can lead to a biased set of samples which overrepresents the high-grade sample population, and, as a consequence, may lead to overestimation of the deposit's average grade. This is the reason why traditional univariate summary statistics such as the histogram, mean, median, variance, for example, all lead to flawed outcomes if clustering is not addressed.

A number of different techniques exist which allow the resource modeler to tackle clustering by determining sample weights which permit the declustering of a set of drillhole samples. One such method is the polygonal declustering method (Isaaks & Srivastava, 1989) which assigns each sample with a weight proportional to the area or volume of interest of the respective sample (see Figure 3.1).

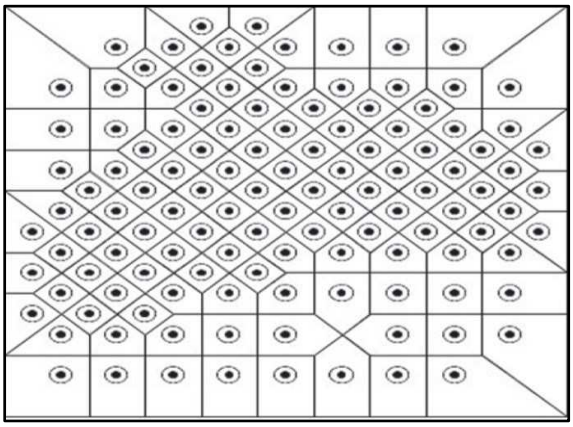

Figure 3.1: Polygonal declustering. Samples and their respective area of influence.

The cell declustering technique (Journel, 1983; Deutsch, 1989) offers a popular alternative to polygonal declustering by accounting for the sampling density inside predefined grid cells (see Figure 3.2).

The method works as follows:

1. Divide the volume of interest into uniform grid cells $k = 1, \ldots, K$
2. Determine the number of occupied cells $K_0$, and the number of data in each occupied cell $n_{k0}$; $k_0 = 1, \ldots, K_0$
3. Weight each data point (inversely) according to the number of data falling in the same cell:

$$w_i = \frac{1}{n_k K_0} \tag{3.1}$$

$$0 \leq \sum_{i=1}^{N} w_i \leq 1 \quad \forall i \tag{3.2}$$

This method is reliant on the specific choice of cell size for the declustering procedure. It is common to experiment with a number of different cell sizes and to choose that which minimizes the declustered weighted average.

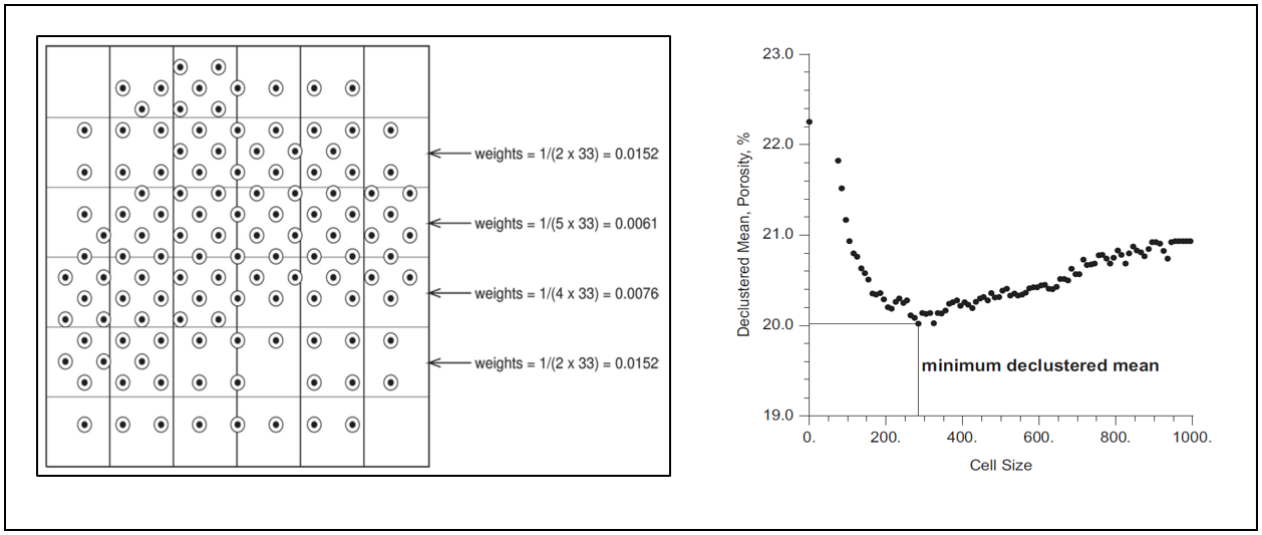


Figure 3.2: Cell declustering method illustration. On the right, declustered weights for a specific cell size; on the left, plot of cell size vs. declustered mean (Rossi & Deutsch, 2014)

Owing to its ease of application, cell declustering by the nearest neighbor technique is also very popular although the specifics of its implementation are not discussed in the present thesis.

## 3.3 Graphical Methods - Scatterplots

Best practice in the context of reserve estimation recommends that all consequential geostatistical analysis be preceded by detailed exploratory data analysis (EDA) studies covering most of the univariate central tendency statistics, as well as common distribution dispersion measures. These tools do not obviate, however, the need for a sound geological knowledge of the deposit and its combination with the extensive use of adequate graphical or "visualization"

statistical tools. Among others, such tools include so-called "indicator maps," moving window statistics, contour and symbol maps, but also, crucially, the scatterplot. These are important bivariate statistical tools which allow for visualizing the strength of the relationship between two random variables but, perhaps more importantly in the context of geostatistics, they facilitate the detection of anomalies and clusters in the data. The dots on a scatterplot correspond to (x, y) pairs in which each of the coordinates is associated with one of the variables (see Figure 3.3). On the left of said figure, points that fall in quadrants I and III make the correlation negative, while quadrants II and IV make it positive. In the center, uncorrelated data show strong relationship due to outliers of estimates. On the right, strongly correlated data show low correlation due to outlier data Also, the strength of the relationship between the variables, as measured by the correlation coefficient, is very sensitive to aberrant data, increasing the importance of being able to visualize the data and checking that correlation values are not unduly influenced by a small set of data values which depart markedly from the general trend in the sample set.

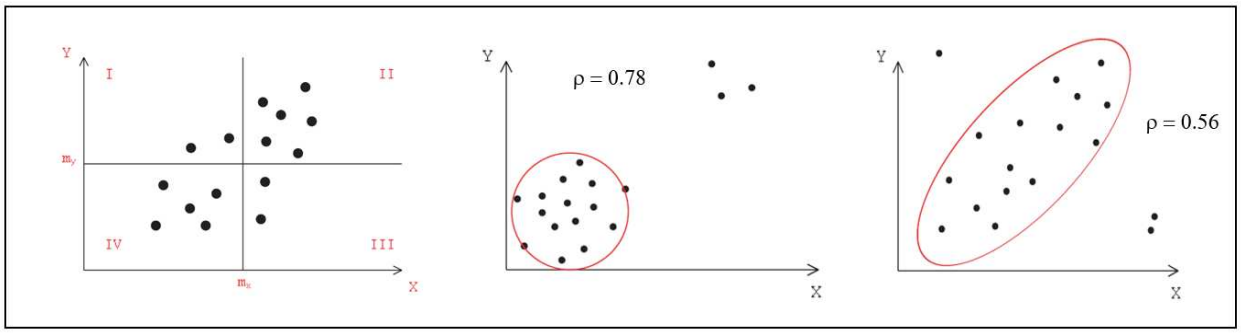


Figure 3.3: Scatterplots highlighting the impact of outlier data to the strength of the correlation coefficient. (Rossi & Deutsch, 2014).

Importantly, scatterplots also denounce the mixing of more than one statistical population in the data set. This is usually viewed in the form of separate clusters on the graphs; and it is important that these have a concrete physical justification, for example, combining more than one geostatistical domain or data originating from different deposits, among others. For instance, Figure 3.4 shows the existence of two distinct populations whose nature of association is also different.

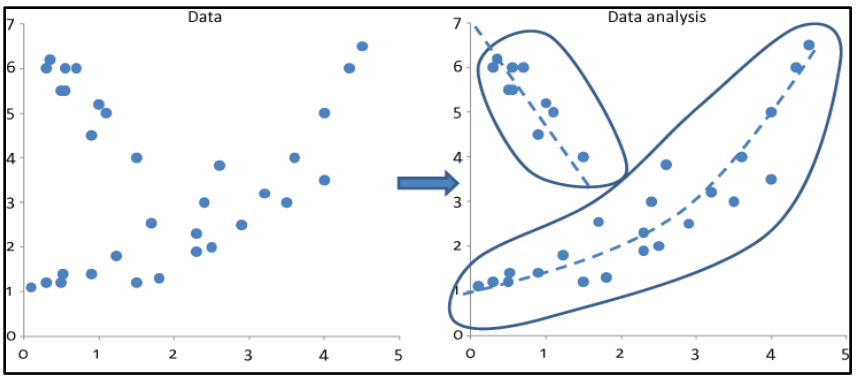


Figure 3.4: Scatterplots. Bivariate data set showing two distinct populations (Caers, 2011).

## 3.4 Measuring Spatial Continuity – Correlograms, Covariograms and Variograms

The concept of spatial continuity is central to geostatistics. In essence, it establishes that all else being equal, data samples that are closer in space tend to have characteristics which are more similar than samples further apart in space. The singular exception being when there exist directions of major and minor geological continuity. The principle of spatial continuity incorporates the existence of strong geological continuity in most ore deposits. This results from the specific nature of the geological processes responsible for the genesis of most ore deposits, and which impart on them physical patterns which allow for reasonable continuity in space, and consequently, increased predictability as well (Isaaks & Srivastava, 1989). For instance, a sedimentary deposit will tend to display greater geologic (spatial) continuity along the direction of its depositional layers, and much smaller continuity (greater variability) across the said layers (see Figure 3.5).

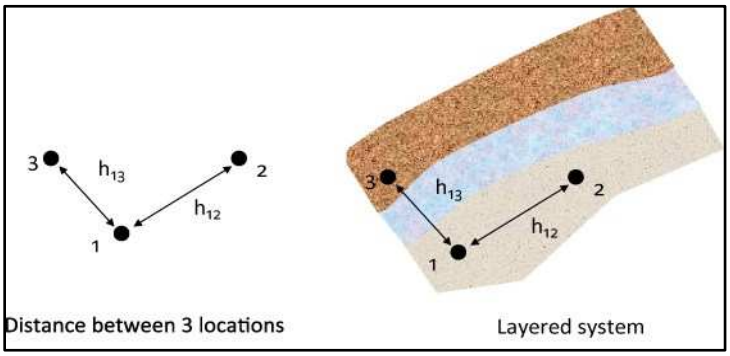


Figure 3.5: Euclidean distance vs. statistical distance. (Caers, 2011).

This implies that in the context of geostatistical data analysis the Euclidean distance differs from the "statistical distance," and, in fact, given the prevailing direction of major continuity, samples aligned along this direction such as samples 1 and 2 in Figure 3.5 might be more closely related than samples aligned in its transversal direction (e.g., samples 1 and 3), despite the latter being further apart physically than the former.

Perhaps the most relevant application of scatterplots in geostatistics is in the form of so-called "h-scatterplots." Considering that "u" stands for a location in space, an h-scatterplot gives a measure of the association between two samples which are "$h$" (distance units) apart: $y(u)$ and $y(u+h)$, respectively.

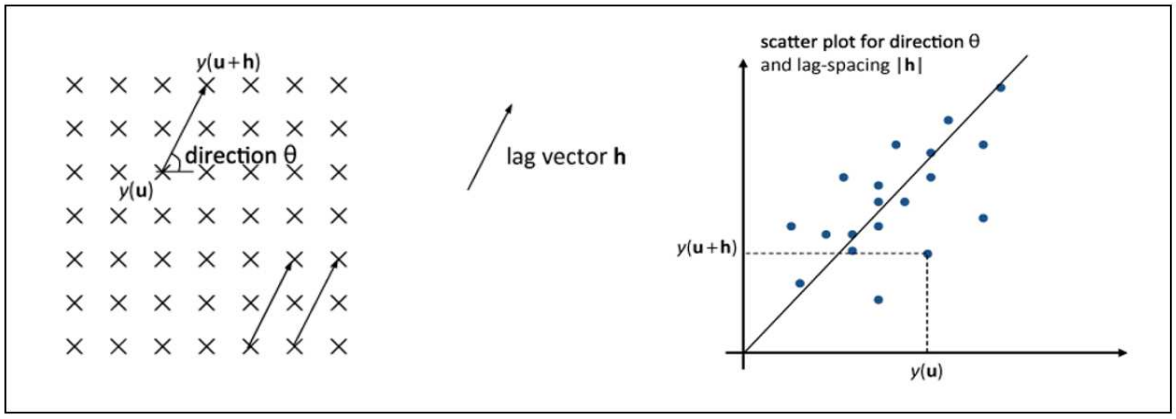


Figure 3.6: H-Scatterplots. On the left, pairing of the data points based on separation (lag) distance "h" and direction Θ. On the right the corresponding h-scatterplot. (Caers, 2011)

H-scatterplots are generated from pairing all the data points which are separated by some lag distance "h" along a certain direction. If, for a given predetermined direction and separation distance, the correlation coefficient ($\rho(h)$) associated to the pairs of data is calculated, then, since the association between points decreases as they become further apart, so too do the respective values of $\rho(h)$. For any direction of choice Θ it is thus possible to plot the value of $\rho(h)$ vs lag distance. Such a graphical display has the advantage of communicating the strength of the association between the variables *across* space and is known as the correlogram or autocorrelation plot (see Figure 3.7).

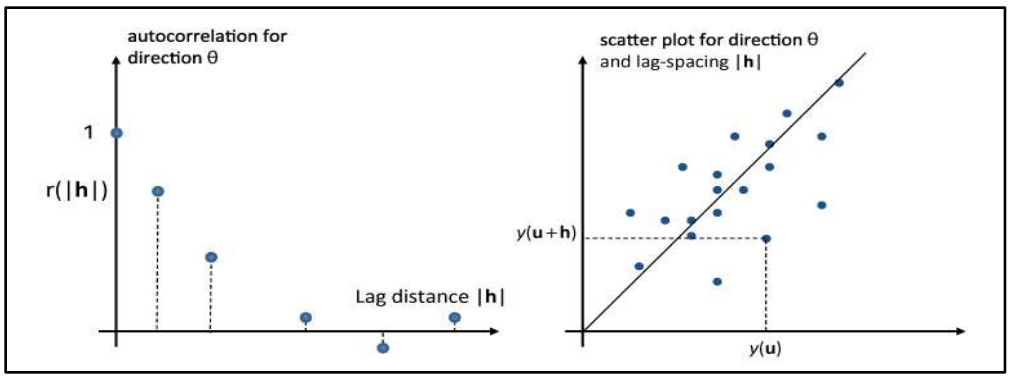

Figure 3.7: Correlograms. On the left each data point corresponds to a (h,ρ(h)) pair. (Caers, 2011).

The correlogram is calculated as:

$$\rho(h) = \frac{E[(Z(u) - m)(Z(u+h) - m)]}{Var(Z)} \tag{3.3}$$

$$m = E[Z(u+h)] = E[Z(u)] \tag{3.4}$$

Correlograms provide a measure of spatial continuity, i.e., a measure of the statistical similarity between nearby data samples as their separation distance increases. Clearly, an identical similarity measure can be generated by calculating covariance values for the set of data points, rather than correlation values $\rho(h)$, and plotting them against lag distance values $h$. In such cases, the spatial statistic generated is called a covariogram $C(h)$.

The covariogram is calculated as:

$$C(h) = \rho(h) * Var(Z) = E[(Z(u) - m)(Z(u+h) - m)] \tag{3.5}$$

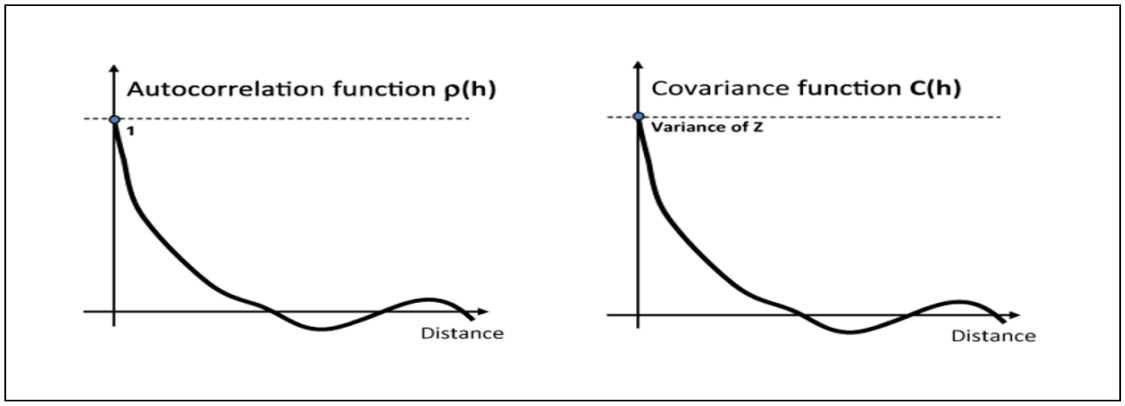

Figure 3.8: Correlogram (autocorrelation function) versus covariogram (covariance function). (Caers, 2011).

Traditionally, and for historical reasons, it is a measure of *dissimilarity*, related to both the correlogram and the covariogram, that has enjoyed the most popularity within geostatistics: the variogram. This statistic in constructed similarly to the other two measures referenced, with the main difference being that at each lag distance (for some predefined direction) it is the spread ("fatness") of the cloud of points about the 45-degree line that is measured.

The variogram is calculated as:

$$\gamma(h) = \frac{1}{2}E[(Z(u) - Z(u+h))^2] \tag{3.6}$$

Also, there exists a clear relationship between the covariogram and the variogram, defined as:

$$\gamma(h) = Var(Z) - C(h) \tag{3.7}$$

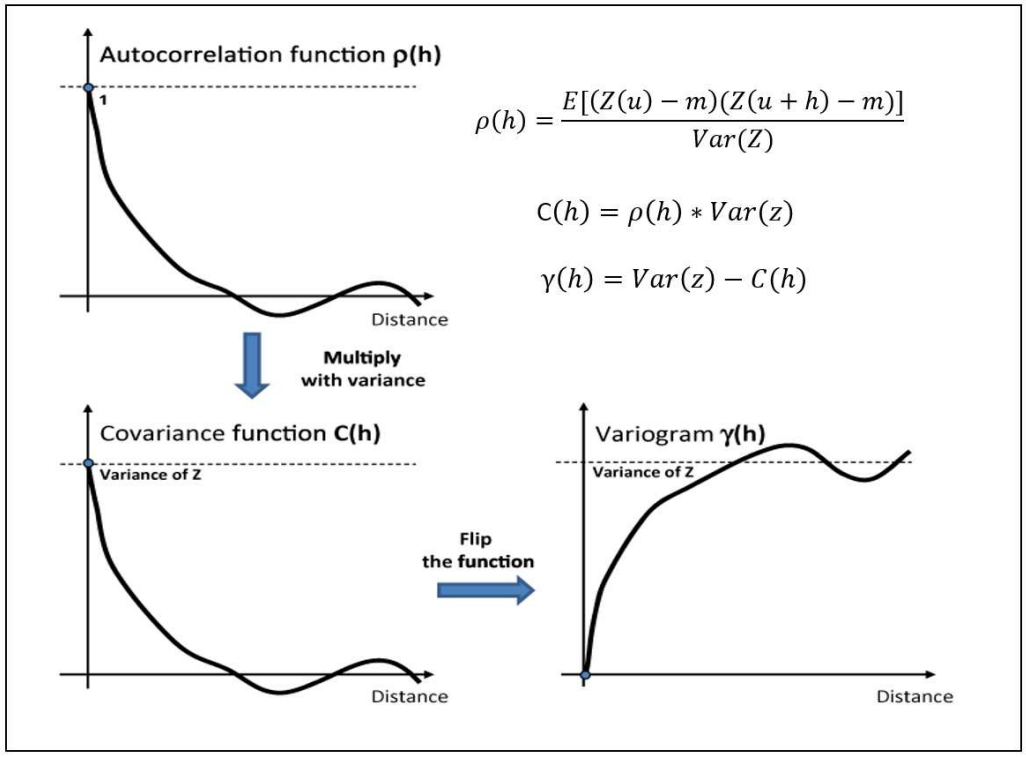


Figure 3.9: Relationship between correlogram, covariogram and variogram functions (Caers, 2011).

The main components of the variogram are its nugget effect, sill and range (Figure 3.10):

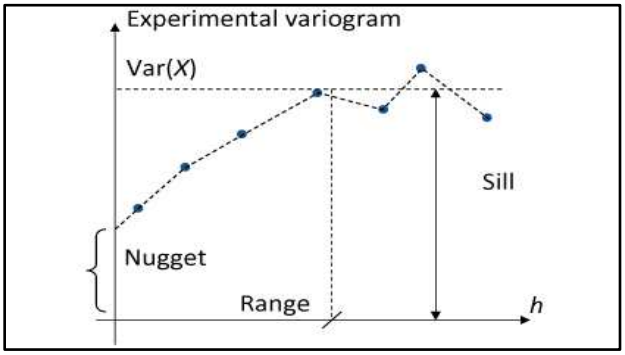


Figure 3.10: Variograms. Major components of experimental variograms (Caers, 2011).

Historically the term nugget effect refers to the small scale variability observed in gold mines when a sample contains a gold nugget but, this may also be due to a multitude of causes, including possible error ("noise") in the sampling instruments. The sill constitutes a plateau in which the variogram values tend to level off. It often equals the overall population variance. The range corresponds to the separation distance about which the variogram reaches the sill, and beyond which samples are no longer spatially correlated (Figure 3.11).

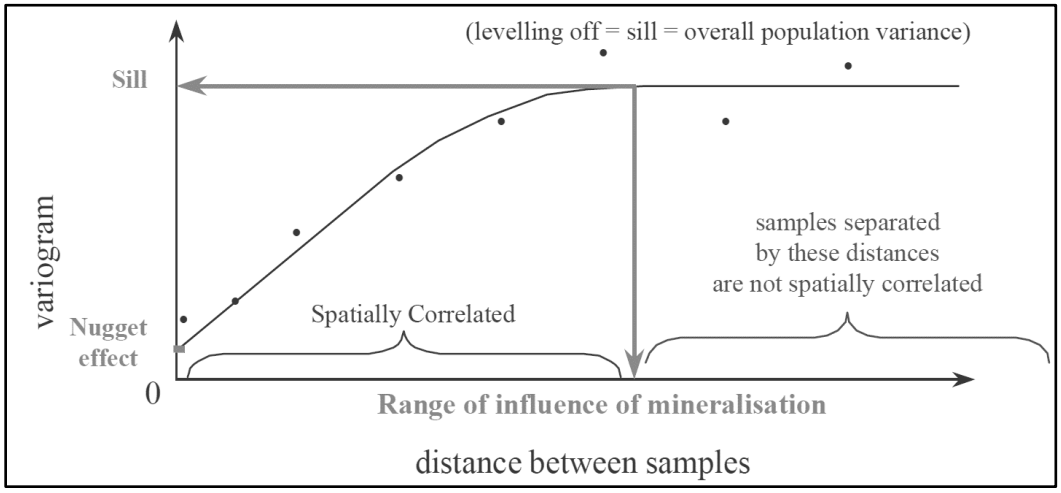


Figure 3.11: Experimental variogram values together with fitted spherical model (Snowden, 2000).

In practice, it is always necessary to fit a mathematical model to experimental variograms in order to allow for inferences at separation distances for which no variogram values are available.

## 3.5 Estimation Criteria

For clarity of exposition, it is convenient to discuss in advance of describing the strengths and weaknesses of kriging, how to decide on the performance of a given estimation method. In what follows, we borrow from the discussion found in Isaaks & Srivastava (1989). It is natural to expect an estimation method to be considered adequate if the estimates it produces ($\hat{v}$) are generally very close to the true grade values ($v$) at the locations studied. Also, in the event that the predictions generated deviate from true grade values, it is desirable that they be: (i) as small as possible and (ii) on average, the number of overestimates be approximately equal to the number of underestimates (unbiasedness condition). Often, the deviations between true and estimated grades at a given location are referred to as "residuals" in the geostatistical literature and are defined as:

$$r = \hat{v} - v \tag{3.8}$$

Hence, positive values for "$r$" represent overestimation while negative values for "$r$" represent underestimation. To aid in the assessment of the efficacy of estimation methods traditional univariate and bivariate statistical tools are mobilized, and typically include histograms of the calculated "residual" values and scatterplots of estimated vs true grades. The distribution of residuals should be centered about a mean value of "$m = 0$" so that no clear estimations bias can be evidenced.

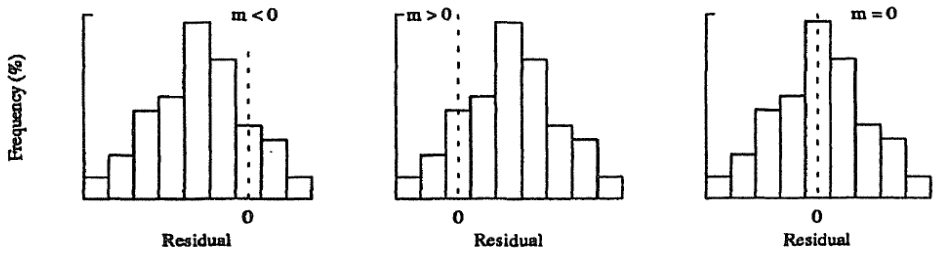


Figure 3.12: Hypothetical distributions of residuals. On the left, the mean of the distribution of residuals is negative which indicates an underestimation bias. On the right, a positive mean indicates an overestimation bias and, in the center, no indication of bias exists.

Analysis of the mean of the distribution might be complemented by the inspection of other measures of central tendency, such as the median and the mode. That is because when a mean

value equals 0, it can easily be the result of a very large number of small underestimates being balanced by a small number of very large overestimates, or vice-versa. This results in skewed distributions of residuals similar to those shown in Figure 3.13 (left). It is desirable, however, that the shape of the distribution be approximately symmetric, signifying that not only the proportion of underestimates and overestimates balance out, but also that the magnitude of said deviations is also fairly similar. Such an ideal is closer to being met when the mean, median and mode of the distribution all coincide at 0.


Figure 3.13: Two different distributions of residuals. On the left, the distribution is (positively) skewed indicating the magnitude of overestimates is significantly larger than that of the underestimates. On the right, an almost-symmetric distribution indicates similar magnitudes of underestimates and overestimates.

An equally desirable feature of the residuals distribution is that it have the smallest possible spread. This gives a measure of how large is the range of values across which the deviations span. Evidently, the variability of the residuals can be adequately quantified by the variance (or standard deviation) statistic.

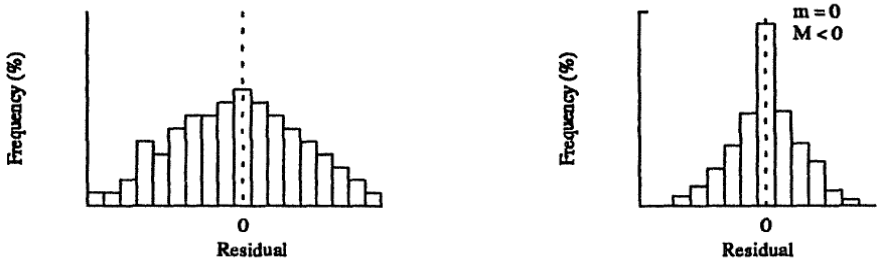


Figure 3.14: Spread of two different distributions of residuals. The variance of the distribution is greater for the one on the left than it is for one on the right.

In addition to analyzing the center and spread of the distribution in its entirety, it is important to also investigate the performance of a given estimator when only specific segments of the full spectrum of estimates are considered. In most ore deposits, for example, it is common that the variance of the population of high-grade samples be much higher than the variance of low-grade samples ("proportional effect"), and this might reasonably be expected to influence the quality of the estimates made. By subdividing the set of estimates into two subgroups: high-grade and low-grade ore, it is possible to check for the existence of any bias in each of the individual subgroups and, if such a bias exists, it is said that the estimator is "conditionally biased" (the "condition" being the cutoff threshold chosen).

Conditional bias can be checked by generating scatterplots of estimated grades versus estimation errors. In Figure 3.15, examples of such scatterplots are shown illustrating the differences in the estimation performance for two different sets of estimates:

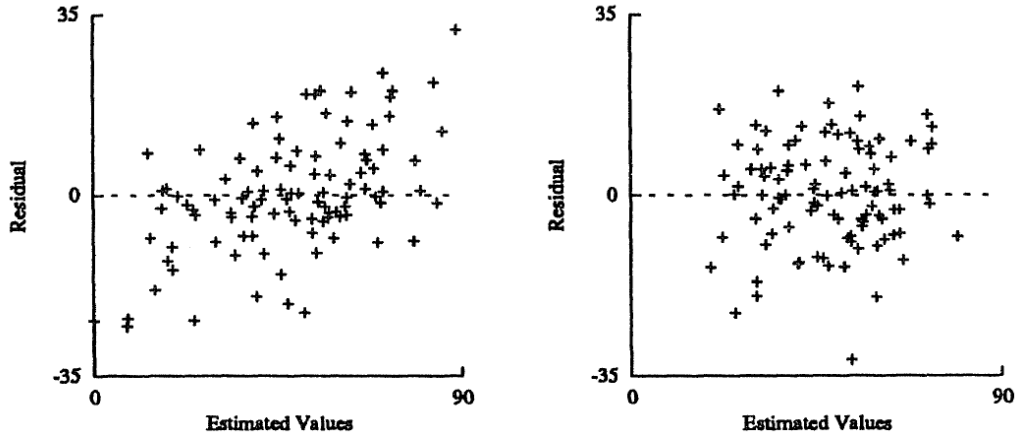


Figure 3.15: Conditional bias. On the left, a clear tendency for overestimation of high grades and underestimation of lower exists. On the right, the propensity for underestimation or overestimation is essentially the same, regardless of grade range under consideration.

In the case of the scatterplot on the right, it is possible to choose any range of grades for inspection and the estimation remains unbiased, i.e., the proportion of underestimates and overestimates approximately compensate each other, meaning that the estimation processes is conditionally unbiased. Also, if the full spectrum of possible grades is inspected as a single unit, the same conclusion is reached, meaning that the estimation processes is also globally unbiased. By the same argument, it can be seen that in the case of the scatterplot on the left, the estimation

process is conditionally biased despite being globally unbiased (see Figure 3.15, left). Finally, scatterplots of true vs estimated grades can be informative of the quality of the estimation by showing the extent to which the cloud of plotted points cluster close to the diagonal 45-degree line passing through the origin (see Figure 3.16).

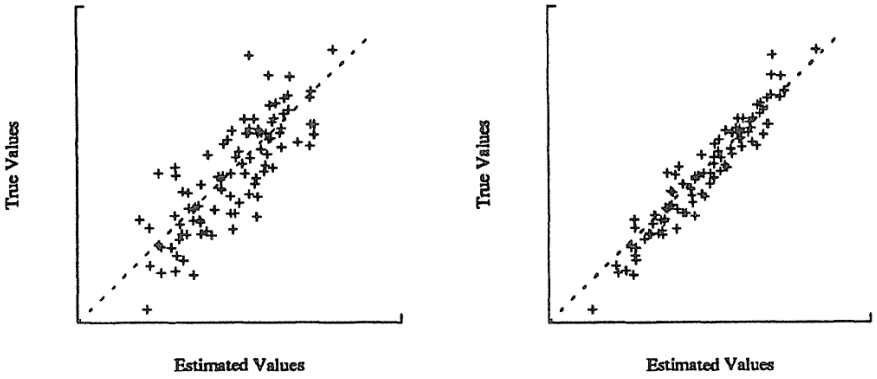


Figure 3.16: Scatterplots of estimated vs. true values, can provide a good sense of the quality of the estimation process.

The diagonal 45-degree line represents the ideal of perfect estimation (true grades = estimated grades) which is unattainable in practice. Nonetheless, the closer the cloud of points is to it, the better the quality of the estimates. Figure 3.17 concludes the discussion regarding the basic criteria underlying judgments on the quality of estimation, by conveying the sense in which the concepts of accuracy and precision are understood in the context of mineral ore reserve estimation.

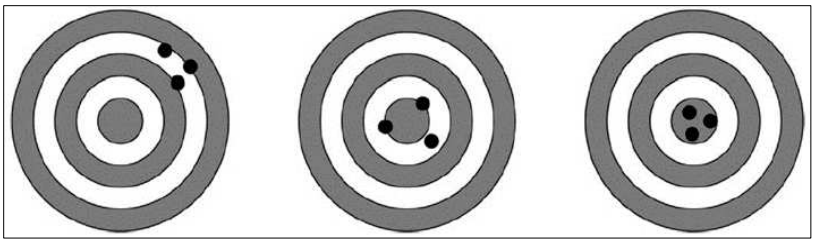

Figure 3.17: Accuracy and precision. Left is precise but inaccurate; center is accurate but imprecise, and right is both precise and accurate.

Aiming at generating probability distributions of residuals centered about zero is a proxy for accuracy in the same way as aiming at minimizing their spread is a proxy for precision.

The discussion of estimation criteria, specifically, the geostatistical meaning of accuracy and unbiasedness, are important to developing an understanding of the popularity and dissemination of the kriging estimation technique. This is will be the subject of the next Section.

## 3.6 Geostatistical Kriging

Geostatistical kriging is a linear interpolation technique first introduced by Danie Krige, who developed the technique while doing ore reserve estimation work in South African gold mines (Krige, 1953). Despite arising initially from empirical experimentation and analytical intuition, kriging was later shown to have a strong theoretical foundation (Matheron, 1971). The method consists of a convex weighted linear combination of the sample data surrounding the location to be estimated within some specified neighborhood. The kriging estimator is formally derived from a constrained optimization problem in which the variance of the estimation residuals is minimized, subject to an unbiasedness condition which translates to the kriging weights adding to one (Isaaks & Srivastava, 1989). In particular, this means that no other set of weights will provide a lower estimation variance than those of kriging. In some contexts, the choice of "minimization of variance" as a criteria can be contested as a wrong optimization criterion (Isaaks, 1987) however, in so far as the choice is made, it partially provides the sense in which kriging is considered the "best linear unbiased estimator."

Using traditional geostatistical terminology some variable definitions are as follows:

$Z(x_i) - value\ of\ the\ random\ variable\ of\ interest\ at\ sample\ location\ x_i$

$\hat{Z}(x_0) - estimate\ of\ the\ random\ variable\ of\ interest\ at\ estimation\ location\ x_0$

$$\hat{Z}(x_0) = \sum_{i=1}^{n} w_i\, Z(x_i) \tag{3.9}$$

$w_i - kriging\ weight\ assigned\ to\ sample\ x_i$
$\mu - Lagrange\ parameter$
$C - Covariance\ matrix\ containing\ the\ cross - variance\ values\ between\ all\ the\ samples\ c_{ij}$
$D - Covariance\ matrix\ between\ individual\ samples\ and\ the\ estimation\ location$

In kriging, the available samples are used in a weighted linear combination to form the estimate. It can be formally shown that the set of (positive valued) weights that minimize the error variance while adding to 1 (satisfying the unbiasedness condition) must satisfy the following set of equations:

$$\sum_{j=1}^{n} w_j C_{ij} + \mu = C_{i0} \qquad \forall\, i = 1, \ldots, n \tag{3.10}$$

$$\sum_{i=1}^{n} w_j = 1 \tag{3.11}$$

This same system of equations is written in matrix notation as:

$$C * W = D \tag{3.12}$$

$$\begin{bmatrix} C_{11} & \cdots & C_{1n} & 1 \\ \vdots & \ddots & \vdots & \vdots \\ C_{n1} & \cdots & C_{nn} & 1 \\ 1 & \cdots & 1 & 0 \end{bmatrix} \begin{bmatrix} w \\ \vdots \\ w_n \\ \mu \end{bmatrix} = \begin{bmatrix} C_{10} \\ \vdots \\ C_{n0} \\ 1 \end{bmatrix} \tag{3.13}$$

It is straightforward to solve for the kriging weights:

$$W = C^{-1} D \tag{3.14}$$

The kriging weights rely on a statistical measure quantifying the spatial interrelation between the samples themselves and between the samples and the unsampled location. This can be provided by, among others, a variogram, covariogram or correlogram function (see discussion in Section 3.4).

### 3.6.1 Small Numerical Example of Estimation by Kriging

In what follows, we draw from the discussions in Hoffman (2014) and provide a succinct description of the (ordinary) kriging estimation which likely helps clarify some of the concepts explored in the prior sections. The algorithm starts with an initial set of measurements of the value of some property of interest (e.g., gold concentration or reservoir porosity) $z_i$ at three locations; and the estimation goal is to determine the value of the same property $z_0$ at unsampled location $x_0$ (represented as a question mark in Figure 3.18).

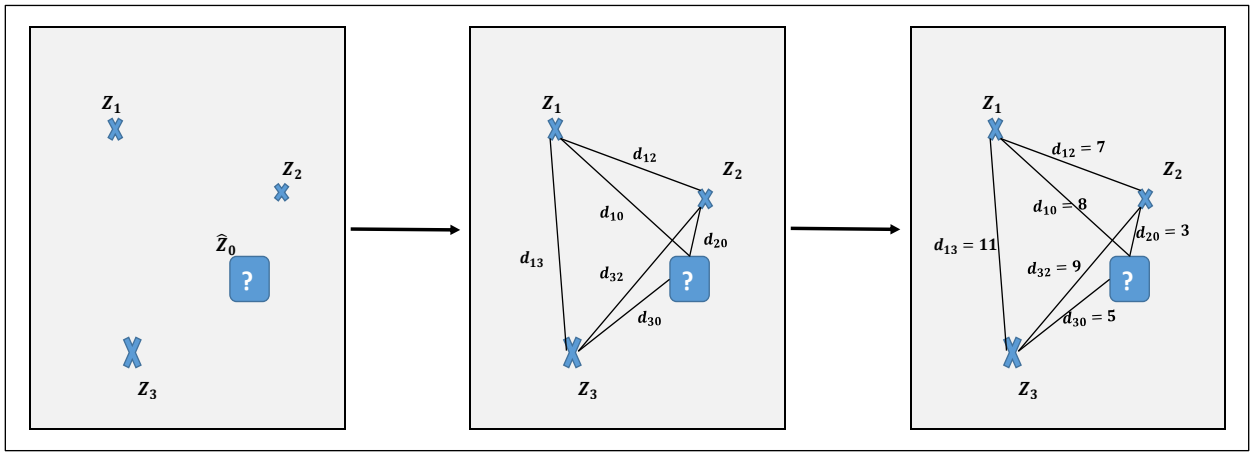


Figure 3.18: Initial set of three sampled locations and the desired estimation location $x_0$ (represented by the blue square with an interrogation mark).

STEP 1

- Calculate the distances between the individual samples themselves $d_{ij}$ and, the distance between each sample and the estimation location $d_{i0}$. Next, store said values in matrices $D_{ij}$ and $D_{i0}$, respectively.

STEP 2

- Determine a spatial continuity function: correlogram, covariogram or variogram function, relating Euclidean separation distances to the degree of (statistical) spatial continuity in the deposit. Recall that kriging takes into account "geological distance" which means that samples which are geologically closer (similar) get larger weights. Likewise, redundant or geologically distant (dissimilar) data get smaller weights (Figure 3.19).

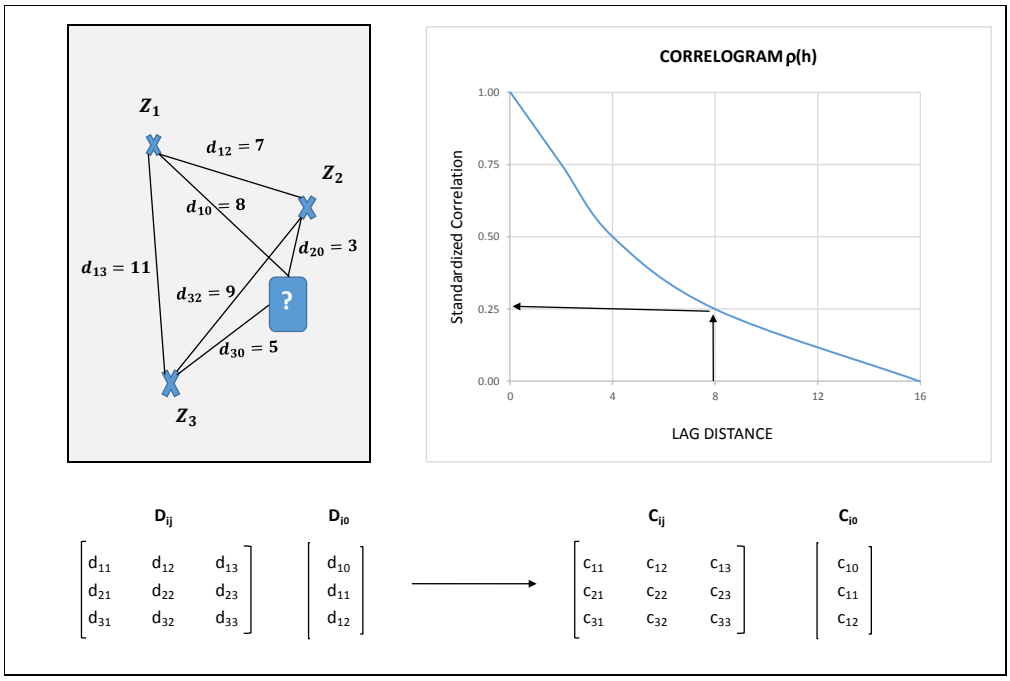


Figure 3.19: Set up of distance matrices and determine the spatial continuity function to use (the correlogram function is shown in the example).

Next, convert distance values $d_{ij}$ and $d_{i0}$, into correlogram values $c_{ij}$ and $c_{i0}$ (Figure 3.20):

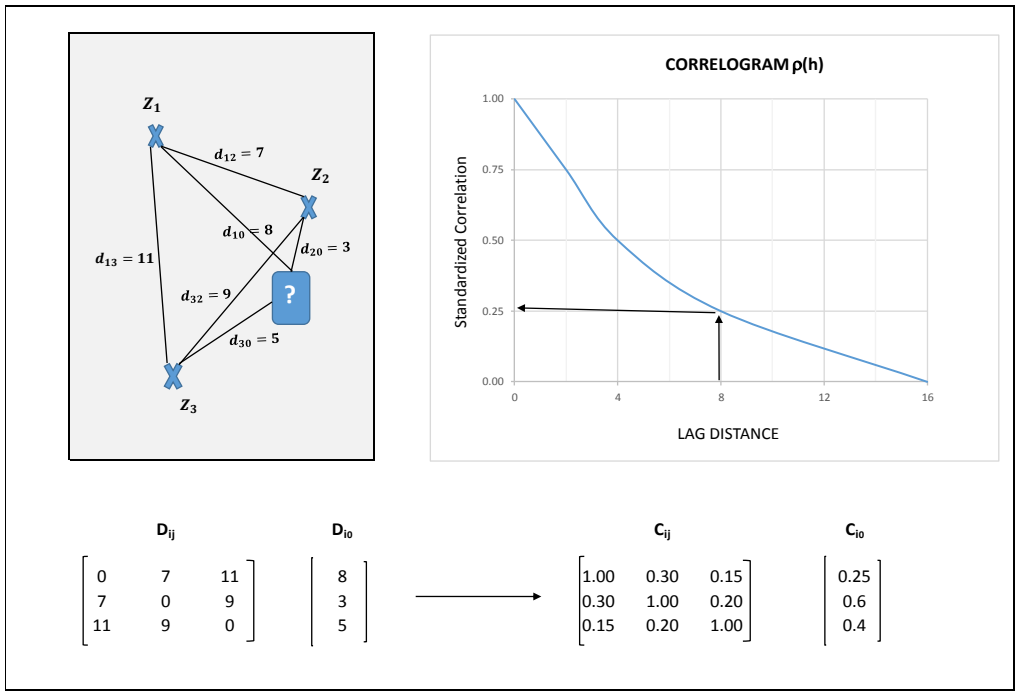


Figure 3.20: Conversion of Euclidean distances into correlogram values. The value $d_{i0} = 8$ corresponds to $c_{i0} = 0.25$.

STEP 3

- Set up the kriging system of equations and solve for the vector of weights $w_i$ (Figure 3.21)

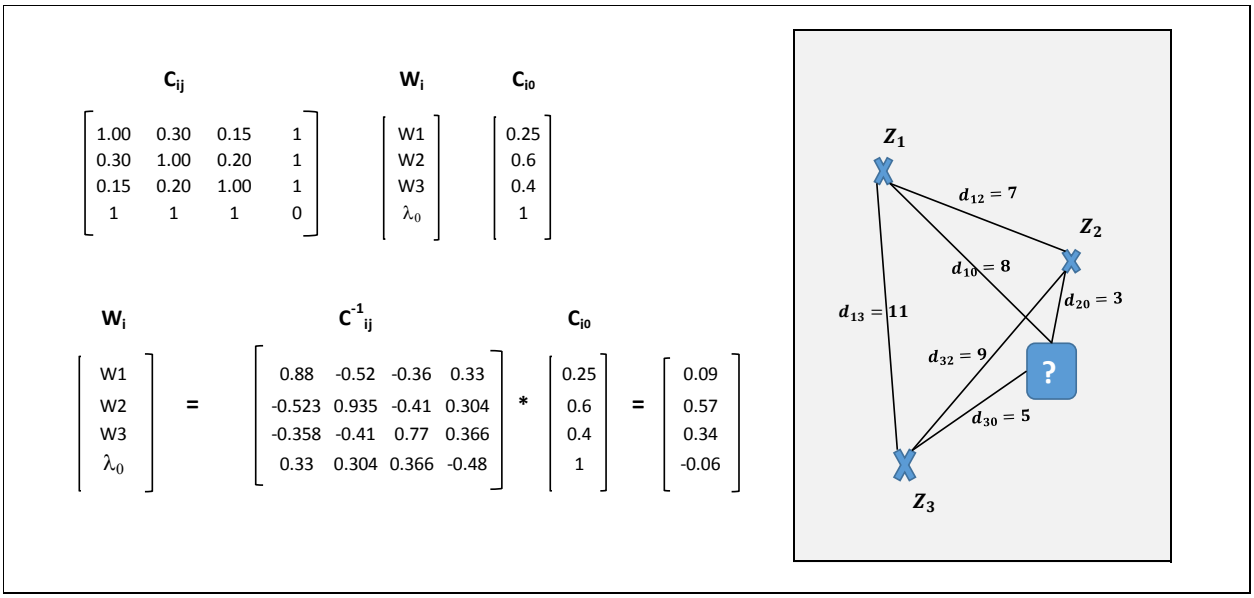


Figure 3.21: The ordinary kriging system of equations.

STEP 4

- Calculate the kriging estimate at unsampled location $\hat{z}(x_0)$ and the kriging variance $\sigma_{ok}^2$

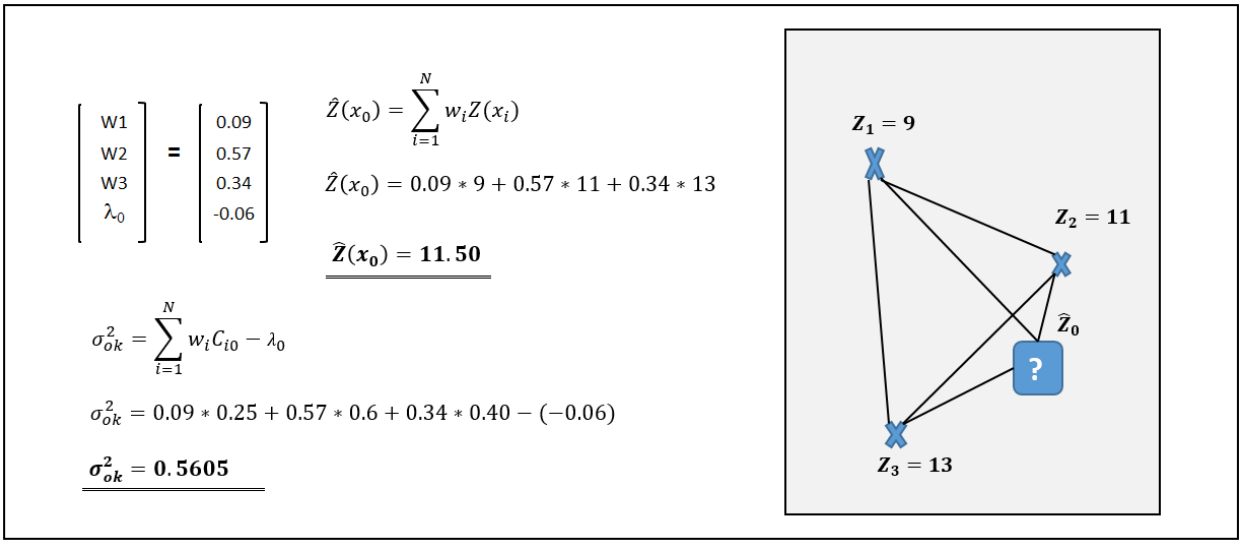


Figure 3.22: Calculating the kriging estimate and corresponding kriging variance.

### 3.6.2 Limitations of the Kriging Estimator

The advent of ever more powerful computers made it possible for kriging to enjoy great popularity in the field of geostatistical resource estimation. However, the method has well-known limitations, one of which being its "smoothing effect." Smoothing occurs because of three key aspects of the kriging estimator, namely: (i) the kriging weights are all positive, (ii) the kriging weights must add to one, and finally, (iii) a linear relationship is assumed between the value to be estimated at a given unknown location, and the known surrounding data. The combined effect of these features leads to estimated values at unsampled locations not reproducing the extreme values (high or low) in the dataset, as they tend to fall somewhere close to the center of the range (spectrum) of sampled values. Alternatively, kriging estimation can be thought of as attempting to approximate a non-linear "grade surface" by a linear interpolation method. This results in kriging's inability to adequately characterize the full spatial variability of the grade distribution in a given deposit (see Figure 3.23 below).

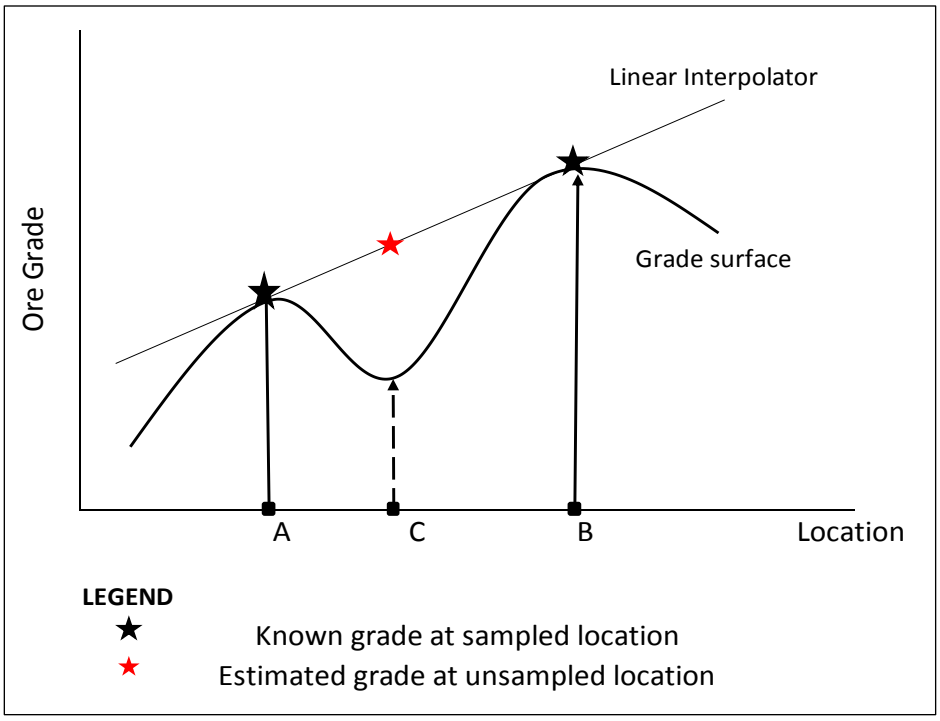


Figure 3.23: Linear interpolation principle underlying kriging. Applying any convex linear estimator to estimate the grade value at location "C" $g_c$ from known locations "A" and "B" will produce an estimate located somewhere in the line segment connecting the grade values at "A" and "B," $g_a$ and $g_b$ respectively. By construction, $g_c$ will not be lower than $g_a$ or higher than $g_b$.

One important reason why Kriging's inability to capture the deposit's variability is consequential is the fact that it could lead to significant misclassification of the material into ore and waste categories at the mine planning stage. In the context of mine planning it is common to define one (or more) operating cutoff grades, below which the total metal contained in the material to be mined is too small to justify the cost of its extraction. The decision on how to classify rock material (e.g., ore or waste), and thus the decision on whether or not to extract and process rock material is contingent on how estimated (rather than true) block grades compare to such predetermined cutoff grades. Rock material with an estimated grade above a specific cutoff grade is classified as ore and potentially mined and sent to the mill plant for processing whereas material below the cutoff grade is (ideally) not mined or, if mined, then sent to a waste dump destination.

Within the realm of geostatistics and ore resource estimation, the challenges posed by incomplete information and its subsequent impact on kriging estimates are commonly represented in the form of schematic "material classification diagrams" such as the one presented in Figure 3.24.

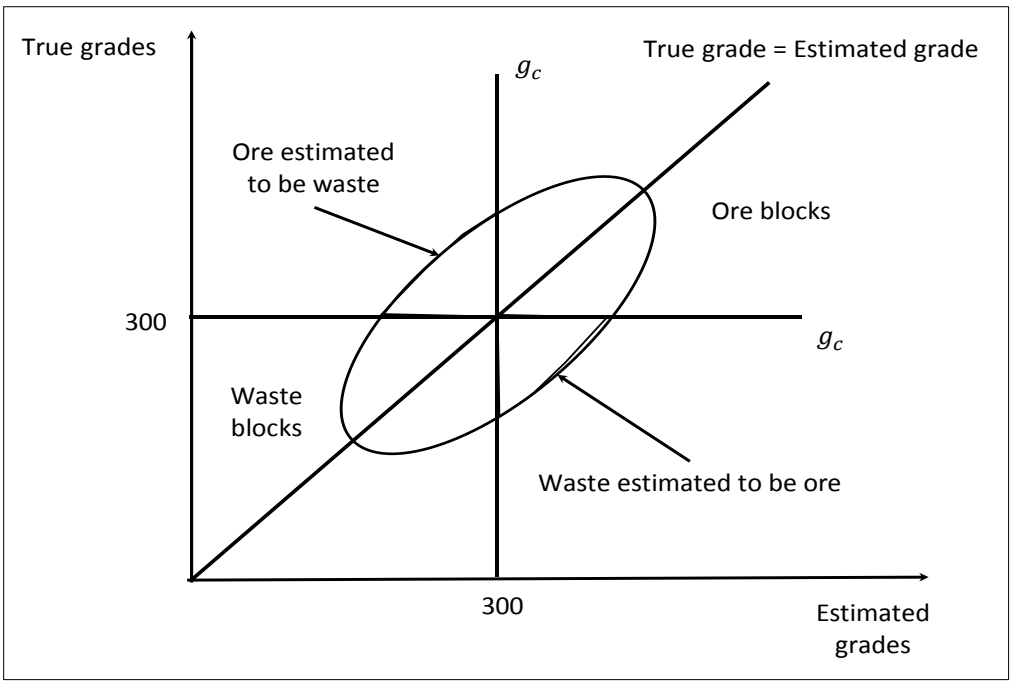


Figure 3.24: Material classification diagram showing possible misclassification due to selection based on estimated, rather than true, values. Misclassification occurs in the upper left and lower right quadrants. All other quadrants represent locations correctly classified, despite the classification not being perfect.

Graphically, the figure reflects a hypothetical scenario in which for every spatial location under study, both true and estimated grades are available. Each point in the graph corresponds to a physical location in the deposit which has as its coordinates (x, y) = (estimated grade, true grade). Also, an example cutoff grade (300 in the present case) is defined, together with the 45-degree line intersecting the origin which represents the unattainable case of perfect estimation (estimated grade = true grade).

Misclassification is said to occur in two distinct circumstances: in the first case, the predicted grade at location $u(x, y, z)$ is smaller than the mining threshold (cutoff grade) while the actual true grade at said location is greater than the threshold. Such occurrences are depicted in the upper left quadrant of the graph and configure what the statistical literature calls "false positive" errors. The second case of misclassification is also formally referred to as "false negative" error and corresponds to occurrences in which, for a given location, the estimated grade is greater than the threshold while the actual true grade is not. Likewise, it is common to construct "loss-functions" that assign penalties to the deviations between estimated and true grades; and to illustrate schematically the influence of imperfect selection on the economic performance of operating mines in the form of graphs such as presented in Figure 3.25 below (Isaaks & Srivastava, 1989; Rossi & Deutsch, 2014):

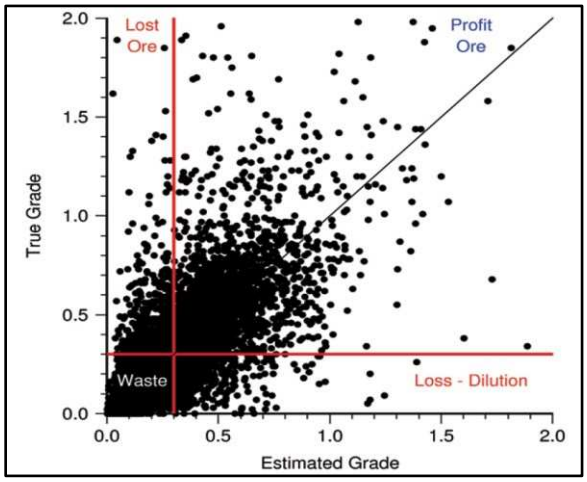


Figure 3.25: Scatterplot of material misclassification showing hypothetical true vs estimated SMU values (Rossi & Deutsch, 2014).

From a mining perspective, portions of the deposit associated with the occurrence of false positive errors are mined when they should not have been; areas corresponding to false negative errors will be left unmined when they should, in fact, have been.

The challenges with misclassification resulting from the smoothing effects of kriging are compounded by a different, though related, aspect of geostatistical ore resource estimation: the "support effect." When making technical and operational decisions or, when reporting ore resources and reserves, mine planners need to consider the scale (or "support") in terms of volume or tonnage at which the grade estimates are made. For instance, operational mining decisions cannot be based on grade estimates made at the scale of composited drillhole samples because one cannot realistically mine at the degree of selectivity represented by such "point estimates." It is thus necessary to define a selective mining unit (SMU), which corresponds to some compromise between factors such as: the expected bench height, the equipment dimensions or the expected ore dilution, and which better corresponds to the true scale at which mining is expected to occur. Since the volumes associated with SMUs are typically much larger than those of drillhole samples, it is natural that a significant degree of "averaging" of extremely low (as well as extremely high) grades take place, leading to a distribution of SMU grades which underrepresents these categories of the original (point-scale) drillhole distribution (see Figure 3.26).

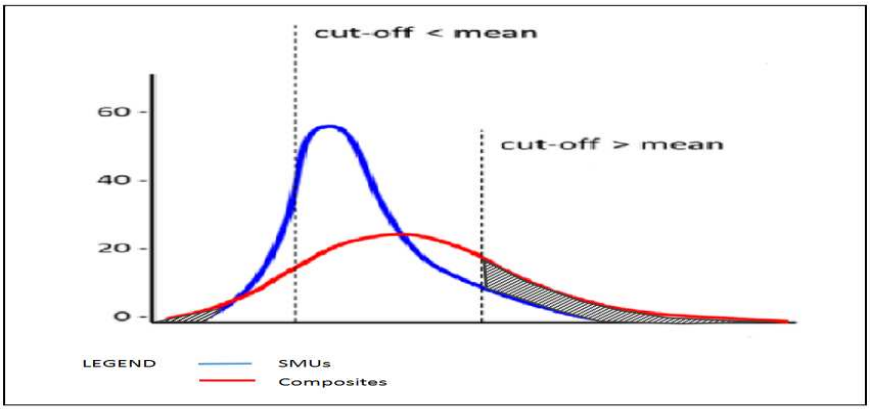


Figure 3.26: Grade distribution of SMUs vs. the grade distribution of composites. Shaded areas represent the proportion of rock material in the extremities (both top and low) of the original composites distribution which is absent from the SMU distribution, (as it "migrates" towards its center).

If the level at which a cutoff grade is placed corresponds to a very high or very low quantile in the grade probability distribution function (pdf), then the smoothing characteristics of the kriging estimator can be particularly impactful, possibly leading to a significant underestimation of both the proportion of (very) high-grade and (very) low-grade material present in the deposit

Correspondingly, it can be theoretically shown that a probability distribution of kriging estimates (e.g., SMU blocks) has mean equal to that of the original sampled data (e.g., drillhole composites), but significantly smaller variability in grades, as measured by the SMU distribution variance (David, 1977; Isaaks & Srivastava, 1989; Goovaerts, 1997). Figure 3.27 shows the general expected differences between original grade pdfs versus estimated grades pdfs. The average grade of the distribution does not change in both cases. However, the spread evidenced in the original composite grade pdf is reduced when compared to the SMU grade distribution, as the tails of the distribution of original grades move to the center (towards the mean).

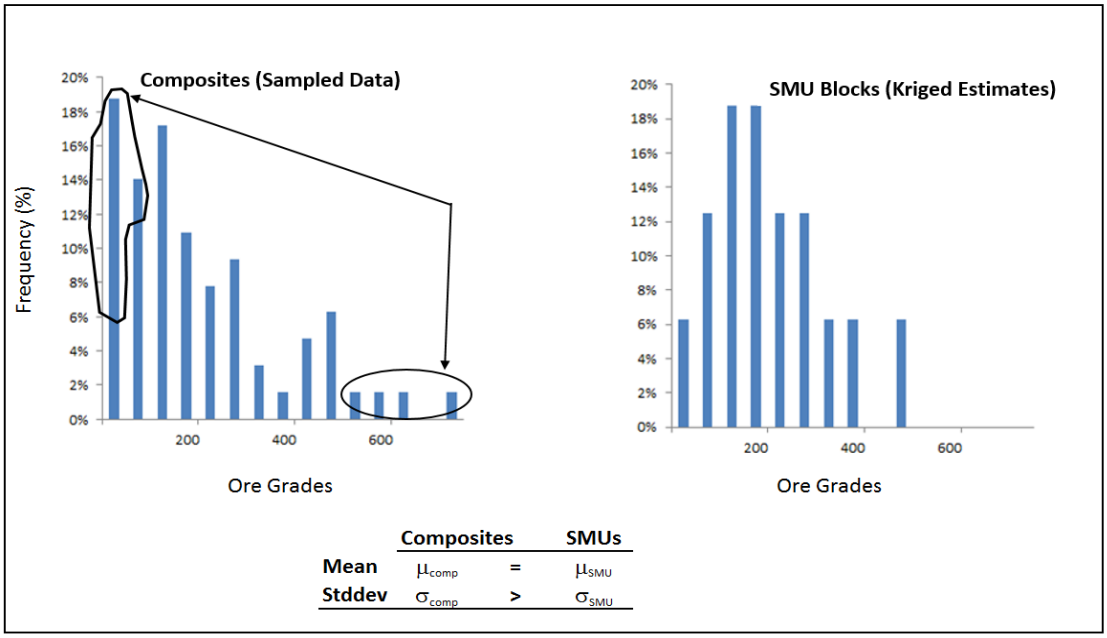


Figure 3.27: Comparison of pdfs for original drillhole sample data (composited) versus estimated (kriged) SMU block data (adapted from Barnes, 2014). Grade units are purposely omitted, for generality of interpretation. Both grade distributions have identical means, approximately 201 "grade units;" however, the composited data has significantly larger variability: 164 vs. 115 for SMUs.

Hence, for circumstances in which preserving the sample data variability is crucial, traditional estimation methods such as kriging (or other convex linear estimator as IDS) do not suffice because, as a result of the smoothing effect, the probability distribution of the set of estimated grades displays a smaller variance than the probability distribution of the original sampled grades. In effect, often times a small fraction of the deposit containing very high grades is critical to its valuation and will tend to be underestimated as a result of smoothing. In the case of gold deposits, for example, it is not uncommon that only 10% of the total deposit tonnage represent 40% (or more) of its total metal content (Parker, 2015). This is one important aspect why a "smoothed" image of the ore deposit, such as the one provided by kriging, might not be fully adequate for mine planning purposes. Additionally, for many operational aspects of mining, there is interest in recognizing the extent to which, uncertainty in the estimated geological models translates into uncertainty in meeting predefined operational or economic targets. These may include ore tons sent to the mill, yearly cash flows to be realized, average grade in the mill feed among others.

Because missing any of the aforementioned operational targets can result in significant financial consequences for mining operators, the ability to quantify uncertainty is of paramount importance. This is the context in which the mineral resource classification methodology is discussed in the subsequent Section.

# CHAPTER 4.
# GEOSTATISTICAL QUANTIFICATION OF GRADE UNCERTAINTY THROUGH MINERAL RESOURCE CLASSIFICATION

For most mining companies, economic and market valuation is reliant, to an important extent, on the total mineral resources it is able to report as assets. Furthermore, in the case of publicly traded companies, most mining jurisdictions require that any event reasonably considered to have a "material" impact on the company's valuation be disclosed to the public.

The exist a variety of reporting codes originated at some of the world's leading mining jurisdictions, namely, the SME code (US), CIM (Canada), SAIM (South Africa) and JORC (Australia). Said codes define Inferred, Indicated and Measured categories for mineral resource classification, which characterize the degree of uncertainty associated with the estimated grade of a block in a given ore deposit.

The following are the internationally accepted definitions for mineral resource together with the distinct mineral resource classification categories:

**Mineral Resource**

A mineral resource is a concentration or occurrence of solid material of economic interest in or on the Earth's crust in such form, grade, or quality and quantity that there are reasonable prospects for eventual economic extraction. The location, quantity, grade or quality, continuity and other geological characteristics of a mineral resource are known, estimated or interpreted from specific geological evidence and knowledge, including sampling.

**Measured Mineral Resource**

A Measured mineral resource is that part of a mineral resource for which quantity, grade or quality, densities, shape, and physical characteristics are estimated with confidence sufficient to allow the application of Modifying Factors to support detailed mine planning and final evaluation of the economic viability of the deposit. Geological evidence is derived from detailed

and reliable exploration, sampling and testing and is sufficient to confirm geologically and grade or quality continuity between points of observation. A Measured mineral resource has a higher level of confidence than that applying to either an Indicated mineral resource or an Inferred mineral resource. It may be converted to a Proved Mineral Reserve or to a Probable Mineral Reserve.

**Indicated Mineral Resource**

An Indicated mineral resource is that part of a mineral resource for which quantity, grade or quality, densities, shape and physical characteristics are estimated with sufficient confidence to allow the application of modifying factors in sufficient detail to support mine planning and evaluation of the economic viability of the deposit. Geological evidence is derived from adequately detailed and reliable exploration, sampling and testing and is sufficient to assume geological and grade or quality continuity between points of observation. An Indicated mineral resource has a lower level of confidence than that applying to a Measured mineral resource and may only be converted to a Probable Mineral Reserve.

**Inferred Mineral Resource**

An Inferred mineral resource is that part of a mineral resource for which quantity and grade or quality are estimated on the basis of limited geological evidence and sampling. Geological evidence is sufficient to imply but not verify geological and grade or quality continuity. An Inferred Resource has a lower level of confidence than that applying to an Indicated mineral resource and must not be converted to a Mineral Reserve. It is reasonably expected that the majority of Inferred mineral resources could be upgraded to Indicated mineral resources with continued exploration.

Depending on a set of modifying factors and on the judgment of the "Qualified Person," Indicated and Measured mineral resources can be converted to Probable and Proved Reserves. Modifying factors involve changes in technical dimensions such as mining, metallurgical, and economic parameters, or societal dimensions such as the legal (regulatory) environment, the requirements for compliance with environmental standards, social perception and governmental policy. It is noted that Inferred resources are not directly convertible into reserves.

In practice, there exists no formal definition for the precise meaning of qualitative statements such as: "sufficient level of confidence to allow mine planning and the evaluation of economic viability…" as stated in the definition of Indicated resources. Nonetheless, industry has converged on a common set of procedures and metrics which have become accepted best practice. Some important mining consultants (e.g., AMEC) recommend that appropriate resource classification analysis focus on three dominant aspects: (i) spatial continuity, (ii) sensitivity of economic parameters to changes in grade and (iii) establishing a target for relative accuracy in grade estimates (Parker *et al*., 2014).

Assessments regarding the spatial continuity of the mineralization entail the following steps:

1. Looking through cross-sectional and plan views of the orebody to get a clearer idea of the degree of connectivity in the ore mineralization across the orebody.

2. Re-evaluating classification (possibly to downgrade) where structural geological features markedly increase local uncertainty. For instance, these features might include geological faults responsible for corridors of Inferred material, or dikes, containing barren or deleterious alteration material (such as talc in iron deposits).

3. Avoiding spottiness, that is, relatively small patches resources belonging to one category to be "mixed" inside a larger pool of resources belonging to a different category.

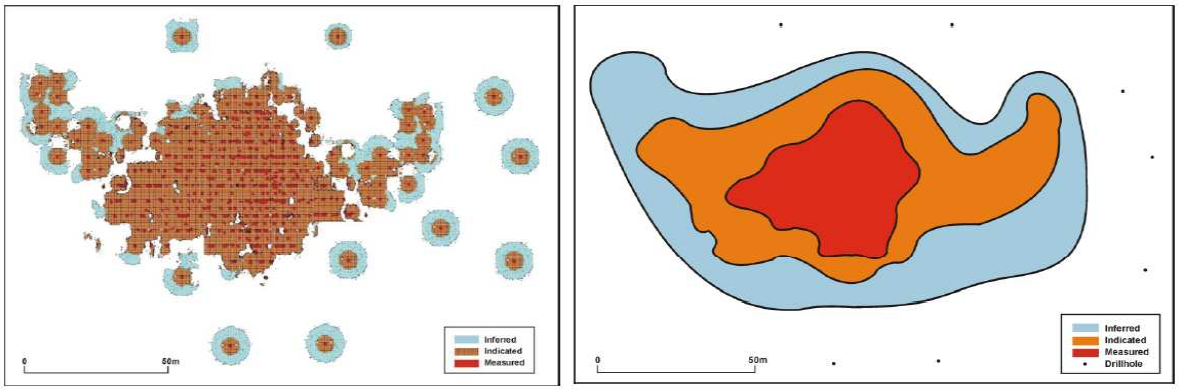


Figure 4.1: Spottiness in mineral resource classification. On the left, a spotted image of the ore deposit is smoothed so as to look like the image on the right. (Stephenson *et al*., 2006).

Assessments regarding the sensitivity of economic parameters to changes in estimated average grade are obviously important because, for most operations, a small error can have a large

impact on cash flows and NPV, particularly if there exists a bias that persists through the life-of-mine.

For illustrative purposes, one real case example of a sensitivity table is extracted from a larger study on a copper deposit by Parker *et al*. (2014) and presented below:

Table 4.1: Sensitivity analysis of economic parameters to deviations in grade estimates

| % Cu | % Chg | Cash Flow Year 2 (M$) | % Chg | NPV(8%) | % Chg | Payback Years |
|---|---|---|---|---|---|---|
| 0.66% | 10% | 218.9 | 30% | 886.5 | 60% | 4 |
| 0.63% | 5% | 193.9 | 15% | 720.4 | 30% | 4 |
| 0.60% | 0% | 169.0 | 0% | 554.3 | 0% | 5 |
| 0.57% | -5% | 144.0 | -15% | 388.1 | -30% | 6 |
| 0.54% | -10% | 119.1 | -30% | 222.0 | -60% | 7 |

Additionally, practitioners doing ore resource modeling frequently target a specific level of estimation accuracy referred to as the "relative accuracy" metric and calculated as:

$$r_a = \frac{(\hat{v} - v)}{v} \tag{4.1}$$

where $\hat{v}$, represents the grade estimate and $v$ represents the true (unknown) grade. The relative accuracy metric is accompanied by the definition of a set of complementary factors which are important to consider, namely, the time period or production increment and the confidence interval (CI) for the average grade estimate.

Different approaches to constructing CI's for mineral resource classification have become popularized, including by using the estimation variance or by the implementing of simulation-based techniques which consist of constructing a bootstrap confidence interval for the estimated grade (Boisvert & Silva, 2014). For methods based on estimation variance, it is of importance to examine what factors affect it most directly. It can be shown formally (Matheron, 1968, Journel & Huijbregts, 1978; Isaaks & Srivastava, 1989) that for any estimator expressed as a convex weighted linear combination of some random variable (sample grades), the estimation variance is expressed as:

$$\sigma_R^2 = \tilde{C}_{00} + \sum_{i=1}^{n}\sum_{j=1}^{n} w_i w_j \tilde{C}_{ij} - 2\sum_{i=1}^{n} w_i\, \tilde{C}_{i0} \tag{4.2}$$

where, $\sigma_R^2$ defines the variance of the estimation errors (estimation variance), $w_i$ defines the estimation weight of sample $i$, $C_{ij}$ defines the covariance value between the pair formed by samples $i$ and $j$, $C_{i0}$ corresponds to the covariance value between each individual sample and the location to be estimated and $\tilde{C}_{00}$

$\tilde{C}_{00}$: *captures the underlying variability of the mineralization*

$\sum_{i=1}^{n}\sum_{j=1}^{n} w_i w_j \tilde{C}_{ij}$ : *captures the redundancy in the data due to the statistical similarity and clustering between samples*

$2\sum_{i=1}^{n} w_i\, \tilde{C}_{i0}$: *captures the statistical similarity between the samples and the location to be estimated*

From the individual terms in equation (4.2), it is clear that estimation variance is influenced by the degree of underlying variability associated with the ore mineralization (first term), the spatial disposition of the samples relative to one another, namely, whether the samples form spatial clusters which lead to redundancy on the information to be extracted (second term), and finally, the (statistical) proximity of the individual samples to the location that is the target of the estimation.

In the case of resource classification, the true goal of estimation is not to generate a point estimate, but rather to obtain a *block* estimate that targets an average value for the grade variable inside a local area $A$ representing a monthly or quarterly volume or tonnage of production. This requires equation (4.2) to be slightly modified, and if ordinary kriging can be assumed as the estimator, a new equation for the estimation variance is constructed, which can be expressed as follows (Isaaks & Srivastava, 1989):

$$\sigma_{OK}^2 = \overline{C}_{AA} - (\sum_{i=1}^{n} w_i \overline{C}_{iA} + \mu) \tag{4.3}$$

where $w_i$ and $\mu$ represent the estimation weight of sample $i$ and the Lagrange parameter respectively and the remaining equation terms are as follows:

$\overline{C}_{iA} = \frac{1}{|A|}\sum_{j|j\in A}\tilde{C}_{ij}$ : *represents the average covariance between a sample i and all the points within A*

$\overline{C}_{AA} = \frac{1}{|A|^2}\sum_{i|i\in A}\sum_{j|j\in A}\tilde{C}_{ij}$ : *represents the average covarince between pairs of locations within A*

Construction of a CI for the estimated average grade of the material requires the following assumptions be made: i) estimation errors are normally distributed; ii) estimation errors are representative of the true (unknown) distribution of errors and iii) the distribution of errors is approximately symmetric. At this point, it is straightforward to build a (symmetric) confidence interval centered on the mean (as given by $\hat{v}$) and with upper and lower extremes defined as a function of the distribution's standard deviation and mean (Figure 4.2). Confidence intervals are defined as follows:

$$CI_\beta = \hat{v} \pm z_{(1-\frac{\alpha}{2})}\frac{\sqrt{\sigma_{OK}^2}}{\hat{v}} \tag{4.4}$$

where $\beta = (1-\alpha)$, with $\alpha \in \{0,1\}$ represents the confidence level, typically 90%, and $z_{(1-\frac{\alpha}{2})}$ represents the $(1-\alpha/2)$ quantile in the distribution of errors (assumed Gaussian).

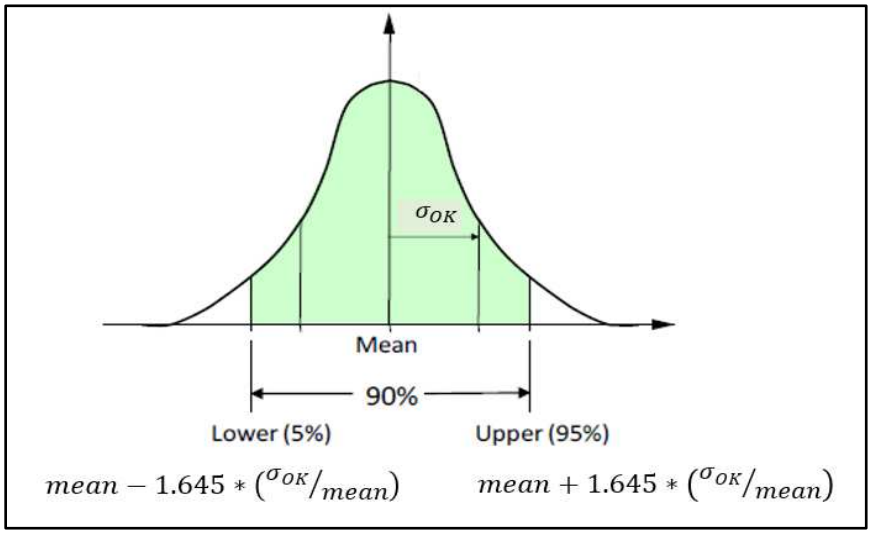


Figure 4.2: Construction of a symmetric two-sided confidence interval for the mean grade of a block (panel) of mine production. In this case, α = 90% but different levels of confidence could have been chosen (adapted from Parker, 2014).

For classification using kriging variance, the relative accuracy is expressed as:

$$r_a = 1.645 * \frac{\sigma_{OK}}{\hat{v}} \tag{4.5}$$

The goal is that relative accuracy not exceed 15% for some production period, i.e., $r_a \in [0, 0.15]$.

It is important to note that conversion from an initial production volume (or tonnage) corresponding to some panel $A$ into a different production panel $B$, possibly corresponding to a different length of time, is achieved simply by re-scaling the initial panel $A$ variance, specifically, by dividing said variance by the number of blocks $(N)$ in panel $B$:

$$Var_B = Var_A/N \tag{4.6}$$

For example, if the initial panel for which $\sigma_{ok}^2$ was calculated corresponds to three months' worth of production then the relative accuracy derived is said to correspond to a "a quarter" (in the sense that 3 months correspond to a quarter of a year). One might be interested in determining the equivalent threshold corresponding to one year's worth of production. In this case, the calculation is straight-forward (David, 1977; Journel & Huijbregts 1978; Verly *et al.*, 2014):

$$Var_{year} = Var_{quarter}/4 \tag{4.7}$$

From the relationship given in equation (4.7) it results that a quarterly relative accuracy threshold of 15% is equivalent to an approximate threshold of 8% $(\frac{15}{\sqrt{4}})$.

Crucially, however, equations (4.2) and (4.3) also show that the estimation variance does not depend on the actual values of samples used for the estimation. This is important because, most ore deposits exhibit, to different degrees, the so-called *proportional effect,* in which high-grade domains of the orebody evidence higher variability than low-grade domains. Thus, for circumstances in which the *proportional effect* is present, the fact that kriging variance ignores grade values can lead to misleading results. Additional drawbacks of the kriging estimation variance approach include the fact that true estimation errors might not follow a Gaussian distribution, and symmetric two-sided confidence intervals might not be appropriate in the case of highly skewed grade distributions.

This motivates the development of new methods replacing kriging variance with bootstrap confidence intervals constructed from incorporating sequential conditional simulations in quantifying risk. Within the conditional simulation framework, the single grade of an individual block is replaced by a set of possible equally-likely grades, each of which associated to an individual simulation of the ore deposit. Hence, instead of a single estimated value, each block is associated to a histogram representing a probability distribution which is expected to fully capture the grade variability at the block's location. It is important to note that, unlike kriging, conditional simulation values are dependent on the actual local grade values (i.e., conditional simulations honor the hard data and are conditioned on both hard data and simulated values) which is desirable for addressing the challenges with the proportional effect. Confidence intervals are constructed centered on the kriged estimate, by counting the number of times the target relative accuracy threshold can be met and dividing it by the total number of simulations generated $|\omega|$. For instance, let $I_{\hat{v}}$ be an indicator variable taking the value 1 if the estimated grade value ($\hat{v}$) is contained in the relative accuracy interval defined as $\varepsilon_{r_a} = \hat{v} \pm r_a$; 0 otherwise. Then $\varepsilon_{r_a}$ is a 90% CI for the mean ($\hat{v}$), if and only if, the following condition is met:

$$CI_{90} = \varepsilon_{r_a} \; iff: \frac{1}{|\omega|} \sum_{\omega} I_{\hat{v}} \geq 0.90 \tag{4.8}$$

As a summary, the general quantitative guidelines for mineral resource classification most widely adopted by the mining industry are presented below (Parker & Dohm, 2014):

**Inferred Resources:** mineral resources for which insufficient geological information exists to establish confidence levels.

**Indicated Resources:** mineral resources for which a 90% confidence interval corresponding to a ± 15% relative accuracy over an annual production increment can be defined. This implies that the true (unknown) average grade will be within 85 and 115% of the estimate 90% of the time. Annual production increments are typically used for Pre-feasibility and Feasibility cash flows. Typically, operating mines can withstand deviations from plan corresponding to one year in 20 as being below 85% of the estimate – normal business risk. Actual realized grades consistently below the 85% threshold, often result in the mine incurring in a loss.

**Measured Resources:** mineral resources for which a 90% confidence interval corresponding to a ± 15% relative accuracy over a quarterly or monthly production increment can be defined. Similar to Indicated resources, this implies that the true average grade is expected to be within 85 and 115% of the estimate 90% of the time. Quarterly or monthly production increments are typically used for determining Operating Budget cash flows.

## 4.1 Geostatistical Conditional Simulations

Geostatistical conditional simulation techniques provide a viable framework for the quantification of grade variability in mineral deposits. Using this approach instead of a single estimated model, a set of equally likely realizations of the orebody are generated. These simulations are such that each single realization honors the hard data at previously sampled locations, reproduce first-order statistics of the dataset (such as data histograms) and second-order statistics including the bivariate spatial distribution of the data (e.g., by reproducing data variograms) (Journel, 1989).

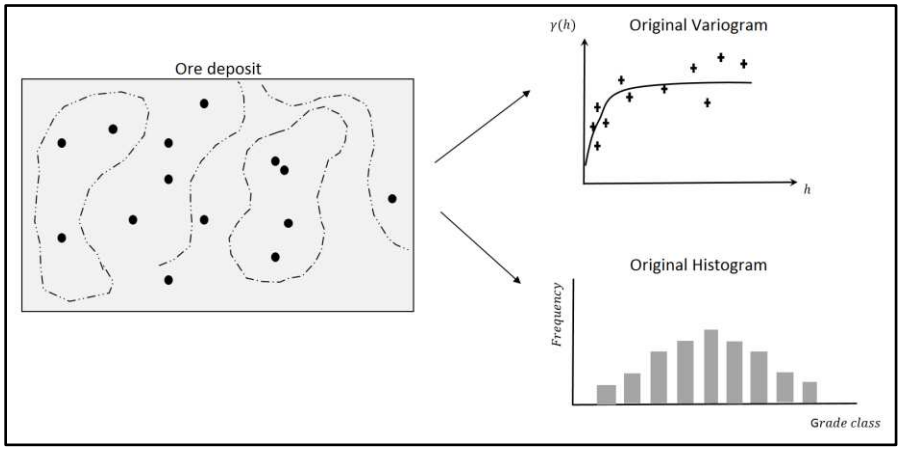


Figure 4.3: Samples collected from the orebody (black dots) are used in exploratory data analysis to build histograms and experimental variograms of the data.

Both the original data variograms and histograms should be honored by the subsequent conditional simulation realizations (see Figure 4.3 and Figure 4.4).

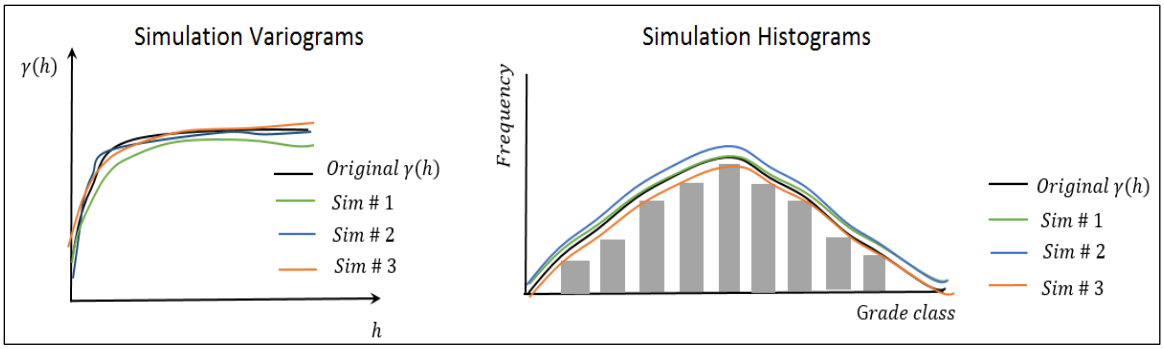


Figure 4.4: Histograms and experimental variograms of the original data should be reproduced by the individual conditional simulations.

There exist quite a large variety of conditional simulation methods being employed and developed in actuality. Their use is not confined to mining but extends notably into oil reservoir characterization (Kelkar & Perez, 2002), environmental (Webster & Oliver, 2007) and health applications (Goovaerts, 2005, 2009). Despite the existence of large swath of distinct conditional simulation methods, the mostly follow a similar basic template (Figure 4.5):

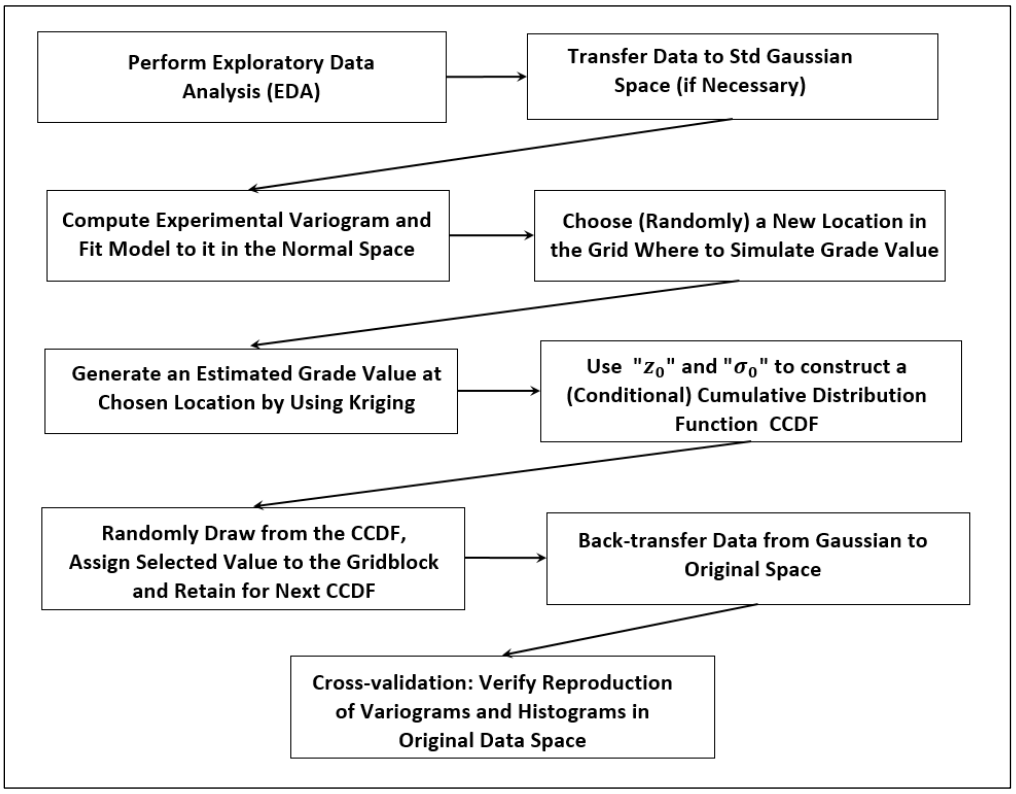


Figure 4.5: Summary of minimum steps required for successful geostatistical conditional simulations.

In essence, exploratory data analysis pertains to traditional first order statistics, including central tendency statistics such as the (declustered) mean, median mode and the construction of histograms of the grade distribution. Spatial data analysis is represented by the computation of variograms, which are used at a later stage (together with data histograms), as an element for cross-validation of the generated simulations. In the next section, a small numerical example of SGS is presented to illustrate the core steps of said methods.

## 4.2 Numerical Example of Sequential Gaussian Conditional Simulation

Similar to ordinary kriging, a succinct description of Sequential Conditional (Gaussian) Simulation is presented to help enlighten some of the key concepts of SGS. Recall that the simulation paradigm is most useful in contexts in which a measure of local uncertainty (other than the kriging variance) is important. The steps of SGS given in Figure 4.5 are illustrated through the example shown in Figure 4.6 to Figure 4.10.

STEP 1

Transfer all data to Standard Gaussian (normal) space by previously ranking the data and converting it to standard normal scores (ns) ≈[-3, 3]

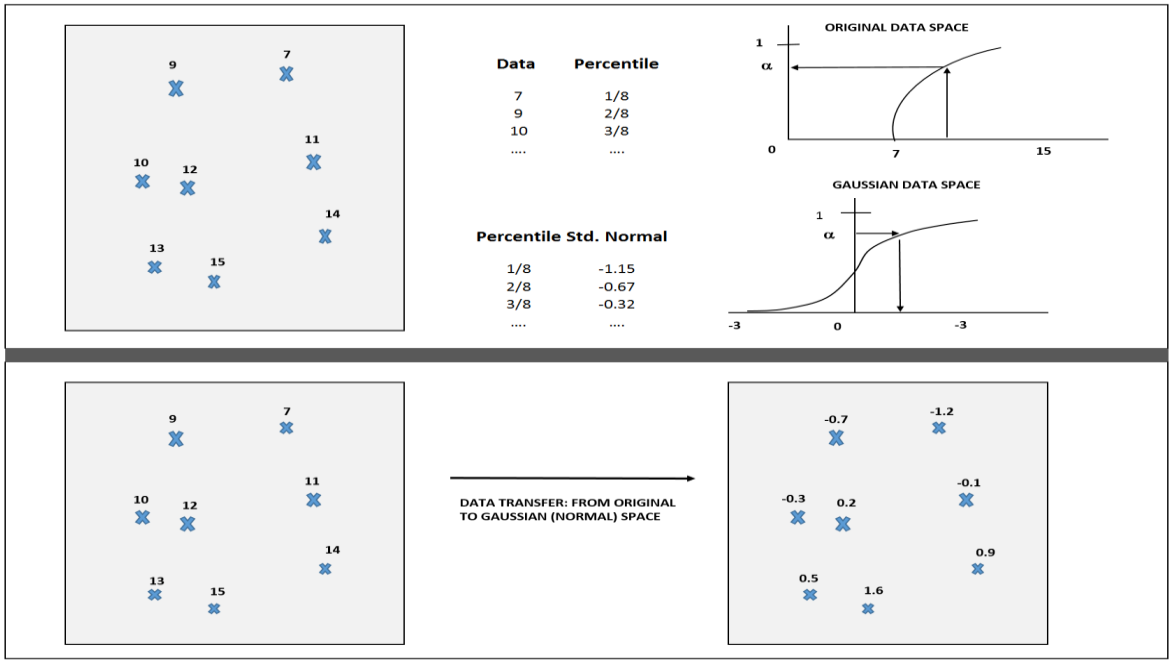


Figure 4.6: Mapping the sample data from the original data into the Gaussian space.

STEP 2

- Assuming a variogram model can be obtained, randomly choose a gridblock where to assign a new simulated grade value. Generate a Kriging estimate for the selected location (using both sampled data and previously simulated nodes), to obtain $z_0$ and $\sigma_0^2$ (Figure 4.7)

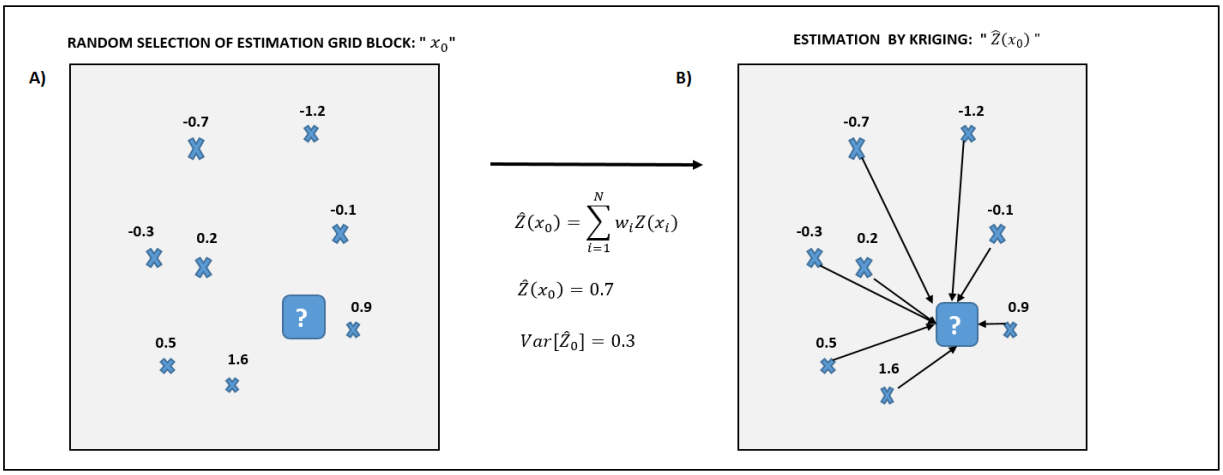


Figure 4.7: Kriging estimation at the location of interest.

STEP 3

- Construct a conditional cumulative distribution function CCDF and randomly draw from it.

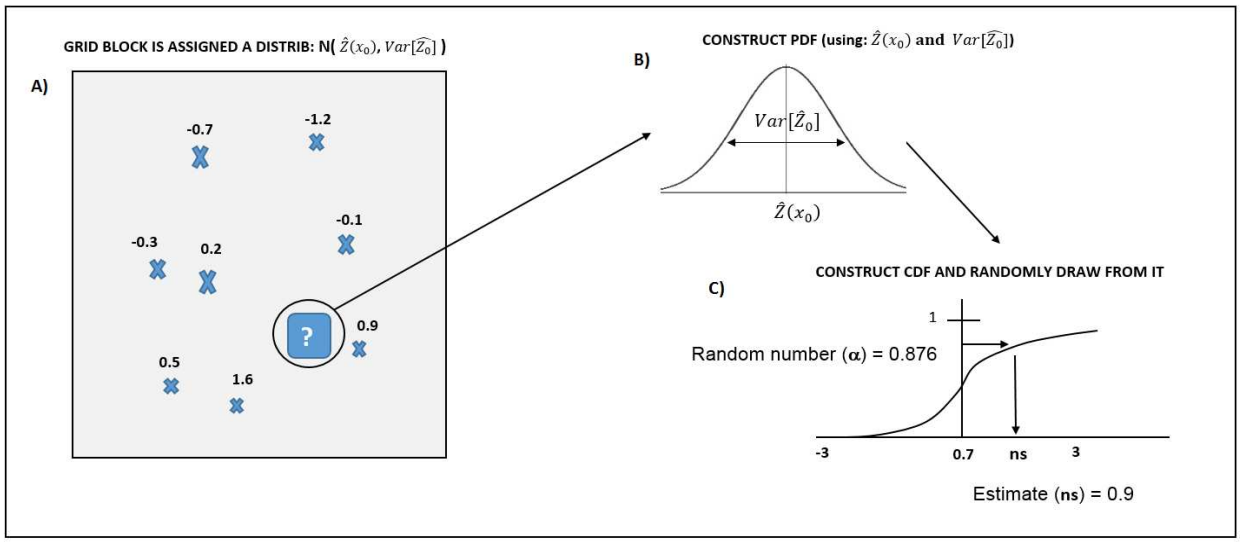


Figure 4.8: Random drawing from generated CCDF.

STEP 4

- Assign simulated grade value to the corresponding gridblock and retain for next CCDF construction.

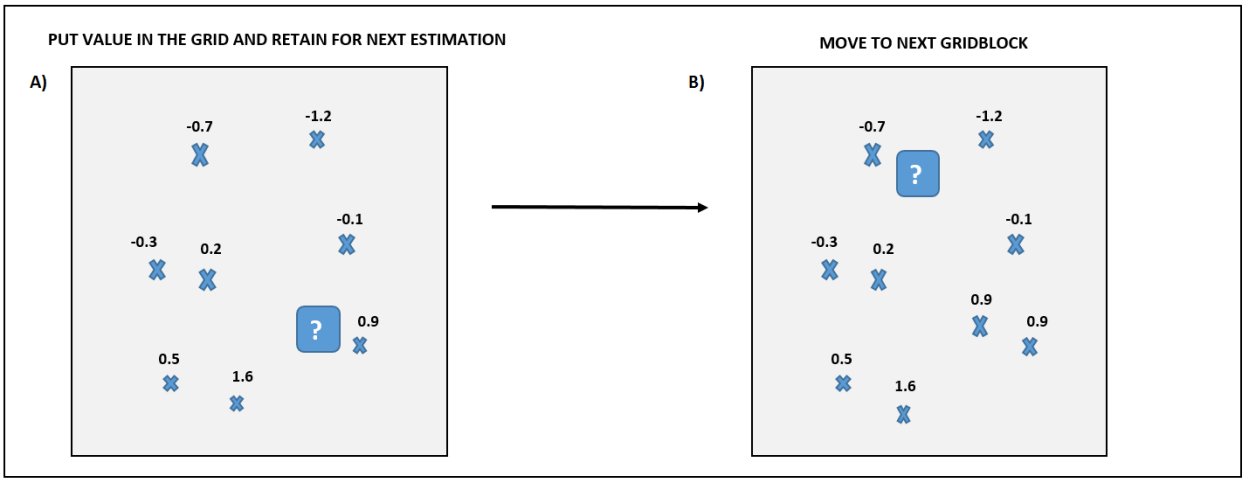


Figure 4.9: Assigning simulated grade value (ns = 0.9) to the grid and moving to the next simulation node.

STEP 5

- Transfer all simulated (as well as original hard) data values back to the original data space

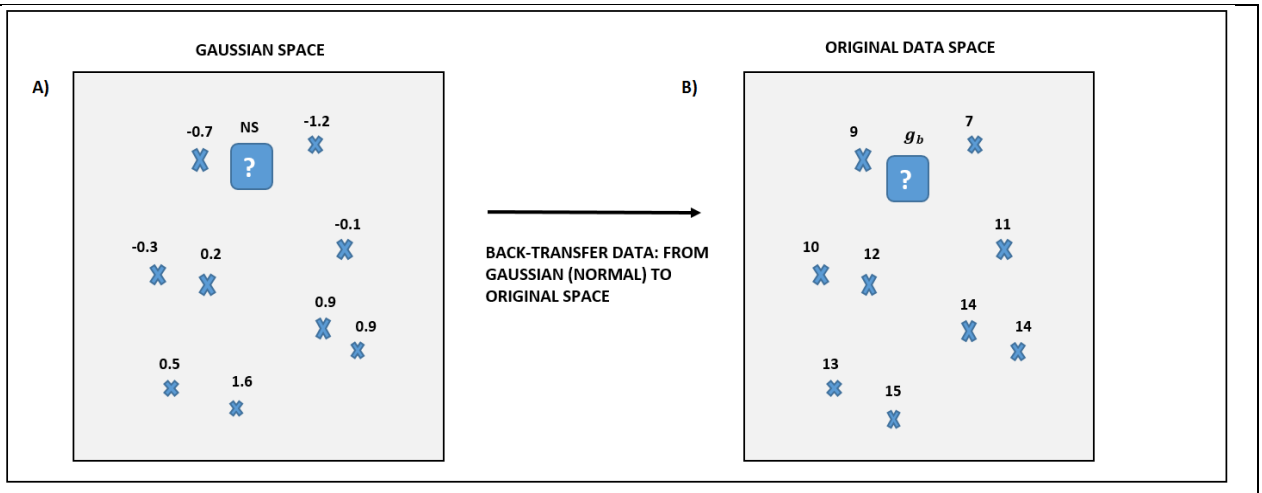


Figure 4.10: All values (simulated and original) are transferred back to the original data space to conclude the simulation.

# CHAPTER 5.
# STOCHASTIC MINE PRODUCTION SCHEDULING OPTIMIZATION

Stochastic open pit mine production scheduling optimization is currently done using grade realizations coming from geostatistical conditional simulations. The essence of the uncertainty-based stochastic optimization framework is best captured by the following schematic figure:

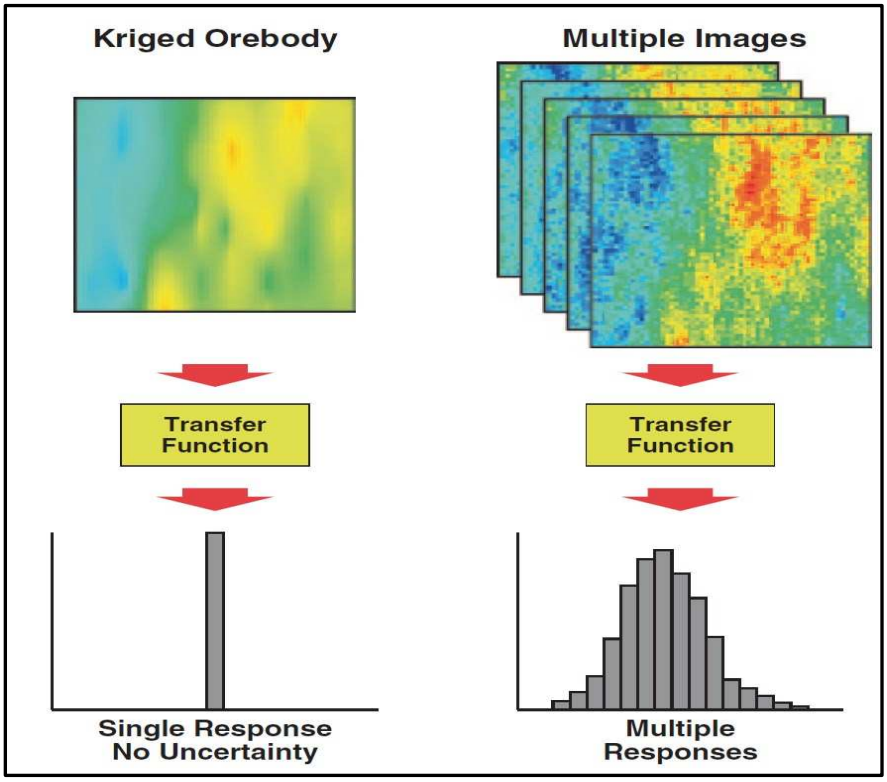


Figure 5.1: Traditional versus Stochastic Production Scheduling (Rossi & Deutsch, 2014)

The left half of Figure 5.1 illustrates how in the traditional approach to mine production scheduling, mine plans are generated based on a single estimated model of the orebody. By contrast, the right half of Figure 5.1 illustrates how, in a risk-oriented approach, many conditionally simulated orebody models serve as the basis for the optimization schedule. Each

conditional simulation is thought of as representing an alternative, equally probable, representation of the mineral deposit.

After passing through a transfer function (such as an optimization model solved using CPLEX), the ensemble of conditionally simulated realizations yields a distribution of possible values for key operational indicators. Said performance metrics might include, among others, yearly discounted cash flows, total ore tonnes mined and average grade of the material sent to the milling plant(s). This is in contrast to the traditional view which ignores uncertainty and assumes a single, perfectly accurate, although usually wrong, estimate of the metric of interest.

Figure 5.2 complements Figure 5.1, and illustrates part of the process of building "risk profiles" for independent production schedules generated for each of the individual conditional simulation realizations.

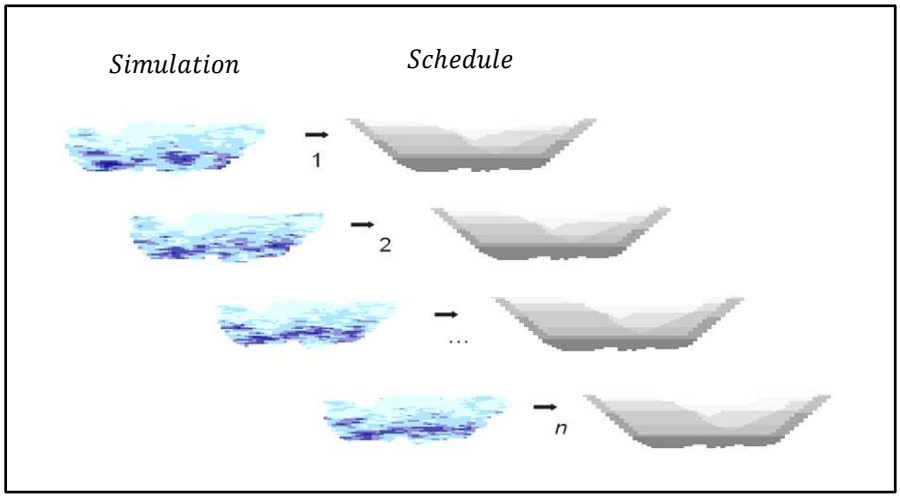


Figure 5.2: Risk-oriented view of open pit optimization (adapted from Leite *et al*., 2007).

Godoy *et al*. (2003) provide an extensive discussion on the role of risk profiles in capturing geological uncertainty and their applicability in incorporating uncertainty into strategic mine production scheduling. In their discussion, the authors cite a variety of case studies which serve as examples. Some of the most effective uses of geostatistical conditional simulations (GCS) include, but are not limited to (Godoy & Dimitrakopoulos, 2007):

- Quantification of uncertainty and risk analysis of an ultimate pit limit, including net value, costs, tonnage, grade and metal,

- Identification of areas of upside potential and downside risk in terms of ultimate pit limits,
- Trade-off analysis for pushback depletion strategies,
- Quantification and assessment of uncertainty related to ore blocks driving the increment between successive pit shells.

Dimitrakopoulos, Martinez and Ramazan (2007) developed a methodology for maximizing the potential upside while also minimizing the downside associated with geological uncertainty using the instances of grade realization resulting from geostatistical simulations. In their approach, the authors first generate a set of conditional simulations of the orebody intended to capture the deposit's geological uncertainty.

All of the mining decisions corresponding to a specific production schedule are then "imposed" on all other orebody realizations, and compliance with a number of pre-specified operational performance metrics - such as average grade or total milling requirements - is verified.

These results are recorded and used to compare the expected performance of an individual mine plan, under the existence of geological uncertainty (which is represented by the previously generated set of orebody realizations). The performance of an individual mining plan regarding each of the chosen operational metrics is summarized in distinct plots which are gathered, and their ensemble is said to correspond to a so-called "risk profile" for the respective plan. From risk profiles, upside and downside statistics are created and added to the objective function to be optimized.

Many interesting discussions on the very latest advances in strategic mine planning can be found in Dimitrakopoulos (2014). The original conceptual framework has been extended and brought to a stage in which researchers use Stochastic Linear Programming ($SLP$) methods to formulate two-stage (and less frequently multi-stage) stochastic models of the mine production scheduling problem. In the most recent $SLP$ formulations of the mine production scheduling problem, researchers draw more explicitly from the formalism presented by authors such as Birge and Louveaux (2011).

Lamghari and Dimitrakopoulos (2013a) provide a paradigmatic formulation of a stochastic rendition of ($OPMPSP$), which is representative of the popular SLP modeling approach. The

authors model a problem which assumes mining decisions can be made separately from processing decisions, and occur under grade uncertainty, that is, mining decisions take place before the true metal content of the ore blocks can be known with certainty. In order to characterize the uncertainty associated with the grades, a finite number of potential outcomes or scenarios are generated, such that each block is assigned a possible grade value per scenario. The problem includes limits on the maximum yearly mining capacity, multiple ore processing destinations with limited milling capacity, as well as a stockpiling option allowing ore material to be stored (whenever more ore is mined than can be processed in a given period), or reclaimed (whenever less ore is mined than must be processed in a given period). In general, the option to stockpile ore material adds flexibility to mine production schedules, relative to the circumstance in which some of the ore mined must be wasted so that richer ore can be processed. However, typically the use of stockpiles is associated with additional re-handling costs resulting from the need to load and haul the previously stored ore. Hence, in an ideal scenario, scheduled ore blocks are sent directly to the processing plant without visiting the stockpiles, so that said re-handling costs can be minimized. The model presented in Lamghari (2013a) can be seen as the deterministic equivalent of a two-stage SLP rendition of the *OPMPSP,* in which decision variables are divided into first-stage (scenario-independent) variables corresponding to mining decisions, and second stage (scenario-indexed) variables corresponding to sending or reclaiming material to and from the stockpile (recourse decisions). First-stage and second-stage decision variables are linked by the fact that, for each scenario considered, initial mining decisions (taken without to regard to the scenario realization) might lead to either excessive or insufficient ore tonnage being sent to the milling plant, and consequently, to the need for sending or reclaiming ore from the stockpile.

The objective function of the model aims at maximizing the expected life-of-mine NPV for the project by: (i) minimizing total (ore and waste) mining costs, together with the losses from sending material to the stockpile, and (ii) maximizing the expected revenue from ore sent directly to the mill, together with the (delayed) gains accrued from the ore reclaimed from the stockpile.

Independently of the solution method selected for generating the actual production schedules, the structure of the formulation model tends to lead to the deferment of mining riskier blocks to later stages of the life of the mine, regardless of whether these blocks could have potentially been mined sooner. Deviations from target production level at the mill plant is

quantified by "slack" variables (in the operational constraints) which are added to the objective function and associated with monetary costs. Said monetary costs could be interpreted as "penalties" for the use of the stockpile.

In practice, the values assigned to the penalty terms in the objective function are adjusted empirically so as to ensure maximum adherence to operational targets. However, by selecting a destination for each individual block *a priori* the models cannot account for cutoff grade optimization, thus, generating suboptimal schedules. Likewise, the models in both this approach and the one discussed in Martinez *et al*. (2007), are representative of the broad spectrum of mining stochastic optimization models and tend, by design, to push the riskier blocks to the latest possible periods in the project's life. Finally, it is noted that the schedules generated by the model in Lamghari (2013), may only be considered optimal in "an expected-value sense."

## 5.1 Shortcomings of Current Deterministic and Stochastic Production Scheduling Models

The traditional, deterministic production scheduling models discussed earlier assume that the estimated grade values in the geologic block model are known with certainty. As such, the corresponding mine schedules are assumed to be achievable during the mining operations when, in fact, due to the existence of uncertainty surrounding the estimation of each block, this is not necessarily true. It is often very difficult to consistently meet the desired production requirements in every singular period throughout the project's mine life. The optimized schedules may not be optimum if one cannot achieve them in practice.

Currently, the framework better suited to address the inevitable geologic uncertainty underlying ore reserve estimates is that of stochastic mine planning. Geostatistical techniques, such as conditional simulations, allow for the generation of a set of equally probable realizations of the orebody which are used as input to a stochastic production scheduling optimizer in place of a single estimated model (Dimitrakopoulos, 2000). The current approach to stochastic mine planning focuses on determining schedules that minimize the risk of not meeting pre-established goals while optimizing financial and operational targets (Whittle, 2014). However, for its many advantages

over a traditional production scheduling optimization framework, the present stochastic paradigm still has weaknesses. One important challenge resides in the fact that one equates variability of grades with risk, such that, the schedules adhere very strictly to operational targets. In the current stochastic mine production scheduling approach, risk is seen as something to be avoided at all costs, leading researchers to design models and solvers that seek to minimize the risk of not meeting predetermined operational targets at the hindrance of realizing potentially higher profits (Ramazan & Dimitrakopoulos, 2007). In particular, it should be noted that the equivalence between risk and uncertainty is faulty because risk is only that fraction of uncertainty which results in unfavorable outcomes. Indeed, risk constitutes part, and not the totality of potential outcomes arising from the underlying uncertainty in ore reserve estimation.

Similarly, there exists the fact that, for fully stochastic optimization models, (including scenario-indexed variables), each of the individual geostatistical simulations represents a new set of decision variables to be added to the model, obviously resulting in dramatic increase in problem size and leading to attempts to solve the models using heuristic (or metaheuristic) solvers. This latest shortcoming is the principal driver for the search of alternative approaches to incorporating grade uncertainty.

## 5.2 The Nature of Uncertainty and the Appeal and Limits of Stochastic Models

An additional, related, though distinct facet of the problem studied, concerns the nature and limits of the most widely used stochastic models, at least as reported in the most recent literature (Dimitrakopoulos, 2014). Increasingly, these models are involved and are characterized by a considerably high degree of mathematical sophistication. This occurs because intuitively there exists a (justified) perception that the higher the degree of complexity in the models, the larger the level of detail that can be captured and, therefore, the more realistic the models are. It is the author's high conviction, however, that in the great majority of the case-studies presented it is still difficult to specify objectively the added insight gained by the increased complexity, or whether it actually exists. Examples include holistic stochastic modeling of mining complexes, encompassing multiple mines, processing streams, transportation schemes, supply contracts, as well as accounting simultaneously for grade and price uncertainty (Zhang & Dimitrakopoulos, 2015). It is stressed that at present, for many real case mine projects, it is still not possible to solve, to proven

optimality, a fully stochastic integer programming model of a single mine. Thus, although holistic stochastic mine planning models represent undeniable advances in mine planning, and are increasingly the subject of added attention, they also carry the risk of "overpromising" on the degree to which one can plausibly quantify and capitalize on uncertainty.

"Mathiness" (Romer, 2015) is particularly misguided when the nature of uncertainty is epistemic, that is, when the sources of uncertainty are the result of either an incomplete understanding of the phenomena one would like to quantify of defective or inadequate information (Loquin *et al.,* 2010). It may occur that, possibly as a result of incomplete drilling, the current state of geological knowledge of the deposit is simply insufficient or lacking to an extent that it does not permit the desired levels of confidence in the mine plans to be achieved in practice. One might imagine, for instance, a scenario in which a hypothetical orebody has just entered the exploration stage and a total of only three (3) samples have been collected. In such circumstances, there will always exist an intrinsically high degree of geological uncertainty and it would be unrealistic to assume that said uncertainty can be overcome or mitigated by additional geostatistical conditional simulations. Increased mathematical sophistication will not suffice either, because that is not the root of the challenge. Clearly, for such a poorly drilled deposit the right answer is simply to conduct more drilling (or alternatively, to decide whether the current level of uncertainty is to be deemed acceptable).

Moreover, there is the important aspect of the sense in which solutions to stochastic mine planning models are optimal. A standard form two-stage stochastic linear programming ($SLP$) model can be formulated as follows:

$$\min_{x,y} \quad c^T x + E_\omega[Q(y,\omega)] \tag{5.1}$$

$$s.t. \quad Ax = b \tag{5.2}$$

$$x \geq 0 \tag{5.3}$$

where $Q(y,\omega)$ is the objective function values of the second stage problem, defined as follows:

$$\min_{y} \quad q(\omega)^T y \tag{5.4}$$

$$s.t.\ \ Wy + Tx = h(\omega) \tag{5.5}$$

$$y \geq 0 \tag{5.6}$$

With $x \in R^n$ the first-stage decision variables, $y \in R^m$ the second-stage decision variables, the vector $\omega(q, h)$ corresponds to a random vector containing the data parameters for the second-stage problem, that is, those parameters about which a certain degree of uncertainty exists, and finally $E_\omega$ is the expectation operator over the uncertainty space defined by $\omega$.

The standard $(SLP)$ formulation makes clear that the appropriate way to interpret the meaning of an optimal solution obtained under uncertainty is to acknowledge that it is optimal only in an expected value sense, i.e., since one can never fully eliminate uncertainty, there remains a possibility that the solution generated from the model be different than the true ("wait-and-see") optimal. Indeed, the true optimal solution is never truly known until uncertainty is resolved, which in the context of grade uncertainty in mining, means only after one mines the deposit, verifies what is in effect "on the ground" and is in a position to confirm that the solution is truly optimal.

This crucial feature of stochastic programs is often lost on many of the discussions found in the stochastic mine planning literature in which, on the contrary, researchers state confidently that a "true optimal' solution has been found. Although $(SLP)$ models are theoretically superior to naïve deterministic models, it is important to recognize the probabilistic nature of statements about optimality. In particular, given the complexity, the difficulty in solving fully stochastic models using exact methods, as well as the inferior transparency, consideration should be given to alternative, more practical modeling approaches.

The solution methodology proposed in this dissertation also provides a contribution to the important problem of the optimal amount of infill drilling $(OID)$. Briefly, the $(OID)$ problem consists of maximizing the benefit (information) derived from a set of drillhole samples while minimizing the costs associated with drilling, i.e., such that the number of drillholes produced does not exceed the minimum necessary to ensure that the continuity of the mineralization can be adequately determined. However, it is evident that "adequate characterization…" is a subjective statement that is directly related to the level of risk that management is willing to accept which, in turn, determines how extensive and rigorous the data collection efforts are. The $(OID)$ is fundamentally a Value of Information problem, in which one must weigh the tradeoff between the

potential benefits from a reduction in grade uncertainty against the costs associated with additional infill drilling (Froyland *et al*., 2007).

By indicating which specific periods violate the pre-defined ore risk requirements, our methodology exposes those areas of the deposit which do require additional infill drilling and provides an effective tool for risk management. Moreover, it is a well-established proposition from decision analysis theory, that information has value only to the extent to which future decisions are affected by it (Clemen, 1997). Therefore it must be emphasized that the $(OID)$ cannot be solved independent of an assessment of the impact of additional information to mine scheduling decisions. By directly linking mineral resource uncertainty to mining decisions, our method is well suited to providing an estimate of an upper bound to the value of additional drilling, in other words, the method helps identify, objectively, the most a decision maker might be willing to invest in additional information gathering given his degree of risk tolerance.

In the solution methodology described in this dissertation, we show how in the context of grade uncertainty, the "curse of dimensionality" can be circumvented by the adoption of mineral resource classification categories, in place of approaching the problem from the perspective of a fully stochastic optimization paradigm. Despite accounting for grade risk, our methodology nonetheless achieves the complementary goals of practicality, transparency and flexibility.

Resource classification categories are central to our solution framework and are presented in greater detail in the subsequent Section.

# CHAPTER 6.
# NEW APPROACH TO OPEN PIT MINE PRODUCTION SCHEDULING UNDER UNCERTAINTY

## 6.1 Defining the Problem

One aspect of mine planning which is of particular concern for mine managers, relates to assessments of the degree of confidence in the estimated average grade of a panel of production, typically corresponding to some period (or volume) of production larger than that of individual mine blocks (see Figure 6.1). The fundamental mine planning problem confronting the mining industry which this dissertation addresses can be stated very simply, it is that, during mine production scheduling optimization, mine planners are often oblivious to the economic implications or do not even consider ore resource risk classification. Indeed, some of the consequences of said omission are rather forcefully illustrated by the events at a mining operation in the Western US (whose name we omit for confidentiality reasons). In this project, the mine planning team developed a mine production schedule which was determined to be "optimal" in a deterministic sense and was thus scrupulously followed by the engineers and operators in the field.

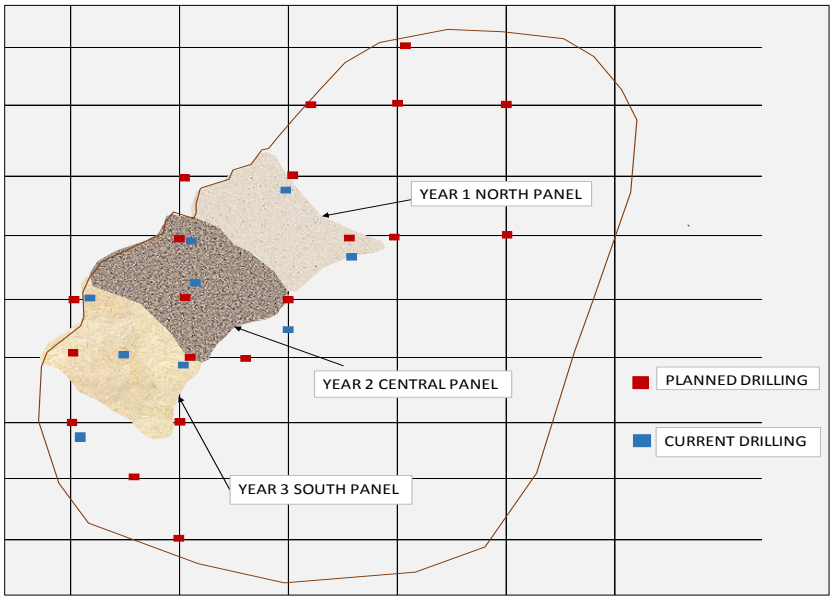


Figure 6.1: Example plan view of the progression of a deterministic mine production scheduling plan. Each of the individual production panels corresponds to 12 months' worth of production.

Despite being considered optimal, however, the plan had ignored any consideration regarding ore resource risk classification, and the result was that by the end of business year 2015 approximately 50% of the total material mined belonged to the Inferred resource category. Furthermore, the mining company concluded that it was missing close to 60 thousand ounces of gold because, although some of the mined material contained metal, the bulk majority did not and was instead barren (as is often the case with Inferred resources).

From an initial stance in which managers relied deeply on qualitative or empirical assessments on the part of geologists, the mining industry has evolved to a position in which the subjectivity in qualitative assessments is increasingly replaced (or complemented) by the objectivity given by quantitative geostatistical methods. Within the realm of geostatistics, the process of assigning categories to mineral resources as a function of the degree of confidence in the grade estimates (and their corresponding spatial continuity) is referred to as "mineral resource classification," and constitutes one of the most important tools for managing grade risk. Traditionally, three mineral resource classification categories are used: Inferred, Indicated and Measured (as discussed in CHAPTER 4). Since each resource classification category has a corresponding level of risk associated with it, it seems natural to generate mine production plans in which the desired composition of the mined material is specified, *a priori*, so that a target mix of the proportion of Inferred, Indicated, and Measured material is known (Figure 6.2).

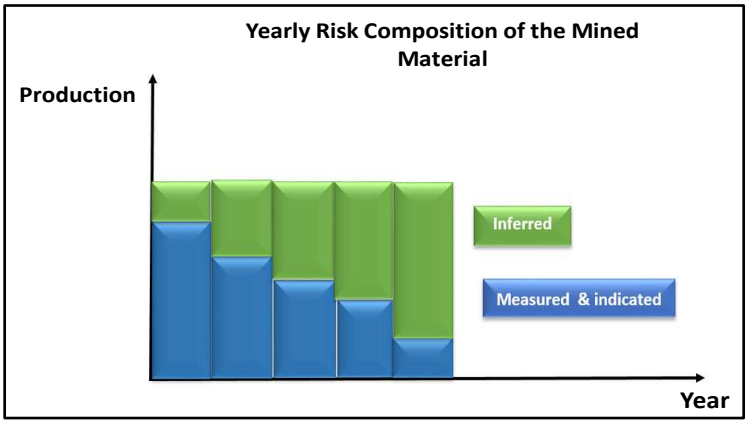


Figure 6.2: Notional depiction of desired "risk mix" in a yearly mine production scheduling plan. Characteristically, Measured and Indicated resources are combined (grouped) and displayed separately from Inferred resources.

For instance, a mine manager might determine that the yearly composition of the ore material in the mill feed, for the first five years of the mine project, must not contain more than 20% of Inferred material, 40% of Indicated ore and at least 40% of Measured material. Moreover, it is often a stated risk management strategy that later years of the mine life accommodate a greater fraction of Inferred material while earlier years be composed mostly of Indicated and Measured material. In addition, Inferred resources do not qualify for reserves (cannot be reported as assets in the financial accounting of any mining company), only Measured and Indicated resources do. However, it is inevitable to mine through some proportion of Inferred material because it is too expensive to convert all resources into Indicated and Measured categories.

In any event, one heuristic (although possibly plausible) mitigation strategy available to mine planners consists of generating a geostatistical risk map where the riskiest portions of the deposit are highlighted, so that once mine plans are generated, it is possible to visualize and avoid particularly risky portions of the orebody. This would allow deferring (sharing) the risk associated with the resources across the different time periods and increased predictability in meeting production targets. Note that these are important objectives for operational and financial motives as well. Whenever a (publicly listed) mining company reports to the market, it is typically expected to produce an estimate of the amount of metal to be realized; for example, a company might publicly state that it expects to produce 400 thousand ounces of gold and if such pre-established targets are not met, it may suffer severe financial penalization, be it in the form of a decrease in its stock price, a lowering of its creditworthiness leading to increased difficulty in financing, or others. Therefore, one key goal of geostatistical modeling of ore resources (and production planning) is not to "overcharge" any single period with an excessive volume of Inferred material.

The drawback of relying solely on a geostatistical map of grade uncertainty lies in the fact that uncertainty is only influenced by factors such as the number of available samples, their relative spatial distribution, and proximity (drilling pattern) as well as the underlying nature of the mineralization (e.g., very erratic in the case of gold, or, very continuous in the case of coal). It does not, *a priori*, have any association with the constraints shaping mining decisions to be taken in an optimized mining plan. It is, therefore, desirable to bridge the disconnect between geostatistical modeling on the one hand, and deterministic optimization on the other. This is achieved by means

of explicitly including constraints enforcing the requirement for a certain pre-specified composition of the mill feed, which accounts for mineral resource uncertainty.

The mine production scheduling model described in this thesis sheds light on and increases the visibility of the consequences resulting from the absence of ore resource classification parameters in current state-of-the-art stochastic (or deterministic) mine planning models. In the same spirit, a solution methodology is developed that is simple, but capable of addressing grade uncertainty as expressed in the form of various levels of risk in mine production plans.

## 6.2 Flowchart of Solution Methodology

The goal of the solution methodology presented in this dissertation is to provide an effective and practical tool for realistic mine production scheduling, that incorporates geological uncertainty, and also avoids the known "curse of dimensionality" associated with the traditional integer ($IP$), mixed integer linear programming ($MILP$), or even linear ($LP$) formulations of the ($OPMPSP$). The approach is distinct from others in the literature in that it explicitly incorporates traditional, industry accepted, ore resource classification categories, namely, the Inferred, Indicated and Measured categories in describing uncertainties associated with block grade estimation.

Similar to other related research (Dimitrakopoulos *et al.*, 2000), the prior generation of a set of geostatistical conditional simulations (GCS) is considered an important indispensable first task. This is because GCS provide a necessary account of the grade variability at the local scale, as well as the best current framework for the classification of ore resources into the traditional risk classification categories (although this task can be achieved by means of traditional geostatistical methods alone). Assuming GCS can be obtained from the ore modeling team or generated by mining engineers, each of the individual blocks is classified into an appropriate resource classification category. Although the specific details related to the process and techniques needed for generating GCS can be decisive (Journel & Kyriakidis, 2004), their in-depth treatment is considered beyond the scope of the present discussion (although a small qualitative example is provided in Section 4.2.

It is important to note that recent resource classification criteria are derived to offer a measure of the degree of uncertainty associated with a group of blocks (i.e., the volume corresponding to 3 months or 1 year production), rather than to individual blocks. In the proposed methodology a choice is made to first generate a mine production schedule, and only then verify if, relative to the set of all geostatistical conditional simulations, the required risk criteria are met. For instance, one possible such criterion could consist of counting the number of times that a specific volume of material belongs to some resource classification category, out of the total number of GCS generated. If the risk threshold consists of a positive answer at least nine times out of ten, then clearly this would amount to a proxy for a ninety percent probability that said material belong to the specified resource category. Indeed, this result follows directly from the definition of the probability of an event "A" over an uncertainty space ω:

$$P(A) = E_{\omega}[I_{\omega}(A)] = \frac{1}{|\omega|}\sum_{\omega} I_{\omega}(A) \tag{6.1}$$

Where:

$E_{\omega}$: *expectation operator defined over the uncertainty space* $\omega$

$I_{\omega}(A)$: *Indicator variable for event A, over the uncertainty space* $\omega$

In the event that a mine plan, including risk constraints, meets all the required risk criteria, then the production schedule is adopted as the optimal plan. Alternatively, if the mine plan fails to meet the desired risk requirements, then the decision maker is able to choose among a set of alternatives which may include: (i) revisiting the original ore risk constraint parameters, and defining new ones if deemed appropriate; (ii) analyzing the tradeoff associated with the cost of investing more capital into drilling campaigns versus the potential benefit of reducing geological uncertainty or (iii) after consideration of the specific characteristics of the schedule obtained, simply choose to accept the additional risk associated with the current plan. If option one (i) is chosen, a new production schedule will be generated that is consistent with the new updated risk constraints. Also note that, by allowing the decision maker to modify the requirements regarding the uncertainty constraints, the practitioner is allowed to state, explicitly and transparently, the accepted degree of risk tolerance, as well as to better adjust to the present level of geological knowledge of the deposit. This is a crucial distinction between the proposed approach and current

practice: by allowing for the aforementioned modifications the new plans incorporate explicitly the decision maker's preferences and are more likely to meet the required risk criteria.

A condensed schematic diagram of the general steps involved in the proposed methodology is provided in Figure 6.3:

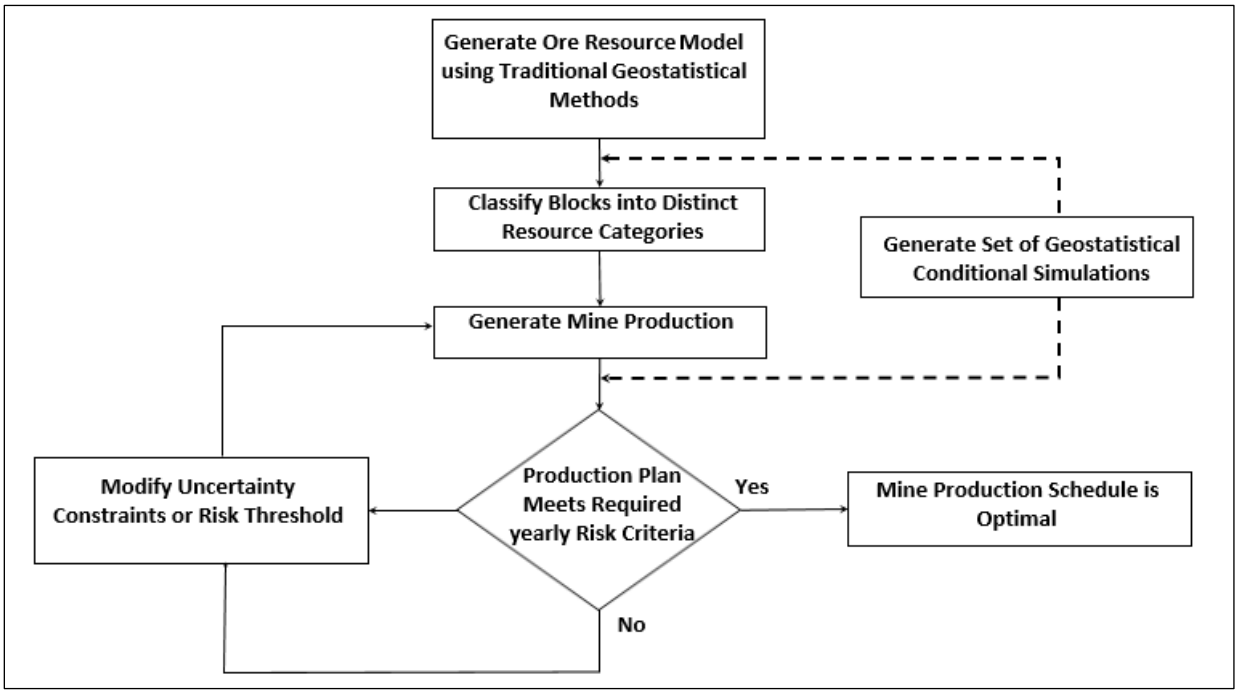


Figure 6.3: Schematic diagram of the steps of the proposed solution methodology. The dashed lines connected to GCS indicate distinct stages of the methodology in which these might be used.

This iterative process is the basis of the proposed methodology. In brief summary, the method proposed allows for controlling of the proportion (a user defined proportion) of material in each of the resource classification categories, exactly as a blending constraint, then running through the simulations and verifying if the derived mining schedule meets predefined risk criteria. The resource risk classification criteria are a proxy for the variability associated with the grade of the block, and when utilized according to the framework proposed herein, they are thought to be a definite improvement compared to the alternative of inspecting the grade of every block individually as is the case with fully stochastic solvers.

The generic stages of the proposed solution methodology, presented in condensed form in the schematic diagram of Figure 6.3, are further expanded and presented in Figure 6.4, in the view

of providing a detailed presentation of the individual steps in the methodology. The flowchart is in effect comprised of two distinct blocks; one which is referred to as the "optimization block," whose constituent elements are depicted in black, and a second block referred to as the "validation block," whose constituent elements are depicted in purple. The optimization block terminates once the entirety of the BZ algorithm is concluded and a deterministic optimal solution is obtained. However, said solution is considered provisional until it has met all the validation criteria in the second block, that is, until it can be verified that the plan satisfies some predefined risk threshold. Once an optimal plan passes satisfactorily through the validation block, it is accepted as an optimal plan and the overall solution procedure terminates.

The list of steps illustrated in the flowchart (see Figure 6.4) are described as follows:

STEP 1:

Read initial set of partitions ($V$)

STEP 2:

Solve the master problem ($MP$) and obtain the corresponding vector of duals ($\mu^0$)

STEP 3:

Check if the iteration counter $k$ (variable defining the current iteration number) is greater than one. If so, proceed to step 4 otherwise proceed to step 5

STEP 4:

Check if the current dual vector $\mu^k$ is equal to the previous iteration's dual vector $\mu^{k-1}$. If true, terminate the algorithm (optimization block) and proceed to step 9, otherwise, proceed to step

STEP 5:

Adjust the block values using dual vector extracted from the side constraints in the master problem ($MP$) and, setup the pricing subproblem ($SP$)

STEP 6:

Solve the pricing subproblem ($SP$) using the PseudoFlow algorithm

STEP 7:

Read the solution $v^k$ obtained from solving $(SP)$ in step 6 and generate a new set of partitions (set $V^k$)

STEP 8:

Check if the new partition set $V^k$ is equal to the previous partition set $V^{k-1}$ and, if so, terminate the algorithm (optimization block) and proceed to step 9; otherwise, proceed to step 2

STEP 9:

Check if plan meets the user-defined acceptable risk threshold; if so, the plan is accepted as an optimal plan; otherwise, re-start the algorithm by re-initializing the optimization block.

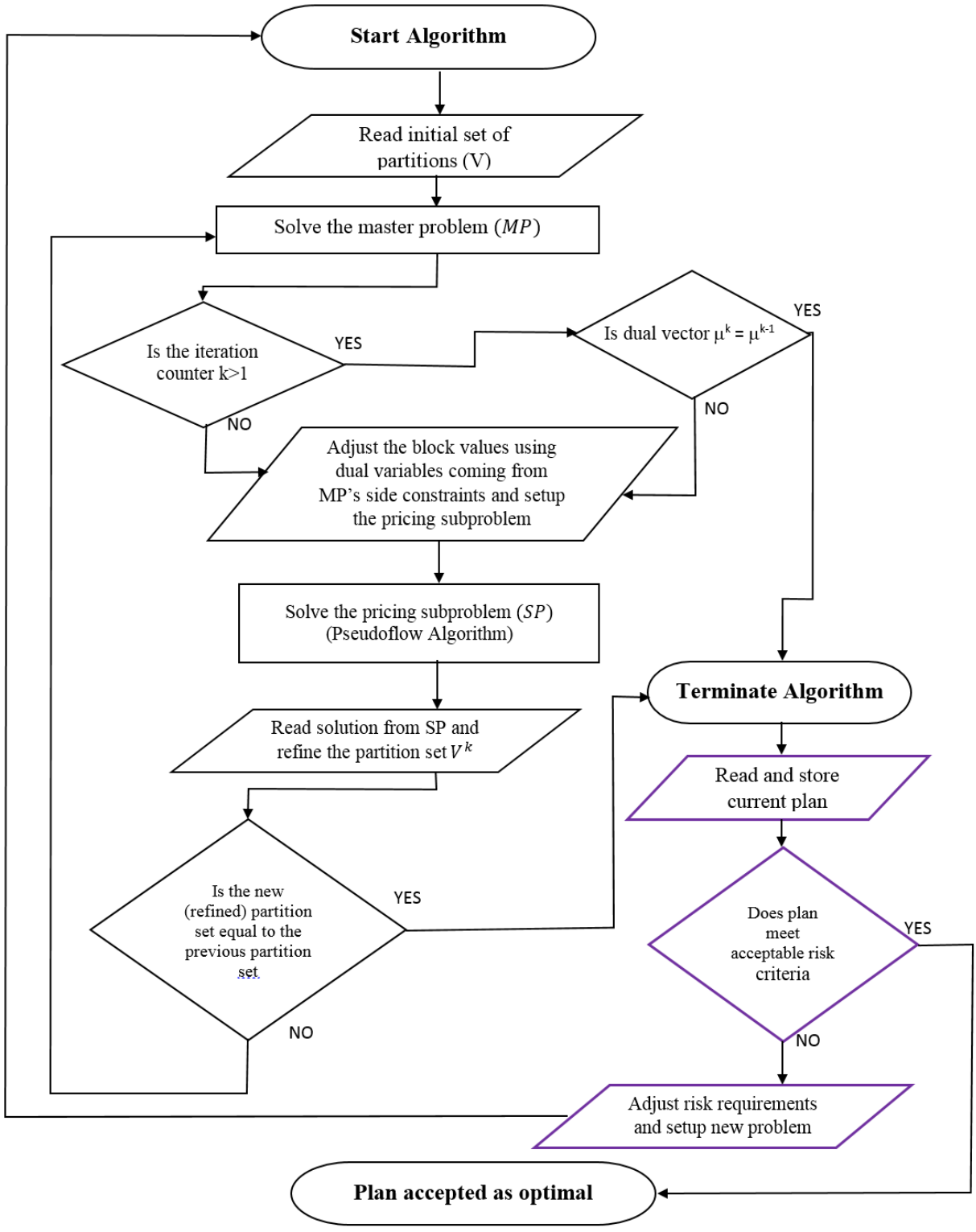


Figure 6.4: Solution methodology flowchart.

# CHAPTER 7.
# RISK-QUANTIFIED OPEN-PIT MINE PRODUCTION SCHEDULING UNDER UNCERTAINTY

.

The problem addressed in this research consists of a rendition of the Open Pit Mine Production Scheduling Problem ($OPMPSP$), which seeks to maximize NPV by determining when, if ever, an open pit mine block should be mined, and if mined, what is the most profitable destination where to send the previously mined block. The models include (per period): (i) minimum requirement and maximum resource capacity constraints, (ii) minimum and maximum average grade requirements for the mill feed, (iii) minimum and maximum average ore risk requirements for the mill feed, expressed in the form of specific targets for the proportions of Inferred, Indicated and Measured material. A deterministic risk-quantified formulation of $(OPMPSP)^r$ is presented, which excludes scenario-indexed decision variables. Furthermore, fractional solutions are allowed, as decision variables are modeled as continuous. Note, however, that said (deterministic) models include ore resource risk classification constraints and are solved under a probabilistic framework that allows for management to incorporate its degree of risk tolerance by specifying whether the schedules generated meet some desired (predefined) risk threshold.

In addition, the models are general enough that multiple block destinations can be considered, allowing the optimal block destination to be selected during the solution procedure, as a function of the state of the overall mining system at a certain point in time. Moreover, the solution algorithms adopted produce exact provably optimal solutions.

The models formulated incorporate the following underlying assumptions:

- Ore blocks can be mined over a continuum of time periods, rather than being mined fully in a single time period.
- The operation holds no stockpiles.

The first model assumption is an indispensable requirement for modeling the $(OPMPSP)$ as a linear program, with continuous variables. The second assumption has implications regarding the importance of stockpiles and their respective modeling in mine production scheduling.

Ideally, mining operations should avoid adopting stockpiles since these necessarily involve additional maintenance and re-handling costs that add to the overall operational cost structure. However, practice shows that, as a result of operational and economic uncertainty, specifically, the challenges with determining future fleet downturn and future evolution of commodity prices, most mines do choose to hold stockpiles as a hedging strategy against risk. For example, mine stockpiles can be used to sustain the mill plant operation, in the event that ore excavators break down, and reallocation of transportation equipment is required. Similarly, mine stockpiles allow for lower grade (marginal) ore material to be stored, rather than sent to the waste dump, if it is believed that future commodity prices will rise significantly enough that currently marginal ore might be considered profitable in the near future. Exclusion of ore material stockpiling (or destinations other than the mill plant and the Waste Dump) in the models is that such hedging strategies cannot be captured. However, it is reasonable to consider that the model formulation could include stockpiles with some additional research.

Finally, although the models proposed are intended to address long-term mine production schedules, it is anticipated that, given appropriate adjustments to time resolution and per-period constraint parameters, the models can be applicable to short-term production planning as well.

## Risk Quantified Open Pit Mine Production Scheduling Problem Formulation

We present a detailed formulation of the Risk Quantified Open Pit Mine Production Scheduling Problem which adheres accurately to the set of problems modeled and solved in this research. Indeed, apart from expanding the constraint sets, the sole distinction from the generic variant of $(OPMPSP)$ resides in the inclusion of risk constraints defining, *a priori*, the risk composition of the mill plant feed. Owing to the fact that risk uncertainty constraints are present, we refer to the new problem as $(OPMPSP)^r$ with the "$r$" superscript standing for "risk." In our notation we keep an additional parameter index "$r$" to better differentiate the treatment of the

specific resource classification component of the model from the remaining capacity constraints (although the notation could arguably be simplified by using a single index "$d$" for destination).

The detailed formulation of $(OPMPSP)^r$ is as follows:

Indices and Sets:

$b \in B$: $set\ of\ all\ blocks\ b$

$b' \in B_b \subseteq B$: $set\ of\ blocks\ b'\ that\ must\ be\ extrated\ before\ block\ b\ (block\ b'\ precedes\ block\ b)$

$b \in B^I \subseteq B$: $set\ of\ all\ blocks\ b\ classified\ into\ the\ Inferred\ resource\ category$

$b \in B^j \subseteq B$: $set\ of\ all\ blocks\ b\ classified\ into\ the\ Indicated\ resource\ category$

$b \in B^k \subseteq B$: $set\ of\ all\ blocks\ b\ classified\ into\ the\ Measured\ resource\ category$

$d \in D$: $set\ of\ all\ destinations\ d\ (1 = mill\ Plant, 2 = waste\ dump)$

$t \in T$: $set\ of\ all\ time\ periods\ t$

$r \in R$: $set\ of\ all\ operational\ resources, such\ that$:

$r = 1\ refers\ to\ processing\ capacity$

$r = 2\ refers\ to\ mining\ capacity$

$f \in F$: $set\ of\ all\ operational\ resources\ associated\ solely\ with\ the\ composition\ of\ the\ mill\ feed$:

$f = 1\ refers\ to\ the\ proportion\ of\ Inferred\ material\ in\ the\ mill\ feed$

$f = 2\ refers\ to\ the\ proportion\ of\ Indicated\ material\ in\ the\ mill\ feed$

$f = 3\ refers\ to\ the\ proportion\ of\ Measured\ material\ in\ the\ mill\ feed$

Data:

$v_{bt}$: $net\ present\ value\ (NPV)\ generated\ by\ extracting\ block\ b\ in\ period\ t$ ($)

$a_{rb}$: $nonnegative\ amount\ of\ operational\ resource\ r\ associated\ with\ block\ b$

$g_b$: $estimated\ ore\ grade\ associated\ with\ block\ b\ (\frac{units\ of\ metal}{units\ of\ weight})$

$\underline{e}_{rt}$: $nonnegative, minimum\ required\ target\ for\ operational\ resource\ r\ in\ period\ t\ (ton)$

$\bar{e}_{rt}$: $nonnegative\ maximum\ required\ target\ for\ operational\ resource\ r\ in\ period\ t\ (ton)$

$\underline{h}_{ft}$: $nonnegative\ minimum\ target\ for\ the\ proportion\ of\ material\ belonging\ to\ mineral\ resource\ classification\ \ category\ f, at\ the\ mill\ feed\ in\ time\ period\ t\ (percent)$

$\bar{h}^{ft}$: $nonnegative\ maximum\ target\ for\ the\ proportion\ of\ material\ belonging\ to\ mineral\ resource\ classification\ \ category\ f, at\ the\ mill\ feed\ in\ time\ period\ t\ (percent)$

$\underline{G_t}\backslash\overline{G_t}$: $minimum\ and\ maximum\ average\ grade\ targets\ for\ the\ mill\ feed\ in\ period\ t$

$\overline{M_t}$: $maximum\ total\ (ore\ plus\ waste)\ mining\ capacity\ in\ time\ period\ t$

Decision Variables:

$x_{bdt} = the\ fraction\ of\ block\ b, that\ is\ extracted\ in\ time\ period\ t, and\ sent\ to\ destination\ d$

Objective Function:

$$(OPMPSP)^r \quad \max \sum_{b\in B}\sum_{d\in D}\sum_{t\in T} v_{bdt}x_{bdt} \tag{7.1}$$

Constraints:

Block Precedence:

$$\sum_{d\in D}\sum_{t'<t} x_{bdt'} \le \sum_{d\in D}\sum_{t'<t} x_{b'dt'} \qquad \forall b \in B, b' \in B_b, t \in T \tag{7.2}$$

Maximum Processing Capacity at mill plant:

$$\sum_{b\in B} a_{1b}x_{b1t} \le \bar{e}_{1t} \qquad \forall\, t \in T \tag{7.3}$$

Minimum Processing requirement at mill plant:

$$-\sum_{b\in B} a_{1b}x_{b1t} \le -\underline{e}_{1t} \qquad \forall\, t \in T \tag{7.4}$$

Total Mining Capacity:

$$\sum_{b\in B} a_{1b}x_{b1t} + \sum_{b\in B} a_{2b}x_{b2t} \le \overline{M}_t \qquad \forall t \in T \tag{7.5}$$

Maximum Proportion of Inferred Material in the mill feed:

$$\sum_{b\,\in\, B^I} x_{b1t} - \bar{e}_{1t}\sum_{b\in B} x_{b1t} \le 0 \qquad \forall t \in T \tag{7.6}$$

Minimum Proportion of Inferred Material in the mill feed:

$$\underline{e}_{1t} \sum_{b \in B} x_{b1t} - \sum_{b \in B^I} x_{b1t} \leq 0 \quad \forall t \in T \tag{7.7}$$

Maximum Proportion of Indicated Material in the mill feed:

$$\sum_{b \in B^j} x_{b1t} - \bar{e}_{2t} \sum_{b \in B} x_{b1t} \leq 0 \quad \forall t \in T \tag{7.8}$$

Minimum Proportion of Indicated Material in the mill feed:

$$\underline{e}_{2t} \sum_{b \in B} x_{b1t} - \sum_{b \in B^j} x_{b1t} \leq 0 \quad \forall t \in T \tag{7.9}$$

Maximum Proportion of Measured Material in the mill feed:

$$\sum_{b \in B^k} x_{b1t} - \bar{e}_{3t} \sum_{b \in B} x_{b1t} \leq 0 \quad \forall t \in T \tag{7.10}$$

Minimum Proportion of Measured Material in the mill feed:

$$\underline{e}_{3t} \sum_{b \in B} x_{b1t} - \sum_{b \in B^k} x_{b1t} \leq 0 \quad \forall t \in T \tag{7.11}$$

Maximum Allowable Average Grade in the mill feed:

$$\sum_{b \in B} (g_b - \overline{G}_t) x_{b1t} \leq 0 \quad \forall t \in T \tag{7.12}$$

Minimum Allowable Average Grade in the mill feed:

$$\sum_{b \in B} (\underline{G}_t - g_b) x_{b1t} \leq 0 \quad \forall t \in T \tag{7.13}$$

Maximum Mineable Block Proportion:

$$\sum_{d \in D} \sum_{t \in T} x_{bdt} \leq 1 \quad \forall b \in B \tag{7.14}$$

$$\sum_{d \in D} \sum_{t' \leq t} x_{bdt} \leq 1 \quad \forall b \in B, t \in T \tag{7.15}$$

Decision Variable Domain:

$$x_{bdt} \in [0,1] \qquad \forall b \in B, t \in T, d \in D \qquad (7.16)$$

The objective function (7.1) seeks to maximize the discounted value of all extracted blocks across all destinations and time periods. Constraints (7.2) enforce block precedence requirements between a block $b$ and its predecessor blocks $b'$ by ensuring that the cumulative proportion of block $b$ (mined in period $t$ or earlier), across all destinations $d$ is not greater than the cumulative proportion of any of its predecessor blocks $b'$ mined in time period $t$ or earlier. Constraints (7.3) enforce an upper bound on the maximum milling capacity at the mill plant. Constraints (7.4) enforce lower bounds on the yearly minimum milling requirement at the mill plant. Note that for implementation reasons (i.e., to conform to the format expected by the BZ algorithm) the formulation slightly modifies lower bounding constraints so as to expresses them in the form of upper bounding constraints.

Constraints (7.5) enforce yearly maximum total (ore plus waste) mining capacity. Constraints (7.6) and (7.7) enforce yearly maximum and minimum limits on the proportion of Inferred material in the mill feed. Constraints (7.8) and (7.9) enforce maximum and minimum limits on the proportion of Indicated material in the mill feed. Similarly, constraints (7.10) and (7.11) enforce maximum and minimum limits on the proportion of Measured material in the mill feed. Constraints (7.12) and (7.13) enforce upper and lower bounds on the average grade in the mill feed. Constraints (7.14) restrict the total mineable proportion of any given block $b$ across all destinations and time periods, not to exceed the totality of the block. Constraints (7.16) ensure all decision variables assume continuous values between zero and one.

# CHAPTER 8.
# SOLUTION ALGORITHMS ADOPTED FOR RISK-QUANTIFIED OPEN-PIT MINE PRODUCTION SCHEDULING UNDER UNCERTAINTY

Due to the "curse of dimensionality" and the large scale of realistic instances of the ($OPMPSP$), many researchers adopt heurist or metaheuristic methods to solve their models. Part of said techniques include: Tabu Search algorithms (Lamghari *et al*., 2012, 2014), Simulated Annealing algorithms (Godoy *et al*., 2002; Montiel *et al*., 2015), and a hybrid of Simulated Annealing and Particle Swarm (Goodfellow *et al*., 2015) among others.

Although Heuristic solvers have the advantage of producing good quality solutions in reasonable amounts of time (Kirkpatrick, 1983; Sattarvand & Niemann-Delius, 2013), they introduce an additional layer of uncertainty, because these methods are highly sensitive on (user-defined) initial and boundary conditions, so that one cannot be certain that the solution obtained is truly optimal, even if all problem parameters are known with absolute certainty. This poses the question of how much should one care about modeling and adequately characterizing uncertainty in cases in which the deviations from optimality caused by grade uncertainty may be small compared to the ones resulting from a heuristic modeling approach?

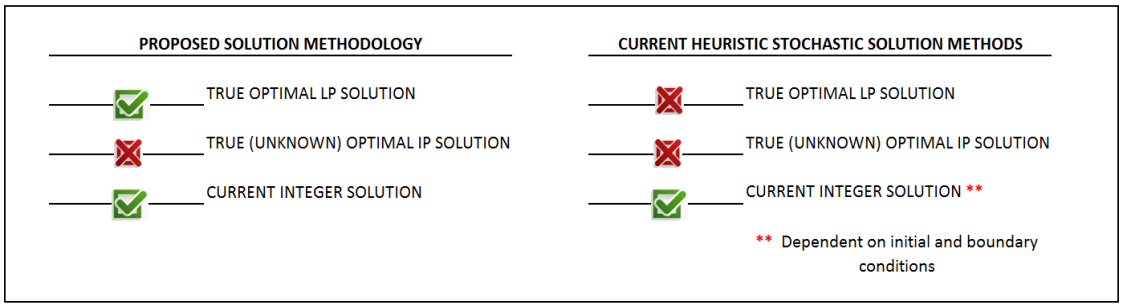


Figure 8.1: Comparison of the characteristics of solutions to proposed methodology vs. current heuristic stochastic solution methods.

It is, therefore desirable to define a provably optimal starting point from where to look for optimal solutions. The most current literature frequently alludes to two related streams of research as being the most promising: (i) the Bienstock-Zuckerberg (BZ) algorithm by Bienstock and Zuckerberg (2009, 2010, 2015) and (ii) the improvements and extensions to BZ introduced by Espinoza *et al.* (2012, 2014, 2016) leading to the OMP Solver; an academic research software developed by the authors.

The framework proposed in this dissertation for addressing uncertainty relies extensively on the incorporation of both the Bienstock-Zuckerberg algorithm (Bienstock & Zuckerberg, 2009, 2010, 2015) and the PseudoFlow algorithm (Hochbaum, 2001, 2008). In effect, the Bienstock-Zuckerberg algorithm (BZ) can be made significantly more competitive if the PseudoFlow algorithm is integrated within its steps and used to solve the successive subproblems which arise at each iteration and constitute an integral part of its solution procedure. Given their importance to the overall methodology, both algorithms are discussed in greater detail in the subsequent sections.

## 8.1 The Bienstock-Zuckerberg Algorithm (BZ)

At present, the BZ Algorithm is regarded as the most effective algorithm for solving to proven optimality linear programming relaxations of the $(OPMPSP)$. In a recent journal article, Munoz *et al.* (2016) discuss the BZ algorithm within the context of Delayed Column Generation algorithms, and show that BZ applies to a broader class of Resource Constrained Project Scheduling Problems $(RCPSP)$ of which the $(OPMPSP)$ can be thought of as a special case. Similar to the formal discussions in Munoz *et al.* (2016), we introduce the BZ algorithm from an initial vector algebra perspective followed by more traditional framing of the algorithm in terms of large-scale decomposition techniques. Also, we strive to be (mostly) consistent with the notation therein.

Let $V = \{\vec{v}_1, \vec{v}_2, \dots, \vec{v}_n\}$ be the matrix containing the set of vectors $\vec{v}_i \in R^n$, $i = 1, .., n$. Then the span of $V$ is defined as:

$$Span\ (V) = \{x_i \in R^n:\ x_i = c_1\vec{v}_1 + c_2\vec{v}_2 + \cdots + c_n\vec{v}_n,\quad c_i \in R^n\ \ \forall i\}$$

Let $lin.Hull(V)$ the linear hull of be the smallest linear space spanned by $V$. Also, let $B = \{\vec{b}_1, \vec{b}_2, \dots, \vec{b}_n\}$ be a set of linearly independent vectors $\vec{b}_i, i = 1, \dots, n$. Then $B$ is a basis for the subspace $S$ iff: $S = span(\vec{b}_1, \vec{b}_2, \dots, \vec{b}_n)$

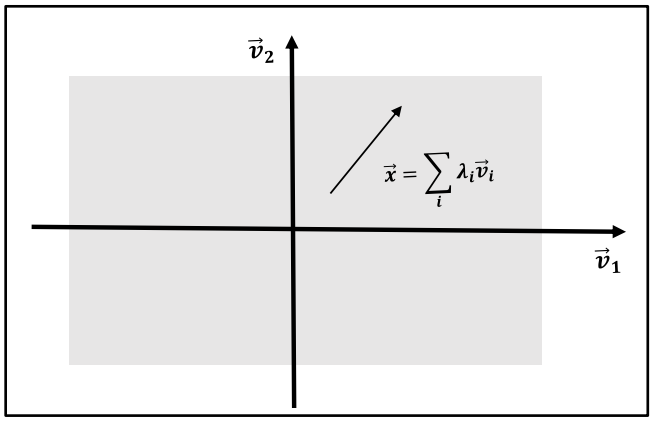


Figure 8.2: Vector $\vec{x} \in lin.hull(\vec{v}_1, \vec{v}_2)$, i.e., vector $\vec{x}$ can be expressed as a linear combination of the vectors in the set $V\{v_1, v_2\}$.

In Figure 8.2 above, the (orthogonal) vectors $\vec{v}_1$ *and* $\vec{v}_2$ span the entirety of $R^2$ and the vector $\vec{x}$ belongs to $lin.hull(V)$ because it can be expressed as a linear combination of vectors $\vec{v}_1, \vec{v}_2$. Similarly, the convex hull for a set of points $X \in R^n$ is defined as the minimal convex set containing the set $X$ (Figure 8.3).

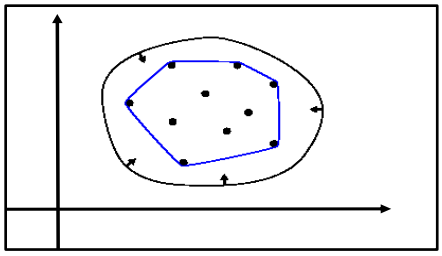

Figure 8.3: The convex hull is represented by the region in space encircled by the blue line and the set $X$ corresponds to the black points on display.

Let $V = \{\vec{v}_1, \vec{v}_2, \dots, \vec{v}_n\}$ be the matrix containing the set of vectors $\vec{v}_i \in R^n$, $i = 1, .., n$. Then, the convex hull of $V$, is referred to as $con.hull(V)$, and is defined as the set of all convex linear combinations of the vectors $\vec{v}_i$:

$$con.hull(V) = \{y_i \in R^n : y_i = c_1\vec{v}_1 + c_2\vec{v}_2 + \cdots + c_n\vec{v}_n, 0 \leq c_i \leq 1, \sum_{i=1}^{n} c_i = 1\}$$

The convex hull can be thought of as the set that would result from allowing a rubber band to collapse around the set of extreme points in Figure 8.3 above (the rubber band corresponding to the outer black circle in the figure).

The Bienstock-Zuckerberg algorithm belongs in the same category as the General Column Generation algorithms (Munoz *et al.*, 2016). This class of algorithms is most effective when the structure of the problem addressed is such that the number of decision variables $x \in R^n$ is very large relative to the number of effective constraints $Gx \leq g;\ G \in R^{mxn}$; i.e., whenever $|n| \gg |m|$. Also, from elementary linear programing theory, it can be shown that at any extreme point solution $x_b = G_b^{-1}e$ the number of basic variables (those whose value is different than zero) is at most $|m|$, and the remaining $|n - m|$ are non-basic variables $x_{nb}$ with value: $x_{nb} = 0$, meaning they do not contribute to the current solution (Bertsimas & Tsitsiklis, 1997). The fact that a number smaller than the cardinality of the full set of decision variables might be sufficient to determining the problem's optimal solution $x^*$ is a crucial observation for General Column Generation algorithms (GCG). Figure 8.4 illustrates this same concept via a hypothetical optimization problem defined in decision variables $v_i \in R^3$. The initial feasible region (image on the left), expressed as a function of the three unit vectors $\vec{v}_1, \vec{v}_2$ and $\vec{v}_3$, is equivalent to the feasible region on the right, if only unit vectors $v_2$and $v_3$ are considered.

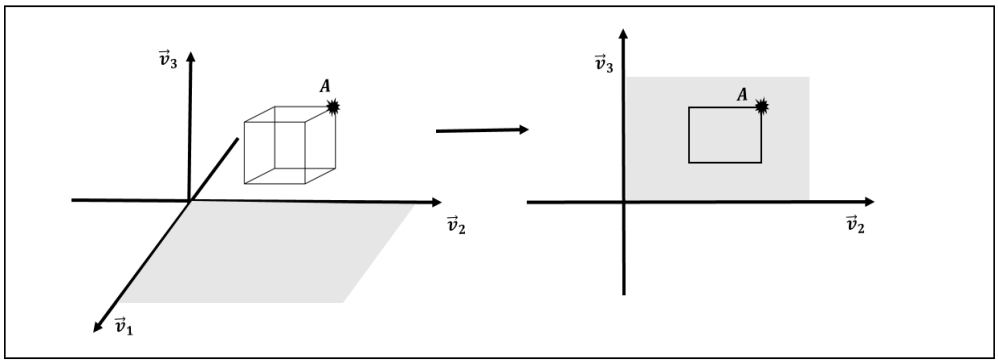


Figure 8.4: Solution to optimization problem defined in $R^3$. The initial LP feasible region defined by the cube on the left is reduced to the new LP feasible region on the right by collapsing (setting to zero) the axis corresponding to decision variable $v_1$. (Objective function contour omitted for clarity).

Assuming the optimal solution to the LP problem corresponds to extreme point "$A,$" and that this point resides in the plan defined by $\overline{v_2 v_3}$, then it is clear that an optimal solution to the LP problem can be found if only decision variables $v_2$ and $v_3$ are basic (and $v_1$ is non-basic).

In effect, the key insight of GCG algorithms is to take advantage of said observation to avoid directly solving the full original problem, and instead, decompose the initial problem into two "smaller" problems, usually referenced as the "Master" and the "Pricing" subproblems. The algorithm may start from the assumption of an initial feasible solution to the master problem, and successively solve the pricing subproblem to generate new incoming variables (columns) to add to the master problem. It is useful to briefly recall some of the principles underlying such algorithms.

Considering problems of the form:

$$max \quad c'x \tag{8.1}$$

$$s.t. \quad Dx \leq d \tag{8.2}$$

$$Ex \leq 0 \tag{8.3}$$

$$Ix \leq 1 \tag{8.4}$$

$$x \geq 0 \tag{8.5}$$

Define the polyhedron $P = \{x \in \{0,1\}^n : Ex \leq 0;\ Ix \leq 1\}$ and let the set $V = \{\vec{v}_1, \vec{v}_2, \dots, \vec{v}_n\}$ constitute a basis for the $lin.hull(P)$. Then, by definition, any vector $\vec{x} \in lin.hull(p)$ can be expressed as:

$$\vec{x} = \sum_{i=1}^{n} \lambda_i \vec{v}_i\ , \quad for\ \lambda_i \in R \tag{8.6}$$

The GCG algorithm calculates an upper bound on a relaxed version of the problem, expressed in the form:

$$max \quad c'x \tag{8.7}$$

$$s.t. \quad Dx \leq d \tag{8.8}$$

$$Ex \leq 0 \tag{8.9}$$

$$Ix \leq 1 \tag{8.10}$$

$$x \in lin.hull(P) \tag{8.11}$$

By the variable substitution in equation (8.6) the problem can be rewritten as:

$$max \quad c'V\lambda \tag{8.12}$$

$$s.t. \quad DV\lambda \leq d \tag{8.13}$$

$$EV\lambda \leq 0 \tag{8.14}$$

$$IV\lambda \leq 1 \tag{8.15}$$

In the spirit of GCG algorithms, Dantzig and Wolfe developed a large-scale decomposition algorithm named the Dantzig-Wolfe decomposition algorithm ($DW$) after the authors. At the time, the motivation for their efforts was to exploit the fact that certain optimization problems tend to display a specific block diagonal (or block angular) structure, which makes them particularly amenable to decomposition algorithms (Dantzig & Wolfe, 1961). Instances of such problems include network-flow problems with multiple commodities, or resource allocation problems with competing activities. An example of a block diagonal structure problem is given below:

$$min \quad c_1x_1 + C_2x_2 + \cdots + c_Tx_T \tag{8.16}$$

$$s.t. \quad A_1x_1 + A_2x_2 + \cdots + A_Tx_T = b \tag{8.17}$$

$$B_1x_1 \leq b_1 \tag{8.18}$$

$$B_2x_2 \leq b_2 \tag{8.19}$$

$$\ldots \tag{8.20}$$

$$B_Tx_T \leq b_T \tag{8.21}$$

Apart from the block of constraints in equation (8.17), the set of problem constraints defining the feasible region consists of blocks of decision variables which are independent of each other. This suggests an effective solution methodology for such problems, by decomposition into several smaller subproblems which can then be solved separately (and more efficiently). By contrast to GCG algorithms, the DW algorithm solves for problems expressed as so:

$$max \quad c'x \tag{8.22}$$

$$s.t. \quad Dx \leq d \tag{8.23}$$

$$Ex \leq 0 \tag{8.24}$$

$$Ix \leq 1 \tag{8.25}$$

$$x \in conv.hull(P) \tag{8.26}$$

Given that the $conv.hull(P)$ is a subset of $P$, i.e., $conv.hull(P) \subseteq P$, equations (8.24) and (8.25) can be omitted, and the problem might be rewritten as:

$$max \quad c'x \tag{8.27}$$

$$s.t. \quad Dx \leq d \tag{8.28}$$

$$x \in conv.hull(P) \tag{8.29}$$

Again, by the variable substitution in equation (8.6), a new problem can be rewritten as:

$$max \quad c'V\lambda \tag{8.30}$$

$$s.t. \quad \lambda.1 = 1 \tag{8.31}$$

$$DV\lambda \leq d \tag{8.32}$$

$$\lambda \geq 0 \tag{8.33}$$

Let $\lambda^j$ be an optimal solution to the master problem at iteration $j$, and let ($x^j = V^j\lambda^j$) be the corresponding feasible solution to the original problem. Let $\pi^j$ be the dual vector associated with constraints $DV\lambda \leq d$. Assuming an initial feasible solution is available (or can be found), the

algorithm might start by using the dual prices corresponding to the current solution of the master problem to solve a Pricing subproblem given by:

$$SP(v) \qquad \max \quad c'v - \pi'(Dv - d) \tag{8.34}$$

$$s.t.\ Ev \leq 0 \tag{8.35}$$

$$Iv \leq 1 \tag{8.36}$$

$$v \in \{1, 0\}^n \tag{8.37}$$

If $v^j$ is a solution to the current $SP^j(v)$ then it is added as a new column to the master problem until for two consecutive iterations $SP^{j-1}(v) = SP^j(v)$ or, equivalently, if the set of dual values is unchanged for two consecutive iterations, that is, $\pi^{j-1} = \pi^j$. At termination, the optimal solution to the original LP problem is expressed as a convex linear combination of the successive solution values for the individual pricing subproblems that are generated (see Figure 8.5).

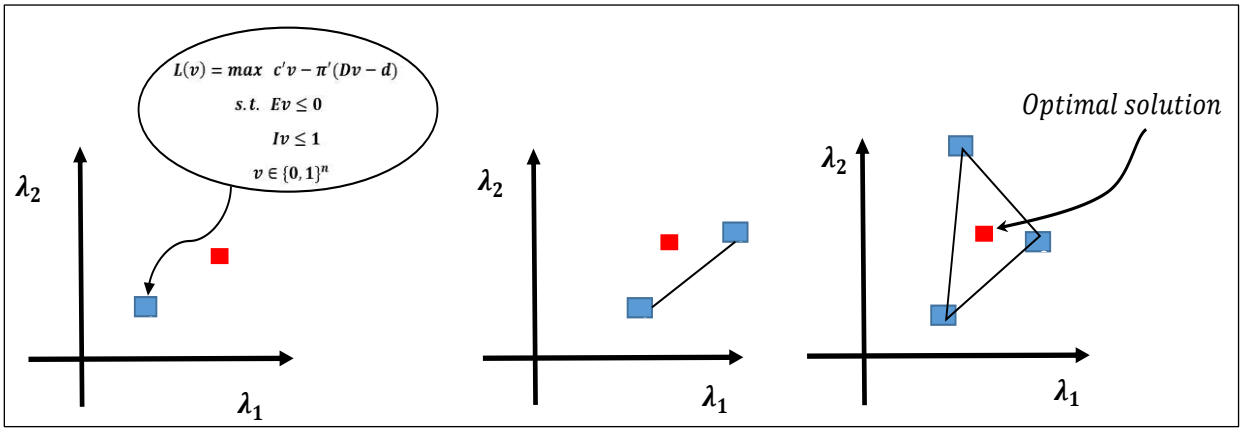


Figure 8.5: From left to right, consecutive iterations of the DW algorithm originate new columns $v^j$ which can be mapped to the master space and be represented as the blue dots in the graphs. The LP optimal solution is a convex linear combination of the blue dots.

Johnson (1968) is credited with having first applied the DW decomposition principle to a mine production scheduling problem. In his and subsequent discussions, including by Picard (1976), Barnes (1980) and Dagdelen (1985), further intuition is provided as to the specific meaning of the individual problems in the context of mining. In particular, it is noted that the pricing subproblem results simply in the classical ultimate pit limit (or max closure) problem with the values for the individual blocks adjusted by a factor of the dual prices. Thus, the algorithm initiates

with feasible solutions for the closure problem, which are unlikely to be close to optimal columns for the master problems at the onset. The algorithm proceeds to rely on the duals generated from the master problems to "shape" the solutions originated at the pricing subproblems by adjusting the values of relevant individual blocks and guiding the problem to convergence.

Recall that for a maximization problem, the DW master problem objective constitutes a lower bound on the objective function value of the original problem. This is intuitive to see since both problems are exactly equal except for the fact that the feasible region of the DW master problem is a subset of the original problem's feasible region. Likewise, the pricing subproblem provides an upper bound on the original problem since it is equivalent to exactly rewriting the original problem with the exception that the side constraints $Dv \leq d$ are dualized (moved to the objective function) and penalized with the dual vector $\pi'$. The algorithm stops when either: i) two consecutive iterations of the pricing problem produce the same solution or ii) two consecutive iterations of the master problem produce the same dual vector.

Similar to the DW algorithm, the BZ algorithm fits into the category of GCG algorithms. However, in the case of the BZ algorithm, the vector columns in the set that constitutes a basis for the original problem space form an orthogonal set; that is, for each individual column in the set $\overrightarrow{v_i}.\overrightarrow{v_j} = 0$ which, in a mining context, means the two columns do not share any block. Also, at each iteration the new set $V^{k+1}$ generates a space which includes the previous iterations solutions $z^k$. The sets $V^k$are obtained by a process referred to as the "refining procedure" by Muñoz *et al*. (2016).

The refining process consists of obtaining a new generator matrix $V^k$, by performing set intersection and set difference operations on $V^{k-1}$ and the current solution to the subproblem $v^k$. The authors define set intersection operations as such: for two vectors $x, y \in \{0,1\}^n$, define $x \cap y \in \{0,1\}^n$ such that: $(x \cap y)_i = 1 \; iff \; x_i = 1$ and $y_i = 1$. Additionally, set difference operations are defined as such: for two vectors $x, y \in \{0,1\}^n$, define $x \backslash y \in \{0,1\}^n$ such that $(x \backslash y)_i = 1$ iff $x_i = 1$ and $y_i = 0$.

Assuming $V^k$ is comprised of $\{v^1, \dots, v^r\}$ then $V^{k+1}$ is matrix a of non-zero vectors obtained as:

$$\{v^j \wedge \hat{v}: 1 \leq j \leq r\} \cup \{v^j \backslash \hat{v}: 1 \leq j \leq r\} \cup \left\{\hat{v} \backslash \left(\sum_{j=1}^{k} v^j\right)\right\} \tag{8.38}$$

Given that each of the solutions $\hat{v}$ to the subproblem can be thought of as representing a physical pit (closure), then it is intuitive to think of the set intersection and difference operations as the intersections and differences of distinct mine pits (Figure 8.6 and Figure 8.7). This is what occurs through the refining process which yields the matrix $V^k$.

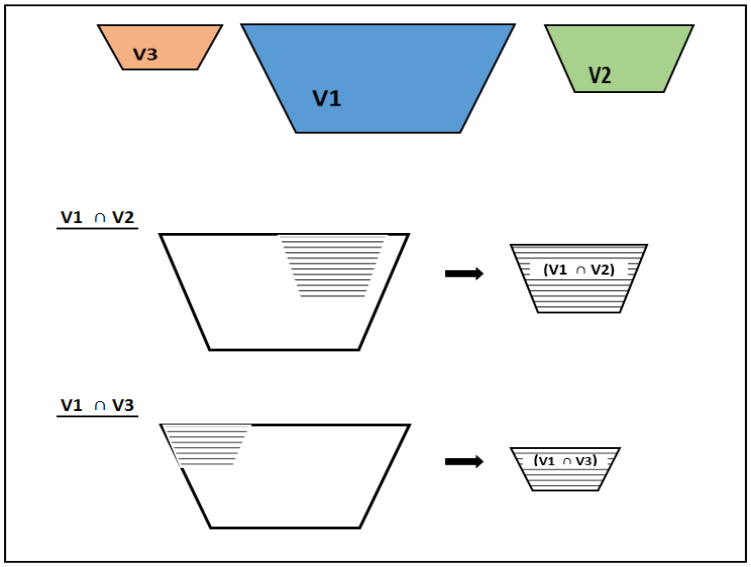


Figure 8.6: "Physical" depiction of set-intersection operations.

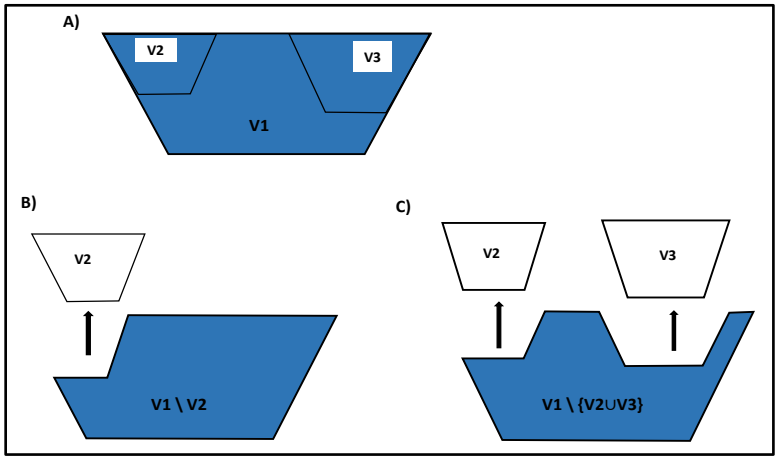


Figure 8.7: "Physical" depiction of set-difference operations. A) Three initial sets are shown together, although resulting from different consecutive iterations. B) Set difference operation $v_1 \backslash v_2$ and C) Set difference operation $v_1 \backslash \{v_2 \cup v_3\}$.

Using terminology from set algebra, Bienstock and Zuckerberg refer to the columns $v^j$ as "partitions" (as in set partitions), and indicate that for each such individual partition the non-zero member elements of the set all assume the same value, i.e., $x_i = x_j \; if \; x_i, x_j \in v^k$. Hence, a potentially large number of individual variables can be eliminated, being replaced by a single variable ($\lambda_i$) representing the entire set, resulting in dramatic reductions on the size of decision variables and originating large sets of redundant problem constraints which can also be eliminated. It is important to note, however, that this observation could already have been made with regards to the DW algorithm and, therefore, in our view it does not in fact constitute a differentiating factor.

The key advantage of the BZ algorithm relative to DW resides in the fashion in which consecutive solutions to the pricing subproblems are used in the general algorithmic scheme. Although both algorithms include and define the same exact class of subproblems, in the case of the DW algorithm, the solutions $v^k$ generated at each iteration "$k$" are mapped "directly" (exactly as they are, coming from the subproblem) into the space of the restricted master problem; resulting in a newly generated data point on the space defined on "$\lambda$." It is from the convex combination of said data points that the DW algorithm attempts at reaching optimality, but, by the same token, there exists an inherent risk that the total number of data points to be enumerated until optimality is reached be very large. For instance, in Figure 8.8 a notional example polyhedron is provided to further illustrate this point. It can be seen that in a pathological case, the number of extreme point solutions potentially visited (the set of corners along the surface) can be quite large.

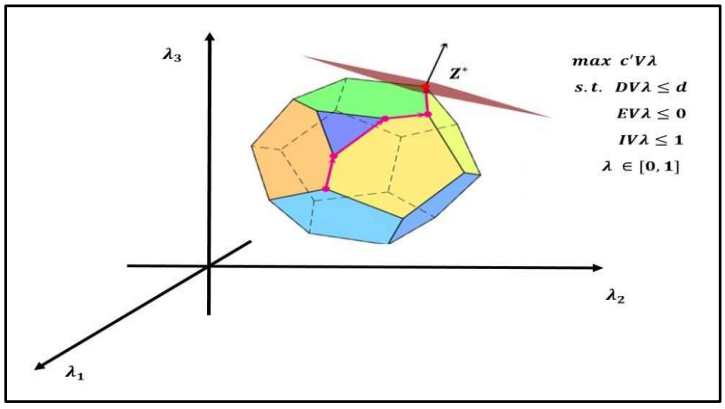


Figure 8.8: Enumeration of extreme point solutions in the DW algorithm. The algorithm travels across the extreme points of the feasibility polyhedron until an optimal solution $x^*$ maximizing the objective function $Z^*$ is reached.

On the contrary, in the case of the BZ algorithm the pricing subproblem solutions $v^k$ generated at each iteration are not mapped directly into the master problem space, but are instead combined with the set of preexisting solutions $V^{k-1}$, to refine it, and generate a new set of orthogonal columns $\vec{v}_i$, which span the entire space of the decision variables $\lambda_i$ in the master problem. Each new orthogonal column $\vec{v}_i$ is associated to a new decision variable $\lambda_i$ in the master problem. The idea is that an orthogonal column, by adding a new decision variable ($\lambda_i$) to the master problem, be the equivalent of adding a new axis to the problem space along which it can be represented. Here again resides an important distinction between the two algorithms, namely in that, at each iteration of the DW a single data point is generated, whereas with BZ the number of columns generated might grow in the order of $(2|V^k| + 1)$, with $|V^k|$ defined as the cardinality of the current set of columns $v^j$. Figure 8.9 emphasizes and makes clear the distinct behavior of both algorithms:

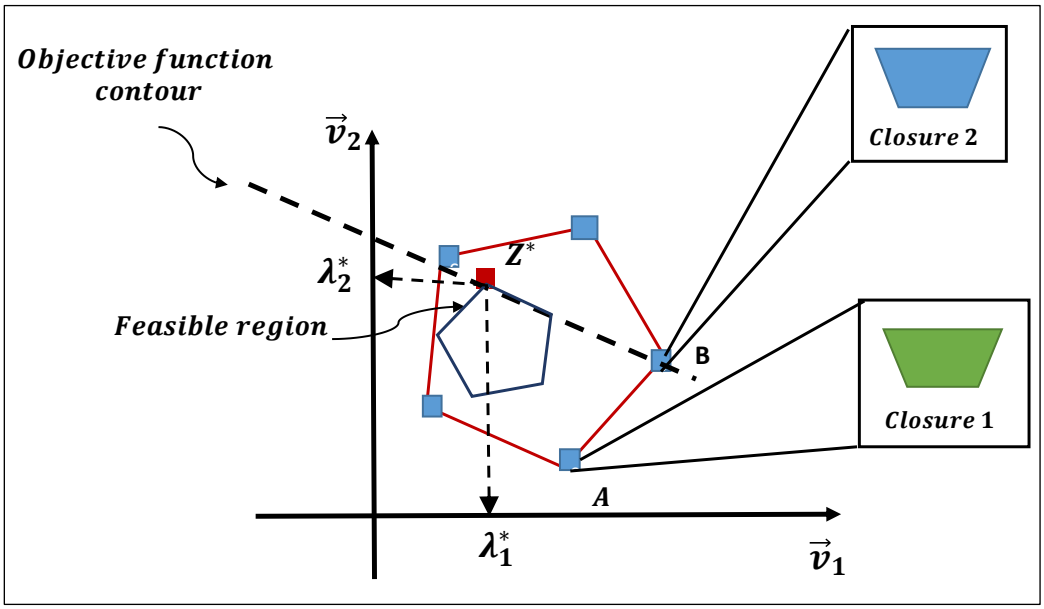


Figure 8.9: Qualitative differences between the BZ and DW algorithms. The convex hull defined by the set of points (blue squares) illustrate the DW algorithm is contrasted with the two orthogonal axes ($\vec{v}_1, \vec{v}_2$) associated with decision variables ($\lambda_1$, $\lambda_2$), in the BZ master problem.

It should be noted that the convex hull (represented by the red lines in Figure 8.9) is associated with the constraint set $P = \{EV\lambda \leq 0;\ IV\lambda \leq 1\}$. Recall, however, that the constraint set

$DV\lambda = d$ defines a distinct polyhedron which further constrains the feasible region of the original problem and has one extreme point coinciding with extreme point $Z^*$.

Considering that two consecutive closures $v^i$ and $v^{i+1}$ are generated from two consecutive solutions to the subproblem, then in the case of the DW algorithm, the closures are mapped as the data points "A" and "B," respectively. Note that at the current iteration, the DW algorithm can only look for the optimal solution in the *line segment* uniting point "A" to point "B," for that corresponds to the linear convex combination of the two data points available so far. In other words, the DW algorithm does not currently "see" beyond the line segment defined by $\overrightarrow{AB}$. In fact, the convex hull of the DW is not fully defined *a priori*, but is "revealed" (exposed) as the iterations progress and new data points are generated. The optimal objective function value $Z^*$ and the optimal solution ($x^*$) are expressed as linear combinations of the decision variables $\lambda_i$:

$$x^* = \sum_i (v_i)\lambda_i \tag{8.39}$$

$$Z^* = \sum_i (c_i v_i)\lambda_i \tag{8.40}$$

Note that we differentiate the closures ($v_i$) used in the DW algorithm from the orthogonal partitions ($\vec{v}_i$) used in the BZ algorithm by omitting the vector arrow (in the first case) and preserving it (in the second case).

Contrary to the DW, in the case of the BZ algorithm, it is not a new data point that is originated by the second closure, but rather *a new axis* $\vec{v}_2$ (associated with a new decision variable $\lambda_2$) with which to solve the master problem. Note that by the introduction of a new axis, the new set of refined orthogonal vectors $\{\vec{v}_1, \vec{v}_2\}$ spans the entirety of $R^2$, and the totality of data points (extreme points) in the figure is exposed. In particular, this means that the true optimal solution $x^*$ corresponding to the optimal objective function value $Z^*$ is already available, and can be reached by some linear combinations of the decision variables $\lambda_i$. Stated differently, we have:

$$x^* = \sum_i (\vec{v}_i)\lambda_i \tag{8.41}$$

$$Z^* = \sum_i (c_i \vec{v}_i)\lambda_i \tag{8.42}$$

### 8.1.1 Algorithmic Steps of the Bienstock- Zuckerberg Algorithm

In what follows, the key steps of the BZ algorithm are presented. In doing so, we first describe the problem to be solved, show how it is decomposed into a Master problem and a (pricing) subproblem, present them, and finally, describe how they are used within the scheme of the Bienstock-Zuckerberg algorithm.

Let us assume a general formulation of the scheduling problem ($OPMPSP$) in the form:

$$(OPMPSP) \quad max \quad c'x \tag{8.43}$$

$$s.t. \quad Dx \leq d \tag{8.44}$$

$$Ex \leq 0 \tag{8.45}$$

$$Ix \leq 1 \tag{8.46}$$

$$x \in [0,1] \tag{8.47}$$

Where the $x \in R^n$ vector is the decision variable vector establishing whether or not to mine a given block $b$ in time period $t$, the $E$ matrix includes the constraints associated with the block precedence constraints, the $I$ matrix contains the constraints relating to the "finitude" of all blocks and the matrix $D$ represents all constraints other than precedence or finitude of blocks. The block of constraints associated with the matrix $D$ might include, among others, capacity (or demand) constraints, blending (and/or risk) constraints, and is often referred to as the group of "side" or "hard" constraints because their presence destroys the underlying network structure of the ($OPMPSP$) (Johnson 1968). Indeed, it is the recognition of said network structure - and the fact the network problems can often be solved efficiently - that motivates a decomposition strategy which divides the original problem into two easier to solve problems, typically named: the "Restricted master problem" ($MP$) and the "Pricing Subproblem" ($SP$). In the context of discussing the BZ algorithm, we refer to the master problem as ($BZ^{MP}$) and to the subproblem as ($BZ^{SP}$).

Considering that the $(OPMPSP)$ is tendentially a multi-time-period problem, i.e., that due to resource limitations mine production typically spans across a range of time periods, it is helpful to present the $(OPMPSP)$ in its multi-time-period form.

$$(OPMPSP) \quad max \quad c_1x_1 + c_2x_2 + c_3x_3 + \cdots + c_Tx_T \tag{8.48}$$

$$s.t. \quad Dx_1 \leq d_1 \tag{8.49}$$

$$Dx_2 \leq d_2 \tag{8.50}$$

$$\cdots$$

$$Dx_T \leq d_T \tag{8.51}$$

$$Ex_1 \leq 0 \tag{8.52}$$

$$Ex_1 + Ex_2 \leq 0 \tag{8.53}$$

$$\cdots$$

$$Ex_1 + Ex_2 + \cdots + Ex_T \leq 0 \tag{8.54}$$

$$Ix_1 + Ix_2 + \cdots + Ix_T \leq 1 \tag{8.55}$$

$$x_t \in [0,1] \qquad \forall t \tag{8.56}$$

For clarity of exposition, facilitating an easier comprehension of the steps in the algorithm, the $(OPMPSP)$ is assumed re-stated in terms of $\lambda$ variables, such as in equations (8.12) – (8.15), so that a definition of both the master and the pricing subproblem can ensue.

Let $V_t$ represent the matrix containing only the period $t$ subsets of the vector columns in the partition matrix $V^j$, and $\lambda_t$ represent only the period $t$ subset of the full column vector $\lambda$, then the multi-time-period formulations of the BZ master problem can be re-stated as follows:

$$(BZ)^{MP} \quad max \quad c_1V_1\lambda_1 + c_2V_2\lambda_2 + c_3V_3\lambda_3 + \cdots + c_TV_T\,\lambda_T \tag{8.57}$$

$$s.t. \quad DV_1\lambda_1 \leq d_1 \tag{8.58}$$

$$DV_2\lambda_2 \leq d_2 \tag{8.59}$$

$$\cdots$$

$$DV_T\lambda_T \leq d_T \tag{8.60}$$

$$EV_1\lambda_1 \leq 0 \tag{8.61}$$

$$EV_1\lambda_1 + EV_2\lambda_2 \leq 0 \tag{8.62}$$

...

$$EV_1\lambda_1 + EV_2\lambda_2 + \cdots + EV_T\lambda_T \leq 0 \tag{8.63}$$

$$IV_1\lambda_1 + IV_2\lambda_2 + \cdots + IV_T\lambda_T \leq 1 \tag{8.64}$$

$$\lambda_t \in [0,1] \quad \forall t \tag{8.65}$$

Similarly, the Pricing subproblem for the BZ is one that results from dualizing the set of hard constraints in the original problem, i.e., moving said constraints to the objective function and penalizing potential constraint violations, such that a new (easier) problem containing only block precedence and finitude constraints can be solved. Let $\pi_t$ define the vector of dual variables associated with the block of hard constraints $DV_t\lambda_t \leq d_t$, then $(BZ)^{SP}$ can be stated as follows:

$$\begin{aligned}\left(BZ_j\right)^{SP} \; max \; & c_1v_1 + c_2v_2 + \ldots + c_Tv_T - \pi_1(Dv_1 - d_1) \\ & - \pi_2(Dv_2 - d_2) - \ldots - \pi_T(Dv_T - d_T)\end{aligned} \tag{8.66}$$

$$s.t. \quad Ev_1 \leq 0 \tag{8.67}$$

$$Ev_1 + Ev_2 \leq 0 \tag{8.68}$$

...

$$Ev_1 + Ev_2 + \cdots + Ev_T \leq 0 \tag{8.69}$$

$$Iv_1 + Iv_2 + \cdots + Iv_T \leq 1 \tag{8.70}$$

$$v_t \in [0,1] \tag{8.71}$$

Recall at this stage that the vector $v$ represents solution values of so-called "at" decision variables, and that stated in this form, the network structure of $(BZ)^{SP}$ is not readily apparent. However, this new problem does in fact have an underlying network structure and, in Section 8.3

we review in greater detail how $(BZ)^{SP}$ can be solved very efficiently by incorporating the PseudoFlow algorithm.

The BZ algorithm can be initiated with either an original set of values for the dual vector associated with the side constraints or, with the choice of an original configuration for the set of partitions. However, for our discussions we will assume without loss of generality, a given initial set of partitions is readily available.

Assuming initial values for the matrix $V^0$ (i.e., an initial set of partitions), set the iteration counter $j$ to one and proceed as follows:

STEP 1:

Solve the BZ master problem for iteration $j$:

$$(BZ)^{MP} \quad max \quad c_1V_1\lambda_1 + c_2V_2\lambda_2 + c_3V_3\lambda_3 + \cdots + c_TV_T\lambda_T \tag{8.72}$$

$$s.t. \quad DV_1\lambda_1 \leq d_1 \tag{8.73}$$

$$DV_2\lambda_2 \leq d_2 \tag{8.74}$$

$$\cdots$$

$$DV_T\lambda_T \leq d_T \tag{8.75}$$

$$EV_1\lambda_1 \leq 0 \tag{8.76}$$

$$EV_1\lambda_1 + EV_2\lambda_2 \leq 0 \tag{8.77}$$

$$\cdots$$

$$EV_1\lambda_1 + EV_2\lambda_2 + \cdots + EV_T\lambda_T \leq 0 \tag{8.78}$$

$$IV_1\lambda_1 + IV_2\lambda_2 + \cdots + IV_T\lambda_T \leq 1 \tag{8.79}$$

$$\lambda_t \in [0,1] \quad \forall t \tag{8.80}$$

STEP 2:

Read the values for the dual vector $\pi_t^j$ associated with the period $t$ hard constraints and proceed to step 3

STEP 3:

Check if $\pi_t^j = \pi_t^{j-1}$ for all periods $t$. If true, then stop: the current solution $x^* = V^{j-1}\lambda^{j-1}$ is optimal. Else, proceed to step 4

STEP 4:

Solve the BZ Pricing subproblem for the $j^{th}$ iteration:

$$\left(BZ_j\right)^{SP} \quad max \;\; c_1v_1 + c_2v_2 + \ldots + c_Tv_T \;\; - \pi_1(Dv_1 - d_1) - \pi_2(Dv_2 - d_2) - \ldots - \pi_T(Dv_T - d_T) \tag{8.81}$$

$$s.t. \quad Ev_1 \leq 0 \tag{8.82}$$

$$Ev_1 + Ev_2 \leq 0 \tag{8.83}$$

$$\ldots$$

$$Ev_1 + Ev_2 + \cdots + Ev_T \leq 0 \tag{8.84}$$

$$Iv_1 + Iv_2 + \cdots + Iv_T \leq 1 \tag{8.85}$$

$$v_t \in [0, 1] \tag{8.86}$$

STEP 5:

Let $v^j$represent an optimal solution to $\left(BZ_j\right)^{SP}$. If $v^j = v^{j-1}$ then STOP; the current problem solution is optimal, i.e., $x^* = V^{j-1}\lambda^{j-1}$ is optimal. Else, proceed to step 6

STEP 6:

Obtain a new set of non-overlapping partitions by refining $V^{j-1}$ using the current solution $v^j$ and following the refining rules defined below to obtain the new partition set $V^j$.

STEP 7:

Increment the iteration counter $j$ by one unit and proceed to step 1

In what follows we describe the BZ Algorithm more formally as pseudocode:

**DESCRIPTION**: An algorithm to solve a feasible LP relaxation of $(OPMPSP)^r$

**INPUT**: A feasible instance of $(OPMPSP)^r$, and an initial partition set $V^0$

**OUTPUT**: An optimal set of decision variables $\lambda^*$ such that an optimal solution $x^*$ to the original $(OPMPSP)$ can be determined: $x^* = \lambda^* V^*$.

Said solution will obey block precedence constraints, system capacity\demand constraints, as well as grade and resource risk blending constraints.

{

/* set the iteration counter $j$ to one, set the current partition set $V$ to $V^0$, and assume an initial feasible solution to the Pricing subproblem $v^i$ */

j ←1; $V^0 \leftarrow V$; $v^0 \leftarrow v^i$

Solve $(BZ_j)^{MP}$

/* Read the values for the dual vector $\pi_t \ \forall t$ associated with the period $t$ hard constraints, and update the vector of duals $\pi_t^j$ */

$\pi_t^j \leftarrow \pi_t$

/* If two consecutive vectors of duals are equal, then stop, the current solution is optimal. Define the optimal solution to the original $(OPMPSP)^r$ as: $x^* = V^{j-1}\lambda^{j-1}$ and break the "while" loop. Otherwise, proceed to solve the Pricing subproblem $(BZ_j)^{SP}$ */

If $(\pi^j = \pi^{j-1})$ then {

$V^* \leftarrow V^j = V^{j-1}$

$x^* \leftarrow V^{j-1}\lambda^{j-1}$

break while

}

else {

Solve $(BZ_j)^{SP}$

$v^j \leftarrow v$

}

/* If the new solution $v^j$ to the Pricing subproblem $(BZ_j)^{SP}$ equals the previous solution $v^{j-1}$, then stop; the set of partitions $V^{j-1}$ is optimal. Define the optimal solution to the

original $(OPMPSP)^r$ as: $x^* = V^{j-1}\lambda^{j-1}$. Otherwise, use the current solution $v^j$ to execute the refining operations and generate a new partition set matrix $V^j$ */

If $\left(v^j = v^{j-1}\right)$ then{

$$V^* \leftarrow V^j = V^{j-1}$$

$$x^* \leftarrow V^{j-1}\lambda^{j-1}$$

break while

}

else {

$$V^j = \left\{v^j \wedge \hat{v}: 1 \le j \le r\right\} \cup \left\{v^j \backslash \hat{v}: 1 \le j \le r\right\} \cup \left\{\hat{v} \backslash \left(\sum_{j=1}^{k} v^j\right)\right\}$$

}

/* Update the iteration counter $j$ to start a new iteration. */

$$j \leftarrow j + 1$$

/* Move to repeat the iteration loop until either of the two conditions for the "while" loop is not met, i.e., until two consecutive vectors of duals are equal or until two consecutive solutions to the Pricing problem are equal */

While $((v^j \neq v^{j-1})\ and\ (\pi^j \neq \pi^{j-1}))$

}

### 8.1.2 Small Numerical Example of the Bienstock–Zuckerberg Algorithm

The Bienstock-Zuckerberg algorithm was studied for its validity and effectiveness in solving LP relaxations of the Open Pit Mine Production Scheduling Problem ($OPMPSP$) and, in this context, the arguments underlying the algorithm have very specific (and intuitive) physical interpretations which we attempt to highlight.

Consider a synthetic numerical example in the form of the 2-D block model presented in Figure 8.10, and the application of the steps of the BZ algorithm as described in Section 8.1.1.

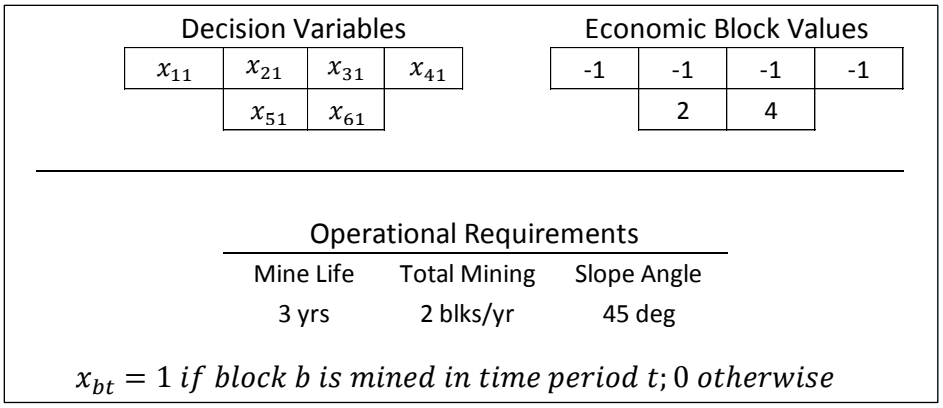


Figure 8.10: Two-dimensional block model, including original economic block values, as well as the operational requirements for the problem considered.

This simple mine plan considers only two destinations (mill and waste dump), spans through 3 years, includes an upper bounding constraint on the total yearly mining capacity of 2 blocks per year, and 45-degree pit wall slope angle requirements. In order for the BZ algorithm to be applicable, it is assumed that the original problem is stated in the following matrix form:

$$max \quad Z = c_1x_1 + c_2x_2 + c_3x_3 \tag{8.87}$$

$$s.t. \quad D_1x_1 \leq d_1 \tag{8.88}$$

$$D_2x_2 \leq d_2 \tag{8.89}$$

$$D_3x_3 \leq d_3 \tag{8.90}$$

$$E_1x_1 \leq 0 \tag{8.91}$$

$$E_1x_1 + E_2x_2 \leq 0 \tag{8.92}$$

$$E_1x_1 + E_2x_2 + E_3x_3 \leq 0 \tag{8.93}$$

$$Ix_1 + Ix_2 + Ix_3 \leq 1 \tag{8.94}$$

$$x_t \in [0,1] \quad \forall t \tag{8.95}$$

The objective function (8.87) maximizes the NPV of the deposit. Constraints (8.88) - (8.90) impose an upper bound $d_t$ on the total amount of material (ore and waste) mined during each time period *t*. Mining precedence requirements are enforced by constraints (8.91) - (8.93). Block

finitude constraints are imposed by equation (8.94), and finally, constraint (8.95) ensures all decision variables are bounded to be between 0 and 1, i.e.; $x_i \in [0,1]\ \forall i$.

The algorithmic steps start by defining the initial matrix $V$, also referred to, originally, as the "partition set" by Bienstock & Zuckerberg. The correspondence between the presentation in Muñoz *et al*. (2016) and Bienstock & Zuckerberg's (2009) original presentation, is that the columns in the $V$ matrix are equivalent to the partition sets of the discussion in Bienstock & Zuckerberg.

STEP 1:
Defining the initial partition set ("$V$" matrix)

As alluded to in Section 8.1, it is a strict requirement for the application of the BZ algorithm that the partition set $V$ be comprised of disjoint columns $v$. This same condition is met in the column generation formalism of Muñoz *et al*. by ensuring that all the columns comprising the $V$ matrix are orthogonal to each other. The intuitive physical interpretation of this condition in the case of mining is that, at any given time period, none of individual partitions shares any blocks in common.

Although any feasible orthogonal set of partitions could have been used as the starting partition set, for simplicity, the initial set chosen is one whose individual columns consist of mining all the blocks in the pit in a single time period. Again, since all the mine blocks contained in a single set can be set equal to each other, this means that the initial individual decision variables for the distinct blocks in one set can be replaced by a single variable representing the entire set which will be referred to as "$\lambda_i$." Since the considered life of mine spans three time periods, then three starting sets are adopted, $\lambda_1, \lambda_2$, and $\lambda_3$ each representing a single partition set for periods 1, 2 and 3 respectively.

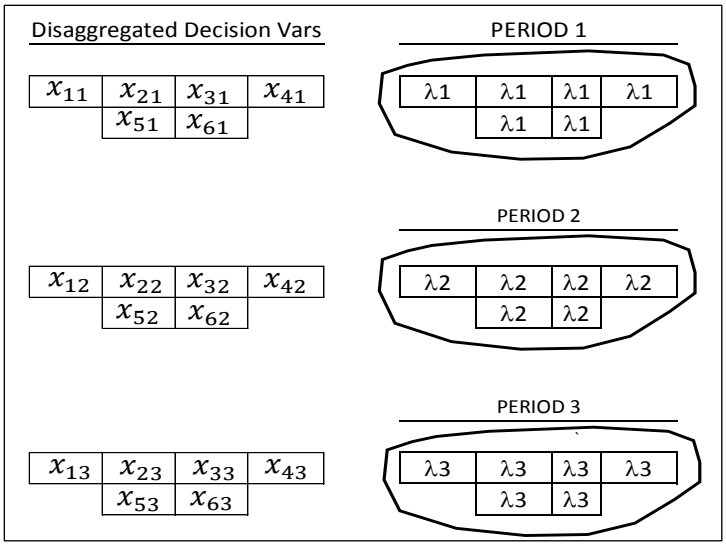


Figure 8.11: Initial grouping of the disaggregated blocks into individual aggregated partitions sets "$\lambda_i$."

Figure 8.11 above illustrates the initial grouping of blocks into distinct partition sets. For clarity of exposition, and given that the problem addressed is a multi-time period problem, it is convenient to conceptualize additional replicas of the ore deposit, one per time period, representing the possibility of mining a given block in either of the three time periods under consideration. Next, the initial (orthogonal) columns for the partition set $V$ are presented, and sided by a schematic depiction of the corresponding (conceptual) time-extended "physical" pits (see Figure 8.12).

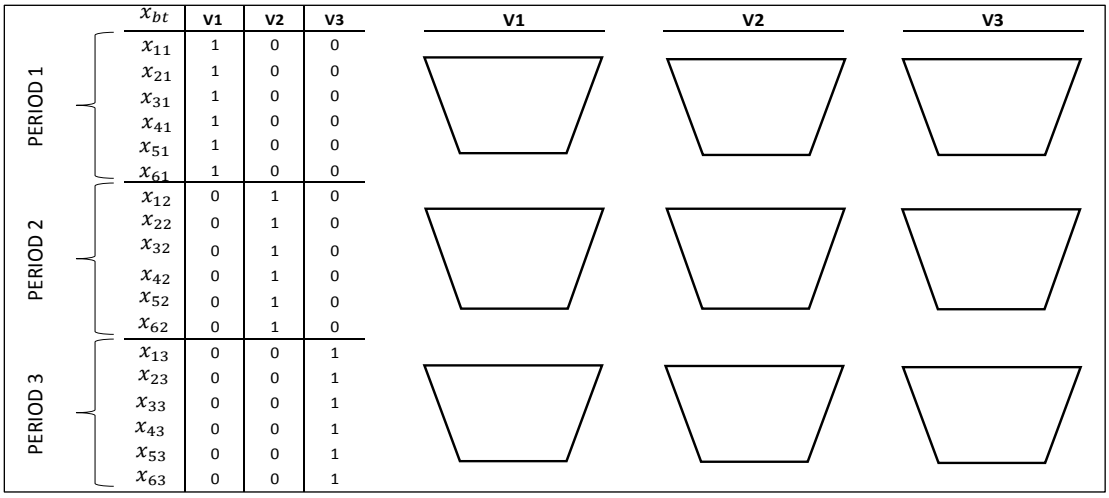


Figure 8.12: Initial partition sets $V^0$ for the three time period problem and their corresponding orthogonal "$v$" columns. Shaded areas correspond to the time period in which blocks are mined.

Figure 8.12 shows columns associated with mining decisions corresponding to mining a given block "at" time period *t*. It is noted, however, that this is not a strict requirement as one can obtain the same results using variables expressing the decision to mine a given block "by" time period *t*, instead. Figure 8.13 (below) presents economic block values for both "at" and "by" decision variables.

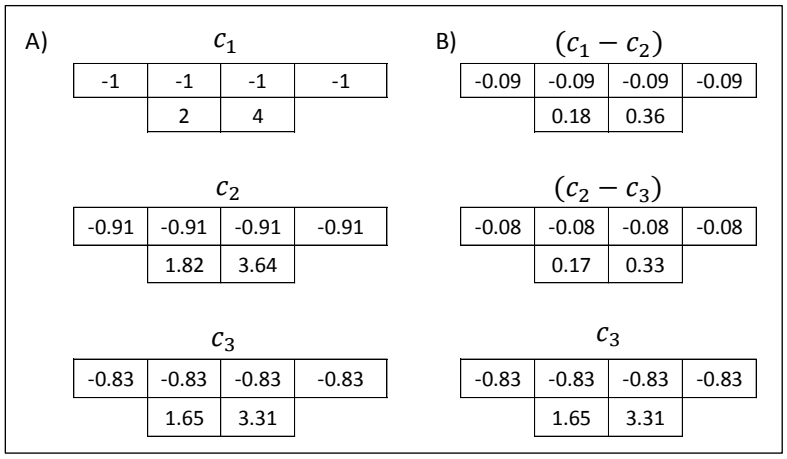


Figure 8.13: Discounted economic block values for (A) mining block *b* "at" time period *t*, and (B) mining block *b* "by" time period *t*. The yearly discount rate applied is 10%.

STEP 2:

Solving the restricted BZ master problem, presented in the form:

$$(BZ)^{MP} \qquad max \;\; c'V^j\lambda \tag{8.96}$$

$$subject\ to: \quad DV^j\lambda \leq d \tag{8.97}$$

$$EV^j\lambda \leq 0 \tag{8.98}$$

$$IV^j\lambda \leq 1 \tag{8.99}$$

$$\lambda \in [0,1] \tag{8.100}$$

At this stage, it is straightforward to derive the system of equations for the BZ master problem. The equation for the objective function in the master problem, as well as the equations containing the sets of constraints $Ex \leq 0$ and $Ix \leq 1$ and $Dx \leq d$ are expressed in terms of the $\lambda$ decision variables as $cV\lambda$, $EV\lambda \leq 0$, $IV\lambda \leq 1$ and $DV\lambda \leq d$, respectively.

Note that, in the simple example we consider, the $(Dx \leq d)$ block of constraints has the following generic fixed structure:

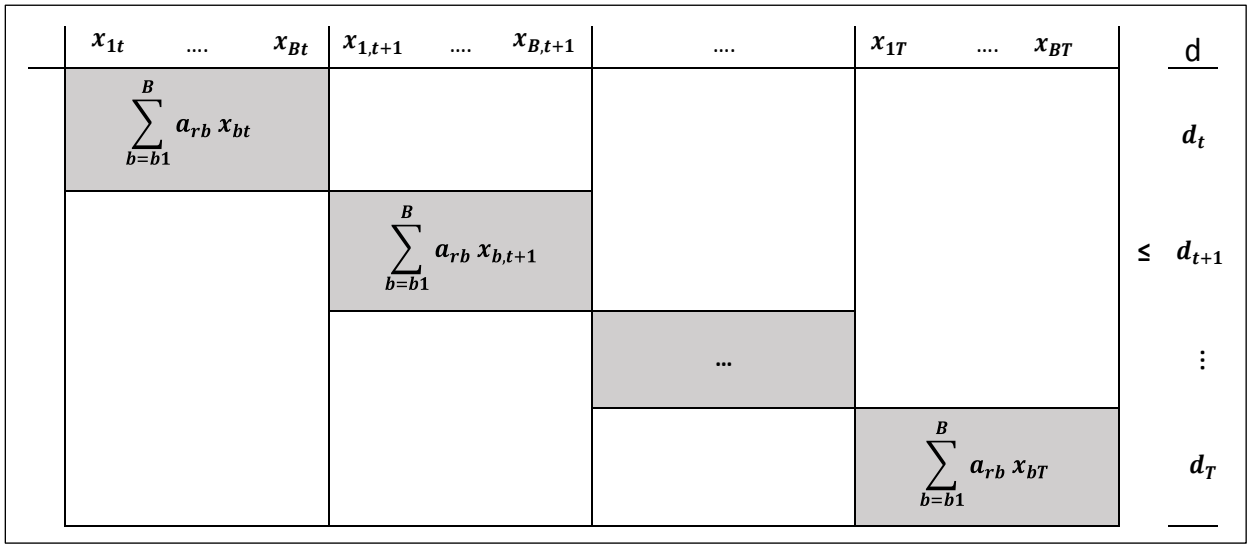


Figure 8.14: Block structure of the sparse precedence (*Dx*) matrix. Shaded areas correspond to non-zero entries.

Similarly, note that the $(Ex \leq 0)$ block of constraints corresponding to block precedence constraints has a generic fixed structure, as shown in Figure 8.15:

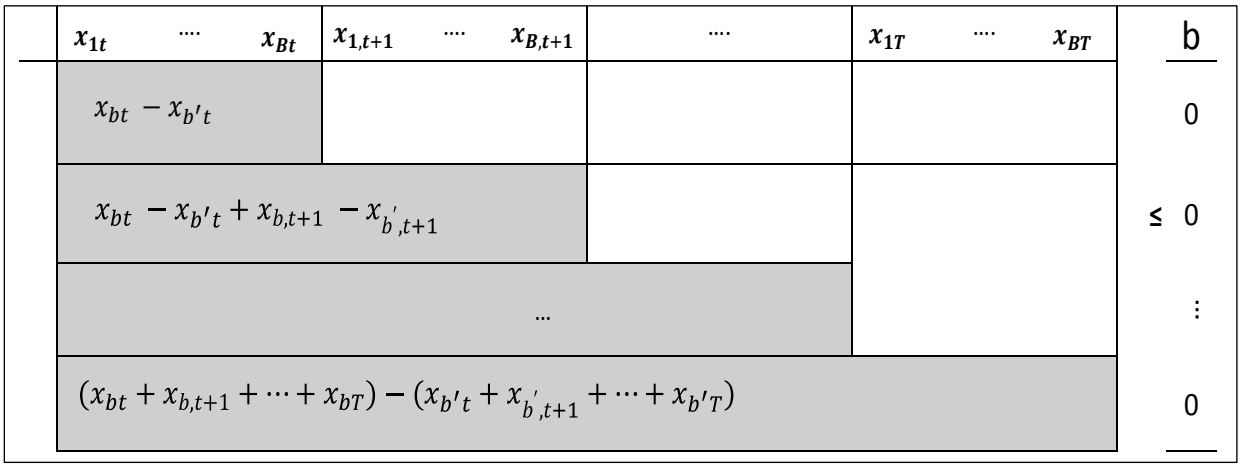


Figure 8.15: Block structure of the sparse precedence (*Ex*) matrix. Shaded areas correspond to non-zero entries. For each pair (*b*, *b*'), block *b*' is a predecessor block to *b*.

The $(Ix \leq 1)$ block of constraints has the following fixed structure:

| | $x_{1t}$ | .... | $x_{Bt}$ | $x_{1,t+1}$ | .... | $x_{B,t+1}$ | .... | $x_{1T}$ | .... | $x_{BT}$ | | b |
|---|---|---|---|---|---|---|---|---|---|---|---|---|
| | $x_{1t}$ | | + | $x_{1,t+1}$ | | + | ... | | + | $x_{1T}$ | | 1 |
| | | $x_{2t}$ | + | | $x_{2,t+1}$ | + | | ... | + | | $x_{2,t+1}$ | ≤ 1 |
| | | | | | | ... | | | | | | ⋮ |
| | | | $x_{Bt}$ | | + | $x_{B,t+1}$ | | + | ... | | + | $x_{BT}$ | 1 |

Figure 8.16: Block structure of the sparse finitude ($Ix$) matrix. Shaded areas correspond to non-zero entries. The summation of each individual block $b \in B$, across all time periods $t \in T$ must not exceed 1.

Referring specifically to the example under consideration and to the cost parameters in Figure 8.13, it is clear that the original objective function coefficients values corresponding to equation $z = cx$, are expressed as shown in Figure 8.17:

| | (cx) | | | | | | | | | | | | | | | | | |
|---|---|---|---|---|---|---|---|---|---|---|---|---|---|---|---|---|---|---|
| | $x_{11}$ | $x_{21}$ | $x_{31}$ | $x_{41}$ | $x_{51}$ | $x_{61}$ | $x_{12}$ | $x_{22}$ | $x_{32}$ | $x_{42}$ | $x_{52}$ | $x_{62}$ | $x_{13}$ | $x_{23}$ | $x_{33}$ | $x_{43}$ | $x_{53}$ | $x_{63}$ |
| | -1.00 | -1.00 | -1.00 | -1.00 | 2.00 | 4.00 | -0.91 | -0.91 | -0.91 | -0.91 | 1.82 | 3.64 | -0.83 | -0.83 | -0.83 | -0.83 | 1.65 | 3.31 |

Figure 8.17: Original objective function coefficients values.

The coefficients associated with the set of requirement constraints $Dx \leq d$ are expressed as shown in Figure 8.18. Recall that said constraints partake only in the BZ master problem and are not included in the Pricing subproblem.

| | (Dx) | | | | | | | | | | | | | | | | | | | (d) |
|---|---|---|---|---|---|---|---|---|---|---|---|---|---|---|---|---|---|---|---|---|
| | $x_{11}$ | $x_{21}$ | $x_{31}$ | $x_{41}$ | $x_{51}$ | $x_{61}$ | $x_{12}$ | $x_{22}$ | $x_{32}$ | $x_{42}$ | $x_{52}$ | $x_{62}$ | $x_{13}$ | $x_{23}$ | $x_{33}$ | $x_{43}$ | $x_{53}$ | $x_{63}$ | | |
| | 1 | 1 | 1 | 1 | 1 | 1 | 0 | 0 | 0 | 0 | 0 | 0 | 0 | 0 | 0 | 0 | 0 | 0 | | 2 |
| | 0 | 0 | 0 | 0 | 0 | 0 | 1 | 1 | 1 | 1 | 1 | 1 | 0 | 0 | 0 | 0 | 0 | 0 | ≤ | 2 |
| | 0 | 0 | 0 | 0 | 0 | 0 | 0 | 0 | 0 | 0 | 0 | 0 | 1 | 1 | 1 | 1 | 1 | 1 | | 2 |

Figure 8.18: Matrix coefficients for the system of equations $Dx \leq d$.

The specific values calculated for the system of equations $Ex \leq 0$ are given in Figure 8.19:

| (Ex) | | | | | | | | | | | | | | | | | | | (b) |
|---|---|---|---|---|---|---|---|---|---|---|---|---|---|---|---|---|---|---|---|
| $x_{11}$ | $x_{21}$ | $x_{31}$ | $x_{41}$ | $x_{51}$ | $x_{61}$ | $x_{12}$ | $x_{22}$ | $x_{32}$ | $x_{42}$ | $x_{52}$ | $x_{62}$ | $x_{13}$ | $x_{23}$ | $x_{33}$ | $x_{43}$ | $x_{53}$ | $x_{63}$ | | |
| -1 | 0 | 0 | 0 | 1 | 0 | 0 | 0 | 0 | 0 | 0 | 0 | 0 | 0 | 0 | 0 | 0 | 0 | | 0 |
| 0 | -1 | 0 | 0 | 1 | 0 | 0 | 0 | 0 | 0 | 0 | 0 | 0 | 0 | 0 | 0 | 0 | 0 | | 0 |
| 0 | 0 | -1 | 0 | 1 | 0 | 0 | 0 | 0 | 0 | 0 | 0 | 0 | 0 | 0 | 0 | 0 | 0 | | 0 |
| 0 | -1 | 0 | 0 | 0 | 1 | 0 | 0 | 0 | 0 | 0 | 0 | 0 | 0 | 0 | 0 | 0 | 0 | | 0 |
| 0 | 0 | -1 | 0 | 0 | 1 | 0 | 0 | 0 | 0 | 0 | 0 | 0 | 0 | 0 | 0 | 0 | 0 | | 0 |
| 0 | 0 | 0 | -1 | 0 | 1 | 0 | 0 | 0 | 0 | 0 | 0 | 0 | 0 | 0 | 0 | 0 | 0 | | 0 |
| -1 | 0 | 0 | 0 | 1 | 0 | -1 | 0 | 0 | 0 | 1 | 0 | 0 | 0 | 0 | 0 | 0 | 0 | | 0 |
| 0 | -1 | 0 | 0 | 1 | 0 | 0 | -1 | 0 | 0 | 1 | 0 | 0 | 0 | 0 | 0 | 0 | 0 | | 0 |
| 0 | 0 | -1 | 0 | 1 | 0 | 0 | 0 | -1 | 0 | 1 | 0 | 0 | 0 | 0 | 0 | 0 | 0 | ≤ | 0 |
| 0 | -1 | 0 | 0 | 0 | 1 | 0 | -1 | 0 | 0 | 0 | 1 | 0 | 0 | 0 | 0 | 0 | 0 | | 0 |
| 0 | 0 | -1 | 0 | 0 | 1 | 0 | 0 | -1 | 0 | 0 | 1 | 0 | 0 | 0 | 0 | 0 | 0 | | 0 |
| 0 | 0 | 0 | -1 | 0 | 1 | 0 | 0 | 0 | -1 | 0 | 1 | 0 | 0 | 0 | 0 | 0 | 0 | | 0 |
| -1 | 0 | 0 | 0 | 1 | 0 | -1 | 0 | 0 | 0 | 1 | 0 | -1 | 0 | 0 | 0 | 1 | 0 | | 0 |
| 0 | -1 | 0 | 0 | 1 | 0 | 0 | -1 | 0 | 0 | 1 | 0 | 0 | -1 | 0 | 0 | 1 | 0 | | 0 |
| 0 | 0 | -1 | 0 | 1 | 0 | 0 | 0 | -1 | 0 | 1 | 0 | 0 | 0 | -1 | 0 | 1 | 0 | | 0 |
| 0 | -1 | 0 | 0 | 0 | 1 | 0 | -1 | 0 | 0 | 0 | 1 | 0 | -1 | 0 | 0 | 0 | 1 | | 0 |
| 0 | 0 | -1 | 0 | 0 | 1 | 0 | 0 | -1 | 0 | 0 | 1 | 0 | 0 | -1 | 0 | 0 | 1 | | 0 |
| 0 | 0 | 0 | -1 | 0 | 1 | 0 | 0 | 0 | -1 | 0 | 1 | 0 | 0 | 0 | -1 | 0 | 1 | | 0 |

Figure 8.19: Matrix coefficients for the system of equations $Ex \leq 0$ expressed in terms of "at" variables. Shaded areas correspond to matrix blocks including non-zero entries.

Similarly, the specific values for the block finitude constraints $(Ix) \leq 1$ in the small numerical example presented are as so:

| (Ix) | | | | | | | | | | | | | | | | | | | (b) |
|---|---|---|---|---|---|---|---|---|---|---|---|---|---|---|---|---|---|---|---|
| $x_{11}$ | $x_{21}$ | $x_{31}$ | $x_{41}$ | $x_{51}$ | $x_{61}$ | $x_{12}$ | $x_{22}$ | $x_{32}$ | $x_{42}$ | $x_{52}$ | $x_{62}$ | $x_{13}$ | $x_{23}$ | $x_{33}$ | $x_{43}$ | $x_{53}$ | $x_{63}$ | | |
| 1 | 0 | 0 | 0 | 0 | 0 | 1 | 0 | 0 | 0 | 0 | 0 | 1 | 0 | 0 | 0 | 0 | 0 | | 1 |
| 0 | 1 | 0 | 0 | 0 | 0 | 0 | 1 | 0 | 0 | 0 | 0 | 0 | 1 | 0 | 0 | 0 | 0 | | 1 |
| 0 | 0 | 1 | 0 | 0 | 0 | 0 | 0 | 1 | 0 | 0 | 0 | 0 | 0 | 1 | 0 | 0 | 0 | ≤ | 1 |
| 0 | 0 | 0 | 1 | 0 | 0 | 0 | 0 | 0 | 1 | 0 | 0 | 0 | 0 | 0 | 1 | 0 | 0 | | 1 |
| 0 | 0 | 0 | 0 | 1 | 0 | 0 | 0 | 0 | 0 | 1 | 0 | 0 | 0 | 0 | 0 | 1 | 0 | | 1 |
| 0 | 0 | 0 | 0 | 0 | 1 | 0 | 0 | 0 | 0 | 0 | 1 | 0 | 0 | 0 | 0 | 0 | 1 | | 1 |

Figure 8.20: Matrix coefficients for the system of equations $Ix \leq 1$.

In order to obtain the new objective function equation for $(BZ)^{MP}$ expressed as a function of $\lambda_i$, we simply multiply the coefficients (entries) in the $c$ vector (see Figure 8.17) with those of columns in $V$ (refer to Figure 8.12). Correspondingly, for the set of capacity constraints in $(BZ)^{MP}$, the entries in the D matrix (see Figure 8.18) are multiplied with those of the columns in partition matrix $V$. As an example, the resulting set of objective function cost coefficients is presented in Figure 8.21.

| (cV)λ | | |
|---|---|---|
| λ1 | λ2 | λ3 |
| 2 | 1.82 | 1.65 |

Figure 8.21: Vector of objective function cost coefficients ($cV$) for the BZ master problem.

The resulting set of capacity constraints is defined as follows:

| (DV)λ | | | | |
|---|---|---|---|---|
| $\lambda_1$ | $\lambda_2$ | $\lambda_3$ | | d |
| 6 | 0 | 0 | | 2 |
| 0 | 6 | 0 | ≤ | 2 |
| 0 | 0 | 6 | | 2 |

Figure 8.22: Matrix coefficients for the system of capacity constraints $(DV)\lambda \leq d$.

Following the same procedure it is possible to define the precedence constraints for the $(BZ)^{MP}$ as follows:

| (EV)λ | | | | |
|---|---|---|---|---|
| λ1 | λ2 | λ3 | | b |
| 0 | 0 | 0 | | 0 |
| 0 | 0 | 0 | | 0 |
| 0 | 0 | 0 | | 0 |
| 0 | 0 | 0 | | 0 |
| 0 | 0 | 0 | | 0 |
| 0 | 0 | 0 | | 0 |
| 0 | 0 | 0 | | 0 |
| 0 | 0 | 0 | | 0 |
| 0 | 0 | 0 | ≤ | 0 |
| 0 | 0 | 0 | | 0 |
| 0 | 0 | 0 | | 0 |
| 0 | 0 | 0 | | 0 |
| 0 | 0 | 0 | | 0 |
| 0 | 0 | 0 | | 0 |
| 0 | 0 | 0 | | 0 |
| 0 | 0 | 0 | | 0 |
| 0 | 0 | 0 | | 0 |
| 0 | 0 | 0 | | 0 |

Figure 8.23: Matrix coefficients for the system of block precedence constraints $(EV)\lambda \leq 0$. At the current iteration, the set of physical block precedence constraints is an empty set.

Given that each $\lambda_i$ variable corresponds to grouping together all the blocks in the pit into a single partition, no physical precedence constraints between blocks are required, and this explains why the set of constraints of the form $(Ev)\lambda \leq 0$ is an empty set. Likewise, the constraint set for the block finitude constraints in the $(BZ)^{MP}$ results as follows:

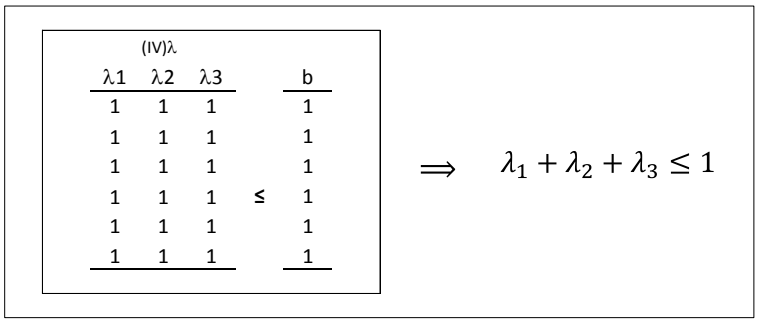


Figure 8.24: Matrix coefficients for the system of block finitude constraints $(IV)\lambda \leq 1$. The set of redundant constraints can be replaced by a single constraint.

The resulting master problem formulation for the first iteration of the BZ algorithm is given as follows:

$$(BZ_1)^{MP} \quad max \quad 2\lambda_1 + 1.82\lambda_2 + 1.65\lambda_3 \tag{8.101}$$

$$s.t. \quad 6\lambda_1 \leq 2 \tag{8.102}$$

$$6\lambda_2 \leq 2 \tag{8.103}$$

$$6\lambda_3 \leq 2 \tag{8.104}$$

$$\lambda_1 + \lambda_2 + \lambda_3 \leq 1 \tag{8.105}$$

$$\lambda_i \in [0,1] \quad \forall i \tag{8.106}$$

The objective function coefficients in equation (8.101) correspond to the economic value of each individual $\lambda_i$ variable, i.e., the summation of economic values of the individual blocks contained in the partition represented by $\lambda_i$. Constraints (8.102) - (8.104) ensure that no more than two blocks be mined per time period. In the same way, constraint (8.105) is the equivalent of the block finitude constraints expressed in terms of the $\lambda_i$ decision variables, ensuring that the cumulative fraction of a block mined, across all time periods, does not exceed one (i.e., 100% of the block), and constraints (8.106) bound the individual $\lambda_i$ variables to be between zero and one.

STEP 3: Solving the BZ maximum closure problem (pricing problem)

For clarity of exposition, the full discussion of the specific algorithmic steps undertaken to solve the BZ Pricing subproblem, including details on the PseudoFlow algorithm, are omitted at this stage (please refer to Section 8.3.2 for a detailed discussion of HPF). For simplicity, assume a feasible solution to the multi-time-period pricing problem $v_4$ is generated and consists of the plan shown in Figure 8.25:

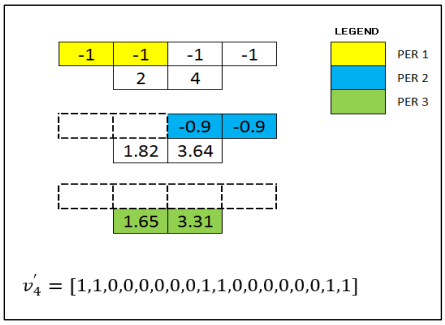


Figure 8.25: A feasible mining plan resulting from the BZ pricing problem. (Numeric values shown are the time discounted economic block values).

Figure 8.26 shows the resulting partition matrix $V^j$ once the newly generated solution $v_4'$ is added to it. As can be seen, the new matrix $V^j$ is composed of partitions which are not (initially) orthogonal.

| | $x_{bt}$ | V1 | V2 | V3 | **V4** |
|---|---|---|---|---|---|
| PERIOD 1 | $x_{11}$ | 1 | 0 | 0 | 1 |
| | $x_{21}$ | 1 | 0 | 0 | 1 |
| | $x_{31}$ | 1 | 0 | 0 | 0 |
| | $x_{41}$ | 1 | 0 | 0 | 0 |
| | $x_{51}$ | 1 | 0 | 0 | 0 |
| | $x_{61}$ | 1 | 0 | 0 | 0 |
| PERIOD 2 | $x_{12}$ | 0 | 1 | 0 | 0 |
| | $x_{22}$ | 0 | 1 | 0 | 0 |
| | $x_{32}$ | 0 | 1 | 0 | 1 |
| | $x_{42}$ | 0 | 1 | 0 | 1 |
| | $x_{52}$ | 0 | 1 | 0 | 0 |
| | $x_{62}$ | 0 | 1 | 0 | 0 |
| PERIOD 3 | $x_{13}$ | 0 | 0 | 1 | 0 |
| | $x_{23}$ | 0 | 0 | 1 | 0 |
| | $x_{33}$ | 0 | 0 | 1 | 0 |
| | $x_{43}$ | 0 | 0 | 1 | 0 |
| | $x_{53}$ | 0 | 0 | 1 | 1 |
| | $x_{63}$ | 0 | 0 | 1 | 1 |

Figure 8.26: Set of matrix $V^0$ columns after appending the column corresponding to the new $v^4$ solution. At this stage colunms are not orthogonal.

It is necessary to obtain a new matrix $V^{j+1}$ by performing refining operations on the current set of partitions (columns) $V^j$ and by using the newly obtained subproblem solution $v_4$ (Figure 8.27). Recall, the partitioning rules are presented in Section 8.1.

| | λ1 | λ2 | λ3 | λ4 | λ5 | λ6 | ~~λ7~~ |
|---|---|---|---|---|---|---|---|
| $x_{bt}$ | V1 ∩ V4 | V2 ∩ V4 | V3 ∩ V4 | V1 \ V4 | V2 \ V4 | V3 \ V4 | V4 \ (V1+V2+V3) |
| $x_{11}$ | 1 | 0 | 0 | 0 | 0 | 0 | 0 |
| $x_{21}$ | 1 | 0 | 0 | 0 | 0 | 0 | 0 |
| $x_{31}$ | 0 | 0 | 0 | 1 | 0 | 0 | 0 |
| $x_{41}$ | 0 | 0 | 0 | 1 | 0 | 0 | 0 |
| $x_{51}$ | 0 | 0 | 0 | 1 | 0 | 0 | 0 |
| $x_{61}$ | 0 | 0 | 0 | 1 | 0 | 0 | 0 |
| $x_{12}$ | 0 | 0 | 0 | 0 | 1 | 0 | 0 |
| $x_{22}$ | 0 | 0 | 0 | 0 | 1 | 0 | 0 |
| $x_{32}$ | 0 | 1 | 0 | 0 | 0 | 0 | 0 |
| $x_{42}$ | 0 | 1 | 0 | 0 | 0 | 0 | 0 |
| $x_{52}$ | 0 | 0 | 0 | 0 | 1 | 0 | 0 |
| $x_{62}$ | 0 | 0 | 0 | 0 | 1 | 0 | 0 |
| $x_{13}$ | 0 | 0 | 0 | 0 | 0 | 1 | 0 |
| $x_{23}$ | 0 | 0 | 0 | 0 | 0 | 1 | 0 |
| $x_{33}$ | 0 | 0 | 0 | 0 | 0 | 1 | 0 |
| $x_{43}$ | 0 | 0 | 0 | 0 | 0 | 1 | 0 |
| $x_{53}$ | 0 | 0 | 1 | 0 | 0 | 0 | 0 |
| $x_{63}$ | 0 | 0 | 1 | 0 | 0 | 0 | 0 |

Figure 8.27: Set of matrix $V^{(1)}$ columns obtained after performing the refining operations to the columns of $V^0$.

Since a new "$\lambda_i$" variable is associated to each of the columns in $V^{j+1}$, it is possible to contrast and compare the original versus the new (refined) partition set.

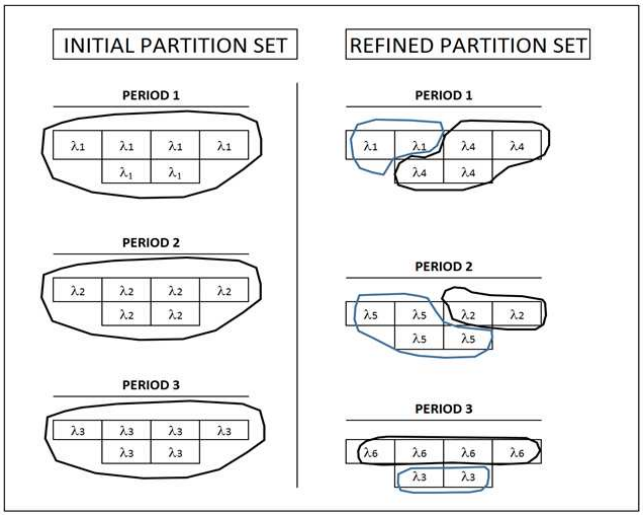


Figure 8.28: Comparison between initial partitions in $V^0$ versus the newly generated partitions in the refined partition matrix $V^{(1)}$.

As shown in Figure 8.28 the refining process results in six distinct partitions, as opposed to the initial three partition sets used in the previous master problem. Repeating the steps taken in the first iteration, the required coefficient matrices $(cV)$, $(EV)$, $(IV)$ and $(DV)$ are built by straightforward matrix multiplication operations, as illustrated in Figure 8.29:

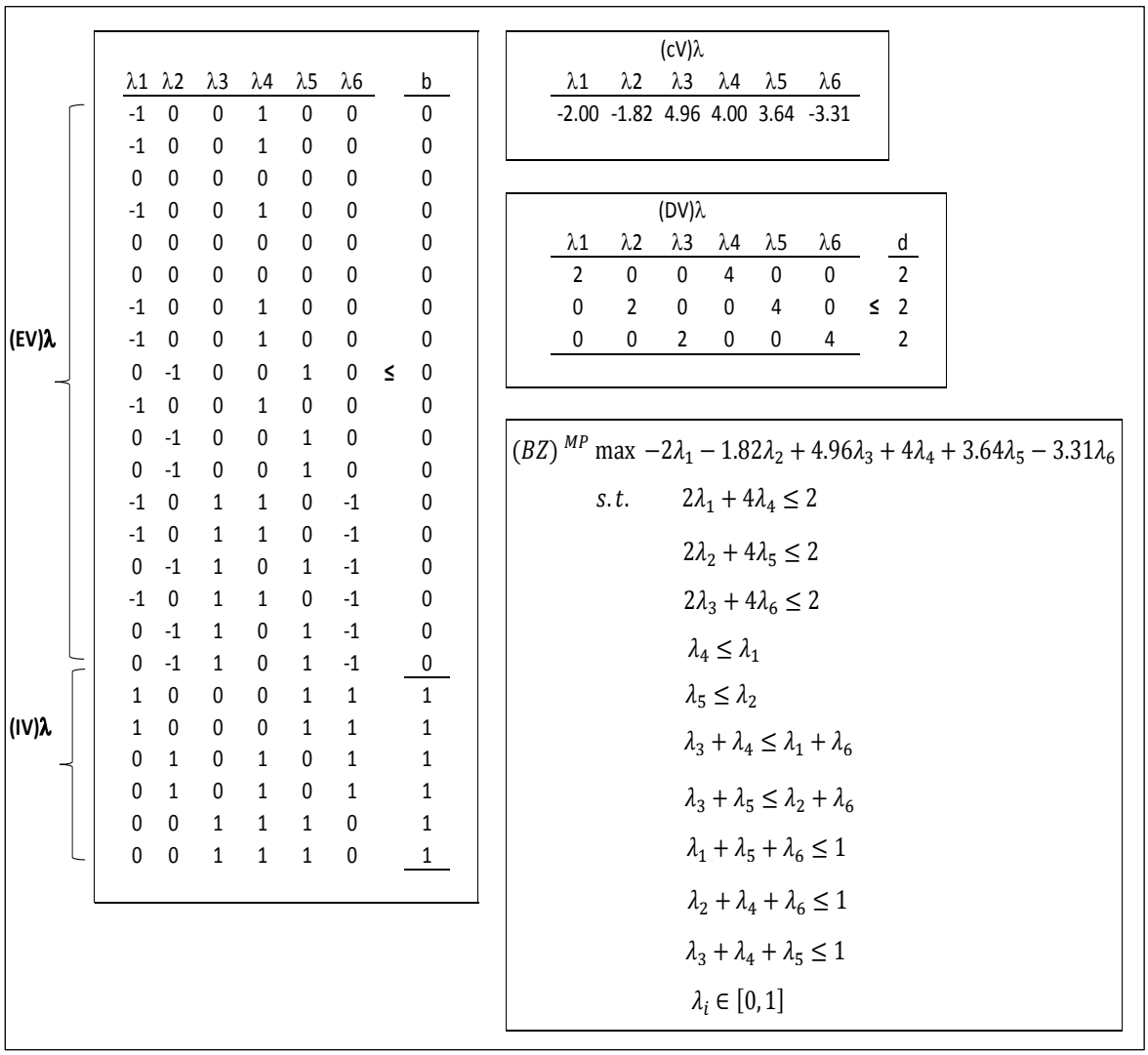


Figure 8.29: Constraint coefficient matrices and master problem formulation associated with the second iteration of the BZ algorithm.

After replacing redundant constraints by single effective constraints, the new master problem that results for iteration #2 is formulated as follows:

$$(BZ_2)^{MP} \quad max \quad -2\lambda_1 - 1.82\lambda_2 + 4.96\lambda_3 + 4\lambda_4 + 3.64\lambda_5 - 3.31\lambda_6 \tag{8.107}$$

$$s.t. \qquad 2\lambda_1 + 4\lambda_4 \leq 2 \tag{8.108}$$

$$2\lambda_2 + 4\lambda_5 \leq 2 \tag{8.109}$$

$$2\lambda_3 + 4\lambda_6 \leq 2 \tag{8.110}$$

$$\lambda_4 \leq \lambda_1 \tag{8.111}$$

$$\lambda_5 \leq \lambda_2 \tag{8.112}$$

$$\lambda_3 + \lambda_4 \leq \lambda_1 + \lambda_6 \tag{8.113}$$

$$\lambda_3 + \lambda_5 \leq \lambda_2 + \lambda_6 \tag{8.114}$$

$$\lambda_1 + \lambda_5 + \lambda_6 \leq 1 \tag{8.115}$$

$$\lambda_2 + \lambda_4 + \lambda_6 \leq 1 \tag{8.116}$$

$$\lambda_3 + \lambda_4 + \lambda_5 \leq 1 \tag{8.117}$$

$$\lambda_i \in [0, 1] \qquad \forall i \tag{8.118}$$

By analyzing the objective function coefficients associated with each individual $\lambda_i$ variable in the master problem, it is readily apparent that on a period-by-period basis, positive-valued variables are more beneficial to the objective than negative-valued ones (for example, in period 1, $\lambda_4$ is preferable to $\lambda_1$, and in period 2, $\lambda_5$ is preferable to $\lambda_2$).

Ignoring the impact of the set of problem constraints in the choice of the specific $\lambda_i$ by the solver – as constraint requirements can cause an otherwise attractive $\lambda_i$ to be precluded – it is assumed, for simplicity, that the vector of duals originated by the $(BZ)^{MP}$ indicate that the blocks mined at each period be selected from the highest valued $\lambda_i$ for said period. In this case, one might consider a new feasible solution to the multi-time-period pricing problem $v_7$ consisting of the plan shown in Figure 8.30.

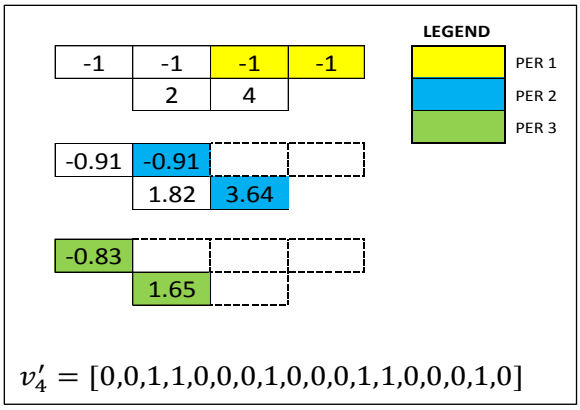


Figure 8.30: A feasible mining plan $v_7$ resulting from the second iteration of the BZ pricing problem. Periods 1, 2 and 3 blocks, originate from $\lambda_4$, $\lambda_5$ and $\lambda_3$, respectively.

Our (informed) qualitative reasoning leads to assuming that, when searching for a solution to the Pricing problem, the solver considers essentially two aspects: (i) the indication obtained from the master problem to prioritize a set of blocks belonging to a specific $\lambda_i$ variable, and (ii) ensuring the satisfaction of block precedence constraints. Hence, it is reasonable to assume that in the case of period 1, blocks are chosen based on combining the intent to pick from $\lambda_4$ (which is the most valuable $\lambda_i$ variable in said period) with the need to obey slope constraints. Correspondingly, the priority for period 2 is to select from out of the subset of blocks belonging to $\lambda_5$, those which give the highest contribution to the objective (maximizing it), while simultaneously obeying block precedence constraints.

Finally, period 3 blocks might also be chosen because they provide a net benefit to the objective and observe precedence constraints. At this point, it should be noted that feasible solutions to $(BZ)^{SP}$ can take many forms and, in particular, they are under no obligation to produce results including two blocks per period only, as this is not one of the problem requirements (for the subproblem). In effect, our goal is only to illustrate the interplay between $(BZ)^{MP}$ and $(BZ)^{SP}$, as well as to describe how solutions to the Pricing subproblem shape the outcomes of the restricted master problem.

By adding the newly generated solution $v_7$ to the current partition set, a new set of non-orthogonal columns is generated. This is illustrated in Figure 8.31 as follows:

| | $x_{bt}$ | V1 | V2 | V3 | V4 | V5 | V6 | **V7** |
|---|---|---|---|---|---|---|---|---|
| PERIOD 1 | $x_{11}$ | **1** | 0 | 0 | 0 | 0 | 0 | 0 |
| | $x_{21}$ | **1** | 0 | 0 | 0 | 0 | 0 | 0 |
| | $x_{31}$ | 0 | 0 | 0 | **1** | 0 | 0 | **1** |
| | $x_{41}$ | 0 | 0 | 0 | **1** | 0 | 0 | **1** |
| | $x_{51}$ | 0 | 0 | 0 | **1** | 0 | 0 | 0 |
| | $x_{61}$ | 0 | 0 | 0 | **1** | 0 | 0 | 0 |
| PERIOD 2 | $x_{12}$ | 0 | 0 | 0 | 0 | **1** | 0 | 0 |
| | $x_{22}$ | 0 | 0 | 0 | 0 | **1** | 0 | **1** |
| | $x_{32}$ | 0 | **1** | 0 | 0 | 0 | 0 | 0 |
| | $x_{42}$ | 0 | **1** | 0 | 0 | 0 | 0 | 0 |
| | $x_{52}$ | 0 | 0 | 0 | 0 | **1** | 0 | 0 |
| | $x_{62}$ | 0 | 0 | 0 | 0 | **1** | 0 | **1** |
| PERIOD 3 | $x_{13}$ | 0 | 0 | 0 | 0 | 0 | **1** | **1** |
| | $x_{23}$ | 0 | 0 | 0 | 0 | 0 | **1** | 0 |
| | $x_{33}$ | 0 | 0 | 0 | 0 | 0 | **1** | 0 |
| | $x_{43}$ | 0 | 0 | 0 | 0 | 0 | **1** | 0 |
| | $x_{53}$ | 0 | 0 | **1** | 0 | 0 | 0 | **1** |
| | $x_{63}$ | 0 | 0 | **1** | 0 | 0 | 0 | 0 |

Figure 8.31: Set of matrix $V^2$ columns after appending the column corresponding to the new solution to the pricing subproblem $v^7$.

Performing refining operations on the current set of partitions (columns) $V^2$ and by using the newly obtained subproblem solution $v_7$ (Figure 8.31), a new refined set of partitions is obtained (see Figure 8.32).

| | $x_{bt}$ | (~~λ1~~) | (~~λ2~~) | λ3 | λ4 | λ5 | λ6 | λ7 | λ8 | λ9 | λ10 | λ11 | λ12 | (~~λ13~~) |
|---|---|---|---|---|---|---|---|---|---|---|---|---|---|---|
| PERIOD 1 | $x_{11}$ | 0 | 0 | 0 | 0 | 0 | 0 | **1** | 0 | 0 | 0 | 0 | 0 | 0 |
| | $x_{21}$ | 0 | 0 | 0 | 0 | 0 | 0 | **1** | 0 | 0 | 0 | 0 | 0 | 0 |
| | $x_{31}$ | 0 | 0 | 0 | **1** | 0 | 0 | 0 | 0 | 0 | **0** | 0 | 0 | 0 |
| | $x_{41}$ | 0 | 0 | 0 | **1** | 0 | 0 | 0 | 0 | 0 | **0** | 0 | 0 | 0 |
| | $x_{51}$ | 0 | 0 | 0 | 0 | 0 | 0 | 0 | 0 | 0 | **1** | 0 | 0 | 0 |
| | $x_{61}$ | 0 | 0 | 0 | 0 | 0 | 0 | 0 | 0 | 0 | **1** | 0 | 0 | 0 |
| PERIOD 2 | $x_{12}$ | 0 | 0 | 0 | 0 | 0 | 0 | 0 | 0 | 0 | 0 | **1** | 0 | 0 |
| | $x_{22}$ | 0 | 0 | 0 | 0 | **1** | 0 | 0 | 0 | 0 | 0 | 0 | 0 | 0 |
| | $x_{32}$ | 0 | 0 | 0 | 0 | 0 | 0 | 0 | **1** | 0 | 0 | 0 | 0 | 0 |
| | $x_{42}$ | 0 | 0 | 0 | 0 | 0 | 0 | 0 | **1** | 0 | 0 | 0 | 0 | 0 |
| | $x_{52}$ | 0 | 0 | 0 | 0 | 0 | 0 | 0 | 0 | 0 | 0 | **1** | 0 | 0 |
| | $x_{62}$ | 0 | 0 | 0 | 0 | **1** | 0 | 0 | 0 | 0 | 0 | 0 | 0 | 0 |
| PERIOD 3 | $x_{13}$ | 0 | 0 | 0 | 0 | 0 | **1** | 0 | 0 | 0 | 0 | 0 | 0 | 0 |
| | $x_{23}$ | 0 | 0 | 0 | 0 | 0 | 0 | 0 | 0 | 0 | 0 | 0 | **1** | 0 |
| | $x_{33}$ | 0 | 0 | 0 | 0 | 0 | 0 | 0 | 0 | 0 | 0 | 0 | **1** | 0 |
| | $x_{43}$ | 0 | 0 | 0 | 0 | 0 | 0 | 0 | 0 | 0 | 0 | 0 | **1** | 0 |
| | $x_{53}$ | 0 | 0 | **1** | 0 | 0 | 0 | 0 | 0 | 0 | 0 | 0 | 0 | 0 |
| | $x_{63}$ | 0 | 0 | 0 | 0 | 0 | 0 | 0 | 0 | **1** | 0 | 0 | 0 | 0 |

Figure 8.32: Refined partition set corresponding to the second iteration.

A comparison of the individual partition matrices is provided in Figure 8.33. As expected, the new solution $v_7$ subdivides (refines) the previous grouping of blocks represented by $\lambda_4$ and $\lambda_5$ into new subsets of blocks, while leaving $\lambda_3$ and $\lambda_6$ unaltered.

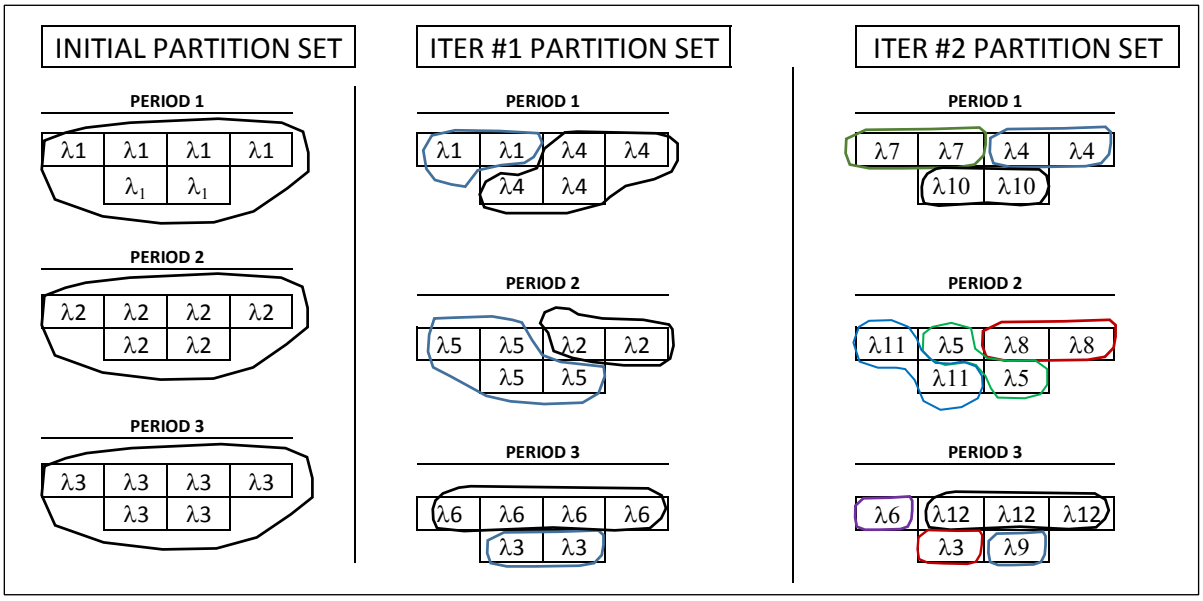


Figure 8.33: Grouping of individual blocks into the partitions contained in matrices $V^0$,$V^1$ and $V^2$.

Similar to iteration one, the current set of partitions $V^2$ gives origin to the following formulation of a new $(BZ)^{MP}$:

$$(BZ_3)^{MP} \quad max \quad 1.65\lambda_3 - 2\lambda_4 + 2.73\lambda_5 - 0.83\lambda_6 - 2\lambda_7 - 1.82\lambda_8 + 3.31\lambda_9 + 6\lambda_{10} + 0.91\lambda_{11} - 2.48\lambda_{12} \tag{8.119}$$

$$s.t. \quad 2\lambda_4 + 2\lambda_7 + 2\lambda_{10} \leq 2 \tag{8.120}$$

$$2\lambda_5 + 2\lambda_8 + 2\lambda_{11} \leq 2 \tag{8.121}$$

$$\lambda_3 + \lambda_6 + \lambda_9 + 3\lambda_{12} \leq 2 \tag{8.122}$$

$$\lambda_{10} \leq \lambda_7 \tag{8.123}$$

$$\lambda_{10} \leq \lambda_4 \tag{8.124}$$

$$\lambda_{10} + \lambda_{11} \leq \lambda_5 + \lambda_7 \tag{8.125}$$

$$\lambda_{10} + \lambda_{11} \leq \lambda_4 + \lambda_8 \tag{8.126}$$

$$\lambda_5 + \lambda_{10} \leq \lambda_4 + \lambda_8 \quad (8.127)$$

$$\lambda_3 + \lambda_{10} \leq \lambda_6 + \lambda_7 \quad (8.128)$$

$$\lambda_3 + \lambda_{10} + \lambda_{11} \leq \lambda_5 + \lambda_7 + \lambda_{12} \quad (8.129)$$

$$\lambda_3 + \lambda_{10} + \lambda_{11} \leq \lambda_4 + \lambda_8 + \lambda_{12} \quad (8.130)$$

$$\lambda_9 + \lambda_{10} \leq \lambda_7 + \lambda_{12} \quad (8.131)$$

$$\lambda_5 + \lambda_9 + \lambda_{10} \leq \lambda_4 + \lambda_8 + \lambda_{12} \quad (8.132)$$

$$\lambda_6 + \lambda_7 + \lambda_{11} \leq 1 \quad (8.133)$$

$$\lambda_5 + \lambda_7 + \lambda_{12} \leq 1 \quad (8.134)$$

$$\lambda_4 + \lambda_8 + \lambda_{12} \leq 1 \quad (8.135)$$

$$\lambda_3 + \lambda_{10} + \lambda_{11} \leq 1 \quad (8.136)$$

$$\lambda_5 + \lambda_9 + \lambda_{10} \leq 1 \quad (8.137)$$

$$\lambda_i \in [0,1] \qquad \forall i \quad (8.138)$$

From visual inspection of Figure 8.10 and Figure 8.33, it is clear that the true optimal integer solution is readily available to the master problem, i.e., the solver could choose to mine $\lambda_4$ in period 1, $\lambda_5$ in period 2, and, $\lambda_3$ and $\lambda_6$ in period 3.

## 8.2 The PseudoFlow Algorithm

In the research presented in this thesis, the pricing subproblem of the Bienstock-Zuckerberg algorithm is solved using the PseudoFlow algorithm (Hochbaum, 2008). The choice of the most efficient approach to solving the pricing subproblem in the BZ algorithm benefits from a brief review of the principles underlying the application of network-flow methods for solving ultimate pit limit problems ($UPL$). The subsequent sections summarize part of the arguments presented in Johnson (1968), Barnes (1980), Dagdelen (1985), Hochbaum (2001, 2008, 2012); and are considered important in providing substantiation for the particular choice made.

## 8.3 Preliminary Review of the Application of Network-flow Methods in Solving Maximum-Closure Problems

Given a directed graph $G = (V, A)$ where $V$ represents the set of all vertices (or nodes), $A$ represents the set of all the arcs (or edges) connecting nodes in $G$, a subset of the nodes $D \subset V$ is $closed$, if for every node in $D$ its successors are also in $D$ (Figure 8.34).

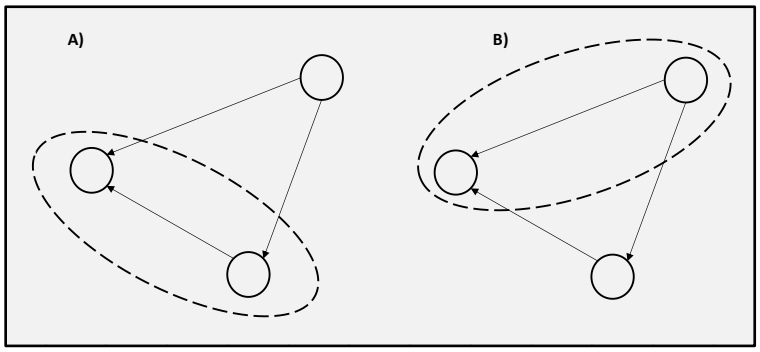


Figure 8.34: Directed graph. In (A) the subset of nodes encircled by the dashed line represents a closed set of nodes while in (B) the encircled subset of nodes is not a closed set (adapted from Hochbaum, 2012).

Given a directed graph $G = (V, A)$ and node weights (positive or negative) $b_i$ for all $i \in V$, the maximum-closure problem consists of finding a closed subset of nodes $V' \subseteq V$ such that $\sum_{i \in V'} b_i$ is maximum.

In the mining literature, the maximum-closure problem has a widely known counterpart in the form of the ultimate pit limit problem ($UPL$). This problem consists of finding the set of blocks in the ore deposit whose extraction maximizes a mining project's total economic value. The profit associated with each individual mine block is defined as the difference between the value of the ore contained in it and the cost involved in its removal and processing. The extraction of mined blocks must be operationally feasible, i.e., it is necessary that physical precedence constraints be enforced such that mine blocks are not mined before other blocks overlying them are removed. Different rock (or soil) formations impose distinct geotechnical considerations determining the maximum (steepest) angle at which mining can occur, which must be obeyed, if mining is to proceed efficiently and safely, i.e., without risking pit slope failure.

These considerations are modeled in the form of block precedence constraints which enforce allowable "mine slope" constraints. Figure 8.35 presents a schematic view of a directed graph over which the maximum-closure is solved:

.

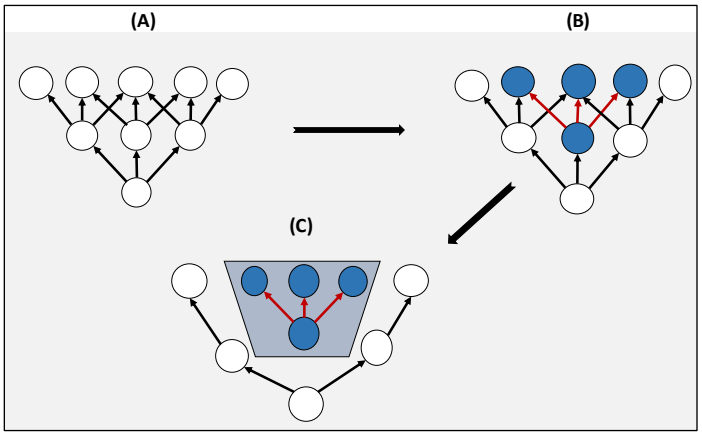


Figure 8.35: Maximum-closure problem. (A) Initial directed graph; (B) the set of blue nodes is identified as forming a closure; (C) Closure identified is one whose the total weight is maximum among all possible closures, therefore it is the maximum-closure.

The goal of maximizing total economic value in the $UPL$ is therefore conditional (constrained) on ensuring these physical requirements are met, but disregards any other operational considerations, including limits on the total resources available, (typically mining and transportation or processing capacities), as well as common mill-feed blending and stockpiling requirements.

The equivalence between maximum-closure problems and the $UPL$ lies in the fact that, for a given discretized orebody, a related directed graph can be constructed such that individual mine blocks can be compared to nodes in the graph, precedence constraints can be compared to arcs in the graph, and block values can be converted into node weights (Figure 8.36).

Hence, in the discussions that follow, mine blocks $(b)$ will be referred to as network nodes $(n)$ interchangeably, depending on whether the context of the exposition relates to mine scheduling problems or network flow problems, respectively.

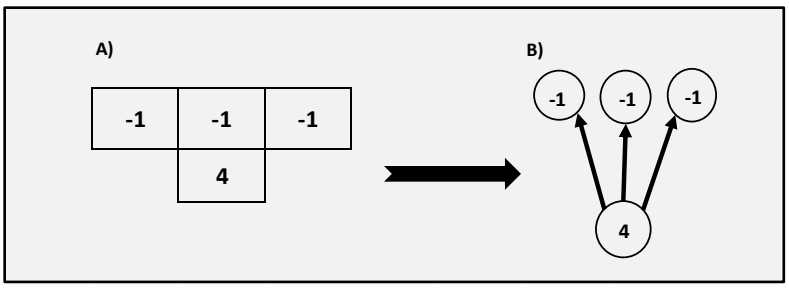


Figure 8.36: Equivalence between mine blocks and the corresponding nodes in a directed graph. In the figure, the original block values $v_b$ shown in A) are converted into the node weights shown in B).

A large number of alternative algorithms exist which solve the maximum-closure problem either by using the concept of "mass" of a subset of nodes, (e.g., the Lerchs-Grossman algorithm), or by the use of flows through a network (e.g., Ford-Fulkerson's labelling algorithm), which constitute some of the more widely used techniques to solve the maximum flow problem (Johnson, 1968; Hochbaum, 2008).

Adopting the mathematical formalism of the field of Operations Research, and in particular that of integer linear programming, it is common to formulate the $UPL$ as follows (Lambert *et al.*, 2014):

Indices and Sets:

$b \in B: set\ of\ all\ blocks\ b,$

$b' \in B_b: set\ of\ all\ predecessor\ blocks\ b'\ that\ must\ be\ extracted\ directly\ before\ b,$

Data:

$c_b: net\ value\ (revenue\ minus\ cost)\ resulting\ from\ mining\ block\ b$

Decision Variable:

$x_b: 1\ if\ block\ b\ is\ to\ be\ extracted; 0\ otherwise.$

$$(UPL) \quad max \sum_{b \in B} c_b x_b \tag{8.139}$$

Constraints:

$$x_b \leq x_{b'} \quad \forall b \in B, \quad b' \in B_b \tag{8.140}$$

$$x_b \; binary \tag{8.141}$$

Or in a compact vector form as:

$$(UPL) \quad max \;\; cx \tag{8.142}$$

$$s.t. \quad Ax \leq 0 \tag{8.143}$$

$$x \;\; binary \tag{8.144}$$

The objective function (8.139) seeks to maximize the total profit realized from mining. Constraints (8.140) ensure the sequencing of mined blocks obeys precedence requirements between a given block $b$, and its set of predecessor blocks $b'$.

It should be noted that the constraint coefficient matrix $(A)$ for the constraint set of the (*UPL*) problem possesses a totally unimodular structure (Johnson, 1968; Picard, 1976), that is, the following necessary and sufficient conditions are satisfied: (i) every row contains at most two non-zero entries; (ii) every entry is 0, 1, or -1; (iii) if two non-zero entries in any row have the same sign, then they must belong to separate columns; (iv) if two non-zero entries in any row have different sign, then they must belong to the same columns. For a constraint set wherein the vector of right-hand-side coefficients is integer, the total unimodularity of the matrix $(A)$ implies that, without loss of generality, the integrality requirements on the decision variables can be relaxed and replaced by the less restrictive condition that $x_b \in [0,1]$ without sacrificing the integrality of the solutions obtained. In other words, total unimodularity of $A$ allows for the UPL to be formulated as a linear program, and solved using linear programming algorithms. Importantly, it also indicates that the dual of the $UPL$ problem is a network-flow problem (Johnson, 1968; Hochbaum, 2001). This is a desirable feature because network problems constitute a subclass of optimization problems which tend to be particularly tractable.

Relaxing the integrality constraints, an equivalent problem can be formulated as follows:

$$(UPL)^r \quad max \;\; \sum_{b \in B} c_b x_b \tag{8.145}$$

$$s.t. \quad x_b \leq x_{b'} \qquad \forall b \in B, \;\; b' \in B_b \tag{8.146}$$

$$0 \leq x_b \leq 1 \qquad \forall b \in B \tag{8.147}$$

Using more compact matrix notation the UPL problem might be expressed as so:

$$(UPL)^r \qquad max \quad c'x \tag{8.148}$$

$$s.t. \quad Ax \leq 0 \tag{8.149}$$

$$x \in [0,1] \tag{8.150}$$

Recall that the problem described by $(UPL)^r$ constitutes a single-time-period problem. This is a special case of the more complex open-pit mine production scheduling problem ($OPMPS$), which takes into account a wider spectrum of operational constraints. Said constraints frequently determine period-limits on the consumption of the available resources, in particular, the existence of period limitations suggests that it might be necessary to consider multi-time-period problems in which mining spans over a discrete set of time periods $T$, and in which the time value of money constitutes a significant factor for net present value (NPV) optimization. Such multi-time-period pit limit problems ($MPLP$) must consider single-time-period physical precedence constraints (such as in the $UPL$), as well as a new set of sequencing constraints (replicated per each individual time period), ensuring block precedence between a given block $b$ and its predecessor $b'$ are obeyed in the context of multiple time periods.

The multi-time-period pit limit problem ($MPLP$) can be formulated as follows:

Indices and sets:

$b \in B$: $set\ of\ all\ blocks\ b$,

$b' \in B_b$: $set\ of\ all\ predecessor\ blocks\ which\ must\ be\ extracted\ directly\ before\ block\ b$,

$t \in T$: $set\ of\ all\ time\ periods\ t$

Data:

$c_{bt}$: $net\ value\ (revenue\ minus\ cost)\ resulting\ from\ mining\ block\ b\ in\ time\ period\ t$

Decision Variables:

$x_{bt}$: $1\ if\ block\ b\ is\ extracted\ at\ time\ period\ t; 0\ otherwise.$

$$(MPLP) \quad max \sum_{b \in B} \sum_{t \in T} c_{bt} x_{bt} \tag{8.151}$$

$$s.t. \quad x_{bt} \leq \sum_{t' \leq t} x_{b't'} \qquad \forall b \in B, \; b' \in B_b, t \in T \tag{8.152}$$

$$\sum_{t \in T} x_{bt} \leq 1 \qquad \forall b \in B \tag{8.153}$$

$$x_{bt} \quad binary \qquad \forall b \in B, t \in T \tag{8.154}$$

Similar to the $UPL$ problem, the objective function (8.151) seeks to maximize the total profit across all time periods, that results from mining each individual block $b$ at a specific time period $t$. Constraints (8.152) enforce block precedence requirements between the pairs of blocks $(b, b')$ across all time periods. Consideration of multiple time periods gives rise to a new set of constraints (8.153) requiring that blocks be mined at most once, which we refer to as "block finitude constraints." The constraint coefficient matrix of $(MPLP)$ preserves the total unimodularity property, implying that the problem can be relaxed and cast as an LP. Henceforth, we refer to the relaxed version of $(MPLP)$ as $(MPLP)^r$, and express the problem in more compact vector notation as follows:

$$(MPLP)^r \quad max \quad c_1 x_1 + c_2 x_2 + c_3 x_3 + \cdots + c_T x_T \tag{8.155}$$

$$s.t. \quad Ex_1 \leq 0 \tag{8.156}$$

$$Ex_1 + Ex_2 \leq 0 \tag{8.157}$$

$$Ex_1 + Ex_2 + \cdots + Ex_T \leq 0 \tag{8.158}$$

$$Ix_1 + Ix_2 + \cdots + Ix_T \leq 1 \tag{8.159}$$

$$x \in [0, 1] \tag{8.160}$$

The underlying network structure present in the $(MPLP)^r$ problem can be made clearer if a variable substitution is employed which replaces so-called "$at$ variables," such as $x_{bt}$, by new variables; frequently called "by variables" $w_{bt}$. These equivalent variables take the value 1 if block

$b$ is mined by period $t$; 0 otherwise. The constraint coefficient matrix resulting from replacing "at" for "$by$" variables is also less dense which is computationally advantageous.

Let:

$w_{bt}$: 1 *if block b is mined by the end of time period t*; 0 *otherwise*

$$w_{bt} = \sum_{t' \leq t}^{t} x_{bt'} \tag{8.161}$$

$$x_{bt} = \begin{cases} w_{bt} & if \ \ t = 1 \\ w_{bt} - w_{b,t-1} & otherwise \end{cases} \tag{8.162}$$

The $(MPLP)^{T}$ problem formulated using "$by$" variables, is expressed as follows:

$$(MPLP)^{\,by} \quad max \sum_{b \in B} \sum_{t=1}^{T-1} (c_{bt} - c_{b,t+1}) w_{bt} + c_{bT} w_{bT} \tag{8.163}$$

$$s.t. \quad w_{bt} \leq w_{b't} \qquad \forall b \in B, \ b' \in B_b, t \in T \tag{8.164}$$

$$w_{bt} \ \leq \ w_{b,t+1} \qquad \forall b \in B, t \in T \tag{8.165}$$

$$w_{bt} \ \ binary \qquad \forall b \in B, t \in T \tag{8.166}$$

Apart from the new set of cost coefficients, the objective function remains unchanged relative to the problem formulation expressed as a function of "at variables." Constraints (8.164) apply to a block $b$ and its physical predecessors $b'$ (per individual time period), and are responsible for ensuring block precedence requirements between pairs of predecessor blocks $(b, b')$ are met. Constraints (8.165) apply to a given block and itself (for two consecutive time periods), and ensure that individual blocks be mined at most once. Indeed, conceptually, it is useful to think of the introduction of multiple time periods as the equivalent of generating "replicas" of the single-time-period network, over the span of "*T*" time periods, which culminate in a new time-extended network such as shown in Figure 8.37.

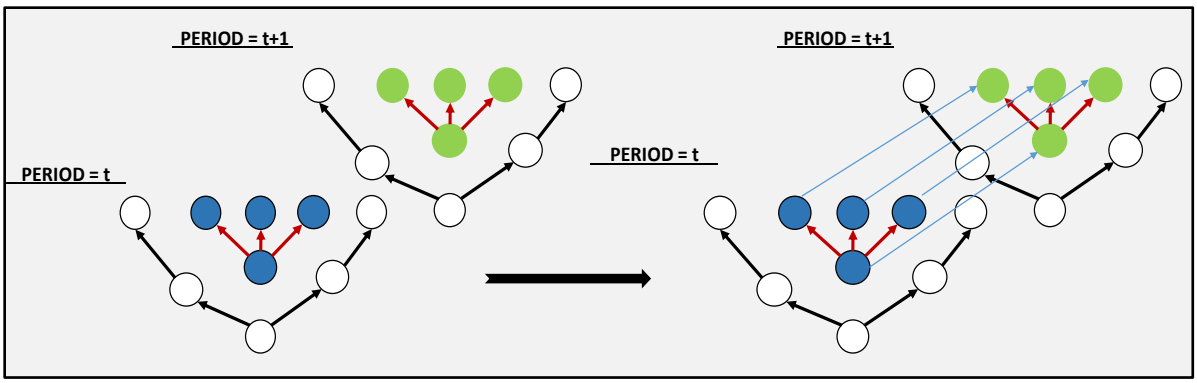


Figure 8.37: Two consecutive periods in a multi-time-period maximum closure problem. On the left, a single time period graph is reproduced to represent the new time-extended graph including period "t+1" nodes. On the right, arcs representing precedence (across time) between nodes, connect nodes and their respective replicas (some arcs are omitted for clarity).

The $(MPLP)^{by}$ problem is expressed in condensed matrix form as follows:

Data:

$c_t$: *coefficient vector including all the cost parameters for period t*

$E$: *coefficient matrix for the physical (slope) precedence constraints between blocks*

$I$: *identity matrix, used as the coefficient matrix in time precendence constraints*

Decision Variables:

$w_t$: *vector of decision variables* $w_{bt}$, *determining whether to mine blocks b by time period t*

$$(MPLP)^{by} \quad \max \quad (c_1 - c_2)w_1 + (c_2 - c_3)w_2 + \cdots + c_t w_T \tag{8.167}$$

$$s.t. \quad Ew_1 \leq 0 \tag{8.168}$$

$$Ew_2 \leq 0 \tag{8.169}$$

$$Ew_T \leq 0 \tag{8.170}$$

$$Iw_1 - Iw_2 \leq 0 \tag{8.171}$$

$$Iw_2 - Iw_3 \leq 0 \tag{8.172}$$

$$Iw_t - Iw_{t+1} \leq 0 \quad (8.173)$$

$$w_T \leq 1 \quad (8.174)$$

$$w_t \in [0,1] \quad \forall t \quad (8.175)$$

From duality theory in linear programming, it can be shown formally that a solution to $(MPLP)^{\boldsymbol{by}}$ is obtained by solving an equivalent problem corresponding to the "dual problem" of $(MPLP)^{\boldsymbol{by}}$ (Johnson, 1968; Barnes, 1982; Dagdelen, 1985). The new dual problem is referred to as $(\boldsymbol{D}MPLP)^{\boldsymbol{by}}$. Note that, in this form, the problem is equivalent to a series of single-time-period ultimate pit limit problems, connected by the "$w_t - w_{t+1}$" block of constraints. In said dual problem, a decision variable is associated to each constraint in the original (primal) problem, and simultaneously, a new constraint is created for each variable in the primal problem. The dual shows more clearly the existence of an underlying network structure, because its coefficient matrix $E'$ corresponds to the transpose of the coefficient matrix for $(MPLP)^{\boldsymbol{by}}$ and displays the features of a network node-arc incidence matrix.

The dual problem $(\boldsymbol{D}MPLP)^{\boldsymbol{by}}$ can be formulated in condensed matrix form as follows:

Data:

$c_t$: *vector of cost coefficients associated with individual primal variables* $w_{bt}$

$E'$: *transpose of the initial coefficient matrix for the physical precedence constraints between blocks*

$I$: *identity matrix*

Decision Variables:

$u_t$: *(vector of) dual decision variables associated with the physical precedence constraint set given in equations* (8.166) − (8.168).

$v_{t,t+1}$: *(vector of) dual decision variables associated with the time precedence constraint set given in equations* (8.169) − (8.171).

$p_n$: *vector of dual decision variables associated with the resource constraints given in equation* (8.172) .

$$(\boldsymbol{D}MPLP)^{\boldsymbol{by}} \qquad min\ Z = Ip_n \tag{8.176}$$

$$s.t. \quad E'u_1 + Iv_{12} \geq (c_1 - c_2) \tag{8.177}$$

$$E'u_2 \quad - Iv_{12} + Iv_{23} \geq (c_2 - c_3) \tag{8.178}$$

$$E'u_{T-1} \quad - Iv_{j,(T-1)} + Iv_{T-1,T} \geq (c_j - c_{T-1}) \tag{8.179}$$

$$E'u_T \quad - Iv_{(T-1),T} + Iv_{nT} + P_n \geq c_T \tag{8.180}$$

$$u_t\ , v_{it}\ , p_n \quad \geq 0 \qquad \forall\ i, n, t \tag{8.181}$$

It can be formally shown that solving $(\boldsymbol{D}MPLP)^{\boldsymbol{by}}$ on its original graph is equivalent to solving an equivalent maximum flow problem on a related graph (Johnson, 1968, 1976; Dagdelen, 1985). Intuitively, it is noted that flow will be induced into the network by positive potential nodes (those corresponding to positive valued mine blocks) and removed from it by negative potential nodes (nodes such that $c \leq 0$) together with $p_n$ arcs. The optimization objective is that flow through the network occurs in such fashion as to minimize the flow on arcs $P_n$ while satisfying the period flow requirements as given by the $(c_t - c_{t+1})$ coefficients. Figure 8.38 shows the original graph representation of $(\boldsymbol{D}MPLP)^{\boldsymbol{by}}$:

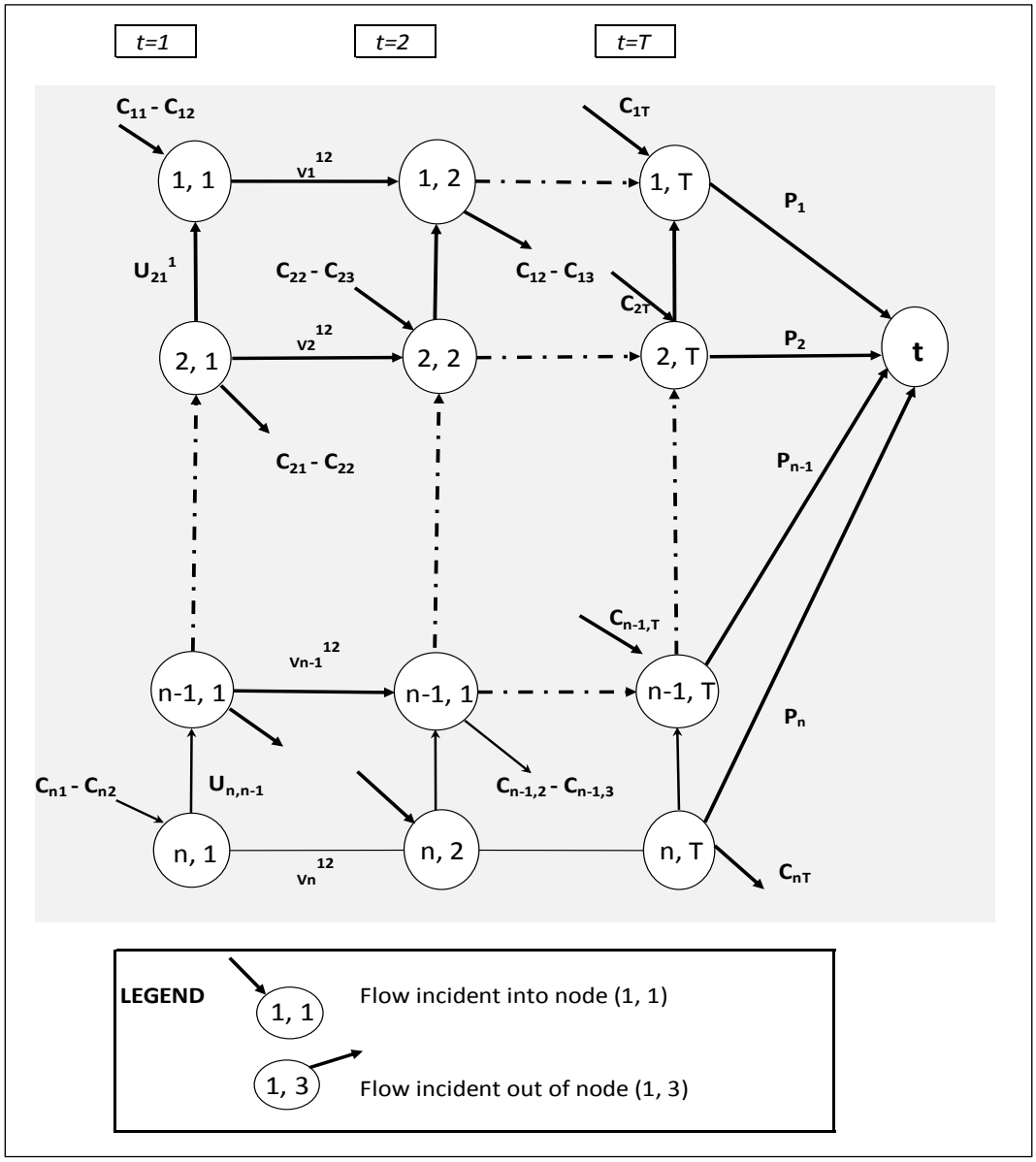


Figure 8.38: A representation of the multi-time-period maximum closure problem (modified from Dagdelen, 1985).

For any given node "$n$" in the network there exist only two possible ways by which, flow that has been induced into the network, is able to leave it: 1) through the $p_n$ arcs or 2) by routing flow to all other outwardly pointing arcs. This implies that the answer to the network problem when the sum of the flow through $p_n$ arcs is minimized, is equivalent to solving a max flow problem in which we push as much flow through the network as possible without considering the $p_n$ arcs. The specific modifications to the original graph transforming it into a graph consistent with finding a maximum flow are:

1. The addition of a source ($s$) and sink node ($t$)
2. The connecting of all nodes with positive gains to the source node
3. The connecting of all nodes with negative gains to the sink node and
4. The elimination of all the remaining $p_n$ arcs connecting to the sink node.

The transformed graph of the problem depicted in Figure 8.38 is shown in Figure 8.39:

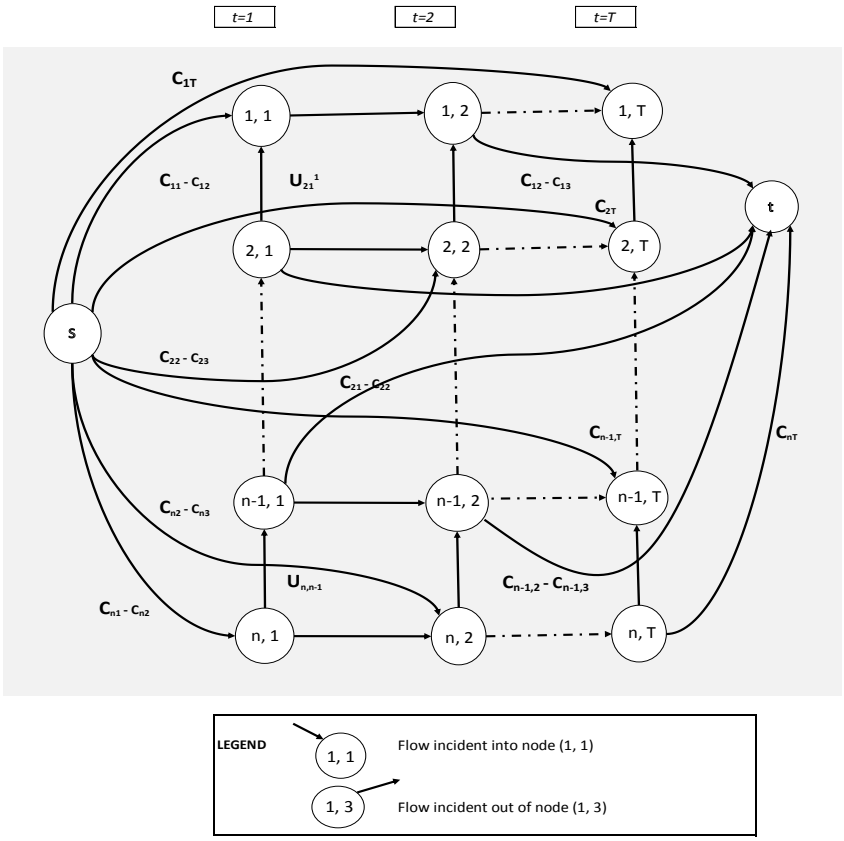


Figure 8.39: Multi-time-period maximum closure problem.

This transformation to a maximum flow problem was first introduced by Johnson (1968) who recognized that the network structure of $(\boldsymbol{DMPLP})^{\boldsymbol{by}}$ on the new extended graph was equivalent to solving a max flow problem, which will be referred to as $(\boldsymbol{EDMPLP})^{\boldsymbol{by}}$.

The equivalent maximum flow problem is formulated as follows:

Indices and sets:

$n \in N_t^+$: $Set\ of\ positive\ nodes$

$m \in N_t^-$: $set\ of\ negative\ \ nodes$

$V$: $set\ of\ all\ nodes\ in\ the\ network\ \{N_t^+\} \cup \{N_t^-\} \cup \{s\} \cup \{t\}$

Variable definition:

$f_{sn}^t$: $Flow\ from\ source\ node\ to\ node\ n\ in\ time\ period\ t$

$f_{mt}^{t'}$: $Flow\ from\ node$ mt$o\ sink\ node$ "$t$" $in\ time\ period\ t'$

$u_{ij}^t$: $Flow\ from\ node\ i\ to\ node\ j\ in\ time\ period\ t$

$v_i^{t,t+1}$: $Flow\ from\ node\ i\ in\ time\ period\ t\ to\ node\ j\ in\ time\ period\ t+1$

$$(\boldsymbol{EDMPLP})^{\boldsymbol{by}} \quad \max \quad \sum_{t \in T} \sum_{n \in N_t^+} f_{sn}^t \tag{8.182}$$

Constraints:

**Period 1**

$$-f_{sn}^1 - u_{in}^1 + u_{nj}^1 + v_n^{12} = 0 \qquad n \in N_1^+ \tag{8.183}$$

$$-f_{mt}^1 - u_{im}^1 + u_{mj}^1 + v_m^{12} = 0 \qquad m \in N_1^- \tag{8.184}$$

$$f_{sn}^1 \leq (c_n^1 - c_n^2) \qquad n \in N_1^+ \tag{8.185}$$

$$f_{mt}^1 \leq -(c_m^1 - c_m^2) \qquad m \in N_1^- \tag{8.186}$$

**Periods $\boldsymbol{t = 2..T-1}$**

$$-f_{sn}^t - u_{in}^t + u_{nj}^t - v_n^{t-1,t} + v_n^{t,t+1} = 0 \qquad n \in N_t^+ \tag{8.187}$$

$$f_{mt}^{t'} - u_{im}^{t} + u_{mj}^{t} - v_{m}^{t-1,t} + v_{m}^{t,t+1} = 0 \qquad m \in N_t^- \tag{8.188}$$

$$f_{sn}^{t} \leq (c_n^t - c_n^{t+1}) \quad n \in N_t^+ \tag{8.189}$$

$$f_{mt}^{t'} \leq -(c_m^t - c_m^{t+1}) \quad m \in N_t^- \tag{8.190}$$

$$-f_{sn}^{T} - u_{in}^{T} + u_{nj}^{T} - v_{n}^{T-1,T} = 0 \qquad n \in N_n^T \tag{8.191}$$

**Last time period**

$$f_{mt}^{t} - u_{im}^{T} + u_{nj}^{T} - v_{m}^{T-1,T} = 0 \qquad m \in N_m^T \tag{8.192}$$

$$f_{sn}^{T} \leq c_n^T \qquad n \in N_n^T \tag{8.193}$$

$$f_{mt}^{t'} \leq -c_m^T \qquad m \in N_m^T \tag{8.194}$$

$$f_{sn}^{t}, f_{mx}^{t}, u_{in}^{t}, u_{nj}^{t}, v_{n}^{t,t+1}, p_n \quad \forall m \in N_t^-, n \in N_t^+, t' \in T, i \in V\{s \cup t\}, \; j \in V\{s \cup t\} \tag{8.195}$$

### 8.3.1 A Numerical Example of the Multi-Time-Period Max Flow Algorithm

Consider the following three-time-period problem:

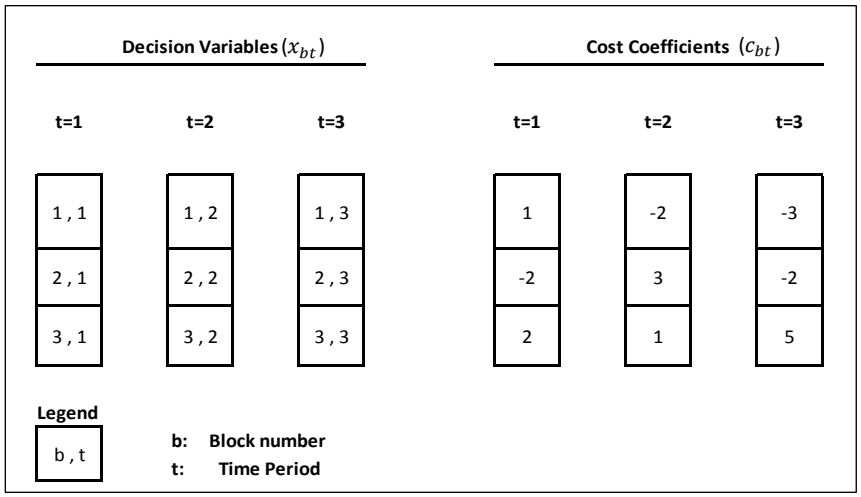


Figure 8.40: Three-time-period maximum closure problem, showing three conceptual mine blocks disposed one on top of the other (adapted from Dagdelen, 1985).

In accordance with the model presented in equations (8.151) - (8.154), a corresponding MPLP is formulated as follows:

$$max\ Z = 1x_{11} - 2x_{21} + 2x_{31} - 2x_{12} + 3x_{22} + x_{32} - 3x_{13} - 2x_{23} + 5x_{33} \quad (8.196)$$

$subject\ to$:

$$-x_{11} + x_{21} \leq 0 \quad (8.197)$$

$$-x_{21} + x_{31} \leq 0 \quad (8.198)$$

$$-x_{11} + x_{21} - x_{12} + x_{22} \leq 0 \quad (8.199)$$

$$-x_{21} + x_{31} - x_{22} + x_{32} \leq 0 \quad (8.200)$$

$$-x_{11} + x_{21} - x_{12} + x_{22} - x_{13} + x_{23} \leq 0 \quad (8.201)$$

$$-x_{21} + x_{31} - x_{22} + x_{32} - x_{23} + x_{33} \leq 0 \quad (8.202)$$

$$x_{11} + x_{12} + x_{13} \leq 1 \quad (8.203)$$

$$x_{21} + x_{22} + x_{23} \leq 1 \quad (8.204)$$

$$x_{31} + x_{32} + x_{33} \leq 1 \quad (8.205)$$

$$x_{bt} \geq 0 \qquad \forall bt \quad (8.206)$$

The variable substitution described in equations (8.170) - (8.171) is applied to transform the problem from an "at" to a "by" formulation, and the cost coefficients are adjusted so as to conform to the new "by" decision variables:

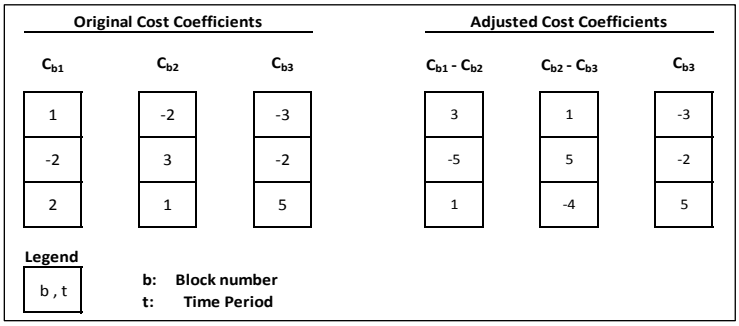


Figure 8.41: Adjusted cost coefficients, consistent with the multi-time-period formulation of the maximum closure problem (Dagdelen 1985).

Objective function:

$$max\ Z = 3w_{11} - 5w_{21} + w_{31} + w_{12} + 5w_{22} - 4w_{32} - 3w_{13} - 2w_{23} + 5w_{33} \quad (8.207)$$

$subject\ to$:

$$-w_{11} + w_{21} \leq 0 \quad (8.208)$$

$$-w_{21} + w_{31} \leq 0 \quad (8.209)$$

$$-w_{12} + w_{22} \leq 0 \quad (8.210)$$

$$-w_{22} + w_{32} \leq 0 \quad (8.211)$$

$$-w_{13} + w_{23} \leq 0 \quad (8.212)$$

$$-w_{23} + w_{33} \leq 0 \quad (8.213)$$

$$w_{11} - w_{12} \leq 0 \quad (8.214)$$

$$w_{21} - w_{22} \leq 0 \quad (8.215)$$

$$w_{31} - w_{32} \leq 0 \quad (8.216)$$

$$w_{12} - w_{13} \leq 0 \quad (8.217)$$

$$w_{22} - w_{23} \leq 0 \quad (8.218)$$

$$w_{32} - w_{33} \leq 0 \quad (8.219)$$

$$w_{13} \leq 1 \quad (8.220)$$

$$w_{23} \leq 1 \quad (8.221)$$

$$w_{33} \leq 1 \quad (8.222)$$

$$\mathrm{w}_{bt} \geq 0 \qquad \forall b, t \quad (8.223)$$

Next, we take the dual of the problem expressed as a function of "by" variables, as in equations (8.207) - (8.223). Recall that in the context of multi-time-period sequencing problems,

a new set of constraints - addressing precedence requirements (*across time*) between a block and itself - must be considered. These requirements are different than those enforcing physical (slope) constraints and, therefore, are associated to distinct dual variables in $(\boldsymbol{D}MPLP)^{\boldsymbol{by}}$ (see Figure 8.42).

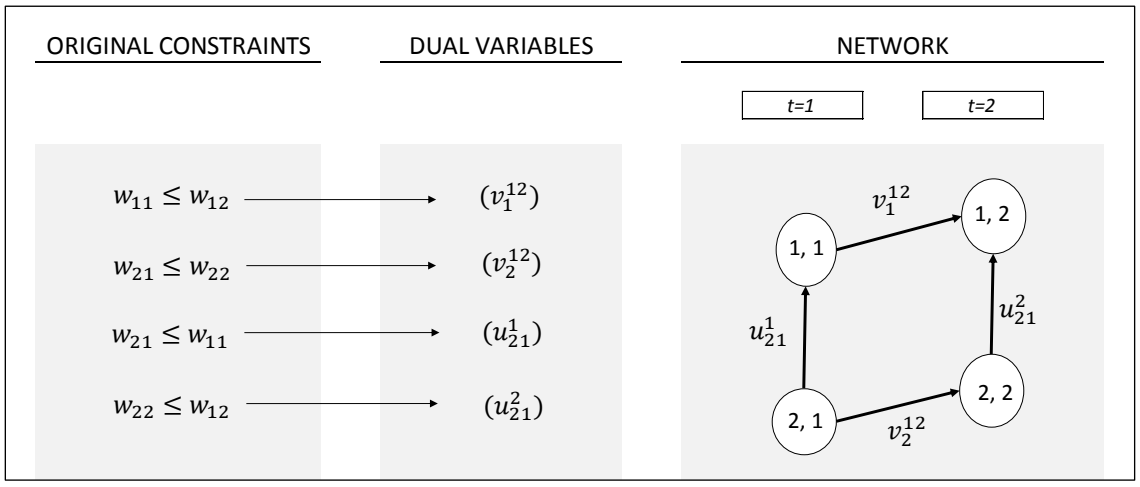


Figure 8.42: Physical versus time precedence constraints in the network flow problem corresponding to $(\boldsymbol{D}MPLP)^{\boldsymbol{by}}$.

In Figure 8.42, the directed vertical arc connecting nodes (2,1) – (1,1) is associated with the dual variable $u_{21}^1$ and represents a physical precedence requirement between said blocks. On the contrary, the directed horizontal arc connecting nodes (1,1) – (1,2) is associated with the dual variable $v_1^{12}$ and represents a time precedence requirement between a given node and its "replica" in a subsequent time period. The new problem $(\boldsymbol{D}MPLP)^{\boldsymbol{by}}$ is formulated as follows:

Variable definition:

$u_{ij}^t$: $flow\ between\ node\ i\ and\ node\ j\ in\ \ time\ period\ t$

$v_i^{t,t+1}$: $flow\ between\ time\ period\ t\ and\ t+1\ for\ node\ i$

$p_i$: $flow\ on\ arcs\ connecting\ to\ the\ terminal\ node$

Objective function:

$$(\boldsymbol{D}MPLP)^{\boldsymbol{by}} \quad min \quad p_1 + p_2 + p_3 \tag{8.224}$$

Constraints:

$$-u_{21}^{1} + v_{1}^{12} \geq 3 \quad (8.225)$$

$$u_{21}^{1} - u_{32}^{1} + v_{2}^{12} \geq -5 \quad (8.226)$$

$$u_{32}^{1} + v_{3}^{12} \geq 1 \quad (8.227)$$

$$-u_{21}^{2} - v_{1}^{12} + v_{1}^{23} \geq 1 \quad (8.228)$$

$$u_{21}^{2} - u_{32}^{2} - v_{2}^{12} + v_{2}^{23} \geq 5 \quad (8.229)$$

$$u_{32}^{2} - v_{3}^{12} + v_{3}^{23} \geq -4 \quad (8.230)$$

$$-u_{21}^{3} - v_{1}^{23} + p_{1} \geq -3 \quad (8.231)$$

$$u_{21}^{3} - u_{32}^{3} - v_{2}^{23} + p_{2} \geq -2 \quad (8.232)$$

$$u_{32}^{3} - v_{3}^{23} + p_{3} \geq 5 \quad (8.233)$$

$$u_{ij}^{t}, \quad v_{i}^{t,t+1}, \quad p_{i} \geq 0 \ \forall i, j, t \quad (8.234)$$

The network representation for $(\boldsymbol{DMPLP})^{\boldsymbol{by}}$ corresponding to the example problem is shown in Figure 8.43:

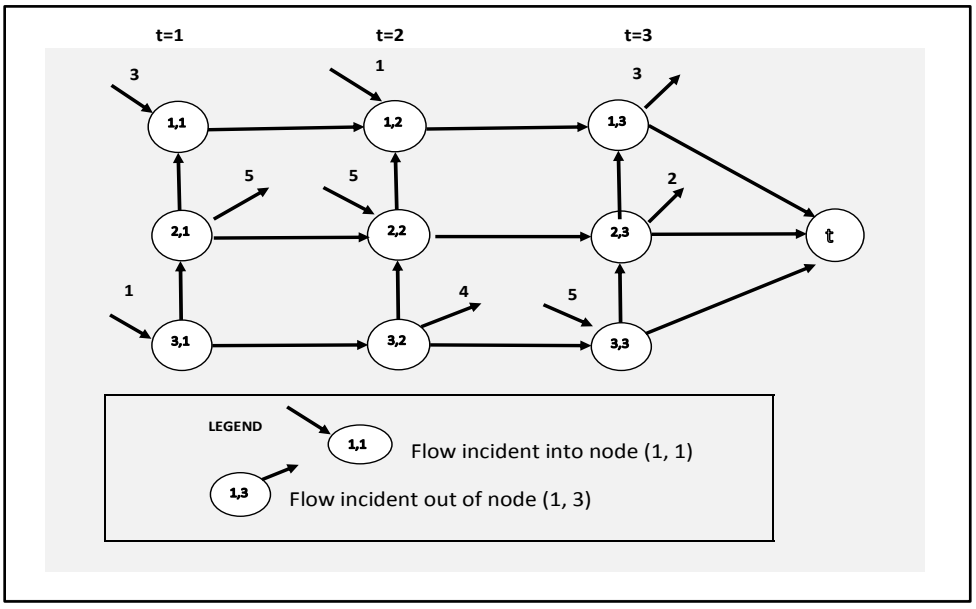


Figure 8.43: Three-time-period maximum closure problem. Inside each node, the first digit corresponds to the node number while the second represents the time period considered. (adapted from Dagdelen, 1985).

An equivalent max flow problem $(\boldsymbol{EDMPLP})^{\boldsymbol{by}}$, consistent with the formulation shown in equations (8.182) - (8.195) is presented as follows:

Variable definition:

$f_{sn}^{t}$: $Flow\ from\ source\ node\ to\ node\ n\ in\ time\ period\ t$

$f_{mt}^{t'}$: $Flow\ from\ node$ m$to\ sink\ node$ "$t$" $in\ time\ period\ t'$

$u_{ij}^{t}$: $Flow\ from\ node\ i\ to\ node\ j\ in\ time\ period\ t$

$v_{i}^{t,t+1}$: $Flow\ from\ node\ i\ in\ time\ period\ t\ to\ node\ j\ in\ time\ period\ t+1$

Objective function;

$$(\boldsymbol{EDMPLP})^{\boldsymbol{by}} \quad max\ f_{s1} + f_{s3} + f_{s4} + f_{s5} + f_{s9} \tag{8.235}$$

Constraints:

$$f_{s1} + u_{21}^{1} - v_{1}^{12} = 0 \tag{8.236}$$

$$u_{32}^{1} - f_{2t} - u_{21}^{1} - v_{2}^{12} = 0 \tag{8.237}$$

$$f_{s3} - u_{32}^{1} - v_{3}^{12} = 0 \tag{8.238}$$

$$f_{s4} + v_{1}^{12} + u_{54}^{2} - v_{4}^{23} = 0 \tag{8.239}$$

$$f_{s5} + v_{2}^{12} + u_{65}^{2} - u_{54}^{2} - v_{5}^{23} = 0 \tag{8.240}$$

$$v_{3}^{12} - f_{6t} - u_{65}^{2} - u_{54}^{2} - v_{6}^{23} = 0 \tag{8.241}$$

$$v_{4}^{23} + u_{87}^{3} - f_{7t} - p_{1} = 0 \tag{8.242}$$

$$v_{5}^{23} + u_{98}^{3} - f_{8t} - u_{87}^{3} - p_{2} = 0 \tag{8.243}$$

$$f_{s9} + v_{6}^{23} - u_{98}^{3} - p_{3} = 0 \tag{8.244}$$

$$f_{s1} \leq 3 \tag{8.245}$$

$$f_{s3} \leq 1 \tag{8.246}$$

$$f_{s4} \leq 1 \tag{8.247}$$

$$f_{s5} \leq 5 \tag{8.248}$$

$$f_{s9} \leq 5 \tag{8.249}$$

$$f_{2t} \leq 5 \tag{8.250}$$

$$f_{6t} \leq 4 \tag{8.251}$$

$$f_{7t} \leq 3 \tag{8.252}$$

$$f_{8t} \leq 2 \tag{8.253}$$

$$f_{sn},\ f_{mt},\ u_{ij}^{t},\ v_{i}^{t,t+1},\ p_i \geq 0 \quad \forall s, n, m, i, j, t \tag{8.254}$$

The network for the modified max flow problem is presented in Figure 8.44:

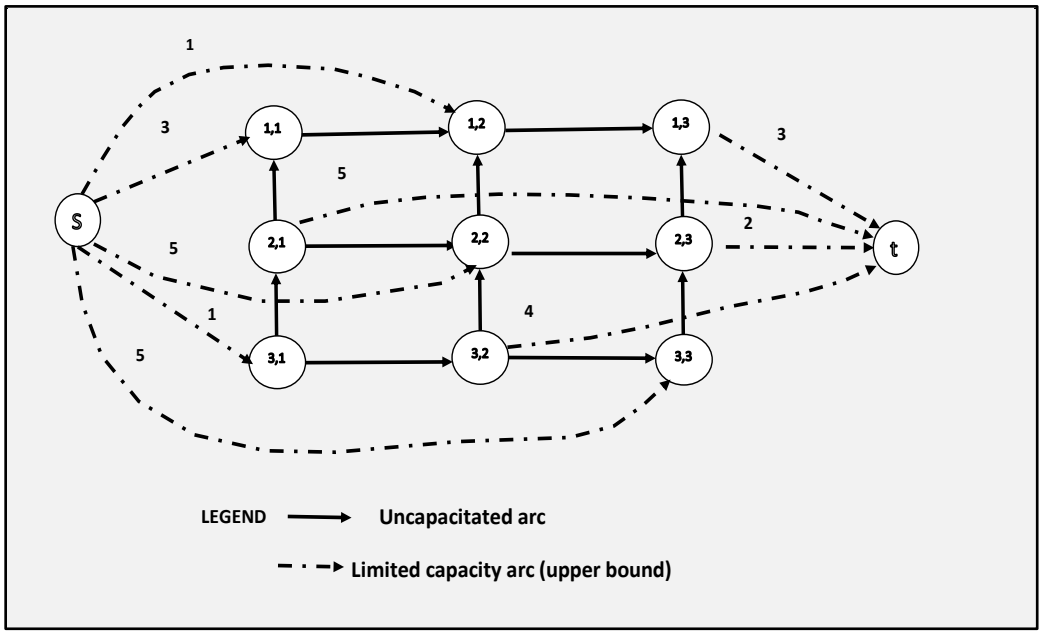


Figure 8.44: Multi-time-period maximum flow problem on the bipartite graph (Dagdelen, 1985).

The preceding discussion showed (in detail) how a multi-time-period pit limit problem can be cast as an equivalent max flow problem, leading to a reasonable expectation that it be solvable efficiently, by the use of specialized algorithms. However, said problems can be solved by a multitude of network algorithms with differing performance (Ahuja *et al.*, 1993), leading to the challenge of determining how to best solve the specific problem one is addressing.

It is in this context that the characteristics of the PseudoFlow algorithm are presented in the subsequent Section.

### 8.3.2 Steps of the PseudoFlow Algorithm

The PseudoFlow algorithm (HPF) is the fastest known algorithm, currently reported in the literature, to solve the maximum flow (or maximum closure) problem (Hochbaum, 2001, 2008). The HPF has marked similarities with the Lerchs-Grossman algorithm, however, contrary to LG which does not use the concept of flow, using instead sets of nodes which have "mass"; the HPF algorithm uses pseudoflows to solve the maximum flow problem. The HPF algorithm operates on a new extended network $G^{ext}$ which differs from the typical graph in traditional max flow problems $G_{st}$. In particular, every node in $G^{ext}$ has two additional arcs associated with it: one connecting it to the source, called an excess arc; and another connecting the sink to the node, called a deficit arc (Figure 8.45). For example, the arc connecting node $(1,1)$ to the source node $(s)$ corresponds to an excess arc, and the arc connecting the sink node $(t)$ to node $(1,3)$ corresponds to a deficit arc.

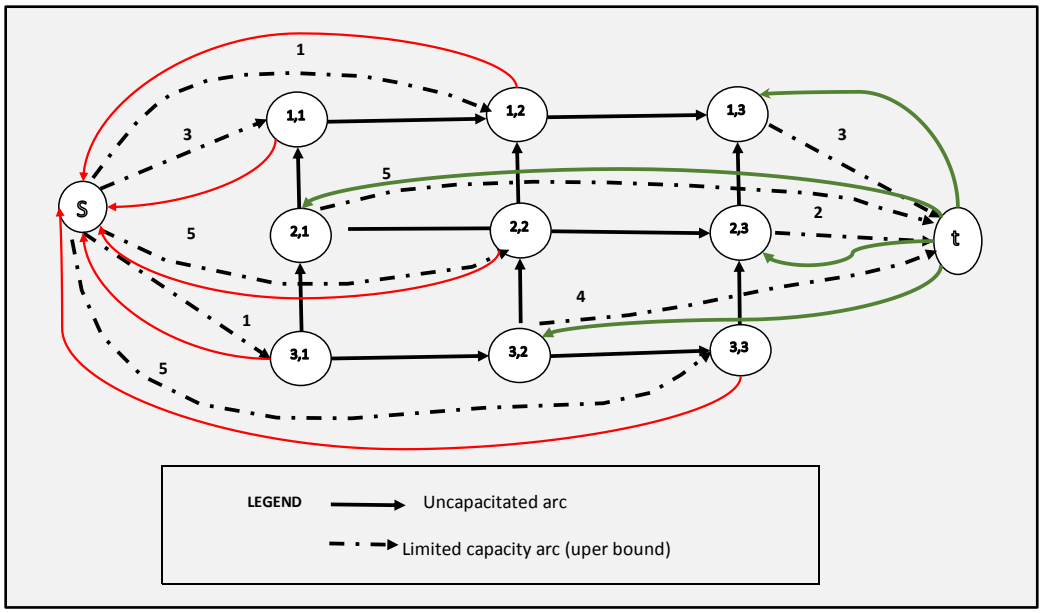


Figure 8.45: The PseudoFlow extended graph $G^{ext}$. In effect, all nodes in the extended graph have two infinite capacity arcs, one connecting it to the source and the other connecting it to the sink, which are partially omitted from the picture for greater clarity.

Prior to describing the iteration steps of the HPF algorithm, it is convenient to introduce part of the terminology as initially suggested by the authors (Hochbaum, 1997, 2001, 2008).

A graph $G = (V, A)$ is considered an $s, t - graph$ if it contains two distinguished nodes $s$ and $t$; source and sink nodes respectively. For $P, Q \subset V$ the set of arcs going from $P$ to $Q$ is denoted by $(P, Q) = \{(u, v) \in A | \, u \in P \; and \; v \in Q\}$. The capacity of an arc $(u, v) \in A$ is a nonnegative real number $c_{uv}$ and the flow on that arc is $f_{uv}$.

A $pseudoflow \; f$ in an arc capacitated $s, t - graph$ is a mapping that assigns to each arc $(u, v)$ a real value $f_{uv}$ so that $0 \leq f_{uv} \leq c_{uv}$. For a given PseudoFlow $f$ in an $s, t - graph$ the residual capacity of an arc $(u, v) \in A$ is $c_{uv}^f = c_{uv} - f_{uv}$, and the residual capacity of the backwards arc $(v, u) \in A$ is $c_{vu}^f = f_{uv}$. Note that flow balance constraints (requiring that the total flow entering a node $n \in V \backslash \{s, t\}$ be equal to the total flow leaving it) are allowed to be violated.

An arc is said to be a $residual \; arc$ if its residual capacity is positive. The set of residual arcs is $A^f = \{(i, j) \in A | \, f_{ij} < c_{ij} \; or \; (j, i) \in A \big| \, f_{ji} > 0\}$. A directed path $(v_1, v_2), \ldots, (v_{k-1}, v_k)$ is said to be a $residual \; path$ if $(v_1, v_2), \ldots, (v_{k-1}, v_k) \in A_f$. An $s, t - graph$ is called a $closure \; graph$ if the only arcs of finite capacity are those adjacent to the source and sink nodes. A $rooted \; tree$ is a collection of arcs that forms an undirected acyclic connected graph $T$with one node designated as a root.

The following are three related equivalent related representations of a graph:

1. $G = (V, A)$ is a directed graph with real node weights $w_i \; \forall i \in V$ and positive arc capacities $c_{ij}$ for $(i, j) \in A$.

2. $G_{st} = (V_{st}, A_{st})$ is an $s, t - graph$ with only arc capacities. It is constructed from the graph G as follows: the set of nodes is $V_{st} = V \cup \{s, t\}$, and the set of arcs $A_{st}$ comprised of the arcs $A$ appended by sets of arcs adjacent to $s$ and $t$, $A(s)$ and $A(t)$. The arcs of $A(s) = \{(s, j) | w_j > 0\}$ connect s to all nodes of positive weight, each of capacity equal to the weight of the respective node, $c_{sj} = w_j$. Analogously, $A(t) = \{(j, t) | w_j < 0\}$ and $c_{jt} = -w_j = |w_j|$ for $(j, t) \in A(t)$. Zero weight nodes are connected neither to the source nor to the sink. Thus, $G_{st} = (V_{st}, A_{st}) = (V \cup \{s, t\}, A \cup A(s) \cup A(t))$.

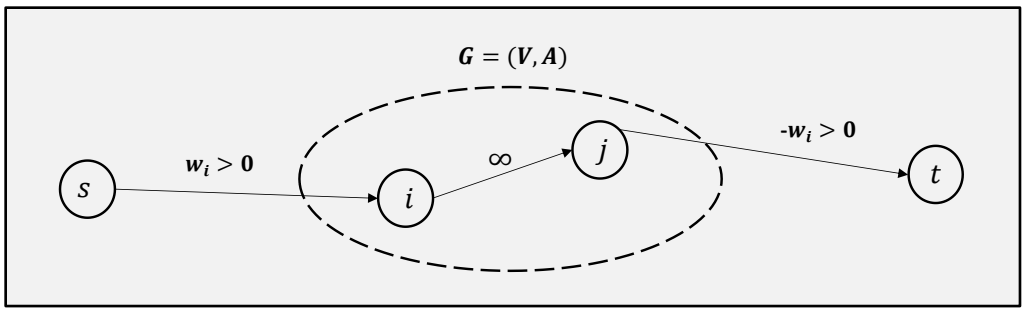


Figure 8.46: Construction of a $G_{st}$ graph starting from an initial G graph (Hochbaum, 2012).

3. $G^{ext}$ the $extended\ network$, corresponds to an $s,t-graph\ G_{st}$ built by adding to $A_{st}$, for each node v, two arcs of infinite capacity – $(t,v)$ and $(v,s)$ – and then shrinking $s$ and $t$ into a single node $r$ called $root$.

The appended arcs from sink $t$ are referred to as $deficit\ arcs$ and the appended arcs to the source s are called $excess\ arcs$; and their set is denoted by $A_\infty = \bigcup_{v\in V}\{(v,r)\cup(r,v)\}$. The $extended\ network$ is the graph $G^{ext} = (V\cup\{r\}, A^{ext})$ where $A^{ext} = A\cup A(s)\cup A(t)\cup A_\infty$.

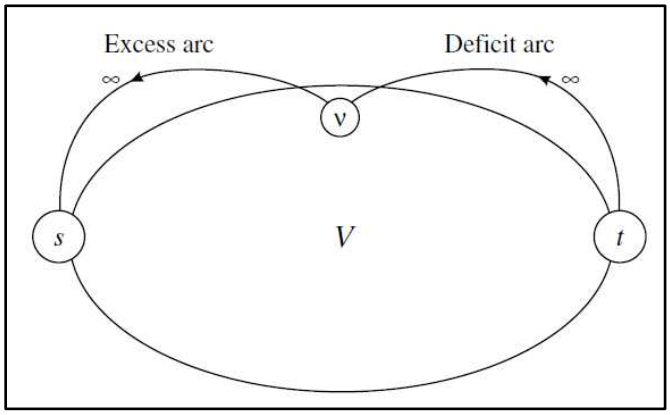


Figure 8.47: Construction of a $G^{ext}$ graph starting from an initial $G_{st}$ graph (Hochbaum, 2012).

An additional important concept, which is borrowed from the LG algorithm jargon, is that of a $normalized\ tree$. $T = (V\cup\{r\}, E_T)$ is a normalized tree if it is defined on a spanning tree in $G^{ext}$ rooted in "$r$" so that $E^T \subset A\cup\bigcup_{v\in V}\{(v,r)\cup(r,v)\}$.

The children of "$r$" in such a spanning tree are designated "$r_i$," and form the roots of their respective $branches$ (also referred to as trees or subtrees). In a normalized tree, only the branch roots "$r_i$" are permitted to carry nonzero deficits or excesses.

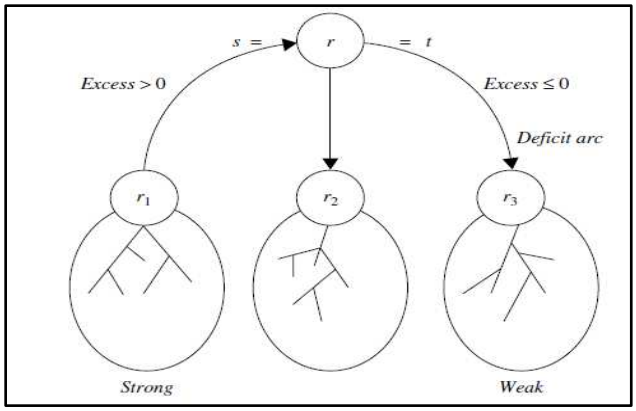


Figure 8.48: Illustration of a normalized tree, with node $r$ representing the root node, and nodes $r_i$ representing the root of branch $i$ (Hochbaum, 2008).

For a given PseudoFlow $f$, a branch is $T_{r_i}$, is called $strong$ if $excess(T_{r_i}) = excess\ (r_i) = f_{r_i,r} > 0$, and $weak$ otherwise. All nodes of strong branches are considered strong, and all nodes of weak branches are considered weak. Branches with zero excess are also considered weak.

One iteration of the PseudoFlow algorithm requires specific steps which can be summarized as follows (Hochbaum 2008):

1. Initialize the algorithm by selecting a normalized tree. One *simple normalized tree* corresponds to a PseudoFlow in $G_{st}$ saturating all arcs adjacent to the source $A(s)$ and all the arcs adjacent to the sink $A(t)$, and zero on all other arcs.

2. Find a residual arc from a strong set of nodes to a week set of nodes – merger arc. If such an arc does not exist, the current solution is optimal.

3. If residual arcs going from a strong node to a weak node exist then, the selected merger arc is appended to the tree, the excess arc of the strong merger branch is removed and the strong branch is merged with the weak branch.

4. Push the entire excess of the respective strong branch along the unique path from the root of the strong branch to the root of the weak branch.

5. Split any arc encountered along the path described in 3) which does not have sufficient residual capacity to accommodate the amount pushed. The tail node of that arc becomes a root of a new strong branch with excess equal to the difference between the amount pushed and the residual capacity.

6. The process of pushing excess and splitting is called *normalization*. The residual capacity of the split arc is pushed further until it either reaches another arc to split or the deficit arc adjacent to the root of the weak branch.

### 8.3.3 Numerical Example of the PseudoFlow Algorithm

Consider the problem described in figure below:

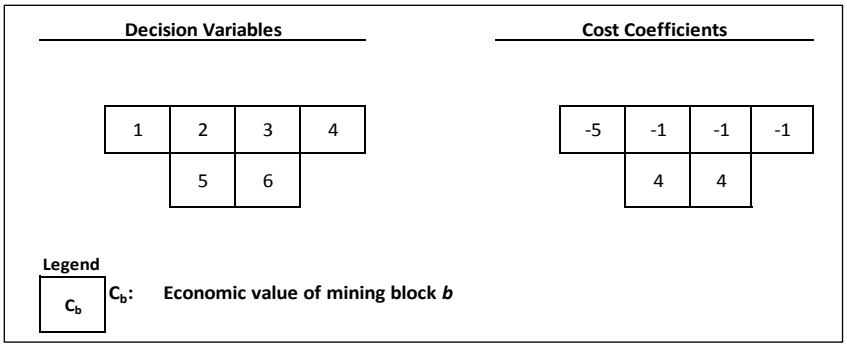


Figure 8.49: Single time period maximum closure problem.

We refer to the steps of the HPF outlined in the previous Section.

- First iteration

For the first iteration source (s) and sink (t) adjacent arcs are saturated and a feasible pre-assignment of flow is decided upon. Four units of flow are induced into the network by the arc connecting nodes (s) and (6); all 4 units of flow reach node (4), only one unit of flow reaches the

sink node (t) from the node (4) and the remainder 3 units of flow are re-routed from node (4) to the source via the excess arc (shown in blue in Figure 8.50). Similar to the arc connecting (s) to (6), the arc from (s) to (5) induces four units of flow into the network, two units of flow originating from (5) are distributed through the arcs connecting node (5) to nodes (2) and (4) by assigning one unit of flow per each of the arcs two units are assigned to node (1) and, from there reach the sink node.

Since the demand in arc connecting node (1) to node "*t*" is greater than the flow on the arc (i.e., 5>2) then, a flow deficit results and flow must be re-routed from "*t*" to node (1). The resulting graph and tree structure are shown in Figure 8.50.

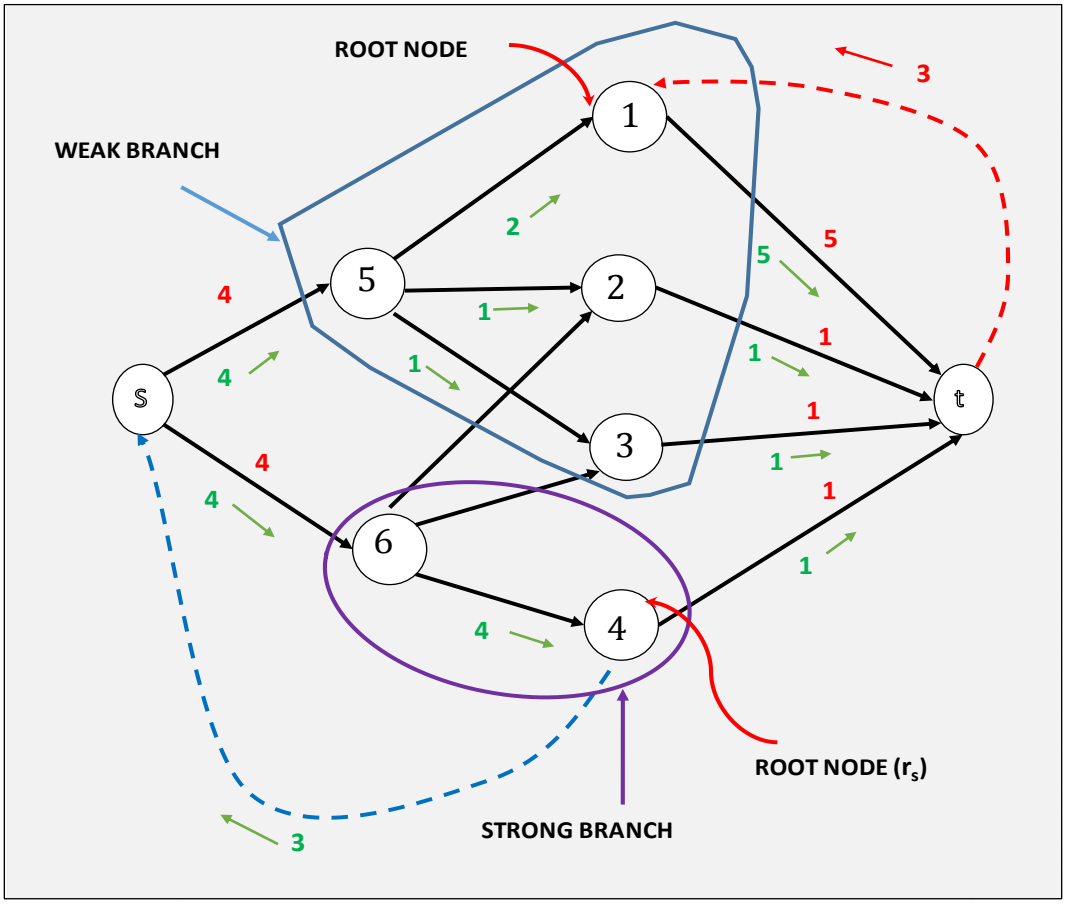


Figure 8.50: An initial normalized tree for the HPF algorithm. The set of arcs *A(s)* and *A(t)* are all saturated. An initial arbitrary flow assignment is chosen in which the strong and the weak group of nodes are circled and the respective root nodes are highlighted as well.

- Second iteration

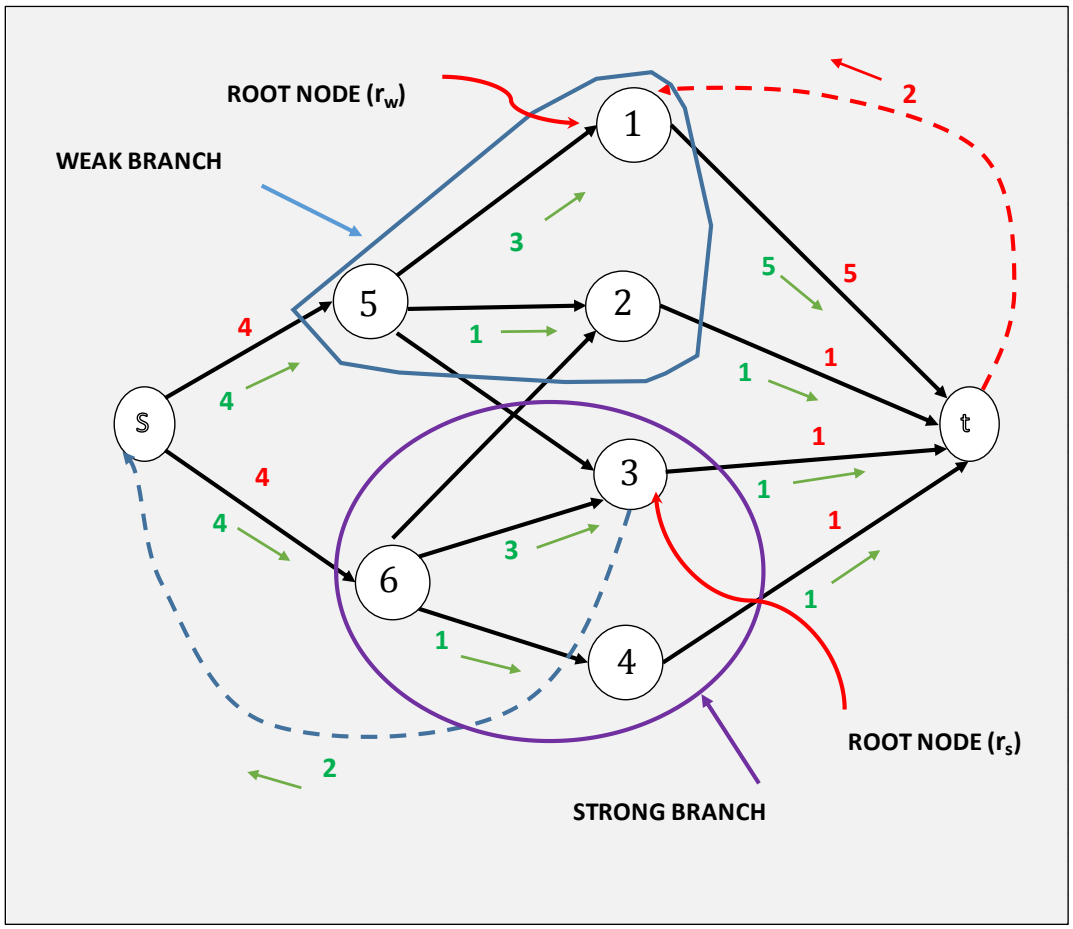


Figure 8.51: At this stage, the excess arc previously connecting (4) to "*s*" is "replaced" by a new arc connecting node (3) to the source and the strong set of nodes is updated.

A residual arc connecting node (6) to (3) is identified going from a strong branch to a weak branch. At this stage, the objective is to re-route as much excess flow as possible from the root of the strong group of nodes (branch) to the root of the weak branch resulting in the graph shown in Figure 8.51. The remaining residual arc connects node (6) to node (2). After re-routing the flow from node (3) (the root of the strong branch) to node (1) (the root of the week branch), the result obtained is shown in the Figure 8.52.

- Third iteration

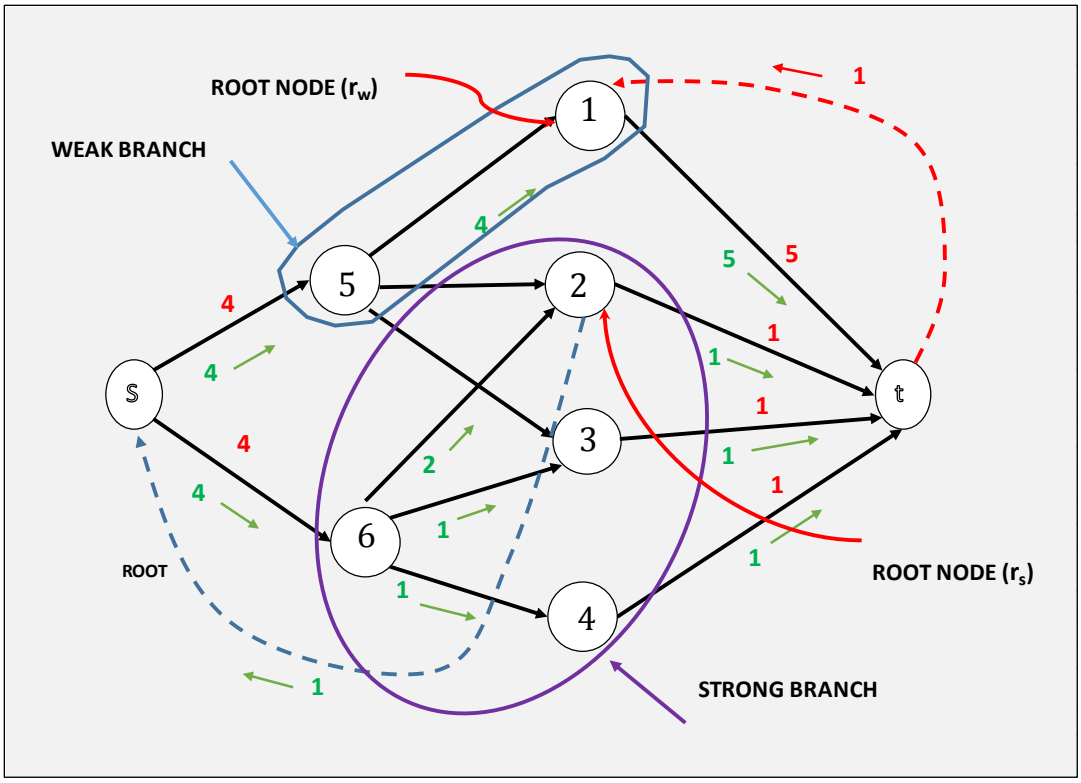


Figure 8.52: Single time period maximum closure problem.

At the current iteration no residual arcs exist which connect a strong set of nodes to a weak set of nodes. This indicates the current *normalized tree* is optimal. The optimal solution corresponds to mining the strong set of nodes as there are no more residual arcs allowing the strong branch to be merged with the weak branch. This is equivalent to mining the blocks associated to nodes (6), (2), (3) and (4); which makes intuitive sense from a mining perspective (Figure 8.53).

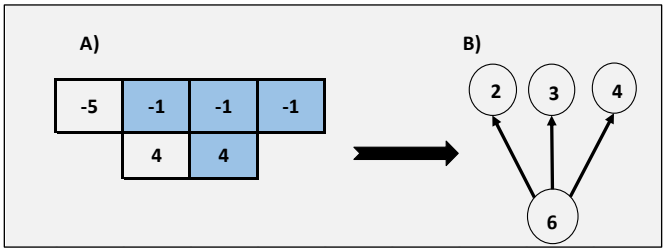


Figure 8.53: Optimal solution to maximum closure problem.

It is noted that, although the maximum flow through the network is not of interest, it could nonetheless be obtained by subtracting the excess flow from the sum of the flows from the source, or by subtracting the deficit flow from the sum of the flows into the sink.

# CHAPTER 9.
# APPLICATION OF THE PROPOSED METHODOLOGY

## 9.1 Two-Dimensional Synthetic Case Studies

The model formulations for the two-dimensional synthetic case studies (as well as for the three-dimensional examples) are coded using the C++ programming language and solved using CPLEX 12.6.0.1 (IBM ILOG CPLEX Optimization Studio, 2015), preserving all of the default settings. The cases are run on a MacBook Pro machine with one 2.5 GHz quad-core Intel Core I7 processor and 16GB of 1600MHz DDR3L onboard memory. For demonstration purposes, the results from the application of the proposed methodology to a synthetic two-dimensional conceptual model of an iron ore mineral deposit are presented and discussed. It is assumed that all blocks have equal tonnage and that only two destinations are available: an ore processing plant and a waste dump. Mine production will occur in three time periods, and time value of money effects are modeled by adopting a 10% discount rate for the economic block values. In order to highlight the importance of incorporating geological uncertainty, two alternative scenarios are tested, one representing a traditional deterministic approach and the other risk-based approach. Specifically, in the case of scenario #1, ore risk constraints are disregarded while in the case of scenario #2 such constraints are enforced. The problem statement also includes distinct constraints for total ore milling capacity, as well as lower and upper bounds on the average grade of material entering the processing plant which are the same in both scenarios.

Figure 9.1 depicts the conceptual grade block model (% Fe) underlying the economic block model of Figure 9.2.

| | 1 | 2 | 3 | 4 | 5 | 6 | 7 | 8 | 9 | 10 | 11 | 12 | 13 | 14 |
|---|---|---|---|---|---|---|---|---|---|---|---|---|---|---|
| 3 | W | W | 67 | 66 | W | W | 64 | 69 | 68 | 68 | W | W | W | W |
| 2 | | W | 62 | W | W | 40 | 60 | 63 | 63 | 62 | 66 | 66 | W | |
| 1 | | | 64 | 65 | 68 | 68 | 68 | 69 | 67 | 66 | 65 | 65 | | |

Figure 9.1: Two-dimensional conceptual cross section of the grade model corresponding to the iron ore deposit used in the computations (% Fe). (The letter “W” standing for waste blocks).

The economic block model corresponding to the ore deposit to be used as input to the proposed solution methodology is shown in Figure 9.2.

| | 1 | 2 | 3 | 4 | 5 | 6 | 7 | 8 | 9 | 10 | 11 | 12 | 13 | 14 |
|---|---|---|---|---|---|---|---|---|---|---|---|---|---|---|
| 3 | -4 | -4 | 9.3 | 3.2 | -0.1 | -4 | 5 | 14.1 | 10.8 | 11.2 | -4 | -1.7 | -4 | -4 |
| 2 | | -4.2 | 2.9 | -1.7 | -4.3 | 4.1 | 4.2 | 1.7 | 1.9 | 4.9 | 2.1 | 1.2 | -4.1 | |
| 1 | | | 0.8 | 1 | 2.5 | 9.6 | 12.9 | 13.3 | 9.2 | 4.3 | 8.3 | 8 | | |

Figure 9.2: Two-dimensional conceptual cross section of an economic block model depicting 1st period undiscounted economic block values ($/ton). (The values in red represent the economic value of waste blocks while values in black correspond to ore blocks).

It is assumed that a significant number of geostatistical conditional simulations can be obtained or generated and that their results may be used in classifying each block into its corresponding resource classification category. For more detailed discussions on the use of geostatistical conditional simulations for mineral resource classification - together with a comparison of the performance of different geostatistical methods - refer to Silva and Boisvert (2014).

Figure 9.3 depicts a cross-sectional view of the classification of the individual blocks into their corresponding ore resource categories.

| | 1 | 2 | 3 | 4 | 5 | 6 | 7 | 8 | 9 | 10 | 11 | 12 | 13 | 14 |
|---|---|---|---|---|---|---|---|---|---|---|---|---|---|---|
| 3 | W | W | IND | IND | W | W | MEAS | MEAS | INF | INF | W | W | W | W |
| 2 | | W | IND | W | W | MEAS | MEAS | INF | INF | INF | MEAS | INF | W | |
| 1 | | | MEAS | INF | IND | INF | IND | MEAS | MEAS | INF | INF | INF | | |

| LEGEND | INERRED | INDICATED | MEASURED | WASTE |
|---|---|---|---|---|
| | INF | IND | MEAS | W |

Figure 9.3: Two-dimensional conceptual cross section of an ore resource classification model.

Table 9.1 provides a summary of the mineral deposit showing proportions of Inferred, Indicated and Measured material for the total (ore and waste), as well as for the economic ore fraction (as a separate unit).

Table 9.1: Proportions of Inferred, Indicated and Measured material considering the entirety of the mineral deposit (ore and waste), as well as ore tonnes exclusively.

| RESOURCE CLASSIFCATION CATEGORY | ORE + WASTE | ORE |
|---|---|---|
| INFERRED (%) | 44.4 | 45.5 |
| INDICATED (%) | 19.4 | 22.7 |
| MEASURED (%) | 36.1 | 40.9 |

A summary of the operational requirements for each period is shown in Table 9.2

Table 9.2: milling capacity, ore blending and mineral resource risk requirements considered for the production scheduling problem.

| PERIOD | ORE MINED (blk) | MIN GRADE (%Fe) | MAX GRADE (%Fe) | INFERRED (%) | INDICATED (%) | MEASURED (%) |
|---|---|---|---|---|---|---|
| 1 | 3 | 64 | 66 | 0.35 | 0.15 | 0.40 |
| 2 | 10 | 64 | 66 | 0.35 | 0.15 | 0.40 |
| 3 | 8 | 64 | 66 | 0.35 | 0.15 | 0.40 |

For the computations carried out in scenario #2, that is, the scenario in which ore risk constraints are considered, it is assumed that in designing the risk plan, the mine planner likely desires to enforce upper bounds on the proportion of Inferred ore material, while choosing to enforce lower bounds on both the proportions of Indicated and Measured ore. Note that different bounds on the risk constraints might be enforced for different time periods, thus allowing for potential risk deferment strategies that postpone the mining of riskier blocks for the later stages of the mineral deposit's mine life. Note that, initially the results are computed and presented on an integer programming basis (i.e., if mined, blocks must be mined fully, as a single unit) so that key differences between the production plans can be more easily communicated. However, this does not alter the central insights about the impact of grade uncertainty on production schedules. The production plans obtained for both scenarios are summarized in Table 9.3 and Table 9.4.

Table 9.3: Mine production schedule corresponding to scenario #1 (risk-free scenario).

| TIME PERIOD | ORE MINED (blk) | AVG GRADE (%Fe) | INFERRED (%) | INDICATED (%) | MEASURED (%) |
|---|---|---|---|---|---|
| 1 | 3 | 64.3 | 0 | 0 | 100 |
| 2 | 10 | 64.0 | 50 | 30 | 20 |
| 3 | 7 | 65.7 | 57 | 14 | 29 |
| NPV ($) | 103.65 | | | | |

Table 9.4: Mine production schedule corresponding to scenario #2 (risk-based scenario).

| TIME PERIOD | ORE MINED (blk) | AVG GRADE (%Fe) | INFERRED (%) | INDICATED (%) | MEASURED (%) |
|---|---|---|---|---|---|
| 1 | 2 | 65.5 | 0 | 50 | 50 |
| 2 | 9 | 64.0 | 33 | 22 | 44 |
| 3 | 4 | 65.8 | 25 | 25 | 50 |
| NPV ($) | 90 | | | | |

From the results in said tables the following observations stand out: (i) the ideal plan of scenario #1, (i.e., the one in which no grade uncertainty exists), shows a much larger presence of Inferred material in its yearly composition of ore sent to the processing plant; (ii) for the first year of mining, enough ore in the Indicated and Measured categories exists (is accessible), that mining can avoid incorporating inferred material in the composition of the mill feed in both scenarios; (iii) comparing the first year of mining in both scenarios, one sees that the inclusion of risk requirements forces production to be redistributed so that a minimum threshold of indicated material is met and the risk composition of the subsequent periods is not jeopardized. This leads to lowering of average grades and decrease of generated cash flow; (iv) in the absence of risk constraints, period two would have much higher proportions of Inferred and Indicated material, indeed substantially higher than the proportion of Measured material for the same year; and finally, (v) using the proportion of Inferred material as the key indicator of risk, period three emerges as the riskiest year, that is, the one in which the greatest correction in this resource classification category occurs (an initial proportion of Inferred material of 57 % in scenario #1 is altered to a new corresponding value of 22 %)

The two alternative scenarios studied show the marked differences between traditional mine production schedules, which disregard any risks associated with geological uncertainty in grades, and mine plans which take due account of grade uncertainty. The physical extent of mining is remarkably different in both cases, with the risk-considerate mine production plans extending

far beyond the limits of the risk-inconsiderate mine production plans. Importantly, the sequencing of production is itself different between the case-studies (see Figure 9.4 and Figure 9.5).

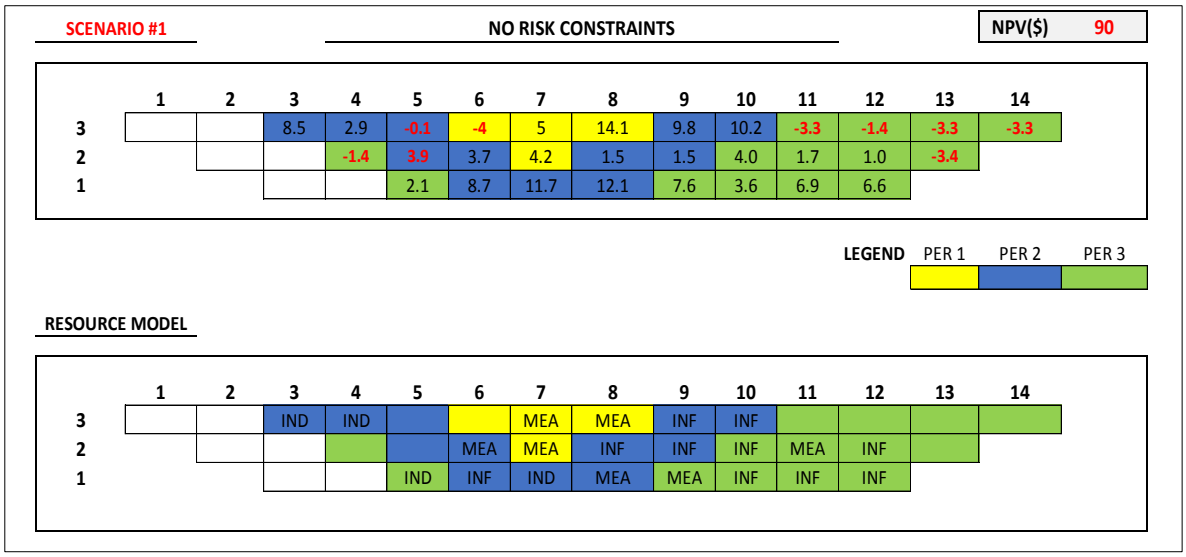


Figure 9.4: Mine production schedule for scenario #1, disregarding all risk associated with grade uncertainty. Values depicted correspond to discounted economic block values.

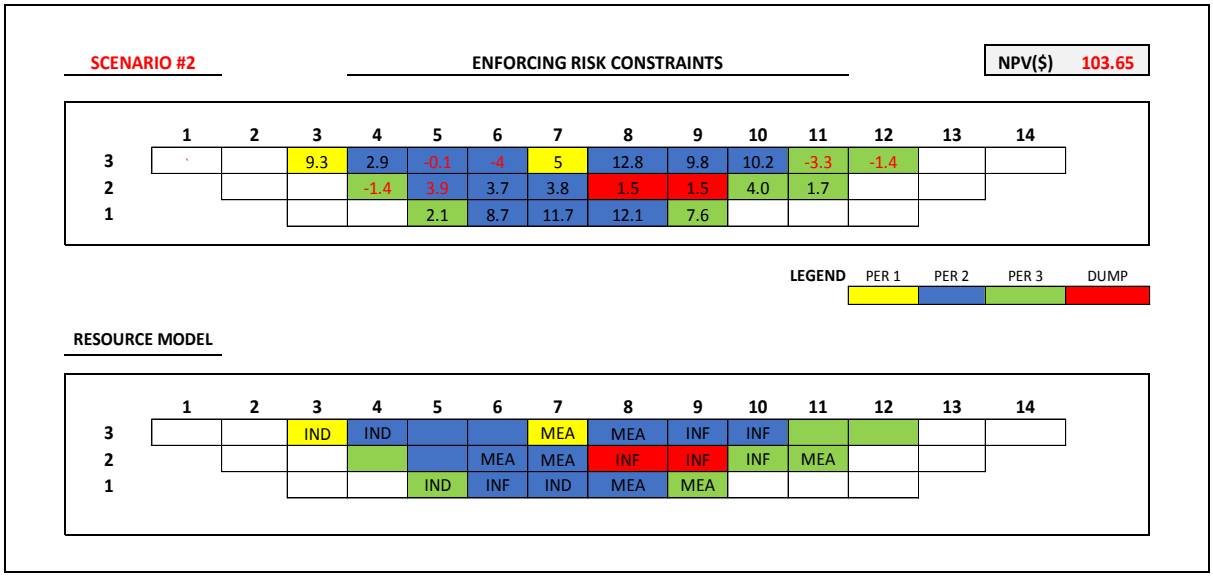


Figure 9.5: Mine production schedule enforcing ore risk constraint (scenario #2). Values depicted correspond to discounted economic block values.

For the mine production plan corresponding to scenario #1 (no risk constraints), mining is scheduled to start at roughly the center of the mineral deposit and then progress outwardly and in depth in the subsequent periods 2 and 3. In the case of scenario #2 mining is more scattered about

the ore deposit in the first period, where blocks positioned at coordinates $(i, j) = (3, 3)$ and $(3, 7)$ are selected. Next, production evolves in depth and roughly to the center of the orebody in period 2. Eventually, in period 3 mining progresses further in depth and outwardly towards the western flank of the orebody. These differences can be readily understood by considering the fact that in the first scenario, the absence of ore risk constraints means that the solver is not considering the need to meet these requirements in the composition of the material it chooses to send to the mill plant. On the other hand, scenario #2 incorporates risk constraints enforcing limits on the proportions of ore material belonging to each of the resource classification categories, causing the solver to deviate from the path it would have otherwise taken, and reach for blocks outside the physical boundary of the mine plan for scenario #1. Additionally, it should be noted that in the case of scenario #2, in period 2, the positive-valued ore block positioned according to coordinates $(i, j) = (2, 8)$ is actually sent to the waste dump rather than the processing plant. This occurs because the scheduler seeks to reach the largely more profitable ore blocks at the bottom of the orebody while staying below the upper limits of total ore sent to the mill plant.

Clearly, NPV for scenario #1 will (necessarily) constitute an upper bound on the total NPV that may be realized by mining according to the schedule associated with scenario #2, as it corresponds to a less constrained optimization model. In the case shown in Figure 9.4 the NPV for scenario #1 is approximately \$111 while scenario #2 has an NPV of approximately \$102.

Next, the proposed methodology is extended to a slightly larger case study emphasizing the importance of allowing for the incorporation of risk tolerance into mine plans.

A cross-sectional view of the resource model for the deposit is as presented in Figure 9.6.

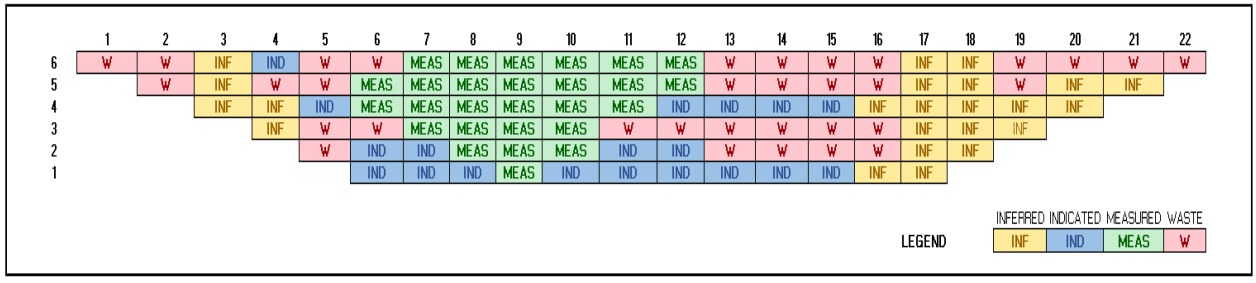


Figure 9.6: Two-dimensional conceptual cross section of the ore resource classification model.

In constructing the conceptual resource model special note has been placed in reproducing appropriately, the typical outcome from drillhole exploration campaigns. Commonly, such campaigns place greater focus on the accurate delineation of those areas of the orebody which display the highest grade results initially and, thus, hold the highest promise in terms of economic profitability.

This results in the richest portions of the deposit being more densely sampled than its poorer areas. In this example, the tendency to focus more on high-grade areas translates into the outer parts of the deposit being less sampled due to their relatively lower grades. Given the lack of detailed drillhole information, these areas have a higher degree of geological uncertainty and are classified into the Inferred resource category. Conversely, the central parts of the deposit, containing relatively higher grade material, are more densely sampled, accrue greater geological information and are classified as Measured or Indicated material.

The set of estimated block grades for this iron ore example deposit are summarized in Figure 9.7 below.

| | 1 | 2 | 3 | 4 | 5 | 6 | 7 | 8 | 9 | 10 | 11 | 12 | 13 | 14 | 15 | 16 | 17 | 18 | 19 | 20 | 21 | 22 |
|---|---|---|---|---|---|---|---|---|---|---|---|---|---|---|---|---|---|---|---|---|---|---|
| 6 | W | W | 67 | 66 | W | W | 64 | 69 | 68 | 68 | 69 | 69 | W | W | W | W | 67 | 66 | W | W | W | W |
| 5 | | W | 62 | W | W | 40 | 60 | 63 | 66 | 65 | 66 | 66 | W | W | W | W | 62 | 10 | W | 40 | 60 | |
| 4 | | | 64 | 65 | 68 | 68 | 68 | 69 | 67 | 66 | 65 | 65 | 65 | 64 | 65 | 63 | 64 | 65 | 68 | 68 | | |
| 3 | | | | 66 | W | W | 64 | 69 | 68 | 68 | W | W | W | W | W | W | 67 | 66 | 68 | | | |
| 2 | | | | | W | 40 | 60 | 63 | 63 | 62 | 66 | 66 | W | W | W | W | 62 | 10 | | | | |
| 1 | | | | | | 68 | 68 | 69 | 67 | 66 | 65 | 65 | 67 | 65 | 62 | 62 | 64 | | | | | |

Figure 9.7: Two-dimensional conceptual cross section of the grade model corresponding to the larger iron ore deposit used in the (% Fe). (The letter “W” standing for waste blocks).

It is important to note that in this model, it is possible for a small number of ore blocks to contain significantly high grades, and to be classified in the Inferred category. That is the case of blocks (3, 17) and (3, 19), and this is intended to induce an incentive for the solver to seek mining blocks which, despite being profitable, can be considered potentially risky. The economic block model for this example is presented in Figure 9.8.

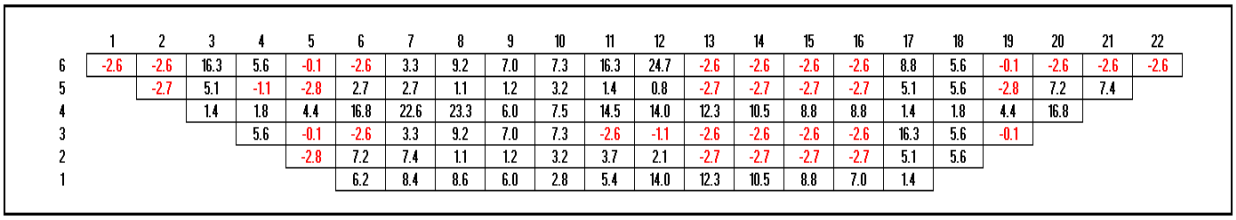


Figure 9.8: Two-dimensional conceptual cross section of an economic block model depicting 1st period undiscounted economic block values ($/ton). (The values in red represent the economic value of waste blocks while values in black correspond to ore blocks).

Two distinct cases in terms of risk preferences are tested. In one scenario, a mine production plan is generated which does not include risk requirements for the composition of the ore sent to the mill. This is called the "risk-free" scenario and it is equivalent to the decision maker having a risk-neutral attitude, which implies indifference towards alternative investment options providing equal economic payoffs, even as they represent very different levels of risk. Such a scenario could be considered extreme or unrealistic but, it is in fact representative of much of the current practice. In the alternative scenario, the decision maker is risk-averse and demands specific requirements on the amount of Inferred, Indicated and Measured material in the ore sent to the mill. Both plans consider three-year mine lives and specific operational constraints. The problem requirements, as well as the summary of the realized mine plan for scenario #1, are presented in Table 9.5 and Table 9.6, respectively.

Table 9.5: Mine production plan requirements for the "risk-free" plan, including lower and upper bounds on the total milling capacity and average grade for the material sent to the mill plant. No requirements placed in the proportions of Inferred, Indicated and Measured material.

| PERIOD | ORE MINED (blk) | MIN GRADE (%Cu) | MAX GRADE (%Cu) | INFERRED (%) | INDICATED (%) | MEASURED (%) |
|---|---|---|---|---|---|---|
| 1 | 10 | 64 | 66 | NA | NA | NA |
| 2 | 15 | 64 | 66 | NA | NA | NA |
| 3 | 15 | 64 | 66 | NA | NA | NA |

Table 9.6: Realized mine production plan including the previously unconstrained proportions of Inferred, Indicated and Measured material.

| PERIOD | ORE MINED (blk) | AVG GRADE (%Cu) | INFERRED (%) | INDICATED (%) | MEASURED (%) |
|---|---|---|---|---|---|
| 1 | 10 | 64.14 | 29 | 7 | 63 |
| 2 | 15 | 64 | 35 | 23 | 42 |
| 3 | 15 | 64 | 40 | 49 | 12 |
| NPV ($M) | 309.968 | | | | |

Figure 9.9 depicts the mine production plan that results from solving for the operational requirements of scenario 1. The decision variables in our optimization model are continuous and allow for the mining of individual blocks across multiple periods. For clarity of exposition, rather than displaying multiple periods in which a block is fractionally mined, we refer to the cumulative proportion of the ore block mined by the end of a given time period *t*. For those blocks which are fully mined by the end of time period *t,* the value displayed in the figure is precisely "*t*" (the completion period). For blocks not fully mined by the end of time period "T" (the last time period) the fraction of the block mined is displayed. Note that this is equivalent to presenting results in terms of so-called "by variables." However, since mine blocks can be mined in multiple periods it might be more consistent to think of said periods not as yearly periods, but as representing a "phase" which may be mined across a spectrum of time periods.

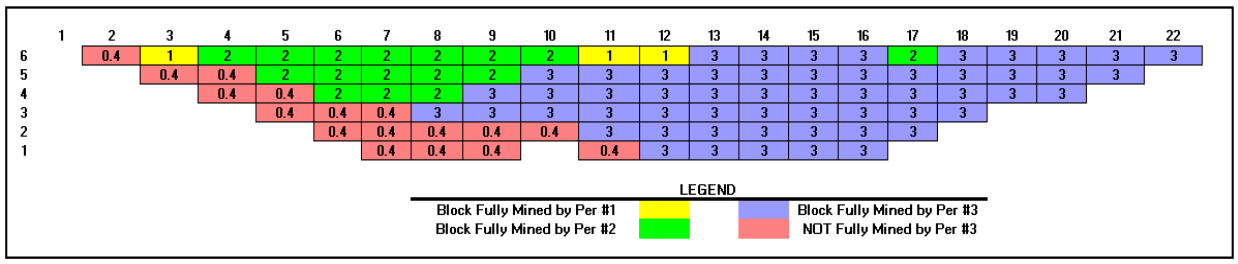


Figure 9.9: Mine production schedules for the "risk-free" scenarios.

For the first scenario, it is noted that the scheduler attempts to mine the center-west areas of the deposit because these contain the highest valued ore blocks and realizes an NPV of $\$(309.97*10^6)$. Also, both year 1 and year 2 productions are very small, while simultaneously, year 3 seems relatively large. Additionally, some of the blocks in the pit are mined only partially (bottom left portion of the deposit). In practice, one would likely combine the advance corresponding to both years 1 and 2 into a single pushback and, combine all of the blocks not fully mined by the end of period 3 into another phase.

Next, it must be determined if the current plan meets the predefined risk criteria. In this case, the adopted criterion was to generate a set of 10 orebody simulations, impose the current schedule onto each of the simulations, and record the number of times the average grade realized stayed within a ±15% accuracy interval around 64 % Fe. It is considered that a schedule can be

accepted (and thus adopted as optimal) if, nine times out of ten, the average grade realized falls inside the required accuracy interval.

Table 9.7 lists the results of testing the current schedule against all ten orebody realizations. As expected, the "risk-free" plan fails to meet the objective risk requirement criteria in all three time periods. Violations occur two times in period 1, three times in period 2 and most notably, four times in time period 3 in which the mine plan includes large proportions of profitable Inferred material.

Table 9.7: Uncertainty validation for current "risk-free" mine production plan

| PERIOD 1 | | | |
|---|---|---|---|
| SIMULATION | LOWER | ACTUAL | UPPER |
| 1 | 54.4 | 56.01 | 73.6 |
| 2 | 54.4 | 65.37 | 73.6 |
| 3 | 54.4 | 59.6 | 73.6 |
| 4 | 54.4 | 60.88 | 73.6 |
| 5 | 54.4 | 63.72 | 73.6 |
| 6 | 54.4 | 63.04 | 73.6 |
| 7 | 54.4 | 52.72 | 73.6 |
| 8 | 54.4 | 67.17 | 73.6 |
| 9 | 54.4 | 63.01 | 73.6 |
| 10 | 54.4 | 54.07 | 73.6 |
| FAILED | | | |

| PERIOD 2 | | | |
|---|---|---|---|
| SIMULATION | LOWER | ACTUAL | UPPER |
| 1 | 54.4 | 61.23 | 73.6 |
| 2 | 54.4 | 62.11 | 73.6 |
| 3 | 54.4 | 63.66 | 73.6 |
| 4 | 54.4 | 67.51 | 73.6 |
| 5 | 54.4 | 67.99 | 73.6 |
| 6 | 54.4 | 62.88 | 73.6 |
| 7 | 54.4 | 77.92 | 73.6 |
| 8 | 54.4 | 51.92 | 73.6 |
| 9 | 54.4 | 76.33 | 73.6 |
| 10 | 54.4 | 54.64 | 73.6 |
| FAILED | | | |

| PERIOD 3 | | | |
|---|---|---|---|
| SIMULATION | LOWER | ACTUAL | UPPER |
| 1 | 54.4 | 51.96 | 73.6 |
| 2 | 54.4 | 68.49 | 73.6 |
| 3 | 54.4 | 72.1 | 73.6 |
| 4 | 54.4 | 67.23 | 73.6 |
| 5 | 54.4 | 75.51 | 73.6 |
| 6 | 54.4 | 81.86 | 73.6 |
| 7 | 54.4 | 64.15 | 73.6 |
| 8 | 54.4 | 49.56 | 73.6 |
| 9 | 54.4 | 71.03 | 73.6 |
| 10 | 54.4 | 68.73 | 73.6 |
| FAILED | | | |

Clearly, the "risk-free" plan would be very difficult to accept as optimal under a probabilistic framework, as all three time periods fail to meet the predefined risk threshold.

Contrasting the outcomes from the "risk-free" scenario, the results obtained in the case of a risk-averse decision maker imposing limits on the proportions of material classified into each of the distinct resource classification categories are presented next. First, Table 9.8 summarizes the specific operational requirements for a feasible mining plan in the second scenario. Limits are enforced on each of the resource classification categories per time period, and these include an upper bound on the proportion of Inferred ore (5%) and a lower bound on both Indicated (10%) and Measured (85%) resources. Next, the risk-based mine production schedule corresponding to the updated risk requirements is presented in Table 9.9.

Table 9.8: Mine production plan requirements for the "risk-based" plan, including upper bounds on the total ore tons, and both lower and upper bounds on the average grade of the ore

material sent to the mill plant. Risk requirements are placed in the proportions of Inferred, Indicated and Measured ore material.

| PERIOD | ORE MINED (blk) | MIN GRADE (%Cu) | MAX GRADE (%Cu) | INFERRED (%) | INDICATED (%) | MEASURED (%) |
|---|---|---|---|---|---|---|
| 1 | 10 | 64 | 66 | 5 | 10 | 85 |
| 2 | 15 | 64 | 66 | 5 | 10 | 85 |
| 3 | 15 | 64 | 66 | 5 | 10 | 85 |

Table 9.9: Realized mine production plan including the proportions of Inferred, Indicated and Measured material.

| TIME PERIOD | ORE MINED (blk) | AVG GRADE (%Cu) | INFERRED (%) | INDICATED (%) | MEASURED (%) |
|---|---|---|---|---|---|
| 1 | 10 | 64.10 | 0.0 | 10.0 | 90.0 |
| 2 | 14 | 66.0 | 0.0 | 14.3 | 85.7 |
| 3 | 7 | 65.0 | 0.0 | 14.3 | 85.7 |
| NPV ($M) | 210.854 | | | | |

The results for the risk-based schedule presented in Table 9.9 differ from the risk-free plan (see Table 9.6) on multiple levels. First, there is a sharp decrease in NPV for the risk-based plan [$(210.854*106)] relative to the risk-free plan [$(309.968*$10^6$)] which is consistent with the fact that the latter corresponds to a more constrained problem than the former, but this is also due to the scheduler being forced to avoid the riskier areas of the deposit which are rich in Inferred and Indicated material. With the exception of period 1, the average grade of the mined material is substantially higher for the risk-based schedule, although less overall tonnage is mined.

What is perhaps of most interest is the composition of the mill feed in terms of proportions of the distinct resource classification categories. In the initial unconstrained production schedules, the solver seeks to maximize profit by including a large fraction of Inferred and Indicated material in the mill feed, thereby "loading" the plan with some of the riskier fractions of the deposit. Specifically, periods 1 and 2 show proportions of Inferred material close to 30 %, and in period 3 this value raises to 40%. However, the central aspect to consider – one that is often missed - is that this may (or may not) be the adequate plan for the mine depending on whether the particular risk preferences of management are satisfied. As shown in Table 9.7, the initial plan obtained might not always be the optimal (is a risk-tolerance sense), and therefore, what is crucial is that management be able to impart its risk preferences on the schedules generated.

The differences between scenario 1 ("risk-free") and its alternative ("risk-averse") extend to the size and shape of the ultimate pit (see Figure 9.9 and Figure 9.10).

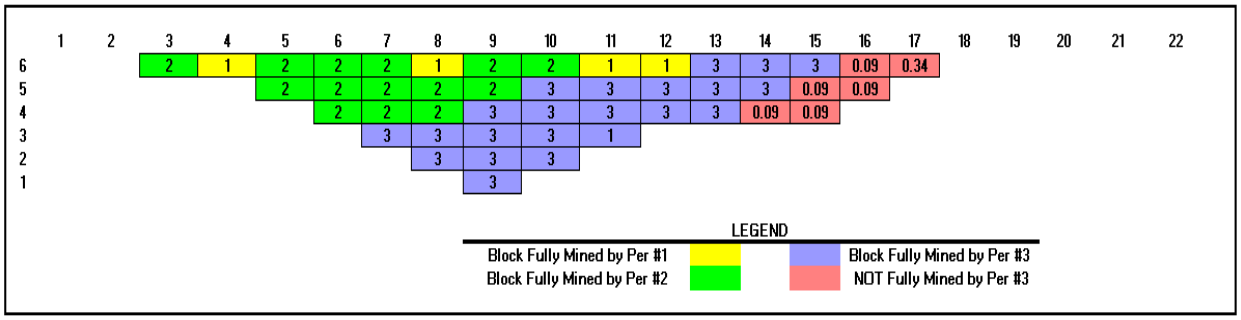


Figure 9.10: Mine production schedules for the "risk-averse" scenarios (scenario #2).

It can be seen (from Figure 9.10) that the production plan for scenario #1 results in a much larger final pit, and with significantly different shape than the one for scenario #2, although there is significant overlap between the two scenarios with regard to the starting location of mining and its subsequent evolution. The differences in shape and size of the production plans also confirm that risk analysis of the impact of uncertainty cannot rely solely on static sensitivity analysis of individual economic parameters, because differences in levels of risk tolerance can result in significantly different production schedules. Instead, it is important that new mine production be generated when risk preference levels are not met, or are themselves updated.

Next, the performance of the "risk-averse" mining plan under conditions of uncertainty is assessed, i.e., in order to be acceptable, it is required that nine times out of ten, the plan meets the required ±15 % accuracy level around the grade of 64% Fe. As can be seen from Table 9.10, the newly generated mine plan does meet the stated risk requirements for all three time periods. This is in accordance with the expected result of enforcing the resource classification constraints. In addition, it is noted that the portions of the pit limits from scenario 1 which display the greatest changes relative to scenario 2 are precisely those being mined in the latest time period. Incidentally, this is the period in which the violations are also the largest.

These small stylized models make clear that despite generating larger life-of-mine NPV, the current level of geological knowledge of the deposit implies that scenario #1 plan is likely unachievable in practice.

Table 9.10: Uncertainty validation for current "risk-averse" mine production plan

| PERIOD 1 | | | |
|---|---|---|---|
| SIMULATION | LOWER | ACTUAL | UPPER |
| 1 | 54.4 | 66.49 | 73.6 |
| 2 | 54.4 | 67.58 | 73.6 |
| 3 | 54.4 | 70.46 | 73.6 |
| 4 | 54.4 | 65.99 | 73.6 |
| 5 | 54.4 | 65.36 | 73.6 |
| 6 | 54.4 | 60.42 | 73.6 |
| 7 | 54.4 | 58.5 | 73.6 |
| 8 | 54.4 | 68.43 | 73.6 |
| 9 | 54.4 | 65.22 | 73.6 |
| 10 | 54.4 | 62.29 | 73.6 |
| PASSED | | | |

| PERIOD 2 | | | |
|---|---|---|---|
| SIMULATION | LOWER | ACTUAL | UPPER |
| 1 | 54.4 | 62.12 | 73.6 |
| 2 | 54.4 | 69.59 | 73.6 |
| 3 | 54.4 | 69.73 | 73.6 |
| 4 | 54.4 | 69.71 | 73.6 |
| 5 | 54.4 | 67.06 | 73.6 |
| 6 | 54.4 | 66 | 73.6 |
| 7 | 54.4 | 67.6 | 73.6 |
| 8 | 54.4 | 60.67 | 73.6 |
| 9 | 54.4 | 66.98 | 73.6 |
| 10 | 54.4 | 66.61 | 73.6 |
| PASSED | | | |

| PERIOD 3 | | | |
|---|---|---|---|
| SIMULATION | LOWER | ACTUAL | UPPER |
| 1 | 54.4 | 64.81 | 73.6 |
| 2 | 54.4 | 59.62 | 73.6 |
| 3 | 54.4 | 63.69 | 73.6 |
| 4 | 54.4 | 57.83 | 73.6 |
| 5 | 54.4 | 65.98 | 73.6 |
| 6 | 54.4 | 69.29 | 73.6 |
| 7 | 54.4 | 62.46 | 73.6 |
| 8 | 54.4 | 62.94 | 73.6 |
| 9 | 54.4 | 61.59 | 73.6 |
| 10 | 54.4 | 60.53 | 73.6 |
| PASSED | | | |

As a final comment, it is noted that although the plan obtained in Figure 9.10 is optimal, and meets all the specified problem requirements, for practical reasons, it cannot be easily implemented on the field, as the scheduler "smears" the production throughout the orebody. Nonetheless, in important regards, these results are still informative and valuable because: (i) they provide a provably optimal solution establishing an upper bound on the value of the optimal integer solution; (ii) they can still offer guidance on the boundary of potential pushbacks or phases. For instance, in presenting mine plans, the numbers inside each block represent the period by which the respective block has been fully mined and this is very useful guidance in terms of the limit times by which certain areas of the pit need to be fully depleted.

## 9.2 Three-Dimensional Synthetic Case Study – KD85

The solution methodology developed in this research is utilized to solve a three-dimensional problem corresponding to a notional copper deposit referred to as KD85, so as to demonstrate the advantage of the methods proposed. The results obtained are compared to those originated from a risk-free approach and further validate the analytical framework proposed. KD85 contains a total of 5,400 blocks, each assigned its individual copper grade value and having the same size and tonnage. In addition, all blocks are classified into one of the three resource classification categories, so that the schedules including grade risk constraints can be contrasted to risk-free schedules. Using the economic assumptions presented in Table 9.11 and assuming pit wall slope constraints require 45-degree slope angles, it was possible to determine ultimate pit

limits for the deposit. These were subsequently loaded into Mintec's MineSight software and visualized as appropriate (see Figure 9.11 below).

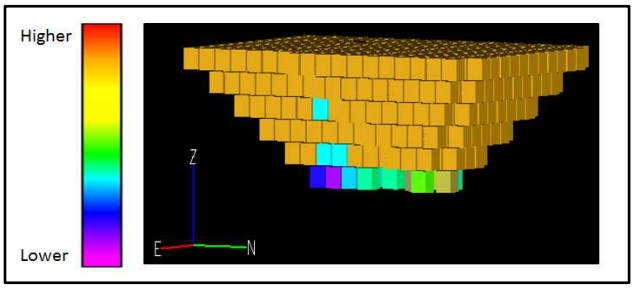


Figure 9.11: Three-dimensional view of the KD85 ultimate pit limits.

It is customary to intersect the topographic contours of the surface terrain with the three-dimensional model of the deposit, as the said contours represent an important consideration in practice. However, for the purpose of the discussions in this methodology this aspect is considered immaterial.

Table 9.11: Economic assumptions used in determining ultimate pit limits for KD85

| Economic Parameter | Value | Unit |
|---|---|---|
| Price of Copper | 0.70 | $/lb |
| Mining Costs | 0.85 | $/ton of material |
| Milling Costs | 2.20 | $/ton of ore |
| Smelting and Marketing | 0.25 | $/lb of Cu |
| G&A | 0.15 | $/ton of ore |
| Discount Rate | 12.5 | % |

Table 9.12 provides a general summary of the characteristics of the material contained within the ultimate pit limits. It can be seen that for KD85 only a small proportion of blocks is considered ore under the adopted economic assumptions, however, the average grade of the ore blocks (3.64% Cu) is such that KD85 is considered a high-grade deposit.

Table 9.12: Characteristics of the ore material inside the ultimate pit limits

| STATISTIC | VALUE | UNITS | RESOURCE CLASSIFICATION CATEGORY | VALUE | UNITS |
|---|---|---|---|---|---|
| TOTAL BLOCKS | 2016 | ** | INFERRED | 20 | % |
| ORE BLOCKS | 64 | ** | INDICATED | 31 | % |
| WASTE BLOCKS | 1952 | ** | MEASURED | 48 | % |
| AVG. GRADE | 3.64 | (% Cu) | | | |

Figure 9.12 depicts three-dimensional grade model for the KD85 conceptual ore deposit:

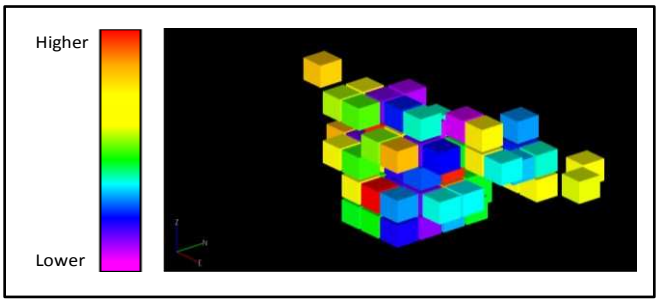


Figure 9.12: Three-dimensional grade model showing ore blocks inside the ultimate pit limits for KD85.

In what follows, we systematically illustrate the disposition of ore blocks throughout the mineral deposit by means of two-dimensional cross-sectional views for both the grade and the resource classification models. The bench-by-bench plan view cross sections corresponding to the grade deposit are as shown in Figure 9.13. Figure 9.14, below depicts North-South cross sections of the grade model for KD85

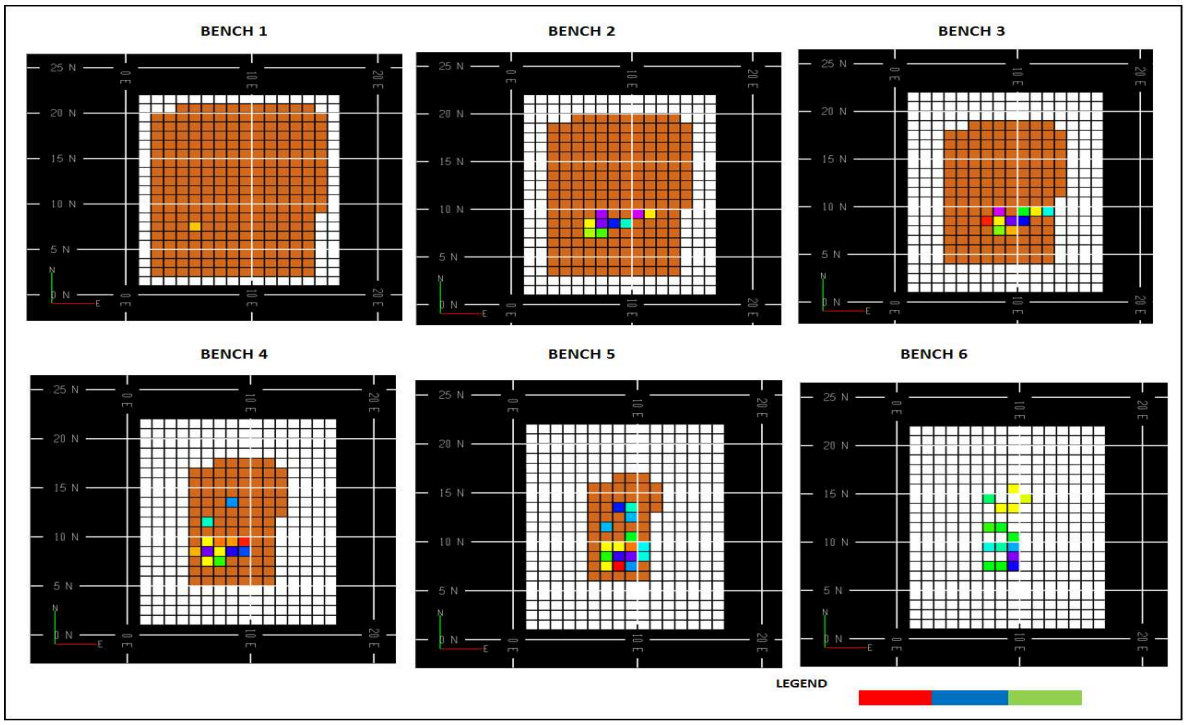


Figure 9.13: Plan view of synthetic mineral grade model. Blocks colored brown represent waste blocks and their contours define the ultimate pit limits for KD85.

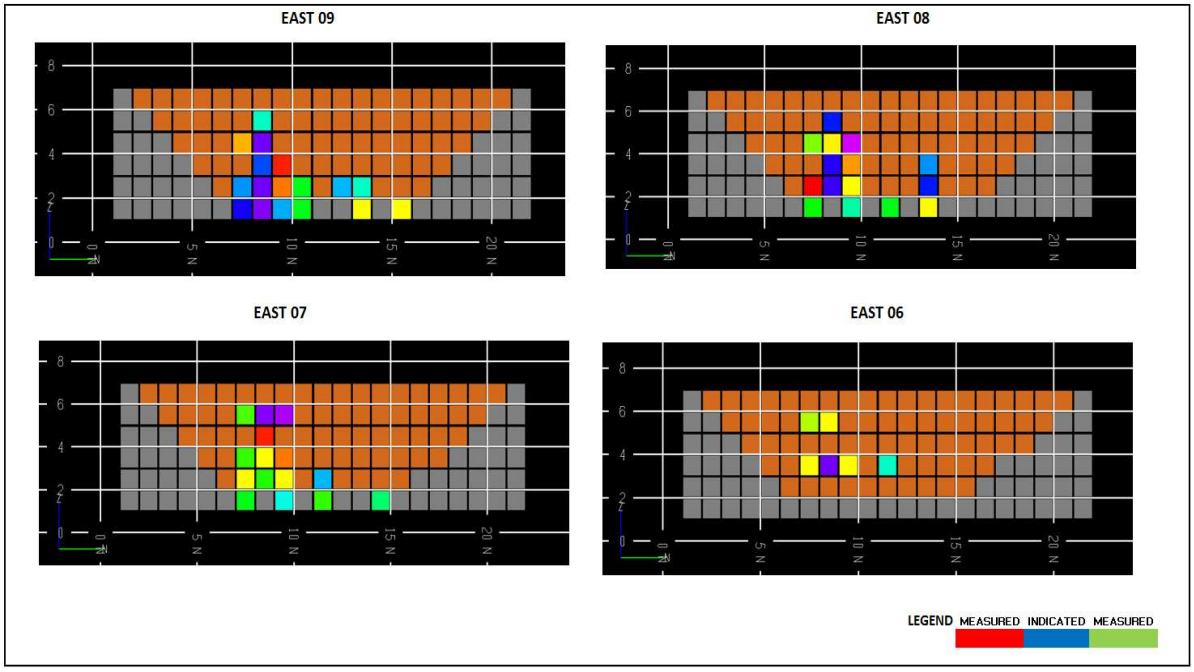


Figure 9.14: North-South two-dimensional cross-sectional view of the KD85 grade block model.

Figure 9.15, below depicts East-West cross sections of the grade model for KD85

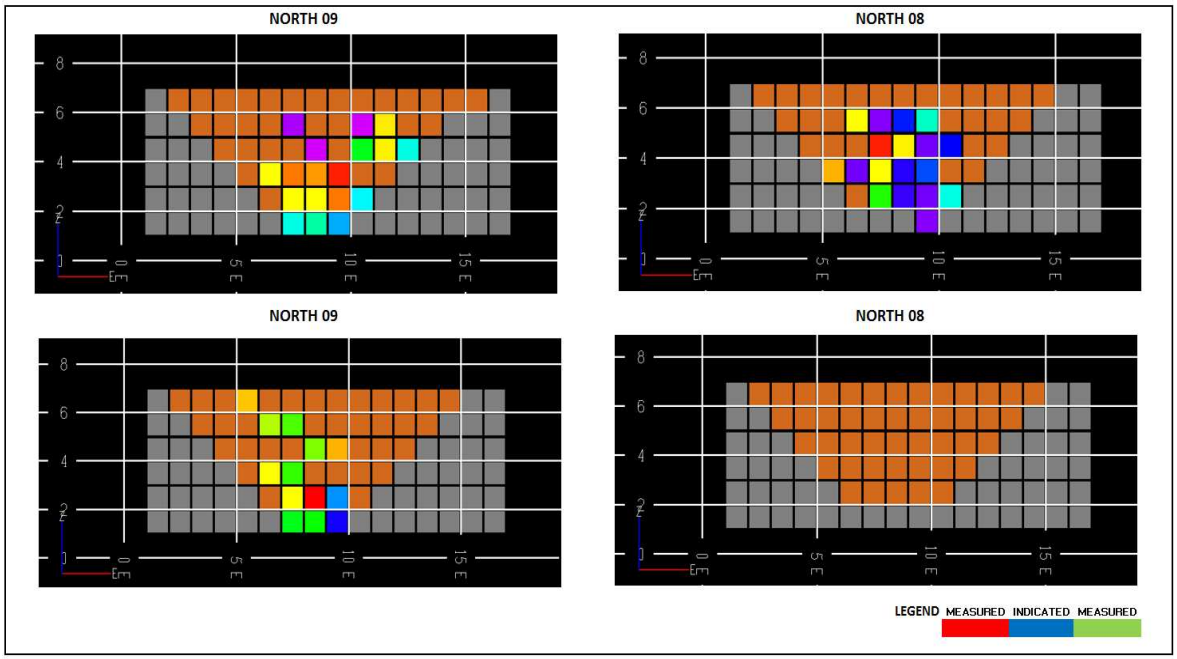


Figure 9.15: East-West two-dimensional cross-sectional view of the KD85 grade block model.

Next, plan cross-sectional views of the deposit, corresponding to the mineral resource classification model are presented.

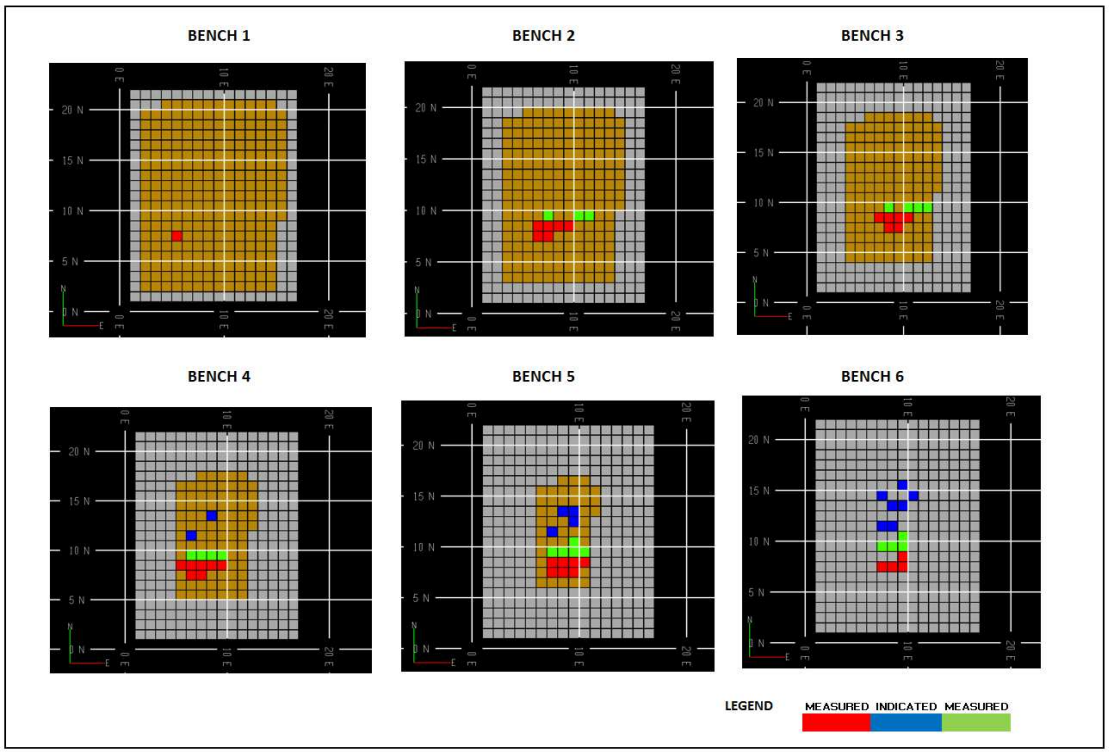


Figure 9.16: Bench-by-bench plan views of mineral resource model for KD85.

Figure 9.17, below depicts North-South cross sections of the mineral resource model for KD85

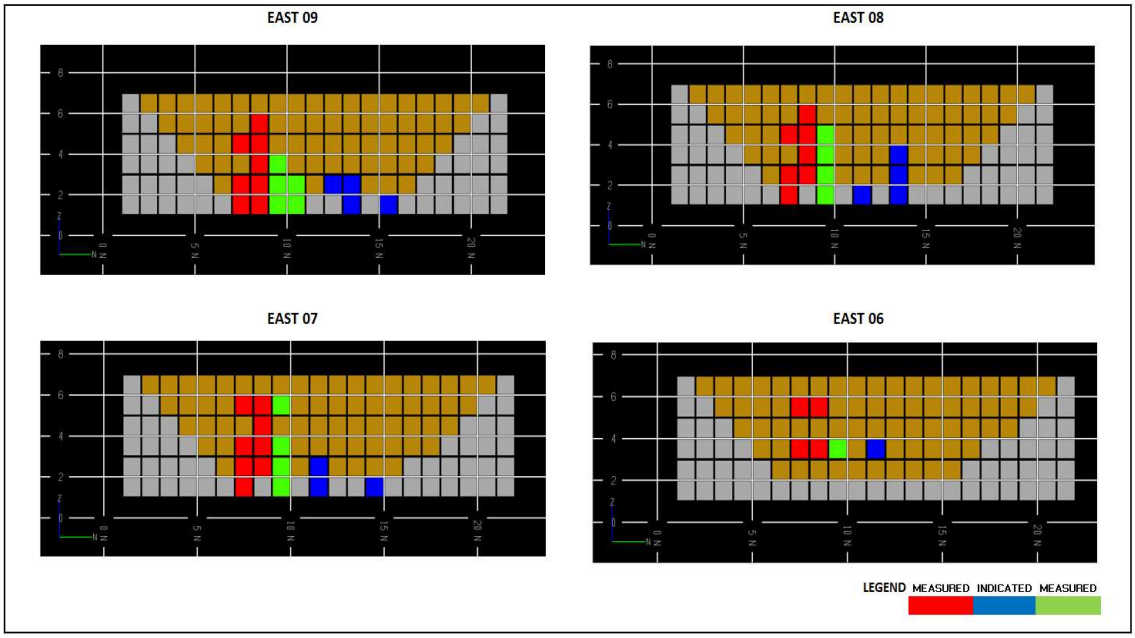


Figure 9.17: North-South two-dimensional cross-sectional view of the KD85 resource classification model.

Figure 9.18, below depicts East-West cross sections of the mineral resource model for KD85.

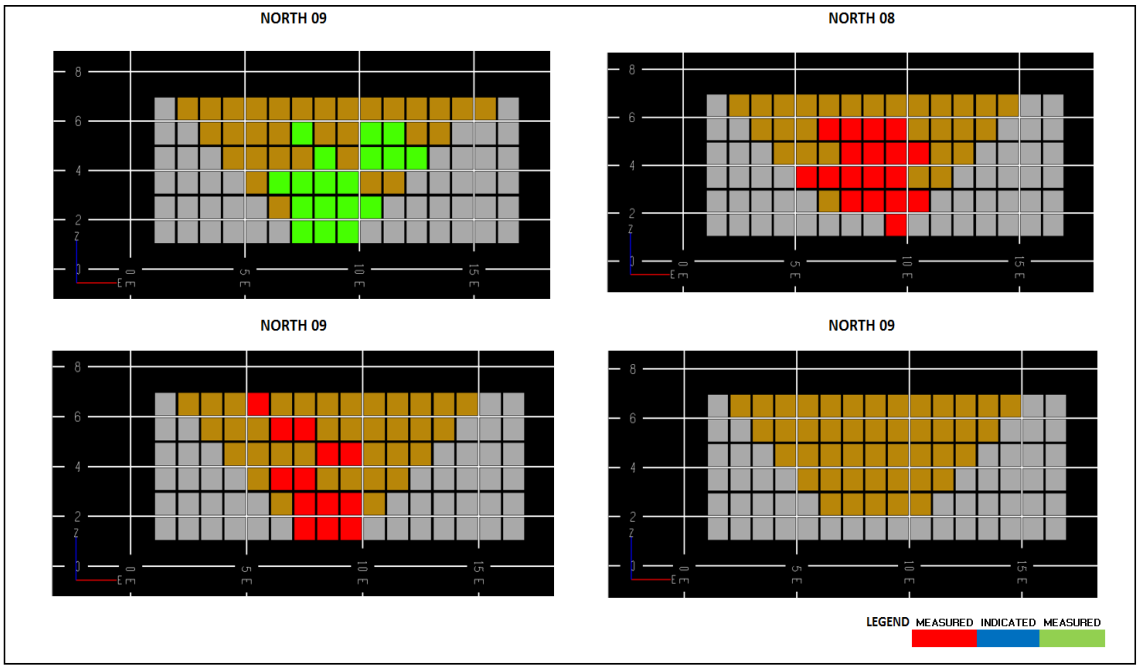


Figure 9.18: East-West two-dimensional cross-sectional view of the KD85 resource classification.

Following the detailed graphical depictions of the grade and resource models, four distinct optimization problems are solved, specifically: (i) the LP relaxation of the original problem $(OPMPSP)^{LP}$ without risk constraints; (ii) the LP relaxation of the original problem, including ore risk constraints $(OPMPSP)^{LPr}$, (iii) the IP formulation of the original production scheduling problem without risk resource constraints $(OPMPSP)^{IP}$, and (iv) the IP formulation of the original production scheduling problem including risk constraints, which will be referred to as $(OPMPSP)^{IPr}$.

Problem (i) provides an upper bound on the maximum NPV value; problem (ii) generates a solution that includes risk constraints, but is considered provisional until it meets management's confidence threshold, problem (iii) generates a solution to the Integer Program that would correspond to the true optimal schedule if mineral grades were known with absolute certainty, and (iv) offers a comparison with respect to the true, typically unknown, risk-based optimal integer production schedule.

Table 9.13 summarizes the economic parameters used to develop the economic block model and for NPV calculations, which are constant for all three problems.

Table 9.13: Economic assumptions for the optimization problem

| PARAMETER | VALUE | UNITS | PARAMETER | VALUE | UNITS |
|---|---|---|---|---|---|
| COPPER PRICE | 0.7 | $/lb | SMELTING & MARKETING | 0.25 | $/lb of Cu |
| MINING COSTS | 0.85 | $/ton of material | G&A | 0.15 | $/ton of ore |
| MILLING COSTS | 2.2 | $/ton of ore | DISCOUNT RATE | 12.5 | % |

For the first model, the linear program $(OPMPSP)^{LP}$ considers three time periods, upper bounding requirements on the maximum yearly ore tonnage sent to the mill plant, lower and upper bounds on the average copper grade of the mill feed , and no yearly ore resource risk constraints. The problem requirements are summarized in Table 9.14.

Table 9.14 Mine production plan requirements for $(OPMPSP)^{LP}$

| TIME PERIOD | MAX ORE MINED (blk) | WASTE MINED (blk) | MIN GRADE (%Cu) | MAX GRADE (%Cu) | INFERRED (%) | INDICATED (%) | MEASURED (%) |
|---|---|---|---|---|---|---|---|
| 1 | 19 | NA | 3.62 | 3.66 | NA | NA | NA |
| 2 | 21 | NA | 3.62 | 3.66 | NA | NA | NA |
| 3 | 23 | NA | 3.62 | 3.66 | NA | NA | NA |

The LP solution to $(OPMPSP)^{LP}$ corresponds to an NPV of $\$(125.717*10^6)$ and is summarized in Table 9.15.

Table 9.15: Summary of realized mine production plan for $(OPMPSP)^{LP}$

| TIME PERIOD | ORE MINED (blk) | AVG GRADE (%Fe) | INFERRED (%) | INDICATED (%) | MEASURED (%) |
|---|---|---|---|---|---|
| 1 | 18.9 | 3.66 | 0.0 | 26.5 | 73.5 |
| 2 | 21 | 3.66 | 8.1 | 40.9 | 51.0 |
| 3 | 23 | 3.66 | 49.1 | 22.6 | 28.3 |
| NPV ($M) | 125.717 | | | | |

For the second model $(OPMPSP)^{LPr}$, milling capacity and blending constraints from $(OPMPSP)^{LP}$ are preserved and incremented by yearly upper bounds on the proportion of Inferred material, and lower bounds on the proportions of Indicated and Measured material in the mill feed . The problem requirements are summarized in Table 9.16.

Table 9.16: Mine production plan requirements for $(OPMPSP)^{LPr}$.

| TIME PERIOD | MAX ORE MINED (blk) | WASTE MINED (blk) | MIN GRADE (%Cu) | MAX GRADE (%Cu) | INFERRED (%) | INDICATED (%) | MEASURED (%) |
|---|---|---|---|---|---|---|---|
| 1 | 19 | NA | 3.62 | 3.66 | 15 | 25 | 45 |
| 2 | 21 | NA | 3.62 | 3.66 | 15 | 25 | 45 |
| 3 | 23 | NA | 3.62 | 3.66 | 15 | 25 | 45 |

The results obtained for $(OPMPSP)^{LPr}$ correspond to an NPV of \$(122.045*$10^6$) and are summarized in Table 9.17.

Table 9.17: Summary of realized mine production plan for $(OPMPSP)^{LPr}$.

| TIME PERIOD | ORE MINED (blk) | AVG GRADE (%Fe) | INFERRED (%) | INDICATED (%) | MEASURED (%) |
|---|---|---|---|---|---|
| 1 | 19 | 3.65 | 15.0 | 29.0 | 56 |
| 2 | 21 | 3.62 | 15.0 | 39.0 | 46 |
| 3 | 18.8 | 3.62 | 15.0 | 28.0 | 57 |
| NPV ($M) | 122.045 | | | | |

Next, the same problem requirements as in Table 9.16 are used to formulate and solve $(OPMPSP)^{IP}$, and the corresponding results are as shown in Table 9.18.

Table 9.18: Summary of realized mine production plan for $(OPMPSP)^{IP}$

| TIME PERIOD | ORE MINED (blk) | AVG GRADE (%Fe) | INFERRED (%) | INDICATED (%) | MEASURED (%) |
|---|---|---|---|---|---|
| 1 | 19 | 3.66 | 0.0 | 36.8 | 63.2 |
| 2 | 21 | 3.66 | 4.8 | 33.3 | 61.9 |
| 3 | 23 | 3.66 | 52.2 | 21.7 | 26.1 |
| NPV ($M) | 125.388 | | | | |

Again, by adopting the risk requirements used in $(OPMPSP)^{LPr}$ a new mine production plan is generated, but this time in terms of integer variables and corresponding to $(OPMPSP)^{IPr}$. The results obtained are summarized in Table 9.19.

Table 9.19: Summary of realized mine production plan for $(OPMPSP)^{IPr}$.

| TIME PERIOD | ORE MINED (blk) | AVG GRADE (%Fe) | INFERRED (%) | INDICATED (%) | MEASURED (%) |
|---|---|---|---|---|---|
| 1 | 18 | 3.62 | 11 | 33 | 56 |
| 2 | 20 | 3.64 | 15 | 30 | 55 |
| 3 | 20 | 3.62 | 15 | 35 | 50 |
| NPV ($M) | 118.253 | | | | |

We see that, as expected, the NPV corresponding to the integer programming formulation is smaller than that of the LP relaxation. Both plans meet all the risk constraints, however, a key distinction between plans seems to result from the first year of mining in which the solution to $(OPMPSP)^{LPr}$ model mines higher grade copper than the $(OPMPSP)^{IPr}$ thus accruing higher revenue.

Figure 9.19 depicts bench-by-bench cross-sectional (plan) views of the integer programming schedules obtained for $(OPMPSP)^{IPr}$.

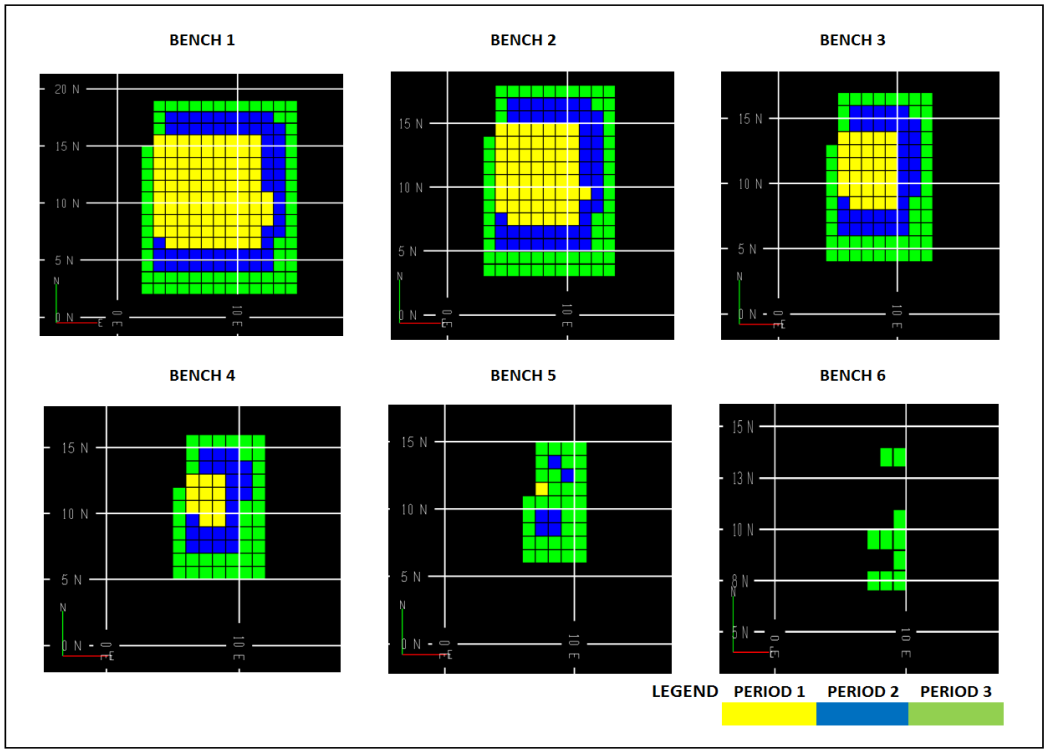


Figure 9.19: Plan view of the true optimal integer solution.

Similarly, Figure 9.20 below depicts North-South cross-sectional views of the integer programming schedules obtained for $(OPMPSP)^{IPr}$.

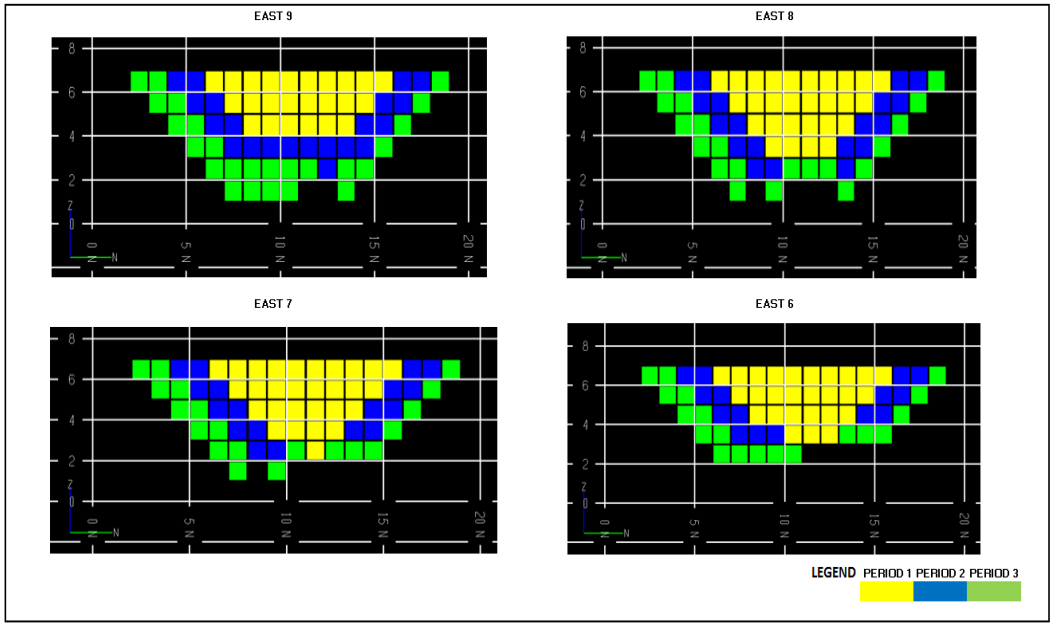


Figure 9.20: North-South two-dimensional cross-sectional view of the KD85 optimal integer solution.

East-West cross-sectional views of the integer programming schedules obtained for $(OPMPSP)^{IPr}$ are also shown in Figure 9.21 below

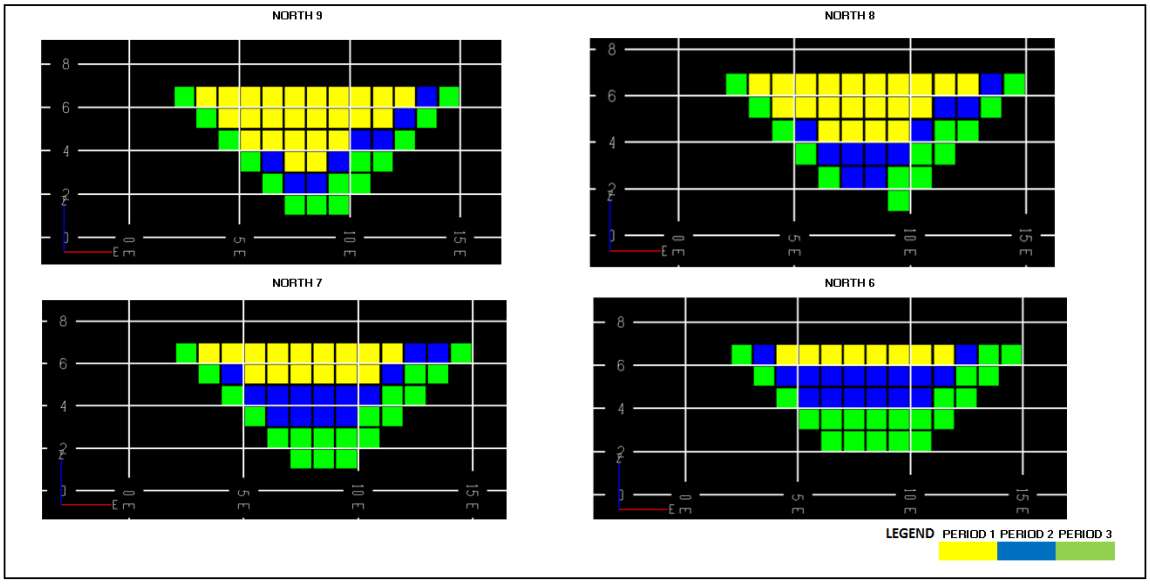


Figure 9.21: East-West two-dimensional cross-sectional view of the KD85 optimal integer solution.

In keeping with the solution methodology developed, we recall that at this stage the current solution to $(OPMPSP)^{LPr}$ consists solely of a "candidate" answer to the full problem. That is, it is still required that the solution be confronted against a risk threshold defined by the decision maker, which in the context of our example, is defined as the total number of times (out of ten possible) that the realized production plan stays within a predefined grade interval. Similar to the synthetic two-dimensional example, it is assumed that ten geostatistical simulations - representing possible realizations for the orebody - can be obtained or generated. Next, all the mining decisions associated with the current solution to $(OPMPSP)^{LPr}$ are superimposed on each of the individual realizations $s$, i.e., we determine the period production statistics (such as average grade) that would result, had the true ore deposit been the one represented by simulation $s$, instead of the estimated (possibly kriged) model that served as a basis for solving $(OPMPSP)^{LPr}$. Finally, per each individual time period, we observe across the full set of geostatistical simulations, whether the realized average grade is contained within the predefined interval, and assign a minimum number of times this condition must be met such that a plan can be deemed acceptable.

If the set of conditional simulations is representative of the full spectrum of uncertainty, then this procedure allows one to determine the robustness of a mining plan relative to grade uncertainty.

The current solution to $(OPMPSP)^{LPr}$ is tested against the ten available orebody realizations to verify the number times the realized average grade is within a ±15% accuracy about the [min, max] grade interval. If, for any time period, the realized average grade is outside the bounds of the predefined interval more than once, then the plan is considered to have failed the desired risk criteria, or equivalently, not to have met the minimum required risk threshold. Obviously, this is akin to the construction of a confidence interval about the target average copper grade. The results of confronting the current $(OPMPSP)^{LPr}$ to the ten conditional simulations are presented in Table 9.20.

Table 9.20: Uncertainty validation for the current solution to $(OPMPSP)^{LPr}$. The current solution fails to meet the desired minimum risk threshold in period 2.

| PERIOD 1 | | | |
|---|---|---|---|
| SIMULATION | LOWER | ACTUAL | UPPER |
| 1 | 3.08 | 3.171 | 4.21 |
| 2 | 3.08 | 3.182 | 4.21 |
| 3 | 3.08 | 3.276 | 4.21 |
| 4 | 3.08 | 3.28 | 4.21 |
| 5 | 3.08 | 3.482 | 4.21 |
| 6 | 3.08 | 3.306 | 4.21 |
| 7 | 3.08 | 3.279 | 4.21 |
| 8 | 3.08 | 3.528 | 4.21 |
| 9 | 3.08 | 3.212 | 4.21 |
| 10 | 3.08 | 3.287 | 4.21 |
| PASSED | | | |

| PERIOD 2 | | | |
|---|---|---|---|
| SIMULATION | LOWER | ACTUAL | UPPER |
| 1 | 3.08 | 3.066 | 4.21 |
| 2 | 3.08 | 3.069 | 4.21 |
| 3 | 3.08 | 3.163 | 4.21 |
| 4 | 3.08 | 3.167 | 4.21 |
| 5 | 3.08 | 3.372 | 4.21 |
| 6 | 3.08 | 3.196 | 4.21 |
| 7 | 3.08 | 3.165 | 4.21 |
| 8 | 3.08 | 3.424 | 4.21 |
| 9 | 3.08 | 3.12 | 4.21 |
| 10 | 3.08 | 3.148 | 4.21 |
| FAILED | | | |

| PERIOD 3 | | | |
|---|---|---|---|
| SIMULATION | LOWER | ACTUAL | UPPER |
| 1 | 3.08 | 3.286 | 4.21 |
| 2 | 3.08 | 3.231 | 4.21 |
| 3 | 3.08 | 3.253 | 4.21 |
| 4 | 3.08 | 3.282 | 4.21 |
| 5 | 3.08 | 3.329 | 4.21 |
| 6 | 3.08 | 3.314 | 4.21 |
| 7 | 3.08 | 3.254 | 4.21 |
| 8 | 3.08 | 3.282 | 4.21 |
| 9 | 3.08 | 3.228 | 4.21 |
| 10 | 3.08 | 3.297 | 4.21 |
| PASSED | | | |

Recall that the current realized production plan results from a problem definition whose risk requirements allowed for the proportion of Inferred material, the riskiest resource classification category, to reach up to 15% of the total mill feed (see Table 9.16).

Given that the current plan fails the desired risk criteria (in period 2), one possible course of action by the decision maker might be to constrain more strictly the proportion of Inferred material allowed into the composition of the mill feed. Such a decision should, in principle, help the newly generated schedules more easily meet the required risk threshold. Hence, the risk requirements are modified such that the maximum allowed proportion of Inferred resources does not exceed 5% of the total composition of the mill feed (see Table 9.21).

Table 9.21: Modified risk requirements enforcing an upper bound on the proportion of Inferred material of at most 5 % of the mill feed .

| | ORE MINED (blk) | MIN GRADE (%Cu) | MAX GRADE (%Cu) | INFERRED (%) | INDICATED (%) | MEASURED (%) |
|---|---|---|---|---|---|---|
| PERIOD 1 | 19 | 3.62 | 3.66 | 5 | 25 | 45 |
| PERIOD 2 | 21 | 3.62 | 3.66 | 5 | 25 | 45 |
| PERIOD 3 | 23 | 3.62 | 3.66 | 5 | 25 | 45 |

In keeping with the developed methodology, said modified production requirements lead to a new, distinct mine production schedule, which must be confronted against the defined risk criteria in order for the solution to be determined optimal. The new solution generated for $(OPMPSP)^{LPr}$ is summarized in Table 9.22.

Table 9.22: Realized mine production plan corresponding to the modified risk requirements to the $(OPMPSP)^{LPr}$

| TIME PERIOD | ORE MINED (blk) | WASTE MINED (blk) | AVG GRADE (%Cu) | INFERRED (%) | INDICATED (%) | MEASURED (%) |
|---|---|---|---|---|---|---|
| 1 | 19 | 95 | 3.66 | 5 | 25 | 70 |
| 2 | 21 | 183 | 3.66 | 5 | 46 | 49 |
| 3 | 23 | 174 | 3.66 | 5 | 35 | 60 |
| NPV ($M) | 114.856 | | | | | |

As expected, the NPV associated with the new plan $(114.856*10^6), is lower than the one obtained for the previous solution to $(OPMPSP)^{LPr}$, $(122.045*10^6). Next, the risk validation stage follows, namely, it is required that the newly generated plan be tested against the user-defined risk threshold for average grade in each time period. As shown in Table 9.23, the new mining schedule meets the desired level of risk.

Table 9.23: Uncertainty validation for the modified solution to $(OPMPSP)^{LPr}$. The current solution meets the desired minimum risk threshold for all periods, and can be accepted as an optimal plan.

| PERIOD 1 | | | |
|---|---|---|---|
| SIMULATION | LOWER | ACTUAL | UPPER |
| 1 | 3.08 | 3.389 | 4.21 |
| 2 | 3.08 | 3.317 | 4.21 |
| 3 | 3.08 | 3.402 | 4.21 |
| 4 | 3.08 | 3.359 | 4.21 |
| 5 | 3.08 | 3.501 | 4.21 |
| 6 | 3.08 | 3.425 | 4.21 |
| 7 | 3.08 | 3.371 | 4.21 |
| 8 | 3.08 | 3.421 | 4.21 |
| 9 | 3.08 | 3.335 | 4.21 |
| 10 | 3.08 | 3.483 | 4.21 |
| PASSED | | | |

| PERIOD 2 | | | |
|---|---|---|---|
| SIMULATION | LOWER | ACTUAL | UPPER |
| 1 | 3.08 | 3.107 | 4.21 |
| 2 | 3.08 | 3.059 | 4.21 |
| 3 | 3.08 | 3.153 | 4.21 |
| 4 | 3.08 | 3.127 | 4.21 |
| 5 | 3.08 | 3.082 | 4.21 |
| 6 | 3.08 | 3.212 | 4.21 |
| 7 | 3.08 | 3.147 | 4.21 |
| 8 | 3.08 | 3.161 | 4.21 |
| 9 | 3.08 | 3.117 | 4.21 |
| 10 | 3.08 | 3.081 | 4.21 |
| PASSED | | | |

| PERIOD 3 | | | |
|---|---|---|---|
| SIMULATION | LOWER | ACTUAL | UPPER |
| 1 | 3.08 | 3.286 | 4.21 |
| 2 | 3.08 | 3.231 | 4.21 |
| 3 | 3.08 | 3.253 | 4.21 |
| 4 | 3.08 | 3.282 | 4.21 |
| 5 | 3.08 | 3.329 | 4.21 |
| 6 | 3.08 | 3.314 | 4.21 |
| 7 | 3.08 | 3.254 | 4.21 |
| 8 | 3.08 | 3.282 | 4.21 |
| 9 | 3.08 | 3.228 | 4.21 |
| 10 | 3.08 | 3.297 | 4.21 |
| PASSED | | | |

In order to be consistent, we compute the solution for a new integer problem which accounts for the same operational requirements as the last $(OPMPSP)^{LPr}$, as stated in Table 9.21. The production plan obtained is presented in Table 9.24.

Table 9.24: Realized mine production schedule for $(OPMPSP)^{IPr}$ with updated risk resource requirements.

| TIME PERIOD | ORE MINED (blk) | AVG GRADE (%Cu) | INFERRED (%) | INDICATED (%) | MEASURED (%) |
|---|---|---|---|---|---|
| 1 | 12 | 3.66 | 0.0 | 25.0 | 75.0 |
| 2 | 20 | 3.66 | 5.0 | 30.0 | 65.0 |
| 3 | 20 | 3.66 | 5.0 | 50.0 | 45.0 |
| NPV ($M) | 109.288 | | | | |

The NPV generated by solving the initial $(OPMPSP)^{LPr}$ \$(122.045*$10^6$), is superior to that of the initial $(OPMPSP)^{IPr}$ \$(118.253*$10^6$). Likewise, the current solution to $(OPMPSP)^{LPr}$ generates an NPV value \$(114.856*$10^6$) that is higher than that of current $(OPMPSP)^{IPr}$ (109,288). In addition, there remains the fact that the existence of fractional values in $(OPMPSP)^{LPr}$ makes their practical implementation a challenge. For this reason, we have adopted a simple heuristic approximation approach whereby, blocks which have been mined beyond a certain user-defined threshold are converted into fully mined blocks. The intuition underlying said approach being that the set of blocks most highly mined by the end of any time period correspond to the ones which an integer solver would visit first, if it were given the freedom to mine fractionally. Thus, it seems natural that these would be made integer first. Moreover, the final set of partitions at the end of the BZ algorithm can be thought of as indicative of the optimal location of phases which could guide mine production scheduling. This is obviously a very simplistic rounding criteria. However, as is shown in the results that follow, the tentative phases thus obtained do provide a very good guide for optimal integer production scheduling.

Similar to the integer solution, the plan and cross-sectional views of the phases obtained by our approach are shown in Figure 9.22 to Figure 9.24.

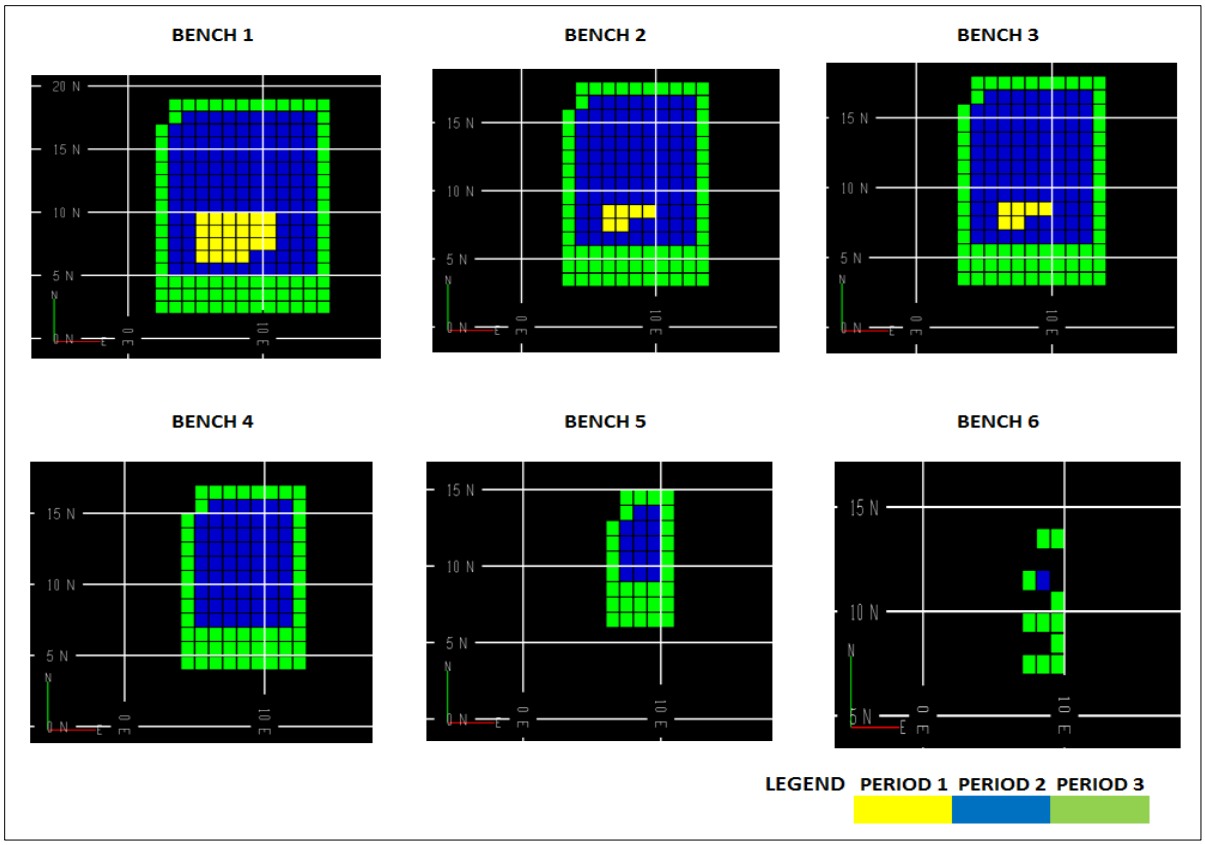


Figure 9.22: Plan view of the phase design solution.

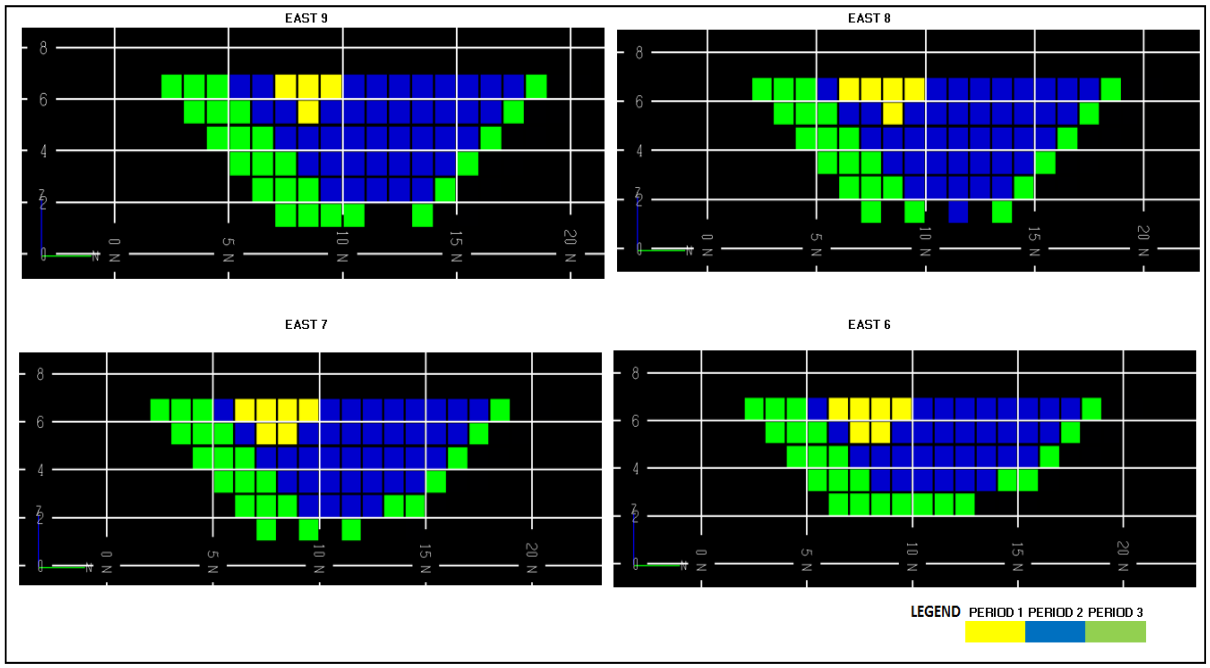


Figure 9.23: North-South two-dimensional cross-sectional view of the KD85 phase design solution.

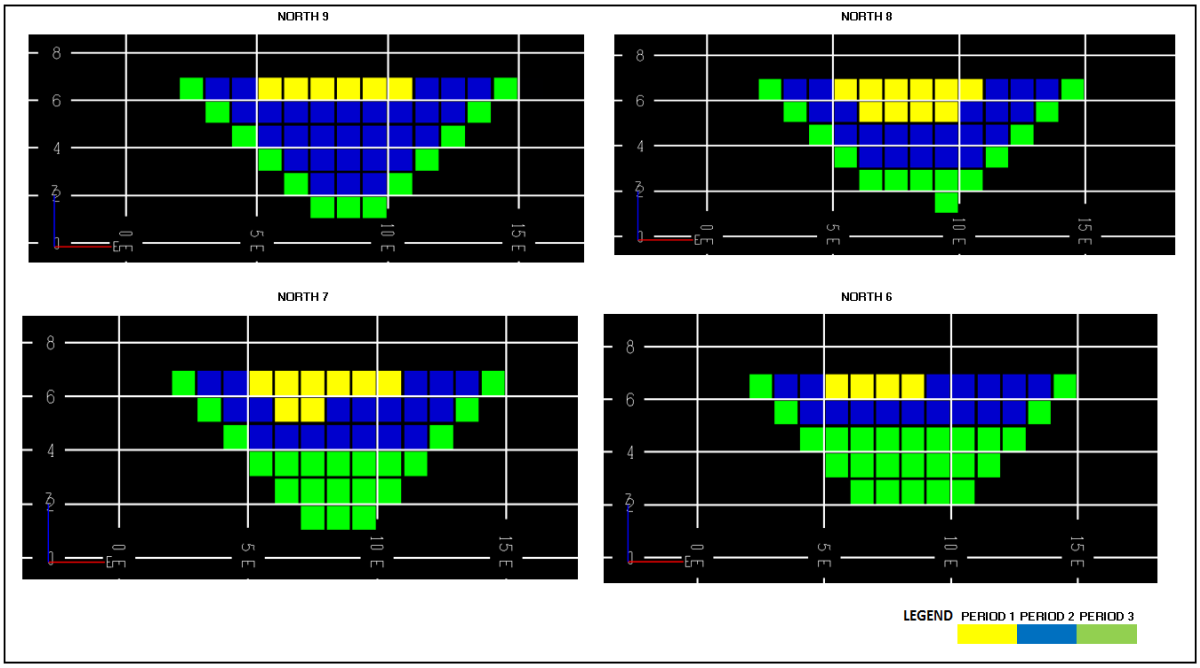


Figure 9.24: East-West two-dimensional cross-sectional view of the KD85 phase design solution.

Table 9.25 summarizes the results for phases obtained using said approach:

Table 9.25: Realized mine production plan for phase design.

| PHASE | ORE MINED (blk) | WASTE MINED (blk) | AVG GRADE (%Cu) | INFERRED (%) | INDICATED (%) | MEASURED (%) |
|---|---|---|---|---|---|---|
| 1 | 7 | 21 | 3.56 | 0 | 0 | 100.0 |
| 2 | 31 | 292 | 3.73 | 22.6 | 45.2 | 32.2 |
| 3 | 22 | 254 | 3.50 | 13.6 | 22.7 | 63.6 |
| NPV ($M) | 119.952 | | | | | |

As expected, given that no mechanism is enforced that prevents violations of either risk or blending constraints these might not be met. In effect, this aspect is referenced in other published work involving rounding heuristics (see Espinoza *et al.,* 2012; Brickey, 2015). However, it can be shown graphically that the phases obtained provide a very good guide for the true integer optimal solution. In order to further emphasize this proposition, the sections corresponding to the integer production schedules are plotted side-by-side with those corresponding to the tentative phases, both for plan and cross-sectional views.

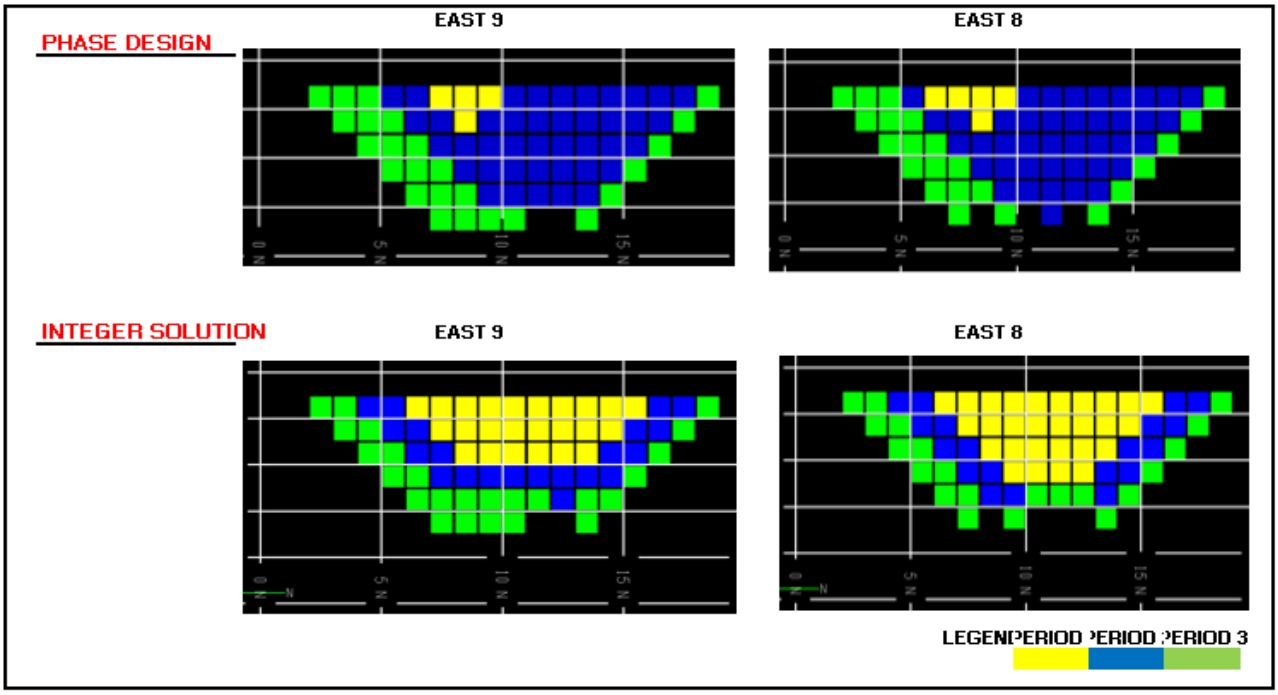


Figure 9.25: Comparison between phase designs and the true optimal integer solution on North-South cross-sectional views.

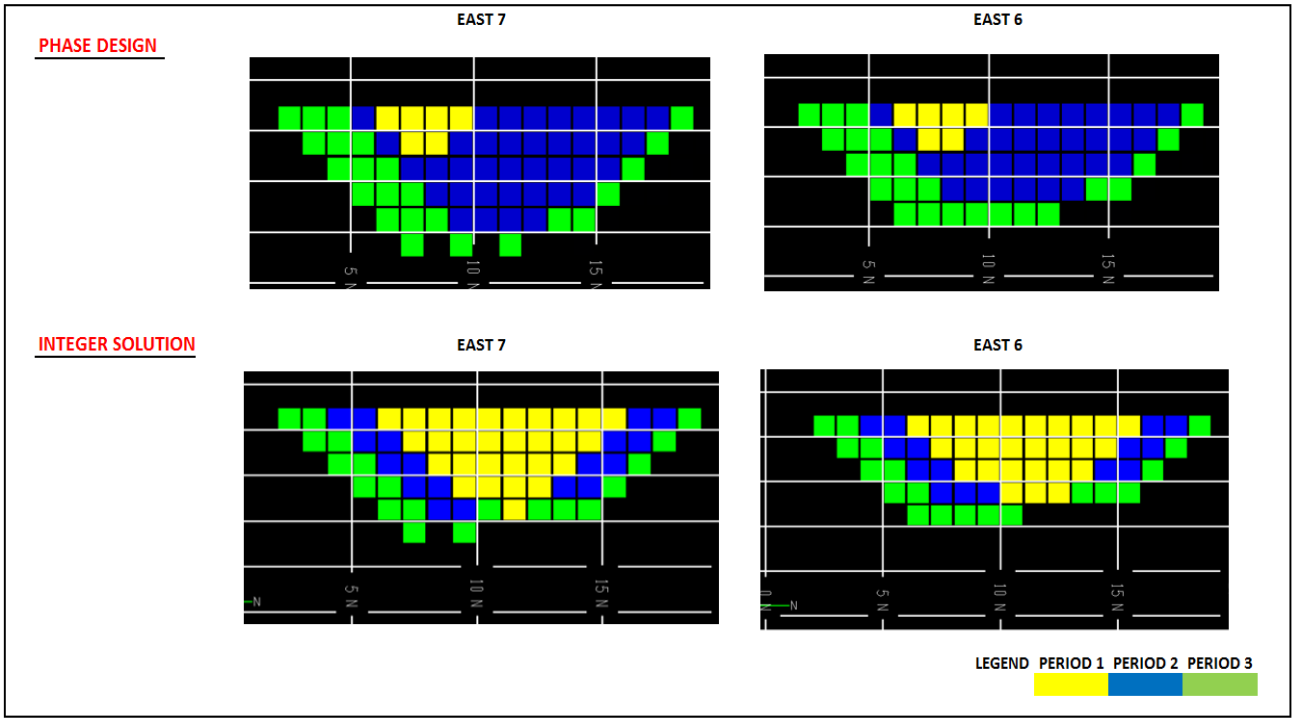


Figure 9.26: Comparison between phase designs and the true optimal integer solution on North-South cross-sectional views.

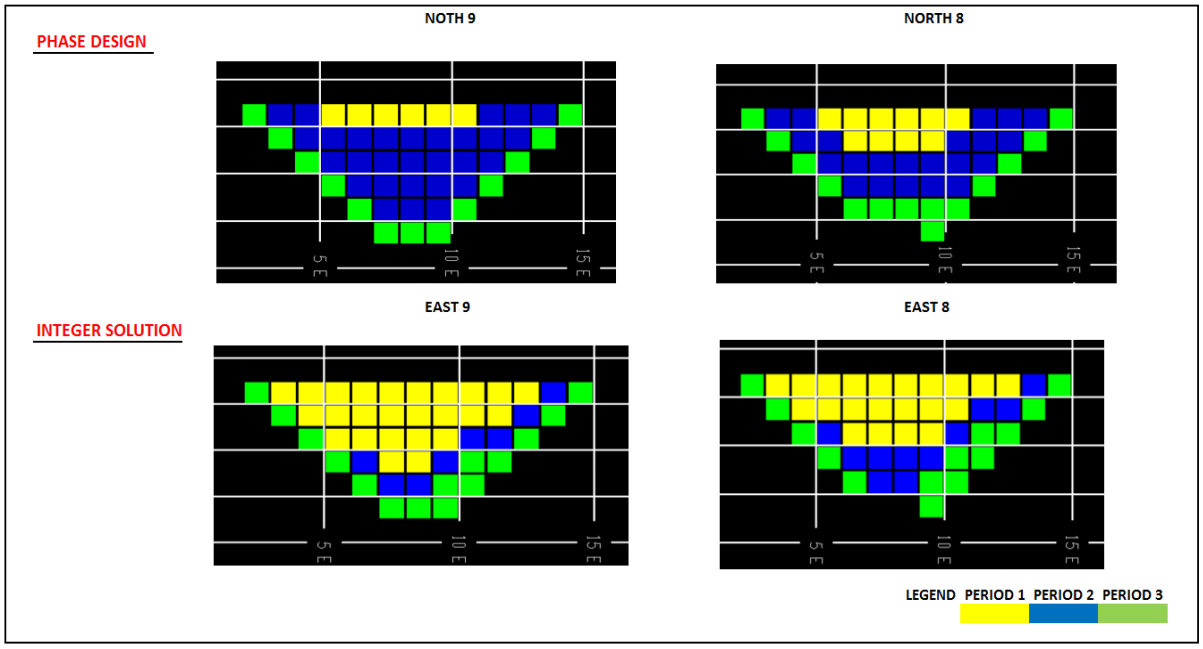


Figure 9.27: Comparison between phase designs and the true optimal integer solution on East-West cross-sectional views.

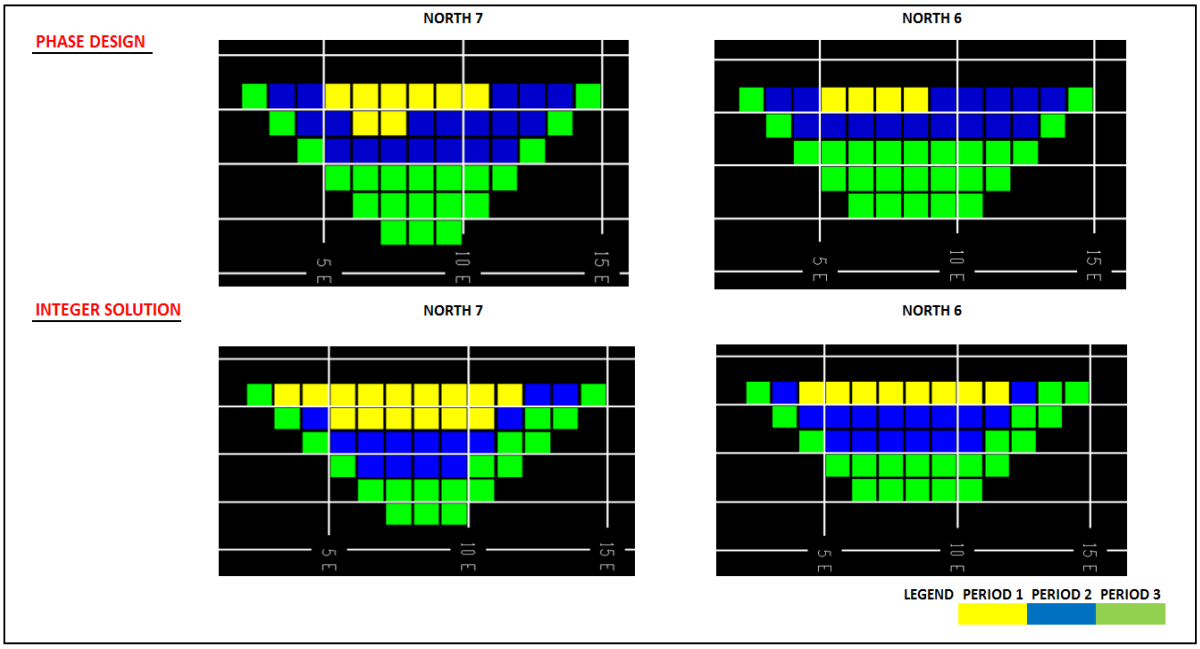


Figure 9.28: Comparison between phase designs and the true optimal integer solution on East-West cross-sectional views.

From a careful analysis of the individual sections in each of the cross-sectional views provided, it can be seen that for circumstances in which the phase size is smaller than the true integer solution, it is fully contained inside the optimal set of blocks corresponding to the true optimal integer solution. Also, it is verified that when the phase obtained is larger than the specified period capacity, it still remained fairly close to the expected progression of mining in the optimal integer case.

# CHAPTER 10.
# CONCLUSIONS

In a multitude of dimensions, social, political, economic or technical, the mining industry is faced with important challenges it needs to meet. It is possible - indeed common – to attempt to address these challenges under a deterministic framework. However, one important topic of concern is the effective management of grade uncertainty, specifically, the important ways in which its effects percolate the mining system and impact project economics. In this context, the practical success of geostatistical conditional simulations (GCS) have consolidated its importance as the method of choice for grade uncertainty characterization. Unfortunately, from an optimization perspective, there exists a crucial obstacle to the direct, explicit incorporation of GCS into mine production schedules in the form of stochastic linear programs: the problems become either intractable or very challenging to solve (by exact methods). This tendency for stochastic models grow to dimensions beyond the reach of exact solution methods has led to a large reorientation of research towards heuristic (or metaheuristic) techniques which - provided some conditions are verified - can obtain a solution to said problems, although one whose optimality cannot be verified.

In this dissertation a novel approach to mine production scheduling is presented which takes into account geostatistical conditional simulations, but models grade uncertainty differently than the current state-of-the-art practice of combining stochastic optimization models with heuristic solution algorithms. We show how the so-called “curse of dimensionality” for stochastic models can be circumvented by means of an integrated solution methodology which, rather than applying the grade realizations of GCS as input parameters in a stochastic model, uses these as elements to be incorporated in two distinct levels of analysis:

(i) as a complement to traditional geostatistical methods for mineral resource classification
(ii) as the means by which a specific, (user-defined) risk criterion can be established

Regarding the first level of analysis, GCS can be central to adequate classification of mineral resources into the Inferred, Indicated and Measured categories which constitutes an integral component of our methodology. We adopt said categories both as a valid proxy for grade

uncertainty and as a tool for quantifying risk in the production schedules generated. Specifically, we show how the precise composition of the mill feed can be defined a priori in terms of the proportions of material belonging to each of the resource categories, and how this impacts the schedules obtained. To our knowledge, this is an approach not yet published in the technical literature, but which carries important implications. On the one hand, these constitute the industry standard for communicating confidence in estimated grades, and this is important because it increases transparency and reduces resistance to adoption of the methods by industry. On the other hand, the inclusion of resource classification categories into the mine plans helps to address the disconnect between demands for robust schedules (on the part of management) and traditional deterministic production schedules which ignore risk.

All optimization models formulated are solved to proven optimality by exploring well-established exact solution algorithms for the mine production scheduling problem. In particular, the Bienstock-Zuckerberg and the PseudoFlow algorithms (both state-of-the-art algorithms) are combined to produce solutions to optimization problems including ore risk constraints $(OPMPSP)^r$. This is in contrast to heuristic (or metaheuristic) techniques which have the advantage of solving large-scale problems, but also the inconvenience that the solutions obtained cannot be proven optimal, and may rely significantly on initial starting conditions.

Regarding the second level of analysis, our method allows for the inclusion for a risk preference measure, expressed in the form of a risk threshold which conditions the acceptance (adoption) of any schedule obtained from the solver. For example, the risk criterion used in the research consisted of finding the number of times (out of ten) that average grades obtained from a production schedule stayed within the limits of some predefined grade interval.

Finally, by allowing direct specification of a critical threshold for risk on the part of the modeler, the method enables decision makers to affect ("shape") the outcome of the desired production schedules transparently and explicitly by imparting risk preferences. In essence, the method developed operates similar to a "price discovery" mechanism in which the variable of interest is the proper level of risk in the mine production schedules, which can be determined by consideration of a range of factors and expectations available to the decision maker, and which may go beyond the simple technical inputs to an optimization solver.

## 10.1 Suggested Future Work

The solution framework presented in this dissertation meets the goal of practicality and transparency, and it is expected that such characteristics should make for an easier incorporation by industry. There remain, however, important directions for future research which should be further explored. First, although uncertainty with regards to *grades* is considered in our models, the true (full) spectrum of uncertainty is much wider and reflects itself in multiple dimensions, including, most notably, the economical and operational.

The stochastic nature of metal prices, in particular, can have an important impact on the production schedules generated (Sabour *et al*., 2009; Mokhtarian & Sattarvand, 2015) - and/or on overall project economics (Davis & Samis, 2006, 2014) - and to the extent to which it affects mining cutoff grades, it is also interdependent with grade uncertainty. Therefore, it is anticipated that the integration of market uncertainty within the proposed framework – provided its implementation be possible while avoiding the "curse of dimensionality" – would prove advantageous.

Similar to (Froyland *et al.*, 2007), our methodology can be used to derive an upper bound on the economic value of additional infill drilling. However, the definitive answer to the question of determining the optimal number of drillholes and their specific location in space encloses an endogenous nature which our models cannot grasp. Indeed, additional drilling should be formulated as an internal decision variable of the optimization model, but one which reduces uncertainty itself. Such problems belong to a broader class of stochastic problems with decision-dependent uncertainty (Goel & Grossman, 2005), and it is not clear how such an integration could be accomplished without making the models intractable. On the other hand, recent years have witnessed dramatic advances in the size of problems incorporating uncertainty which are now solvable in reasonable amount of time, i.e., possibly not exceeding one or two hours per scenario evaluated (Lamghari *et al*., 2012). The methods used frequently avoid the "curse of dimensionality" by employing solution techniques belonging to the class of heuristic (or metaheuristic0 algorithms. This newfound possibility has prompted a large body of research work directed at holistically modelling increasingly large mine planning problems representing entire mining complexes. In our methods all the solution algorithms used are exact, which implies that the limitations resulting from the large size of mining problems must be overcome differently. In

this regard, one specific direction of research seems particularly promising, and involves determining the minimum possible number of realizations (conditional simulations) required for an adequate characterization of the true uncertainty spectrum (Romisch, 2008; Armstrong & Galli, 2010; Bayraksan & Morton, 2011). If scenario reduction techniques result in significantly smaller sets of "high-quality" realizations, it is envisioned that our methods can be extended to solving explicitly stochastic models of the production scheduling problem with risk constraints included $(OPMPSP)^r$.

Another important direction of future research relates to the improvement and scaling of the implementation of our solution algorithms so that they are made more efficient and able to tackle increasingly larger problems. Specifically, more computational testing is required to establish (or refute) dependence of algorithmic performance on specific problem instances, as well as comparisons with heuristic solution times. In this regard, the inclusion to the solution procedure of "hot starts" – defining an initial feasible solution expected to be relatively close to optimal – can accelerate convergence and should therefore be explored. Similarly, our methods provide tentative indication to the generation of "Mining Phases" that differ from the ones obtained by price parameterization, and seem to provide a very good guide to optimal production scheduling. However, in line with some of the research published in the mining literature (Chicoisne *et al*., 2012), much can be done regarding the study of approximation (or exact) techniques that make possible the conversion of initial fractional solutions into integer ones.

# REFERENCES


Ahuja, R., Magnanti, T., & Orlin, J. 1993. *Network Flows: Theory, Algorithms and Applications*. Pearson.

Akaike, A. 1999. "Strategic planning of long-term production schedule using 4D network relaxation method." Ph.D. Thesis, Colorado School of Mines, Golden, CO.

Akaike, A., & Dagdelen, K. 1999. "A strategic production scheduling method for an open pit mine." *Proceedings of the 28th APCOM,* pp. 729-738 of: Dardano, C., Francisco, M., & Proud, J. (eds.).

Armstrong, M., Galli, A., & Meheut, C. 2014. "genetic algorithms and scenario reduction." In *Journal of the Southern African Institute of Mining and Metallurgy*, 114: 237–44.

Armstrong, M., Ndiaye, A., Razanatsimba, R., & Galli, A. 2013. "Scenario reduction applied to geostatistical simulations." *Mathematical Geosciences,* 45(2): 165–82.

Askari-Nasab, H, Pourrahimian, Y., Ben-Awuah, E., & Kalantari, S. 2011. "Mixed integer linear programming formulations for open pit production scheduling." *Journal of Mining Science,* 47(3): 338–59.

Barnes, R. 1982. "Optimizing the ultimate pit." MSc. Thesis, Colorado School of Mines, Golden, CO.

Barnes, T. 2011. "Introduction to Geostatistics" MNGN433 Lecture Notes, Mining Engineering Department, Colorado School of Mines, Golden, CO.

Bayraksan, G., & Morton, D. 2011. "A sequential sampling procedure for stochastic programming." *Operations Research,* 59(4): 898–913.

Benndorf, J., & Dimitrakopoulos, R. 2007. "New efficient methods for conditional simulation of large orebodies." In *Proceedings of the Orebody Modelling and Strategic Mine Planning Conference, edited by Roussos Dimitrakopoulos, 14: 61–67. Australasian Institute of Mining and Metallurgy Publication Series.*

Bernabe, D, & Dagdelen, K. 2002. "Comparative analysis of open pit mine scheduling techniques for strategic mine planning of the Tintaya copper mine in Peru." In *SME Annual Meeting*, 1–7. Phoenix, AZ.

Bienstock, D., & Muñoz, G. 2014. "LP approximations to mixed-integer polynomial optimization problems." *arXiv preprint arXiv:1501.00288*.

Bienstock, D., & Zuckerberg, M. 2009. "A New LP algorithm for precedence constrained production scheduling." Technical report. Columbia University.

Bienstock, D., & Zuckerberg, M. 2010. "Solving LP relaxations of large-scale precedence constrained problems." In *International Conference on Integer Programming and Combinatorial Optimization* (pp. 1-14). Springer Berlin Heidelberg.

Birge, J. R., & Louveaux, F. 2011. *Basic Properties and Theory*. *Introduction to Stochastic Programming*. Springer Science & Business Media.

Bley, A., Boland, N., Fricke, C., & Froyland, G. 2010. "A Strengthened formulation and cutting planes for the open pit mine production scheduling problem." *Computers & Operations Research*, 37(9): 1641-1647.

Boland, N., Dumitrescu, I., Froyland, G., & Gleixner, A. 2009. "LP-based disaggregation approaches to solving the open pit mining production scheduling problem with block processing selectivity." *Computers & Operations Research, 36(*4): 1064-1089.

Brickey, A. 2015. "Underground production scheduling optimization with ventilation constraints." Ph.D. Thesis, Colorado School of Mines, Golden, CO.

Brickey, A., Espinoza, D., Goycoolea, M., Moreno, E., & Newman, A. 2015. "Implications of the Bienstock-Zuckerberg algorithm in mine planning problems." In *Chilean Congress of Operations Research,* Antofagasta, Chile.

Caccetta, L. 2016. "Application of optimization techniques in open pit mining." *International Series in Operations Research and Management Science,* 99: 547–59.

Caccetta, L., & Hill, S. 2003. "An Application of Branch and Cut to Open Pit Mine Scheduling." *Journal of Global Optimization*, 27: 349–65.

Caers, J. 2011. *Modeling Uncertainty in the Earth Sciences*. 1st Edition. Vol. 1. Wiley-Blackwell.

Chicoisne, R., Espinoza, D., Goycoolea, M., Moreno, E., & Rubio, E. 2009. "A new algorithm for the open-pit mine scheduling problem." Working paper, Universidad Adolfo Ibanez and Universidad de Chile.

Chicoisne, R., Espinoza, D., Goycoolea, M., Moreno, E., and Rubio, E. 2012. "A new algorithm for the open-pit mine production scheduling problem." *Operations Research,* 60(3): 517-528.

Chiles, J., & Delfiner, P. 2012. *Geostatistics: Modeling Spatial Uncertainty*. 2nd Edition. Vol. 1. Fontainebleau, Wiley.

CIM. 2006. "International Reporting Template." London. http://www.icmm.com/en-gb.

Clemen; R., & Riley, T. 2014. *Making Hard Decisions with Decision Tools*. 3rd ed. Vol. 1. CENGAGE.

Cullenbine, C., Wood, R. & Newman, A. 2011. "A sliding time window heuristic for open pit mine block sequencing." *Optimization Letters,* 5(3): 365–77.

Dagdelen, K, & Kawahata, K. 2008. “Value creation through strategic mine planning and cutoff-grade optimization.” In *Mining Engineering*, 1–8. Denver, CO: SME.

Dagdelen, K. 2007. “Open pit optimization - strategies for improving economics of mining projects through mine planning.” In *Orebody Modeling and Strategic Mine Planning*, edited by Roussos Dimitrakopoulos, 14:145–48. The Australasian Institute of Mining and Metallurgy (The AusIMM), Perth, Australia.

Dagdelen, K., & Francois-Bongarcon D., 1982. "Towards the complete double parameterization of recovered reserves in open pit mining." *17th APCOM* (pp. 288-296).

Dagdelen, K., & Francois-Bongarcon D., 1982. "Towards the complete double parameterization of recovered reserves in open pit mining." *17th APCOM* (pp. 288-296).

Dagdelen, K., 1985. "Optimum multi-period open pit mine production scheduling." Ph.D. Thesis, Colorado School of Mines, Golden, CO.

Dagdelen, K., 1992. "Cutoff grade optimization." *Proceedings of 23rd APCOM*, pp. 157-165, Tucson, AZ.

Dantzig, G. 1987. “Origins of the simplex method.” *A History of Scientific Computing*, Stanford, CA.

Dantzig, G & Wolfe, P. 1961. “The decomposition algorithm for linear programs.” *Econometrica,* 29(4): 767–78.

David, M. 1977. *Geostatistical Ore Reserve Estimation (Developments in Geomathematics 2)*. 1st ed. Vol. 1. Elsevier.

Davis, G., & Samis, M. 2006. “Using real options to value and manage exploration.” *Society of Economic Geologists*, 12, p. 273.

Deutsch, C., & Rossi, M. 2014. *Mineral Resource Estimation*. 1st Edition. Delray Beach, Florida, Springer.

Dimitrakopoulos, R. 2008. “Orebody modelling and strategic mine planning.” *Economic Geology*, 14: 455–458.

Dimitrakopoulos, R., & Godoy, M. 2014. “Grade control based on economic ore and waste classification functions and stochastic simulations: examples, comparisons and applications.” *Mining Technology,* 123(2): 90–106.

Dimitrakopoulos, R., Farrelly, C. & Godoy, M. 2002. "Moving forward from traditional optimization: grade uncertainty and risk effects in open pit mine design." *Transactions of IMM, Section A Mining Industry*, Vol 111, pp. A82-A89.

Dimitrakopoulos, R., Martinez, L., and Ramazan, S. 2007. “A maximum upside/minimum downside approach to the traditional optimization of open pit mine design.” *Journal of Mining Science,* 43(1): 73–82.

Dimitrakopoulos, R. 2007. “Orebody modelling and strategic mine planning - uncertainty and risk management models (2nd edition).” *The Australasian Institute of Mining and Metallurgy* (The AusIMM).

Dimitrakopoulos, R. 2011. “Strategic mine planning under uncertainty.” *Journal of Mining Science,* 47(2): 138–150.

Dimitrakopoulos, R, & Ramazan, S. 2005. “Uncertainty-based production scheduling in open pit mining.” *SME Annual Meeting,* 316(3): 106–112

Dimitris, B., & Tsitsiklis; J. 1997. *Introduction to Linear Optimization*. Vol. 1. Athena Scientific.

Diwekar, U. 2008. “Optimization under uncertainty.” In *Introduction to Applied Optimization,* (pp. 1–54). Springer US.

Elevli, B., Dagdelen, K., & Salamon, M. D. 1989. "Single time period production scheduling of open pit mines." *SME Annual Meeting,* (pp 1888-1893). Salt Lake City, UT.

Espinoza, D., Goycoolea, M., Moreno, E., & Newman, A. 2013. “MineLib: a library of open pit mining problems.” *Annals of Operations Research,* 206(1): 93–114.

Fishbain, B., Hochbaum, D. & Mueller, S. 2013. “A competitive study of the PseudoFlow algorithm for the minimum s–t cut problem in vision applications.” *Journal of Real-Time Image Processing*, 1–21.

Fisher, M. 2004. “The Lagrangian relaxation method for solving integer programming problems.” *Management Science,* 50(12_suplement): 1861–1871.

Gaupp, M., 2008. "Methods for improving the tractability of the block sequencing problem for open pit mining." Ph.D. Thesis, Colorado School of Mines, Golden, CO

Geovariances. 2014. “Uncertainty of mineral resource estimates to resource classification uncertainty of mineral resource estimates.” White Paper.

Gershon M. 1987b. "An open-pit production scheduler: algorithm and implementation." *AIME Trans*., 282: 793–796.

Gershon, M. 1983. "Optimal mine production scheduling: evaluation of large scale mathematical programming approaches." *International. Journal of Mining Engineering,* 1(4): 315–329.

Gershon, M. 1983. “Mine scheduling optimization with mixed integer programming.” *Mining Engineering*, *(Littleton, Colo.); (United States)*, *35*(4).

Gleixner, A. 2008. “Solving large-scale open pit mining production scheduling problems by integer programming.” MSc Thesis, Technische Universitat, Berlin.

Godoy, M, & Dimitrakopoulos, R. 2004. “Managing risk and waste mining in long-term production scheduling of open-pit mines.” *SME Transactions* 316(3): 43–50.

Godoy, M. 2003. "The effective management of geological risk in long-term production scheduling of open pit mines.” Ph.D. Thesis, The University of Queensland, Queensland.

Goodfellow, R. 2014. “Unified modelling and simultaneous optimization of open pit mining complexes with supply uncertainty.” Ph.D. Thesis, McGill University, Montreal, Quebec Province.

Goodfellow, R., & Dimitrakopoulos, R. 2016. “Global optimization of open pit mining complexes with uncertainty.” *Applied Soft Computing Journal,* 40, pp. 292–304.

Goovaerts, P. 1997. *Geostatistics for Natural Resources Evaluation*. New York: Oxford University Press.

Gröwe-Kuska, N., Heitsch, H., & Römisch, W. 2003. “Scenario reduction and scenario tree construction for power management problems.” *2003 IEEE Bologna Power Tech - Conference Proceedings,* 3: 152–158.

Gupta, V., & Grossmann, I. 2011. “Solution strategies for multistage stochastic programming with endogenous uncertainties.” *Computers and Chemical Engineering,* 35(11): 2235–2247.

Henrion, R., Kuchler, C., & Romisch, W. 2008. “Discrepancy distances and scenario reduction in two-stage stochastic mixed-integer programming.” *Journal of Industrial and Management Optimization,* 4(2): 363–384.

Hochbaum, D. 1997. “The PseudoFlow algorithm: a new algorithm and a new simplex algorithm for the maximum-flow problem.” UC Berkeley manuscript.

Hochbaum, D. 2001. “A new-old algorithm for minimum-cut and maximum-flow in closure graphs.” *Networks,* 37(4): 171–193

Hochbaum, D. 2008. “The PseudoFlow algorithm: a new algorithm for the maximum-flow problem.” *Operations Research,* 56(4): 992–1009.

Hochbaum, D. 2010. “Integer programming and combinatorial optimization.” IEOR269 Lecture Notes, Berkeley, California.

Hochbaum, D. 2012. “The PseudoFlow algorithm graph algorithms and network flows.” IEORR266 Lecture Notes. Berkeley, California.

Hochbaum, D., & Orlin, J. 2012. “Simplifications and speedups of the PseudoFlow algorithm.” *Networks,* 61(1): 40–57.

Hustrulid, W., Kuchta, M., & Martin, R. 2013. *Open Pit Mine Planning and Design*. CRC Press.

IBM. 2012. *ILOG CPLEX*. Incline Village, NV.

IBM. 2014. "IBM ILOG CPLEX Optimization Studio." *Manual for Sequencing of Interval Variables*.

Isaaks, E., & Srivastava, R. 1989. *An Introduction to Applied Geostatistics*. New York, Oxford University Press.

Jélvez, E., Mancilla, D., Morales, N., & Nancel-Penard, P. 2013. "Comparing heuristics for the open pit block scheduling problem." *In Proc. 36th Internat. Appl. Comput. Oper. Res. Mineral Indust. (APCOM) Sympos*, pp. 456-464. Porto Alegre, Brazil.

Johnson, T. 1968. "Optimum open pit mine production scheduling." Ph.D. Thesis, University of California Berkeley, Berkley, CA.

Journel, A. 1990. *Fundamentals of Geostatistics in Five Lessons*. Computers & Geosciences. Vol. 16.

Journel, A., & Kyriakidis, P. 2004. *Evaluation of mineral reserves: a simulation approach*. Oxford University Press.

Kall, P., & Mayer, J. 2011. *Stochastic linear programming - second edition*. Edited by Frederick S. Hillier; Camille C. Price. 2nd Edition. Vol. 156. Zurich, Switzerland: Springer.

Kawahata, K. 2006. "A new algorithm to solve large scale mine production scheduling problems by using the Lagrangian relaxation method." Ph.D. Thesis, Colorado School of Mines, Golden, CO.

Kawahata, K., & Dagdelen, K. 2003. "A mixed integer linear programming approach to limestone quarry scheduling optimization with sequencing and blending constraints." In *SME Annual Meeting*, 1–7. Cincinnati, Ohio.

Kelkar, M., & Perez, D. 2002. *Applied Geostatistics for Reservoir Characterization: SPG*. Society of Petroleum Engineers.

King, B. 2016. "Using integer programming for strategic underground and open pit-to-underground scheduling." Ph.D. Thesis, Colorado School of Mines, Golden, CO.

Kirkpatrick, S., Gelatt, C., & Vecch, M. 2007. "Optimization by simulated annealing." *Science,* 220(4598): 671–680.

Kizilkale, A. & Dimitrakopoulos, R. 2014. "Optimizing mining rates under financial uncertainty in global mining complexes." *International Journal of Production Economics,* 158, pp. 359–365.

Klotz, Ed., & Newman, A. 2013 "Practical guidelines for solving difficult linear programs." *Surveys in Operations Research and Management Science,* 18(1): 1-17.

Klotz, Ed., & Newman, A. 2013. "Practical guidelines for solving difficult mixed integer linear programs." *Surveys in Operations Research and Management Science,* 18(1): 18-32.

Krige, D. 1953. "A statistical approach to some basic mine valuation problems on the Witwatersrand." *OR, 4*(1), p. 18.

Lambert, W. 2012. "Techniques to reduce the solution time of the open pit block sequencing problem." Ph.D. Thesis, Colorado School of Mines Golden, CO.

Lambert, W., & Newman, A. 2013. "Tailored Lagrangian relaxation for the open pit block sequencing problem." *Annals of Operations Research*, 1–20.

Lambert, W., & Newman, A. 2013. "Analyzing solutions of the open-pit: block sequencing problem obtained via Lagrangian techniques." *Mining Engineering,* 65(2): 37–43.

Lambert, W., Brickey, A., Newman, A., & Eurek, K. 2014. "Open-pit block-sequencing formulations: A tutorial." *Interfaces,* 44(2): 127–42.

Lamghari, A., & Dimitrakopoulos, R. 2012. "A diversified Tabu Search approach for the open-pit mine production scheduling problem with metal uncertainty." *European Journal of Operational Research,* 222(3): 642–652.

Lamghari, A., & Dimitrakopoulos, R. 2016. "Network-flow based algorithms for scheduling production in multi-processor open-pit mines accounting for metal uncertainty." *European Journal of Operational Research,* 250(1): 273–90.

Lamghari, A., Dimitrakopoulos, R., & Ferland, J. 2014. "A Variable Neighborhood Descent algorithm for the open-pit mine production scheduling problem with metal uncertainty." *Journal of the Operational Research Society,* 65(9): 1305–14.

Lane, K. 1988. *The Economic Definition of Ore*. 1st Edition. Queensland, Australia: COMET Strategy Pty Ltd.

Leite, A., & Dimitrakopoulos, R. 2007. "Stochastic optimization model for open pit mine planning: application and risk analysis at copper deposit." *Transactions of the Institution of Mining and Metallurgy, 116 A*, 109–118.

Leite, A., & Dimitrakopoulos, R. 2014. "Stochastic optimization of mine production scheduling with uncertain ore/metal/waste supply." *International Journal of Mining Science and Technology,* 24(6). China University of Mining & Technology: 755–62.

Lerchs, H., & Grossman, I. 1965. "Optimum design of open-pit mines." *Transactions of the Canadian Institute of Mining and Metallurgy*, 68(6), 17-24.

Loquin, K., & Dubois, D. 2010. "Kriging and epistemic uncertainty: a critical discussion." *Studies in Fuzziness and Soft Computing,* 256: 269–305.

Matheron, G. 1968. “Lois stables et loi lognormale.” Technical report, Ecole des Mines de Paris, Centre de G´eostatistique, Fontainebleau, 17 p. 13.

Matheron, G. 1971. “The theory of regionalized variables and its applications.” *Les Cahiers du Centre de Morphologie Mathematique,* Ecole des Mines de Paris, *5* p. 211.

Mokhtarian. M., & Sattarvand, J. 2016. “Commodity price uncertainty propagation in open-pit mine production planning by Latin hypercube sampling method.” *Journal of Mining and Environment,* 7(2): 215–27.

Montiel, L., & Dimitrakopoulos, R. 2015. “Optimizing mining complexes with multiple processing and transportation alternatives: an uncertainty-based approach.” *European Journal of Operational Research,* 247(1): 166–178.

Moreno, E., Espinoza, D., & Goycoolea, M. 2010, “Large-scale multi-period precedence constrained knapsack problem: A mining application.” *Electronic Notes in Discrete Mathematics*, 36, pp. 407-414.

Morrison, D. 2009. “The PseudoFlow algorithm for the maximum blocking-cut and minimum-waste flow problems.” Lecture Notes. a) A, 8(5), p.2.

Muñoz, G., Espinoza, D., Goycoolea, M., Moreno, E., Queyranne, M., & Rivera, O. 2016. “A study of the Bienstock-Zuckerberg algorithm, Applications in Mining and Resource Constrained Project Scheduling.” *arXiv preprint arXiv:1607.01104*.

Newman, A., & Weiss, M. 2013. “A survey of Linear and Mixed-Integer optimization tutorials.” *INFORMS Transactions on Education,* 14(1): 26–38.

Newman, A., Rubio, E., Caro, R., Weintraub, A., & Eurek, K. 2010. “A review of operations research in mine planning.” *Interfaces,* 40(3): 222–45.

Osanloo, M., Gholamnejad, J., & Karimi, B. 2008. “Long-term open pit mine production planning: a review of models and algorithms.” *International Journal of Mining, Reclamation and Environment,* 22(1): 3–35.

Parker, H., Hill, E., & Morgan, R. 2015. “Comparison of Fort Knox gold deposit resources from pre-feasibility study (1991) to production (1997 to 2015).” In *37th International Symposium on the Application of Computers and Operations Research in the Mineral Industry*. APCOM.

Picard, J.-C. 1976. “Maximal closure of a graph and applications to combinatorial problems.” *Management Sci.,* 22(11): 1268–1272.

Ramazan, S. 2001. "Open pit mine scheduling based on fundamental tree algorithm." Ph.D. Thesis, Colorado School of Mines, Golden, CO.

Ramazan, S. 2006. “The new fundamental tree algorithm for production scheduling of open pit mines.” *European Journal of Operational Research,* 177(2): 1153–66.

Ramazan, S., & Dimitrakopoulos, R. 2007. “Production Scheduling with Uncertain Supply: A New Solution to the Open Pit Mining Problem.” *Optimization and Engineering,* 14(2): 361–380.

Ramazan, S., Dagdelen, K., & Johnson, T., 2005. “Fundamental tree algorithm in optimizing production scheduling for open pit mine design.” *Mining Technology*, 114(1): 45-54.

Rebennack, Steffen. 2010. “Hydro-thermal scheduling.” EBGN698 Lecture Notes. Golden, CO.

Rockafellar, R., & Uryasev, S. 1997. “Optimization of conditional value-at-risk.” *Journal of Risk,* 2: 21–41.

Romer, P. 2015. “Mathiness in the theory of economic growth.” *American Economic Review: Papers & Proceedings,* 105(5): 89–93.

Sabour, S., & Dimitrakopoulos, R. 2009. “A Multi-criteria decision support system for open pit mine planning under geological and market uncertainties.” In *SME Annual Meeting and Exhibit and CMA’s 111th National Western Mining Conference 2009*. Vol. 1. Denver, CO.

Samis, M., & Davis, G. 2014. “Using Monte Carlo Simulation with DCF and Real Options risk pricing techniques to analyze a mine financing proposal.” *International Journal of Financial Engineering and Risk Management,* 1(3): 264–81.

Sattarvand, J., & Niemann-Delius, C. 2008. “Perspective of metaheuristic optimization methods in open pit production planning.” *Mineral Resources Management,* 24(4): 143–156.

Sattarvand, J., & Niemann-delius, C. 2013. “Past, present and future of metaheuristic optimization methods in long-term production planning of open pits.” *BHM Berg- Und Hüttenmännische Monatshefte,* 158(4): 146–154.

Silva, D., & Boisvert, J. 2014. “Mineral resource classification: a comparison of new and existing techniques.” *Journal of the Southern African Institute of Mining and Metallurgy,* 114(3): 265–273.

Silva, M. 2014. "Solving a large stochastic integer programming model for production scheduling at a gold mine with multiple processing streams and uncertain geology." *Proceedings of Conference on Orebody Modeling and Strategic Mine Planning,* Perth Australia, pp. 389 -396, Dimitrakopoulos, R., (eds.).

Snowden, V. 2000. “Practical interpretation of resource classification guidelines.” *AusIMM 1996 Annual Conference*, Perth, Australia.

Stephenson, P., Allman, A., Carville, D., Stoker, P., Mokos, P., Tyrrell, J., & Burrows, T. 2004. “Mineral resource classification – it’s time to shoot the ‘spotted dog ’!” In *Proceedings Sixth International Mining Geology Conference (pp. 91-95)*.

Verly, G., Postolski, T., & Parker. H. 2014 “Assessing uncertainty with drillhole spacing studies: applications to mineral resources.” Vol. 1. In *Proceedings of Conference on Orebody Modeling and Strategic Mine Planning*, (pp. 109 -118), Perth, Australia, Dimitrakopoulos, R., (eds.).

Wackernagel, H. 2013. *Multivariate geostatistics: an introduction with applications*. Springer Science & Business Media.

Webster, R., & Oliver, M. 2007. *Geostatistics for environmental scientists*. John Wiley & Sons.

Whittle J, 1999. "Four-x strategic planning software for open pit mines." Reference manual.

Whittle, J., 2014. "Not for the faint-hearted." *Proceedings of Conference on Orebody Modeling and Strategic Mine Planning*, pp. 3 – 5, Dimitrakopoulos, R., (eds.) Perth Australia.

Zhang, J., & Dimitrakopoulos, R. 2015. "A dynamic ore-price-based method for optimizing a mineral supply chain with uncertainty." *Application of Computers and Operations Research in the Mineral Industry - Proceedings of the 37th International Symposium, APCOM, pp.*1–9.

Zhang, M., & Middleton, R. 2007. "A study of the impact of price uncertainty to mining project valuation." *Knowledge Creation Diffusion Utilization*, p.1–5.

Zhang, Ye. 2009. *Introduction to Geostatistics - Course Notes*. *Dept. of Geology & Geophysics, University of Wyoming*.

Zhao, Y. 1992. "Algorithms for optimum design and planning of open pit mines." Ph.D. Thesis, The University of Arizona, Phoenix, AZ.